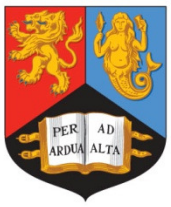

UNIVERSITY OF BIRMINGHAM

EXHAUST GAS FUEL REFORMING FOR IMPROVED GASOLINE DIRECT INJECTION ENGINE EFFICIENCY AND EMISSIONS

by

DANIEL ALEXANDER FENNELL

A thesis submitted to
The University of Birmingham
for the degree of

DOCTOR OF PHILOSOPHY

School of Mechanical Engineering
The University of Birmingham
March 2014

ABSTRACT

The thesis investigates how exhaust gas fuel reforming, also known as reformed exhaust gas recirculation (REGR), may benefit direct injection gasoline (GDI) engine efficiency and emissions. REGR is a thermochemical process that has potential for efficiently producing hydrogen-rich gas onboard a vehicle by using waste exhaust energy to promote endothermic reforming of hydrocarbon fuels. Partially fuelling a gasoline engine with hydrogen generally improves engine thermal efficiency.

The experimental research begins by simulating REGR on single- and multi-cylinder GDI engines, which indicates that REGR can increase engine thermal efficiency by up to 9% and reduce NO_x by up to 96%. Particulate matter (PM) measurements reveal that REGR significantly reduces PM number and mass emissions, beyond that achieved by EGR.

Further experiments with a full-scale prototype exhaust gas fuel reformer integrated with the multi-cylinder GDI engine demonstrate improved fuel efficiency at a wide range of engine conditions, by 8% for conditions typical of motorway driving. The reforming process is observed to be overall endothermic when the exhaust temperature is above 650°C, and the reformed fuel enthalpy is increased by up to 21% in these experiments.

The results demonstrate that REGR can simultaneously increase engine thermal efficiency, and reduce gaseous and PM emissions.

Dedicated to my Dad and Mick

For providing me with endless support and motivation from the start

and for the alternative, two-wheeled education on countless Sundays in muddy fields all over the country...we learnt a lot together...

ACKNOWLEDGEMENTS

Firstly I must thank Dr. Thanos Tsolakis and Dr. Karl Dearn for presenting this opportunity to me, and for their dedicated supervision of the research. The technical and moral support of Dr. Dale Turner and Dr. Jose Martin Herreros has been incredibly useful; they have always been willing to provide guidance and motivation when I've been 'hitting the wall'.

I am grateful to Dr. Steve Dinsdale at Cambustion Ltd for his continued support and helpful advice throughout - I gained a lot from his participation in many technical discussions.

The Technology Strategy Board is acknowledged as co-funder of the industry and academia collaboration project, (ref. 400176/149) *CO2 Reduction through Emissions Optimisation (CREO),* of which the University of Birmingham is a consortium member. This project has provided me a postgraduate scholarship. Many thanks to the following individuals and companies who are acknowledged for their involvement with the CREO project research: Andy Scarisbrick, Dave Chick and Roland Stark at Ford Motor Company for ensuring supply of the engine and associated parts; Paul Millington, Kirsty Cockle and John Pignon at Johnson Matthey Plc for supplying catalysts, parts, data and the prototype fuel reformer; and to Lia Beddow and Malcolm Goddard at Jaguar-Land Rover for providing parts and information relating to the engine installation. I am also grateful to Dr. Roger Cracknell at Shell Global Solutions UK for arranging the supply of gasoline fuel.

Thank you to Carl Hingley, Lee Gauntlett, Jack Garrod, Pete Thornton and Becky Charles, the team of technicians who assisted with the engine test cell installation.

Many thanks must go to my good friend Amy Beaumont, who kindly edited the thesis for conventions of language, spelling and grammar.

TABLE OF CONTENTS

LIST OF FIGURES

LIST OF TABLES

LIST OF ABBREVIATIONS

AFR	Air fuel ratio
AI	Analogue input channel
AO	Analogue output channel
aTDC	After top dead centre
BDC	Bottom dead centre
BSFC	Brake specific fuel consumption, g/kWh
bTDC	Before top dead centre
CA	Crank angle
CH_4	Methane
CI	Compression ignition
CO	Carbon monoxide
COV	Coefficient of variation
CO_2	Carbon dioxide
CR	Compression ratio
CREO	CO_2 reduction through emissions optimisation (TSB funded project)
CZA	Ceria-zirconia-alumina (catalyst washcoat)
DAQ	Data acquisition

D-EGR	Direct - exhaust gas recirculation
DI	Direct injection
DI/O	Digital input/output channel
ECU	Engine control unit
EGR	Exhaust gas recirculation
EGT	Exhaust gas temperature
EVC	Exhaust valve closing
FTIR	Fourier transform infra-red spectrometer
GDI	Gasoline direct injection
GHSV	Gas hourly space velocity
GNMD	Geometric (particle) number mean diameter
GPF	Gasoline particulate filter
HC	Hydrocarbon
HCCI	Homogeneous charge compression ignition
H_2	Hydrogen
IC	Internal combustion (engine)
IEM	Integrated exhaust manifold
IMEP	Indicated mean effective pressure

IVO	Intake valve opening
JM	Johnson Matthey Plc
LHV	Lower heating (calorific) value
LTC	Low temperature combustion
MBT	(Ignition advance for) maximum brake torque
MEP	Mean effective pressure
MFB	Mass fraction burned
NA	Naturally aspirated
NDIR	Non-dispersive infra-red gas analyser
NEDC	New European drive cycle
NO	Nitric oxides
NO_2	Nitrogen dioxide
NO_x	Oxides of nitrogen
NVH	Noise, vibration and harshness
Pd	Palladium
PFI	Port fuel injection
PM	Particulate matter
PMEP	Pumping mean effective pressure

PPCI	Partially premixed compression ignition
ppm	Parts per million (concentration)
Pt	Platinum
PWM	Pulse-width modulated
REGR	Reformed exhaust gas recirculation
Rh	Rhodium
SI	Spark ignition
SMPS	Scanning mobility particle sizer
SOI	Start of injection
THC	Total hydrocarbons
TSB	Technology strategy board
TWC	Three-way catalyst
WGS	Water-gas shift reaction
TDC	Top dead centre
UoB	University of Birmingham
VCT	Variable cam timing
VE	Volumetric efficiency
Vol	Volumetric concentration

VVL	Variable valve lift

NOMENCLATURE

$\frac{dQ}{d\theta}$	Rate of heat release, J/degree (crank angle)
dV	Increment of swept cylinder volume, m^3
LHV_{fuel}	Lower heating value (enthalpy of combustion) of fuel, kJ/kg
$\dot{m}_{EGR}$	EGR mass flow rate, kg/s
$\dot{m}_{fuel}$	Fuel flow, kg/s
$M_{r,EGR}$	Relative molecular mass of EGR, kg/kmol
N	Engine speed, rpm
$\dot{n}_{Air}$	Molar flow rate of air, mol/s
$\dot{n}_{EGR}$	Molar flow rate of EGR, mol/s
p	Cylinder pressure, Pa
$\bar{p}$	Mean cylinder pressure, bar
P_{Br}	Engine 'brake' power, kW
P_{Ind}	Indicated power (one cylinder), kW
QR	Heat release, J
$\dot{Q}_{max}$	Maximum rate of heat release, J/degree (crank angle)
T	Measured engine torque, Nm

V_s	Swept volume, m^3
γ	Ratio of specific heats
ΔH_{ref}	Enthalpy increase of reformed fuel
ΔT	Change in temperature
η_{comb}	Combustion efficiency
η_{Ind}	Indicated engine thermal efficiency
η_{ref}	Reforming process efficiency
θ	Crank angle, degrees
λ	Excess air ‘lambda’ ratio

CHAPTER 1

INTRODUCTION

1.1 Overview

Continued refinement of legislation relating to vehicle emissions and fuel economy in recent years has forced the automotive industry to introduce a variety of new technologies into production vehicles at ever greater cost and complexity. Incremental efficiency gains are achieved by systems across the vehicle architecture. The engine and its related systems offer many potential areas for improving efficiency, not least by reducing the large fraction of fuel energy that leaves the exhaust as waste heat. For this reason there are many new technologies being developed to enable exhaust energy recovery for improved fuel efficiency.

Combustion of hydrogen in automotive engines has been widely researched with the aim of reducing CO_2 emissions, and has shown benefits in terms of engine thermal efficiency and the reduction of other regulated emissions. However, problems encountered with production, onboard storage and infrastructure have prevented a move toward widespread adoption of hydrogen fuelling. The process of reforming hydrocarbon (HC) fuel to hydrogen-rich gas can be implemented onboard a vehicle to partially fuel the engine, eliminating some of the problems associated with stored hydrogen while still retaining attractive combustion properties. Systems developed in the past however have suffered a net energy loss in the reforming process and therefore have not been viable in terms of overall system efficiency. Exhaust gas fuel reforming is a technology with potential to efficiently produce hydrogen by utilising waste exhaust energy.

Exhaust gas fuel reforming aims to extract energy from the exhaust stream using endothermic reforming reactions and produce a gaseous fuel with higher enthalpy than the gasoline fed to the reformer. The principle relies on using a reforming catalyst mounted in the hot exhaust stream, as depicted schematically in Figure 1.1. HC fuel (gasoline in the context of this research) is mixed with a fraction of the engine exhaust gas and passed over the hot reforming catalyst to produce a hydrogen and carbon monoxide (CO) rich gas, known as reformate. The reformate fuel is then inducted into the intake system for combustion, similarly to exhaust gas recirculation (EGR); this system is known as reformed exhaust gas recirculation (REGR). The combination of EGR-like charge dilution and combustion enhancement with hydrogen offers the possibility to increase engine thermal efficiency and reduce exhaust emissions.

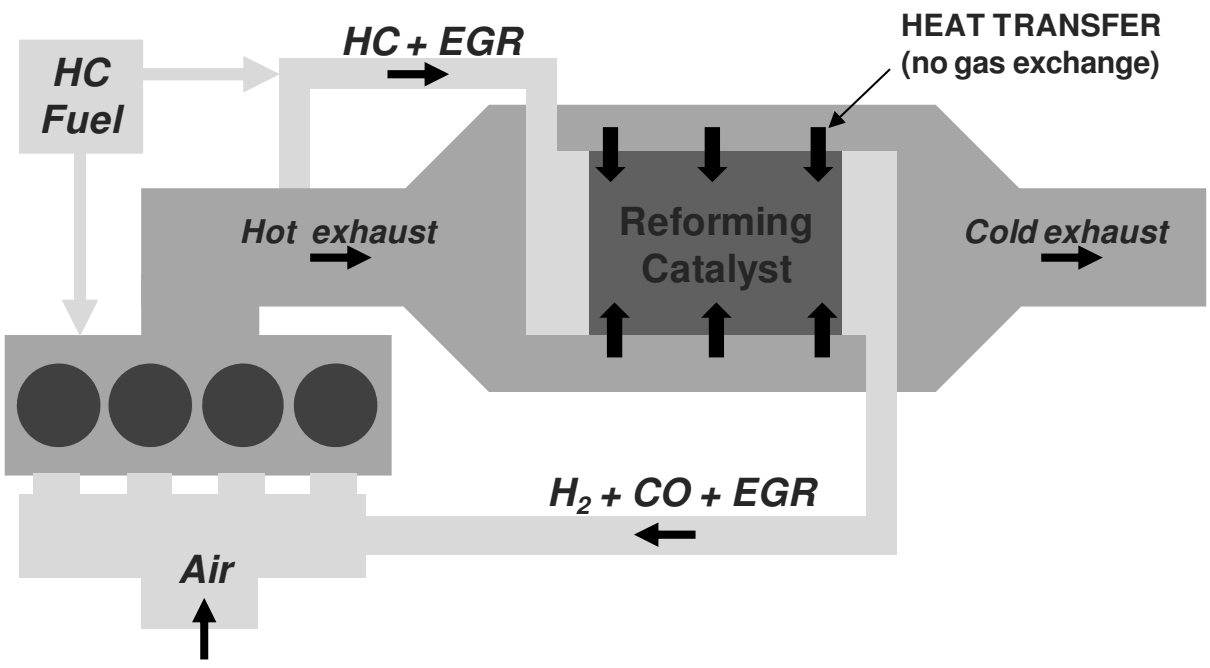

Figure 1.1 - Schematic of an exhaust gas fuel reformer to produce hydrogen (H_2) and CO from HC fuel and EGR

The University of Birmingham's Future Power Systems group has recently been working in collaboration with a number of industrial partners on a Technology Strategy Board (TSB) funded project entitled *CO_2 Reduction through Emissions Optimisation* (CREO). As part of

this project, a prototype exhaust gas fuel reformer system was developed, and much of the research presented in this thesis contributed to achieving the CREO project objectives.

1.2 Research focus

The aim of this research is to demonstrate and quantify the benefit of using exhaust gas fuel reforming to improve gasoline engine efficiency and emissions.

Recent research on the application of exhaust gas fuel reforming has been mostly related to diesel engine combustion [1-3] and aftertreatment enhancement [4-6]. Some studies have investigated exhaust gas reforming of various bio-fuels, with the application of bio-diesel reforming to compression ignition (CI) engines [7, 8] and ethanol reforming to spark ignition (SI) engines [9-13]. There has been less work dedicated to the use of exhaust gas fuel reforming with the gasoline engine, although early work did envisage this application and it has been developed to some degree over the years [14-16]. These studies are discussed in section 2.5.3.

The gasoline engine is a prime candidate for exhaust gas fuel reforming due to the high exhaust gas temperature (EGT) encountered in normal operation, which is important for effective reformer operation. In addition, the exhaust oxygen concentration is low for the homogeneous, stoichiometric charge gasoline engine. This has potentially positive implications for fuel reforming, which will be discussed later. The development of high efficiency gasoline engines now applies direct injection (DI) as standard technology. Therefore, this work sets out to develop the application of exhaust gas fuel reforming to the gasoline direct injection (GDI) engine.

Emphasis was placed on taking a holistic approach throughout the research, which meant considering the performance of each part of the total system. It was therefore necessary to

analyse: the reformer performance in terms of reforming activity and energy recovery capability; how the reformer influences engine performance in terms of combustion, fuel efficiency, gaseous emissions and particulate emissions; and how engine-reformer interactions affect the total system performance. With this in mind the following research objectives were outlined.

1.2.1 Objectives

1. Understand how partially fuelling the GDI engine with reformate affects:
    a. Combustion performance
    b. Engine thermal efficiency
    c. Gaseous and particulate emissions
2. Demonstrate the operation of an integrated, full scale prototype fuel reformer with a production specification, multi-cylinder GDI engine
3. Quantify the prototype fuel reformer performance at steady state engine conditions
4. Understand how the engine operating characteristics influence the fuel reformer performance and reformate composition
5. Understand how fuel reforming influences engine efficiency and emissions
6. Determine how effective reforming can be for exhaust energy capture

1.3 Thesis outline

Chapter 2 provides some relevant background to GDI engine technology, with particular attention given to EGR due to its relevance to engine operation with exhaust gas fuel reforming. The gaseous fuel reformate is then discussed, noting its physical properties relative to gasoline, the inert gas content and their effects on combustion. This is followed by an overview of fuel reforming and the fundamentals of reforming chemistry. Finally, there is a

review of experimental research in the literature relating to hydrogen and reformate combustion in gasoline engines, including some research that has used prototype fuel reformers.

Details of the experimental facilities used throughout the course of the research are provided in **Chapter 3**, as well as details of the calculations used for processing test data.

Chapter 4 begins by presenting results that demonstrate the performance of Platinum-Rhodium (Pt-Rh) reforming catalysts and predict the reformate composition achievable at typical gasoline engine exhaust stream temperature. Single-cylinder GDI engine test results are then reported that indicate the effects of partial reformate fuelling on GDI engine combustion and emissions performance. Most of the content of this chapter was published in a technical paper presented at the SAE World Congress in April 2013 [17].

Chapter 5 describes the experimental simulation of a REGR system which supplies hydrogen and CO to the EGR system of a multi-cylinder GDI engine. Again the hydrogen and CO concentrations in the REGR stream were selected to be achievable in practice at typical gasoline exhaust temperatures. Emphasis was placed on comparing REGR and EGR to the baseline GDI engine performance, as well as the effects of varying reformate quality. Combustion, efficiency and emissions results are presented for a low-load and mid-load engine condition, and a full system analysis attempts to predict total engine-reformer system efficiency. The chapter includes a study of the influence of EGR and REGR on particulate matter (PM) emissions. There is also an investigation into the relative effects of hydrogen and CO concentration in reformate on combustion performance, and the chapter concludes by analysing REGR performance maps across a wider range of engine conditions. **Sections 5.1**

and **5.2** form the basis of a journal paper published by the International Journal of Hydrogen Energy [18].

The experimental work culminates with two chapters focused on studies of a prototype exhaust gas fuel reformer integrated with the multi-cylinder GDI engine. In **Chapter 6** the reformer performance is assessed in terms of the temperature distribution across the catalyst, the reformate composition, the reforming process efficiency and the amount of exhaust heat recovery achieved, as well as an analysis of the variation in exhaust stream exergy. The content of this chapter has been submitted as a research paper to the journal of Applied Energy and is currently *in review*.

Chapter 7 is focused specifically on the influence of reformer operation on the engine performance, in particular the engine fuel efficiency improvement. Combustion performance and engine emissions results are also presented to confirm the trends predicted in earlier chapters. There is then an investigation into the effect of engine down-speeding on the reformer operation and engine fuel efficiency. The chapter concludes with a study of full load engine operation with REGR, which investigates the use of two alternative gas recirculation systems for their influence on engine torque, knock and fuel efficiency.

The conclusions of the thesis are summarised in **Chapter 8** along with some suggestions for future research relating to exhaust gas fuel reforming.

1.4 Novelty of research

This thesis addresses several original points, thus providing an innovative and novel contribution to catalytic fuel reforming research applied in the wider context of internal combustion (IC) engine research. These are outlined below:

- Performing experimental engine research using ‘low quality’ reformate rather than ideal reformate compositions to predict the benefit of a fuel reformer
- Taking a holistic approach to the prediction of GDI engine performance with REGR, with consideration for engine efficiency, gaseous emissions, particulate emissions, effects on combustion and potentially important engine-reformer interactions (e.g. effect of REGR on exhaust temperature, which is important for reformer performance)
- Investigating the combination of hydrogen/reformate with EGR to reduce PM emissions
- Demonstrating results obtained using a full scale prototype exhaust gas fuel reformer integrated with a production specification, multi-cylinder GDI engine
- Analysing the composition of reformate produced by exhaust gas fuel reforming
- Detailed speciation of HCs in reformate
- Analysing the total system thermal efficiency (i.e. the engine and reformer)
- Analysing the combustion process associated with a GDI engine using an integrated exhaust gas fuel reformer
- Estimating exhaust heat recovery achieved by exhaust gas fuel reforming
- Comparing alternative exhaust gas recirculation architectures for used with REGR
- Investigating REGR characteristics and influence on engine performance and knock at high load with elevated (boosted) intake manifold pressure

CHAPTER 2

BACKGROUND AND LITERATURE REVIEW

2.1 Introduction

This research is focused on the application of exhaust gas fuel reforming to the GDI engine. DI has been at the core of SI gasoline engine development in the past decade due to the wide ranging benefits it offers relative to its predecessor, port fuel injection (PFI). DI will continue to increase its share of the gasoline engine market in the future. The brief overview of GDI engine technology that follows is presented both as background information that is relevant to the application of exhaust gas fuel reforming, and also to explore how the various systems will integrate to provide an overall benefit for GDI engine efficiency and emissions. Following an introduction to fuel reforming thermodynamics and catalysis, the more detailed review of literature is concerned with hydrogen and reformate combustion in SI engines, as well as previous attempts at onboard fuel reformer development.

This chapter, and the work that follows, will be focused on the SI gasoline engine with little discussion of the CI engine. In order to keep a sufficiently narrow scope, this work eliminates any detailed reference to conventional diesel combustion or modern low temperature combustion (LTC) modes such as homogeneous charge or partially premixed compression ignition (HCCI or PPCI). As will become apparent, the gasoline SI engine is possibly most well suited to achieving energy recovery with exhaust gas fuel reforming due to its high temperature exhaust stream with low oxygen content. Additionally, the gasoline engine maintains a majority share in the global passenger vehicle market, although less so in Europe.

2.2 The GDI engine

2.2.1 General characteristics and components of the GDI engine

The fuel delivery system is the major difference, in terms of hardware, between the DI and the more traditional PFI gasoline engine. For PFI the injectors are usually mounted in the intake manifold close to the inlet port such that the nozzle delivers fuel into the air path prior to the intake valve. The mixing of fuel and air before the intake valve is a characteristic historically shared by other fuel delivery systems, for instance with single point injection or the carburettor. This approach results in a homogeneous charge where the air/fuel mixture is completely, or almost completely, mixed.

For DI the injectors are mounted to the cylinder head with their nozzles positioned to deliver fuel directly into the combustion chamber. Broadly speaking, the timing of DI during the induction or compression strokes determines whether the charge is homogeneous or stratified (partially mixed).

One of the key advantages of DI over PFI is the superior charge cooling effect as the fuel vaporises inside the combustion chamber, which increases the charge density. This increases volumetric efficiency (VE) and the potential peak engine output. It also reduces the tendency for pre-ignition and knock because the compression temperature is lower, thus allowing an increased compression ratio (CR). In turn, this means that greater pressure charging can be achieved, enabling engine downsizing. DI increases engine efficiency, improves transient response and reduces the EGT, which means that thermal stresses on exhaust components are lower. [19]

In order to enable fuel injection directly into the cylinder with suitable fuel vapourisation over a short time period, significantly higher fuel pressures are required for DI compared to PFI

engines. This has led to the introduction of high pressure mechanical fuel pumps in addition to the low pressure feeder pump. Fuel rail pressures between 50-200bar are now typical, varying across the engine range.

Since the introduction of GDI, injector and combustion system development has led to the definition of three distinct types of DI which are depicted in Figure 2.1. The first generation DI systems became known initially as 'wall-guided' as they used the influence of the combustion chamber walls (in particular the piston crown) on fuel and charge motion to control fuel/air mixing. Generally the first generation DI systems use solenoid injectors located under the inlet port. There is potential for significant fuel impingement, in particular with the piston, which is usually shaped with an asymmetric, 'scooped' cut-out that assists by influencing the charge motion and directing the injected fuel towards the spark plug. Wall wetting by fuel impingement leads to increased unburned HCs and soot formation.

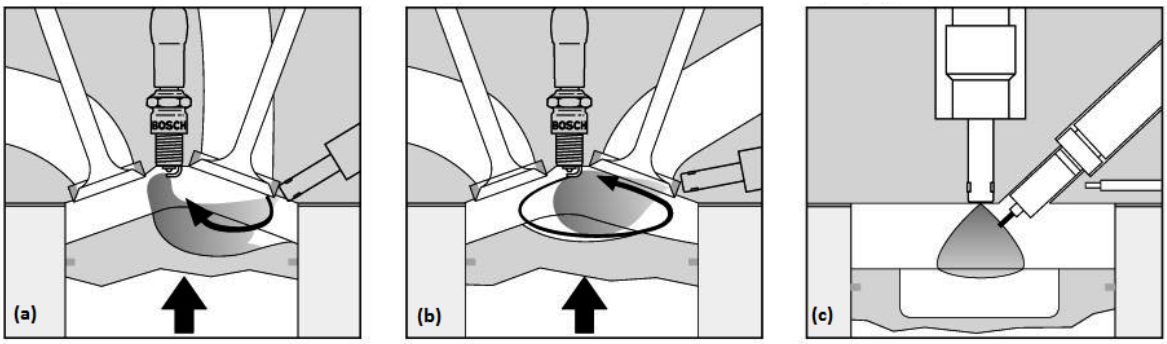

Figure 2.1 - SI engine charge preparation with wall-guided (a), air-guided (b) and spray-guided (c) direct injection [20]

A later variation of first generation DI is the 'air-guided' approach in which the inlet ports are designed to generate the desired amount of tumble charge motion across the speed/load range. Tumble is defined as rotational charge motion perpendicular to the cylinder axis, and facilitates by entraining the injected fuel in the bulk charge motion, thereby reducing

impingement, while achieving sufficient fuel-air mixing. Engine control unit (ECU) controlled tumble flaps located in front of the inlet ports are sometimes used to vary the amount of tumble motion. Although originally developed for stratified combustion, these arrangements are also commonly used in homogeneous SI engines. [19]

The second generation of DI systems use a 'spray-guided' approach to fuel/air mixing (Figure 2.1c). These systems use a central injector and spark plug position that enables the fuel spray to be concentrated locally to the spark plug electrode and helps achieve a stratified charge more effectively. The fuel spray pattern and atomisation is even more important for ensuring the desired fuel distribution and level of stratification/mixing; therefore, increasingly challenging requirements have been placed on the fuel injector. The use of multiple injections provides superior control of fuel distribution in the combustion chamber by reducing the spray penetration distance and improving atomisation, which both help to reduce fuel impingement. Piezoelectric injectors offer faster response and shorter minimum injection duration compared to solenoid injectors and so are often employed in second generation DI systems.

A split injection strategy can be used to generate partial charge stratification in an otherwise homogeneous charge SI engine. The first injection event is timed similarly to normal homogeneous operation, during the induction stroke, and the additional second injection is timed much later during the compression stroke. This results in a partially stratified charge that is locally rich near the spark plug, while the surrounding homogeneous charge is slightly lean to maintain an overall stoichiometric air fuel ratio (AFR). The influence of split injection on combustion and emissions will be discussed later.

2.2.2 Emissions formation

The primary pollutant formed during the combustion of HC fuels is CO_2 and there is worldwide pressure on all industries to reduce the amount of CO_2 released into the atmosphere. The subject of this work, exhaust gas fuel reforming, is concerned primarily with reducing the levels of CO_2 produced by the GDI engine, which are typically used in many modern passenger vehicles. The phrases 'increasing fuel/engine/thermal efficiency' and 'improving fuel economy' may be used interchangeably with 'reducing CO_2 emissions'.

Automotive manufacturers face increasingly strict regulations for CO_2 emissions. Beyond this, the permitted levels of the other regulated emissions become more challenging to achieve with each legislative update. The recent and ongoing priority in the development of vehicles to be sold in Europe is to meet the EU6 regulations (Table 2.1) that will be introduced in 2014. These emissions standards will also include for the first time a particulate number limit for gasoline engines, which will be enforced from 2017.

Table 2.1 - EU6 emissions regulations for gasoline fuelled passenger vehicles [21]

NO_x (g/km)	**CO (g/km)**	**HC (g/km)**	**[1] NMHC (g/km)**	**Particulate mass (mg/km)**	**[2] Particulate number (#/km)**
0.06	1.0	0.1	0.068	4.5	$6x10^{11}$

[1] NMHC: Non-methane hydrocarbons; [2] To be introduced in 2017

In order to achieve emissions reduction with combustion system development and the application of aftertreatment systems it is necessary to understand the various mechanisms of emissions formation. These will now be introduced for the major pollutant species.

Oxides of nitrogen (NO_x)

Oxides of nitrogen in engine exhaust gas consist of mostly of nitric oxide (NO) with a smaller proportion of nitrogen dioxide (NO_2). The formation rate of NO during combustion only becomes significant when the temperature is above 1800K [22]. During the combustion process it is mostly NO that is formed; subsequently, in the exhaust stream and in the atmosphere, NO is oxidised to NO_2, which causes environmental problems by reacting with HCs to form photochemical smog. The quantity of NO formed in the post-flame gas is generally far greater than that produced in the flame itself, firstly because the residence time in the flame front is short, and secondly because the increasing cylinder pressure compresses the combustion products, raising the temperature. The engine operating characteristics that most affect NO formation include the charge equivalence ratio, the residual gas fraction, external EGR rate and ignition timing, due to the influence they have on the oxygen concentration or temperature experienced in the burned gas. [23]

NO formation in SI engines is often assumed to be primarily due to the thermal mechanism and is modelled using the extended Zeldovich mechanism. In this process dissociated oxygen atoms oxidise nitrogen molecules to form NO (Equation 2.1), as well as atomic nitrogen which goes on to produce further NO by reacting with oxygen (Equation 2.2). The hydroxyl radical (OH) also plays a part in NO formation (Equation 2.3). The less significant 'prompt' and 'nitrous oxide' mechanisms involve the reaction of nitrogen with HC molecules and the decomposition of nitrous oxide respectively; the contribution of these mechanisms becomes more important at low combustion temperatures. [22]

$$O + N_2 \rightleftharpoons NO + N$$ Equation 2.1

$$N + O_2 \rightleftharpoons NO + O$$ Equation 2.2

$$N + OH \rightleftharpoons NO + H$$ Equation 2.3

The strong dependence of the rate of NO formation on temperature is clear when the reaction kinetics are considered. For example, the initial rate of NO formation is increased by an order of magnitude if the flame temperature is increased by just 140K (from 2080K to 2220K for a stoichiometric mixture). This is derived from the exponential relationship in Equation 2.4, which also indicates the dependence of NO formation rate on the oxygen and nitrogen equilibrium concentrations. The initial rate of NO formation is strongly influenced by the forward reaction rate constant of Equation 2.1 and the equilibrium constant for the dissociation of oxygen at the instantaneous reaction temperature. [23]

$$\frac{d[NO]}{dt} = \frac{6 \times 10^{16}}{T^{1/2}} exp\left(\frac{-69{,}090}{T}\right)[O_2]_e^{1/2}[N_2]_e \qquad \text{Equation 2.4}$$

Carbon monoxide (CO)

The level of CO emissions is determined mainly by the extent to which combustion is completed; incomplete combustion as a result of insufficient oxygen in a rich fuel-air mixture leads to partial burning and high CO emissions. In contrast to NO formation, higher temperature and oxygen concentration results in lower CO emissions by increasing the rate of CO oxidation. This process continues to some extent during the expansion stroke, but will slow down to become insignificant as the temperature drops. The high oxygen concentration in lean fuel-air mixtures results in very low CO emissions. The prevailing temperature of the burned gases also influences CO emissions through variation of the CO/CO_2 equilibrium, where higher temperature promotes the dissociation of CO_2 to increase CO [22, 23].

Unburned hydrocarbons (HCs)

HC emissions are not formed in the same manner as the other pollutants. Rather, they are a result of incomplete combustion. There are many reasons that the HC fuel may not be completely burned. Air-fuel mixture is forced into crevice volumes (space between

combustion chamber components, e.g. piston rings or valve seats) by high in-cylinder pressure, and some fuel is absorbed by oil layers and cylinder deposits on the combustion chamber walls. Fuel in these locations is not burnt because the flame is quenched as it approaches the combustion chamber walls and cannot penetrate into the small crevice volumes. Less complete and increasingly variable combustion occurs when the engine management system is unable to ensure the optimum fuel-air mixture preparation on a cycle-by-cycle basis, which is particularly challenging during transient operation. In this scenario the end-gas will contain high levels of unburned HCs. Deterioration of combustion stability due to charge dilution has the same effect, and can eventually result in total misfire [22, 23].

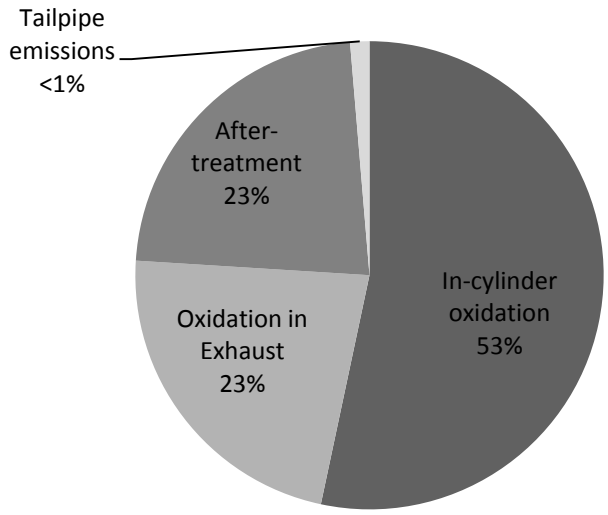

Figure 2.2 - Contribution of the various mechanisms for oxidation of HCs that remain after the main combustion process: data from [22]

HC oxidation in the end-gas proceeds at lower temperature than for CO oxidation, and continues for the duration of the exhaust stroke, both in the cylinder and later in the exhaust manifold. Of the HCs that remain after the main combustion process, approximately half will be oxidised in the cylinder and a quarter in the exhaust manifold (Figure 2.2). The aftertreatment system is able to remove the low levels of HC (usually of the order of 2000ppm C1) with high conversion efficiency, leaving only a small proportion to be emitted to

atmosphere. However, practical limitations make 100% HC conversion impossible, which highlights the importance of the post-oxidation processes on reducing tailpipe HC emissions. [22]

Particulate matter (PM)

PM generated by HC combustion is a mixture of insoluble material, mainly carbonaceous soot particles with smaller amounts of ash and metal oxides, and a considerable volatile fraction consisting of HC compounds and sulphates. The volatile fraction may exist as condensed particles or be adsorbed on other solid particles. [21, 24]

PM from diesel engines usually exists in a clearly defined bi-modal distribution, in terms of particle size. These are termed the nucleation and accumulation modes, and very generally speaking these modes have a mean particle diameter of the order of 30nm and 200nm respectively [24]. Particle size distributions tend to be less well defined in samples of gasoline engine exhaust gas, with more overlap between the two modes and a greater contribution and variation of the nucleation mode. Nucleation mode particles are mostly condensed volatile species, although particles in this size range have been reported to contain a solid core [25]. Adsorption and condensation of the volatile fraction mostly occurs in the exhaust system as the gas cools and is diluted by air (either in the sample system or when released to atmosphere) [23].

In the past, controlling PM emissions from gasoline engines has not been a considerable technical or research focus. In contrast to diesel engines, PM formation is low in PFI gasoline engines due to the substantially pre-mixed charge, and PM emissions only increase under very fuel rich conditions that are avoided at most engine conditions. This changed, however, with the introduction of DI to gasoline engines.

PM formation in GDI engines is generally due to combustion of a non- homogeneous charge containing liquid fuel droplets or locally fuel-rich regions; this is far more likely with DI than PFI. Figure 2.3 identifies the many sources of particle formation in the combustion chamber [21]. These include the various locations for possible fuel impingement (1-4), injector deposits resulting in poor fuel vapourisation (5), inadequate fuel-air mixing (6) and PM formed in the diffusion flame (7) that may occur with a stratified charge during particularly late injections, similarly to diesel engines.

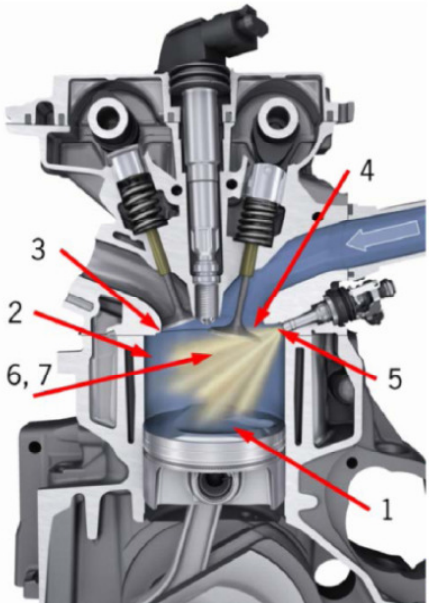

1. Piston wetting
2. Cylinder liner wetting
3. Roof wetting, including spark plug
4. Interaction spray, air flow, intake valve
5. Injector deposits
6. Mixture homogeneity (locally rich regions)
7. Diffusion flame (liquid phase)

Figure 2.3 - In-cylinder particle sources [21]

Final particulate emissions are determined by the extent of various particle formation and destruction mechanisms. Briefly, soot formation begins with the fragmentation and dehydrogenisation of HC fuel molecules in the flame to soot pre-cursor compounds, notably acetylene (C_2H_2) and polycyclic aromatic hydrocarbons (PAHs). These soot pre-cursors partake in condensation reactions that form soot nuclei, which then increase in size by surface growth and collisions resulting in coagulation. In the process of surface growth, which is responsible for producing most of the soot volume, gas-phase HC species become attached to

the particle surface. Agglomeration involves the collision and coalescence of the approximately spherical primary particles to form larger, irregular particles. Particle destruction occurs by soot oxidation that continues throughout the formation process. The oxidation reactions are kinetically controlled, meaning the oxidation rate is strongly influenced by oxygen concentration and temperature. [23, 24]

2.2.3 Emissions control and aftertreatment

Emission control with combustion strategy and calibration

One of the most widely used techniques to reduce emissions from both diesel and gasoline engines is EGR. This will be discussed in a dedicated section later, but briefly its primary benefit is that is greatly reduces NO_x emissions. EGR only slightly reduces CO and actually increases HC emissions, but these species are more readily removed from the exhaust stream than NO_x. The main purpose of oxidation catalysts employed in gasoline powered vehicles following the introduction of emissions legislation was to remove CO and HCs. However, as the permissible NO_x emissions were continually lowered over time, alternative methods were introduced – most notably the three-way catalyst (TWC). A recent resurgence in the use of EGR has occurred with increasing application to turbocharged GDI engines [26-36].

Manipulation of the combustion process by retarding the ignition timing can also be used to attenuate NO_x [37]. The combustion process develops later in the cycle as the ignition timing is retarded, and so the peak cylinder pressure and temperature are lower. While NO_x can be effectively reduced using this method, engine torque and efficiency are also lower so there is a compromise to be considered. That said, at low engine load, retarding the ignition means the engine must be de-throttled to maintain load, which sometimes can lead to increased fuel efficiency; in this case, the reduction in pumping work is greater than the loss of useful

expansion work. PM emissions are also influenced by ignition timing [38, 39], and are generally lower at late ignition timings due to the longer time for fuel mixing and evaporation.

Split injection can be used to enhance combustion and reduce emissions. The concept uses one early injection event during the induction stroke to create a slightly lean homogeneous mixture, followed by a second injection event later in the cycle resulting in a rich mixture in the region of the spark plug electrode; overall the AFR is stoichiometric. The quantity of fuel injected during the second injection event determines the characteristics of combustion in the inner and outer regions of the cylinder (early and late phases of combustion). The formation of a slightly stratified charge improves ignitability and increases the early burn rate due to the rich AFR near the spark plug. With this, HCs are incrementally reduced due to higher in-cylinder temperature and the remaining homogeneous region of the cylinder charge becomes slightly lean. If the level of stratification is increased too far however, greater numbers of rich regions can increase CO and HC emissions. This technique may therefore be used to improve combustion stability, increase EGR tolerance and reduce HC and CO emissions by increasing the rate of flame kernel formation. [29]

Gaseous emissions aftertreatment

The most significant technology in gasoline engine emission control is the TWC which is capable of eliminating the three primary pollutants in the gasoline exhaust stream (HCs, CO and NO_x). The principle of TWC operation relies on a catalyst to promote a series of reactions in order to bring the exhaust stream towards chemical equilibrium. The catalysts employed are typically Pt-Rh or palladium (Pd) only (although other combinations are successfully implemented) on a porous ceramic support known as the washcoat. The washcoat is primarily porous γ-alumina (Al_2O_3), which provides a high surface area support for the precious metals and is applied to a ceramic or metal monolith that is mounted in the engine exhaust stream.

Further additions (e.g. ceria, zirconia) can enhance or stabilise performance depending on the precious metals present and the required catalyst function. Washcoats are designed to enhance the catalyst activity by creating beneficial metal-support interactions, and providing opportunity to prevent or slow catalyst ageing. The most important and widely used washcoat enhancer is ceria (CeO_2). [24]

Effective TWC operation requires a suitable ratio of reducing and oxidising species and the engine's AFR must be controlled such that combustion stoichiometry fluctuates periodically in a narrow band either side of stoichiometric. When the exhaust composition is rich, and once the small amount of oxygen available has been consumed in oxidation reactions (Equation 2.5 and Equation 2.6), CO and HC removal is achieved by the water-gas shift (WGS) and steam reforming reactions (Equation 2.7 and Equation 2.8). When lean, chemical reduction of NO is achieved in reactions with CO, HCs and hydrogen despite the oxygen rich environment (Equation 2.9 - Equation 2.11). One important function of the catalyst that is vital for successful TWC operation is an oxygen storage capacity, which is usually provided by ceria. As the AFR is cycled close to stoichiometric ($\lambda = 1 \pm 0.02$) oxygen is stored on the catalyst during lean periods and released during rich periods, which allows the necessary oxidising and reducing reactions to occur. It is by this mechanism that simultaneous removal of all the gaseous exhaust pollutants is achieved. [22-24]

CO oxidation: $2CO + O_2 \rightarrow 2CO_2$ Equation 2.5

HC oxidation: $C_xH_y + (x + \frac{y}{4})O_2 \rightarrow xCO_2 + \frac{y}{2}H_2O$ Equation 2.6

WGS reaction: $CO + H_2O \rightleftharpoons CO_2 + H_2$ Equation 2.7

Steam reforming: $C_xH_y + xH_2O \rightarrow xCO + (x + \frac{y}{2})H_2$ Equation 2.8

NO reduction by CO: $2CO + 2NO \rightarrow 2CO_2 + N_2$ Equation 2.9

NO reduction by HCs: $4HC + 10NO \rightarrow 4CO_2 + 2H_2O + 5N_2$ Equation 2.10

NO reduction by H_2: $2NO + 2H_2 \rightarrow N_2 + 2H_2O$ Equation 2.11

Gasoline engines have used the TWC almost exclusively since its introduction, with the main exception being DI engines that operate with a lean/stratified charge at lower engine load regions. In these cases, a TWC is unable to remove NO_x from the oxygen-rich exhaust stream. Technologies usually associated with diesel engines have the ability to chemically remove or store NO_x while under strongly oxidising conditions and so have been developed for the lean gasoline engine application. One example is the NO_x trap that enables NO_x conversion above 90% over a wide temperature range, typically 200-550°C. It functions by storing NO as NO_2 on the catalyst during lean engine operation. Periodic rich combustion is required to regenerate the catalyst. The normal products of rich combustion (HCs, CO and hydrogen) decompose the NO_2 stored on the catalyst to form nitrogen, CO_2 and water. [19]

Particulate emissions control

Traditionally PFI and DI gasoline engines have not required aftertreatment to reduce particulate emissions. Combustion in PFI engines does not produce significant PM, certainly relative to diesel engines. But the GDI engine combustion process can generate high PM emissions under certain conditions, particularly at elevated load, during cold starts and as the engine warms up. Most of the recent developments in PM emission reduction technology have been focused around the combustion system, in particular relating to charge motion and fuel delivery to ensure desirable fuel/air mixing. The injector characteristics are of particular importance. The spray pattern and penetration define the initial location and distribution of fuel in the combustion chamber, before charge motion takes over. The influence of the injector on fuel vapourisation is important. The injector spray characteristics change with fuel

pressure, temperature, nozzle design, pulse duration, fuel properties (viscosity etc) and injector location, amongst other factors, and so this is an area of intensive ongoing research. Any developments aimed at reducing PM formation are in essence trying to achieve one or more of the following:

- Low fuel impingement with combustion chamber walls and components
- Complete fuel vapourisation
- The desired type (swirl/tumble) and potency of charge motion at all engine conditions
- Ensure sufficient charge homogeneity (minimise locally fuel rich regions) or appropriate stratification
- Achieve complete combustion
- Avoid the necessity for fuel rich combustion

Recent GDI engine research has demonstrated PM reductions by taking measures to avoid fuel impingement [40], use of cooled EGR or internal EGR [30], and through calibration of the many available parameters including injection timing, fuel pressure and split injection [21, 40]. Other works have shown injector deposits [41] to severely increase PM formation. Through combustion system design alone GDI engines are able to meet future PM number emissions standards (Euro 6c due in 2017), although fuel penalties range between 0 and 5% [42]. Inevitably, this increasingly challenging scenario has led to interest in catalyst-based gasoline particulate filters (GPFs) as a means for reducing or eliminating combustion generated particulate emissions.

GPF systems combine a particle filter with TWC capability to trap PM and remove gaseous pollutant species. TWC materials are usually applied directly to the filter, and the GPF is often used in a close-coupled arrangement with a standard TWC. There is synergy in using

TWC on the filter in that it aids with filter regeneration [43]. There are various types of GPF (e.g. ceramic wall-flow filters, metallic foams and metallic fibre) and in each there is compromise between trapping/conversion efficiency, backpressure, regeneration frequency, thermal mass, range of operating temperature and cost. Impressive durability has already been demonstrated by GPF technology given its early stage of development with filtration performance of 98% and gaseous emission conversion well within regulation after 150,000km [44].

2.2.4 Current technology for improved engine efficiency

Engine downsizing with pressure charging

A trend has emerged in recent years for engine downsizing, whereby the engine displacement is reduced significantly for a given vehicle road load requirement. This raises the average load on each cylinder and forces the engine to run more frequently in the higher efficiency regions of its operational range. Pressure charging is required in order to maintain the peak load achieved by the larger naturally aspirated (NA) engine. There have been many instances of four-cylinder NA engines being downsized to three-cylinder turbocharged engines [45-47]. One example that has been implemented in production is the Ford 1L turbocharged GDI engine that has successfully replaced a 1.6L NA gasoline engine.

Ensuring adequate drivability (i.e. high torque at low engine speeds) is a challenge when implementing engine downsizing, and places a high demand on the pressure charging system. Currently, single exhaust gas turbochargers are the norm for downsized engines but, as downsizing becomes more aggressive, charging systems will become more advanced to meet the increased demand, particularly in terms of the range of operation (engine speed and mass flow). The application of variable turbine geometry (VTG) technology, as used for some

diesel engines, and dual-stage turbocharging are cited as being viable but complex solutions to improve downsized engine performance [19, 48].

A demonstrator engine has showcased the potential for aggressive downsizing with a 0.85L two cylinder, single turbocharged engine [49]. By investigating several turbochargers and combustion system configurations, they demonstrated equal drivability performance compared with a 1.6L NA engine while achieving a 25% reduction of fuel consumption.

The trend for engine downsizing is set to continue in the near-term. This may be important for future implementation of the exhaust gas fuel reformer because engines that operate with a high duty cycle will have high exhaust temperature for more of the time, potentially making heat recovery technology more viable.

Variable valve actuation

Variable valve actuation techniques are now applied to SI engines with increasing frequency, and offer many possibilities for advanced engine control and calibration. The desired level of exhaust residuals varies significantly across the engine range in any calibration designed to offer the best compromise of efficiency, emissions reduction and peak load performance, which is not possible to achieve with fixed valve timings. Variable cam timing (VCT) can be used to modify the amount of cylinder scavenging by changing the intake valve opening (IVO) and exhaust valve closing (EVC) timing, which together define the valve overlap period.

A long valve overlap at low load gives rise to high exhaust residuals, which reduces NO_x emissions and improves efficiency by reducing pumping losses. Retardation of the overlap period generally reduces the trapped residual fraction slightly, and increases HC oxidation before the exhaust valve opens, thus reducing HC emissions [50]. At high load (boosted)

operation a long overlap promotes over-scavenging and increases the fresh charge mass for high peak load performance.

A shorter valve overlap can reduce the amount of trapped residuals if necessary; this is useful if knock is initiated by the hot residual gas increasing the charge temperature, or if external EGR is to be used. Negative valve overlap can also give rise to high residuals, and is an approach used for engines utilising HCCI [51].

Aggressive early or late intake valve closing timing is sometimes used to reduce the effective CR; these approaches are recognised as variations of the Atkinson thermodynamic cycle, or the Miller cycle when combined with pressure charging. This is an effective method for permitting increased geometric CR while avoiding high load knock in highly charged GDI engines, and results in improved thermal efficiency [52]. Engine load control can also be achieved by utilising VCT with Miller cycle valve timings, which results in reduced pumping losses [53].

It is anticipated that VCT could assist engine operation with a reformer by providing a means for varying the residual exhaust gas fraction (internal EGR), and the ratio of internal EGR to REGR. This should help during the transition between different regions of the engine map when the desired reformer flow rate, as well as the total dilution rate, will change. In addition, VCT could be used when switching between alternative combustion strategies. The optimum cam timings are likely to be very different for engine operation with no external dilution (e.g. when the engine/reformer is warming up) compared to those with REGR, once sufficient temperature is reached and the reformer is switched on.

Another variable valve actuation method is cam profile switching, which can allow high and low valve lift configurations to be used in one calibration or for individual cylinders to be deactivated entirely [54].

More recently, research and development has moved on to fully variable valve lift (VVL) and timing solutions; mechanical, electro-magnetic and electro-hydraulic variations have been developed [54] and put into production by many vehicle manufacturers. For a homogeneous charge GDI engine that would usually require intake throttling for load control, VVL allows the engine to be throttled via the valve actuation; load is controlled by varying the valve lift and duration to regulate the charge air mass flow. This provides a significant benefit for fuel efficiency by dramatically reducing pumping work, as the intake manifold is no longer under significant vacuum and is close to atmospheric pressure. Depending on the specific design characteristics, these systems can also reduce parasitic losses (e.g. by avoiding unnecessary valve spring compression), enable individual cylinder control to correct for AFR disparity, and provide cycle to cycle response for improved transient performance. [55]

Integrated exhaust manifolds (IEMs)

By integrating the exhaust manifold into the cylinder head casting there are practical benefits in the fact that production and assembly are simplified and there is a lower overall parts count [19]. But there are also benefits to engine operation: the IEM may be water-cooled such that exhaust heat is transferred to engine coolant, meaning peak exhaust temperatures are lower and there is lower thermal stress on exhaust system components. This reduces, but does not necessarily remove, the requirement for high load fuel enrichment. In addition, warm up times are reduced due to lower thermal inertia, and turbo response is improved as the pre-turbine volume is reduced. [47]

The increasing application of the IEM poses a challenge for possible future implementation of the exhaust gas fuel reformer because the available exhaust enthalpy is lower, which suggests that the technologies may not be compatible if the exhaust temperature is too low for reforming to be practical. However, it should be considered that, with an IEM, heat is rejected to atmosphere via the engine coolant; in contrast, the exhaust gas fuel reformer aims to recover waste exhaust heat.

2.2.5 Future technology for improved fuel efficiency

There are many and wide-ranging solutions currently in development that aim to improve the efficiency of future internal combustion engines. It is not the intention to summarise these here but a select few will be discussed briefly, noting their relevance to REGR.

Low temperature combustion (LTC)

The detailed operating characteristics of the various LTC modes such as HCCI and PPCI will not be discussed here, however it should be noted that they are a subject of much research globally, within both academia and industry. The key advantage of LTC is the potential to dramatically reduce the formation of NO_x and PM, and achieve complete and efficient combustion. The LTC regime is now being considered by major automotive industry suppliers [48] who are developing a four-cylinder, turbocharged GDI engine with part load HCCI capability. Their project objective is to achieve 25% fuel efficiency over a previous V6 engine, but simulation work predicts an optimistic 42% fuel economy benefit.

Exhaust gas fuel reforming has been recognised to assist HCCI combustion [8]. Very high pressure rise rates associated with HCCI generate significant combustion noise and wider noise, vibration and harshness (NVH) issues; fuel reforming can enable higher dilution rates

than with conventional EGR, which reduces the pressure rise rate and therefore may extend the useable range for HCCI.

Ignition systems

The ignition system strongly influences the initiation and later development of the combustion process. This becomes especially apparent when approaching the limits of charge dilution, and it will be seen later that the ability to maintain reliable combustion at high rates of EGR dilution is particularly relevant to engine operation with a fuel reformer. More recently there has been research investigating alternative ignition systems designed to enhance highly dilute combustion. A continuous discharge ignition system that allows variable discharge duration [56] is able to extend the EGR dilution limit between 5-10%, and significantly improve initial burn rates; increasing the discharge energy of these systems [57] can further extend the dilution capability.

A gasoline fuelled turbulent jet ignition system [58] uses a spark plug to ignite a small amount of gasoline in a pre-chamber. The reacting mixture is then directed into the combustion chamber though a series of radial orifices to initiate the main combustion process simultaneously at multiple sites. This approach has proven successful for enhancing the combustion rate in lean and stoichiometric gasoline engines, and could also assist with stabilising and speeding up combustion with high EGR or REGR dilution. Laser ignition systems are being developed for similar reasons and may be an applicable future ignition system solution. [59, 60]

Heat recovery techniques

Exhaust gas fuel reforming is just one of many technologies that aim to achieve exhaust heat recovery. Technologies of note include: 6-stroke cycle engines; exhaust gas turbine-driven

generators; solid-state thermoelectric generators that exploit the Seebeck effect; and many systems based on the Rankine cycle. A detailed description of these technologies would go beyond the scope of this work, but Saidur [61] provides a concise review of current waste heat recovery technology in the automotive context.

Dedicated-EGR, or D-EGR [62], is one technology that does warrant a more detailed description, firstly due to characteristics it shares with exhaust gas fuel reforming, but also because it is due to enter production in 2018 [42]. Similarly to REGR, D-EGR aims to improve engine efficiency and emissions by operating with EGR enhanced with hydrogen and CO, but the system differs in that there is no catalytic fuel reforming. Hydrogen and CO are instead produced by fuel rich combustion in one cylinder, which exhausts directly to the intake manifold resulting in a constant EGR rate (25% for a four cylinder engine). The system benefits from simplified control and has demonstrated brake thermal efficiency of 42%.

Whilst not strictly a heat recovery device, D-EGR uses the availability of high cylinder temperature to promote reforming reactions, producing reformate that allows highly dilute combustion and reduces the energy content of the exhaust. It might be considered, then, a preventative measure that directly increases thermal efficiency, rather than a corrective measure of recovering energy from an inherently less efficient process. The feasibility of D-EGR suggests that REGR should provide similar benefits for enhancing dilute combustion to improve efficiency and emissions. The potential for exhaust stream energy recovery with REGR is a major difference between these two systems. Additional components, control functionality and calibration effort are required to implement a working system in both cases, but to a greater extent for a fuel reformer system.

An approximate timeline of the major SI engine technologies is depicted in Figure 2.4, highlighting how the use of the various technologies discussed above has overlapped from the past to the present day, and noting the key technologies that may emerge in production engines in the future.

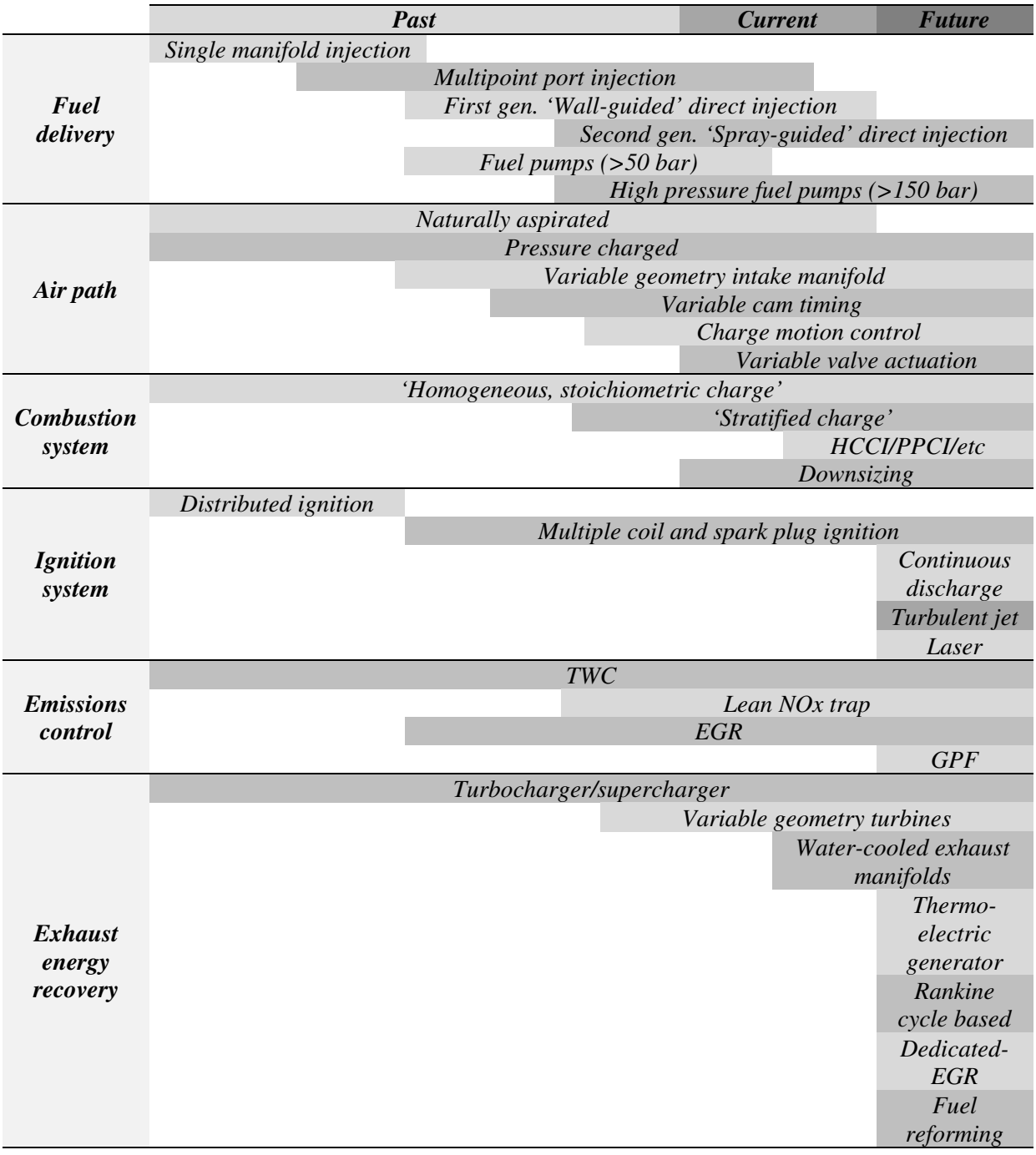

Figure 2.4 - Summary of SI engine technology

This concludes the section relating to current GDI engines and related technology. All future discussion of the GDI engine will be concerned with the homogeneous stoichiometric combustion mode unless otherwise stated.

2.3 Exhaust gas recirculation (EGR)

The following section is dedicated to the use of EGR in gasoline engines given its relevance to exhaust gas fuel reforming and REGR. First the effects of EGR on combustion are discussed, followed by a summary of the mechanisms for improved efficiency and reduced emissions with EGR. Various EGR system configurations are then defined with a discussion of their attributes.

2.3.1 Combustion with EGR

EGR typically has the composition of engine-out exhaust gas, unless the exhaust stream passes through the aftertreatment system before recirculation. In any case, the concentration of the main constituents (nitrogen, CO_2 and steam) varies little. Table 2.2 details the typical range for EGR composition and some thermodynamic properties of the individual species. Each of these compounds dilutes the combustion charge and increases the overall the charge mass (for a given engine load). Because of the higher charge mass the total heat capacity is increased relative to the undiluted charge.

In addition, steam and CO_2 have high specific heat capacity (on a molar basis) so the increase in total heat capacity of the charge is greater than for an equivalent (volumetric) dilution with air. Therefore, for a given quantity of heat released from the combustion process, the cylinder contents will be heated to a lower temperature.

Table 2.2 - Composition and physical properties of EGR [1]

Species	Typical conc. (%)	Specific heat capacity, c_p (kJ/kg.K)	Specific heat capacity, c_p (kJ/kmol.K)	Ratio of specific heats, γ
N_2	76%	1.039	29.1	1.4
CO_2	12-14%	0.846	37.2	1.289
H_2O	12-15%	1.872	33.7	1.327
O_2	<1%	0.918	29.4	1.395
CO	<1%	1.040	29.1	1.4
Air [2] (21% O_2/79% N_2)	-	1.005	29.1	1.4

[1] The EGR composition excludes low concentration pollutants. Data from [63] at 300K

[2] Properties of air included for comparison

The value of the ratio of specific heats, γ, of the charge is changed by dilution with EGR, compared with the normal, undiluted charge; this has implications for the ideal thermodynamic efficiency, seen in Equation 2.12. This value is reduced for the raw charge mixture due to the presence of steam and CO_2 (Table 2.2), but may actually be higher during combustion, relative to that for undiluted combustion, due to lower combustion temperature. This is because the value for γ reduces with increasing temperature.

Ideal thermodynamic efficiency: $$\eta_{,ideal} = 1 - \left(\frac{1}{r_c{}^{\gamma-1}}\right)$$ Equation 2.12

Charge dilution with EGR slows the combustion rate; hence there is a lower rate of heat release. This means that combustion with EGR occurs over a greater portion of the engine cycle, moving away from the ideal case of constant volume heat addition. Additionally, the slower burn leads to higher variability in combustion duration from cycle to cycle, which reduces combustion stability. Using high levels of EGR leads to partial burning and eventually misfires. [23]

The reduction of the heat release rate, and resulting lower pressure rise rate, also lead to lower in-cylinder temperatures compared with undiluted combustion. These effects counter any incremental increase in temperature due to slightly higher peak cylinder pressure (associated with greater charge mass and advanced ignition timing). Further to this, EGR has been shown to reduce the severity of knock in GDI engines [27, 34, 35]. The reduced heat release rate and slower pressurisation of the cylinder means the end-gas is not compressed and heated as significantly, therefore auto-ignition of the end-gas is less likely. The ability of EGR to eliminate or reduce knock tendency may permit increased compression ratio, leading to improved efficiency at all operating conditions.

The fact that EGR reduces combustion temperature is important and will be referred to repeatedly in the explanations of how EGR improves efficiency and affects exhaust emissions in the following sections.

2.3.2 Beneficial effects of EGR on engine efficiency

Improved gasoline engine efficiency with EGR can be attributed to a number of mechanisms. At low load, when the intake manifold is under significant depression due to throttling, pumping losses are a large source of inefficiency for the SI engine. Therefore large efficiency gains can be achieved by methods that reduce the pumping work. For a given throttle opening, the induction of EGR displaces air in the intake manifold. In some cases, EGR also raises the intake air temperature, which exhibits lower density as a result. Both of these effects require de-throttling of the engine to increase the intake manifold pressure and deliver the required fresh charge mass in order to maintain engine load. Hence EGR is able to increase engine efficiency by reducing pumping work.

At high load, further significant fuel savings can be obtained with the use of EGR. The reduced knock tendency with EGR allows the ignition timing to be advanced towards the optimum. This improves the combustion phasing, which increases the work output, hence increasing efficiency. The advanced combustion also reduces the EGT, which can eliminate the requirement for fuel enrichment at high engine speed/load [28], again increasing efficiency. This has been demonstrated in a GDI engine with EGR rates as low as 5% [29].

Whenever EGR is used, the magnitude of the heat loss to the combustion chamber walls is reduced because the combustion temperature is lower with EGR. This results in a lower temperature gradient to the combustion chamber walls, and therefore the rate of heat transfer to the engine coolant and surrounding components is reduced.

2.3.3 Gaseous emissions with EGR

It is well known that EGR reduces NO_x emissions, having had widespread use in SI and CI engines since being introduced in the 1970s. In un-throttled engines EGR lowers the oxygen concentration in the charge and, because there is less oxygen available, the rate of NO_x formation is reduced. Although EGR does reduce the oxygen concentration in the charge slightly for throttled engines, for a given engine load it does not displace oxygen in the same way. The primary reason that EGR reduces NO_x in throttled gasoline engines is that lower combustion and post-combustion temperatures reduce the rate of NO_x formation. [22, 23]

Lower in-cylinder temperature reduces the rate of HC oxidation both during and post-combustion, which results in higher HC emissions. Slightly higher cylinder pressures are experienced with EGR due to increased charge mass, for a given engine condition, which increases the amount of fuel-air mixture forced into crevice volumes to be released during the exhaust stroke. A deterioration of combustion stability will occur as the EGR rate increases,

which will eventually cause the engine to misfire and significantly increase the level of unburned HCs. CO emissions may also be lower with EGR. Lower in-cylinder temperature reduces CO_2 dissociation leading to a higher CO_2/CO ratio, hence lower CO emissions. [22, 29]

In addition, when EGR is used the intake charge temperature is likely to be increased to some degree, even with EGR cooling in place. Higher temperature will improve fuel vapourisation and mixing leading to a more complete combustion process, reducing CO and HC emissions and PM.

2.3.4 PM emissions with EGR

In addition to these benefits to engine efficiency and gaseous emissions, a small amount of research has shown EGR to reduce PM emissions from PFI [64-66] and DI [30] gasoline engines, and so EGR may assist in achieving future PM emission regulations. PM mass reductions of 65% were demonstrated with a GDI engine using cooled, external EGR [30], with a similar trend for internal EGR. Elsewhere though, EGR has been reported to increase particle number emissions from a PFI engine [67]. This is likely to have been a result of increased particle nucleation during sample dilution and caused by the condensation of volatile HC species, which were present in higher concentration with EGR.

2.3.5 EGR system configurations

EGR system configurations are usually defined as either high pressure (HP) or low pressure (LP), and these definitions will be adopted for the application of REGR to the GDI engine. Each approach offers different benefits in terms of EGR cooling and compressor requirements, charge air temperature control, complexity and useable engine range. A LP-EGR system extracts gas from the post-turbine exhaust stream and feeds to the pre-

compressor intake system, i.e. the low pressure regions of the intake and exhaust systems. The EGR cooling may be more easily managed because the EGR gases pass through the charge air cooler, but an additional EGR cooler is still required to maintain acceptable compressor inlet temperature. HP-EGR systems connect the pre-turbine exhaust to the intake manifold (post-compressor), i.e. the high pressure regions. All EGR cooling must be achieved by the EGR cooler and this usually leads to higher charge air temperature relative to LP-EGR. Additional considerations are the build up of PM and other deposits in the EGR system and turbocharger, particularly in diesel engines, as well as the temperature rating of the compressor and related components. A mixed pressure (MP) system combines attributes of the HP and LP configurations and feed exhaust gas from pre-turbine to pre-compressor.

The maximum EGR flow rate in each system is limited by the pressure differential across the manifolds. The HP configuration can only be used when the intake manifold pressure is sub-ambient (or rather, when there is an adequate negative pressure differential from exhaust to intake), so is not suitable for higher loads in a pressure charged engine. At low load, significant intake manifold depression provides a large pressure differential and so high EGR rates are possible. Conversely, the pressure differential across a MP or LP system is much lower for all engine conditions and so the achievable EGR rate may not be as high, but it offers the possibility to use EGR across the entire engine range. The routing of EGR gases through the compressor requires further considerations including: transient engine response; increased compressor work; compressor efficiency, maximum compressor outlet temperature; impact of condensed water droplets; high local compressor blade temperature; and the possible deposition of exhaust gas residue/species. [33]

2.4 Fuel reforming

This section provides some background on typical reformate composition, the chemistry of fuel reforming and the combustion properties of hydrogen and reformate.

2.4.1 Reformate

Reformate is the term given to the mixture of product gases obtained from a reforming process that converts HC fuel into hydrogen and CO, amongst other compounds; depending on the reactant composition, reformate may include nitrogen, methane (CH_4), steam, CO_2 and various other HCs. Synonyms for reformate often encountered in the literature include synthesis gas, syn-gas and hydrogen-rich gas. The specific composition is dependent upon many factors including the type of fuel, the catalyst, process temperature, feed gas composition and the type of reforming mechanism taking place.

Hydrogen content

The combustion characteristics of hydrogen offer a range of benefits for use in automotive engines compared with gasoline, with limited negative effects. When hydrogen is introduced as a constituent of reformate, depending on the concentration, these benefits may be less significant as they are offset by the effects of other combustible and inert gases. Table 2.3 lists some of the important properties of hydrogen, CO and methane compared with gasoline.

With reference to Table 2.3, there are various ways that the properties of hydrogen influence combustion and exhaust emissions when combined in a fuel-air mixture with gasoline. The comparably low minimum ignition energy of hydrogen provides more stable ignition, and high laminar flame velocity speeds up early flame development, reduces combustion variability and may increase indicated efficiency. The higher diffusion coefficient may improve fuel-air mixing, although this is generally determined by turbulent in-cylinder flow.

Table 2.3 – Combustion properties of hydrogen, CO, methane and gasoline (Stoichiometric unless stated) [38, 68-70]

	Hydrogen	**CO**	**Methane**	**Gasoline [1]**	**Syn-gas [2]**
Lower heating value (MJ/kg)	120	10.1	50.4	44	11.9
Energy density (MJ/m^3)	10.3	12.6	34.2	202	9.3
Net energy density of fuel-air mixture (MJ/kmol)	71.5	83.6	84.3	76.3	72.0
Air/fuel ratio	34.1	2.45	17.3	14.7	3.13
Flammability limit, equivalence ratio in air	0.1-7.14	0.34-	0.5-1.42	0.68-3.95	-
Laminar flame velocity (cm/s)	237	40	42	41.4	105
Adiabatic flame temperature (K)	2318	2394	2230	2148	2285
Minimum autoignition temperature (K)	858	882	813	500-744	-
Diffusion coefficient (cm^2/s)	0.61	-	0.05	0.16	-
Quenching distance (cm)	0.06	-	0.2	0.2	-
Minimum ignition energy (MJ)	0.02	-	0.29	0.24	-

[1] Iso-octane (C_8H_{18}), [2] Syn-gas with composition 40:40:20 H_2:CO:N_2

A shorter flame quenching distance should provide a more complete combustion by being able to oxidise HCs closer to the combustion chamber walls, resulting in lower unburned HCs. Wider flammability limits extend the usable range of AFRs, particularly useful for increasing efficiency with lean AFRs. Less positive effects include the reduction of peak engine power because there is a lower energy density of the combustion mixture, and there may be increased NO_x formation if the higher adiabatic flame temperature of hydrogen causes sustained higher combustion temperature. [38]

CO and other constituents

CO is an important component of reformate as it is combustible and its concentration in reformate is often close to that of hydrogen. It has a higher net energy density (for a

stoichiometric mixture with air) than hydrogen, despite its significantly lower calorific value, due to its much lower stoichiometric AFR. This is significant for a gaseous fuel as the combustion mixture is inducted into an engine on a volumetric basis and so, if the air requirement is high, the power potential is reduced (for fixed engine VE). In addition, hydrogen and CO have high octane numbers and "inhibit knock by slowing autoignition chemistry and slightly increasing flame speed" [71], so reformate addition should increase the octane number of the fuel mixture.

Reformate has a significant nitrogen content that provides a diluting effect on combustion similarly to EGR [68]. The source of the nitrogen is either from air supplied for the reforming reactions or from the engine's EGR stream, depending on the reforming mechanism in use. Steam and CO_2 are also present in reformate as products of oxidation in the reformer, or in-cylinder combustion, both of which provide a further diluting effect [16].

HCs may be present in reformate if some fuel breaks though the reactor because the reforming reactions do not reach completion. The HC concentration depends on the thermodynamic equilibrium composition of the reformate and the progression of the reforming reaction towards that equilibrium. Factors that affect fuel conversion include temperature, reactant flow rate (or gas hourly space velocity – GHSV), catalyst formulation and fuel concentration. In a study by Gomes et al. [72] fuel conversion rates varied between 20% and 100% for REGR at a range of temperatures and catalyst mass/fuel flow ratios, showing that higher temperature and catalyst mass tend to increase fuel conversion.

2.4.2 Reforming reactions and thermodynamics

While the context of this discussion is focused on gasoline reforming, it is relevant to reforming of any HC fuel. One significant difference between exhaust gas reforming of

gasoline and diesel is the relatively high oxygen concentration in diesel engine exhaust gas; this means that some diesel fuel must be initially consumed in oxidation reactions, which can be detrimental to the reforming process efficiency. This would also be applicable to gasoline reforming under lean exhaust conditions. For reference, Tsolakis et al. present research investigating reforming of diesel and biodiesel for use in CI engines [6, 73] while Abu-Jrai compares REGR with diesel and GTL fuelling [74] and Rodriguez-Fernandez investigates REGR combined with HC-SCR aftertreatment for diesel engines [5].

The two primary reforming reactions of interest in gasoline reforming are dry reforming and steam reforming (Equation 2.13 and Equation 2.14 in Table 2.4). In all the example equations, C_xH_y is used to represent a general chemical formula for HC fuel. Dry reforming is an endothermic reaction in which fuel reacts with CO_2 to produce hydrogen and CO. Theoretically this reforming reaction exhibits the highest overall process efficiency as it has the highest enthalpy of formation (Table 2.4). The steam reforming reaction is also endothermic and utilises steam to produce hydrogen and CO, and is more active at lower temperature than dry reforming.

If oxygen is present in the exhaust gas then some fuel will be consumed by highly exothermic oxidation reactions. Exhaust gas fuel reforming studies [2, 75] have revealed that the combustion reaction (Equation 2.15) prevails, but there may feasibly be some partial oxidation (Equation 2.16). In some applications such as the partial oxidation reformer, these reactions are used to increase the catalyst temperature and promote the endothermic reactions to improve the hydrogen yield, but at the expense of overall process efficiency.

The slightly exothermic WGS reaction (Equation 2.17) can be useful for increasing the hydrogen concentration by reacting CO, which has already been produced by the other reforming reactions, with excess steam not consumed by steam reforming.

Table 2.4 - General formulae for the key reforming reactions in HC reforming

Reaction	General chemical formula	Enthalpy of reaction, kJ/mol [1]	
Dry reforming:	$C_xH_y + xCO_2 \rightarrow 2xCO + \frac{y}{2}H_2$	Δh_R = (+ 1588)	Equation 2.13
Steam reforming:	$C_xH_y + xH_2O \rightarrow xCO + (x + \frac{y}{2})H_2$	Δh_R = (+ 1259)	Equation 2.14
Combustion:	$C_xH_y + (x + \frac{y}{4})O_2 \rightarrow xCO_2 + \frac{y}{2}H_2O$	Δh_R = (– 5116)	Equation 2.15
Partial oxidation:	$C_xH_y + \frac{x}{2}O_2 \rightarrow xCO + \frac{y}{2}H_2$	Δh_R = (– 676)	Equation 2.16
Water-gas shift:	$CO + H_2O \rightleftharpoons CO_2 + H_2$	Δh_R = (– 283)	Equation 2.17
Methanation:	$CO + 3H_2 \rightleftharpoons CH_4 + H_2O$	Δh_R = (– 206)	Equation 2.18
Methanation:	$CO_2 + 4H_2 \rightleftharpoons CH_4 + 2H_2O$	Δh_R = (– 165)	Equation 2.19

[1] when calculating the enthalpy of reaction it was assumed that: HC fuel is *n*-octane; reactions go to completion; products and reactants are at 25°C and 1 atm; and water is in the gas state
Thermodynamic data from [63]

The WGS reaction is reversible and so the local catalyst temperature defines the reaction equilibrium position. The variation of the WGS reaction equilibrium constant with temperature is illustrated in Figure 2.5, which indicates that the molar fraction of hydrogen at equilibrium reduces with increasing temperature.

Finally, under certain reforming conditions methanation reactions may occur. These are not preferable as, firstly, they are exothermic and, secondly, they consume hydrogen in reactions with CO (Equation 2.18) and CO_2 (Equation 2.19) to produce methane, and so reduce the potential hydrogen yield.

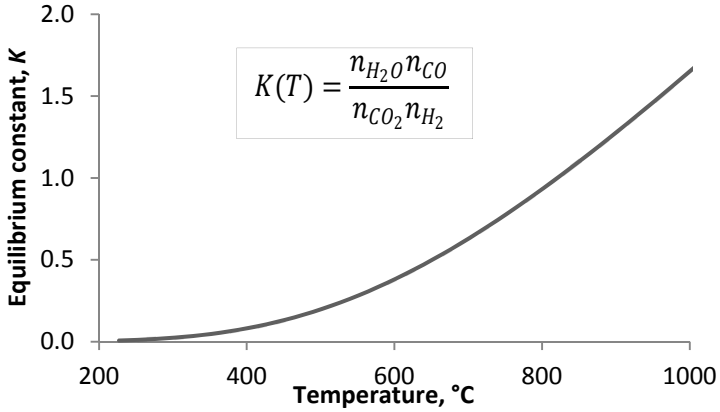

Figure 2.5 - Variation of the WGS reaction equilibrium constant, *K* with temperature

2.4.3 Reforming catalysts

In order to achieve effective exhaust gas reforming at realistic exhaust temperature a precious metal catalyst is required. This work is not concerned with the development of the reforming catalyst, rather the application of existing catalysts to the gasoline engine application. Johnson Matthey developed and supplied the catalysts used in this work. Some catalyst development was performed as part of the wider CREO research project. The catalysts used in the research presented here were Pt-Rh with a ceria-zirconia-alumina (CZA) support, applied to ceramic or metallic substrates. The exact specification will be detailed for each investigation.

Rhodium is possibly the most important precious metal catalyst in this application as it effectively promotes the hydrogen generating steam and dry reforming reactions. Platinum is included to catalyse the exothermic oxidation and reforming reactions, and there is synergy between rhodium and ceria regarding promotion of the steam reforming reaction [75]. Zirconia is a valuable addition to the washcoat as it is known to inhibit methanation reactions in partial oxidation of iso-octane [77], and also works to stabilise the Pt, Rh and ceria [75].

There are various deactivation mechanisms that cause degradation of reformer activity. Sintering is a process of thermal deactivation, instigated by high temperature (typically

>500°C), and is characterised by the accumulation of precious metal into larger particles; this reduces catalytic surface area, hence there is a reduction in activity. The temperature at which this process begins, and to what extent it occurs, varies with catalyst formulation. Fouling also results in lower catalyst surface area, but is caused by carbonaceous material (coke) or fuel additives physically blocking active sites and filling catalyst pores. The effect of coking can often be reversed by regeneration at high temperature under oxidising conditions, however sintering is a permanent effect. [78]

Sulphur is well known to deactivate precious metal catalysts; even the low concentration of sulphur in gasoline may cause degradation of reformer performance. The precious metal catalyst and support compositions will influence the degree of deactivation. In one ethanol reforming study [75], Rh-only catalysts were more resistant to sulphur poisoning than Pt-Rh catalysts, as well as being easier to regenerate, particularly when combined with a silica-enriched alumina support. Continued catalyst development will be important to ensure the best combination of reformer performance and long-term stability, but is beyond the scope of the research documented in this thesis.

2.4.4 Reformer catalyst development

The performance of early reforming catalysts at typical exhaust temperatures was relatively poor. In 1996, Jamal et al. [16] reported the performance of a prototype exhaust gas fuel reformer operating at moderate reactor temperatures (600-650°C). Figure 2.6 shows the comparison between predicted and experimental reformate compositions from the prototype reformer, with significantly lower concentrations of hydrogen and CO obtained compared to the equilibrium composition. The low yields were attributed to a relatively inactive catalyst resulting in poor fuel conversion rates.

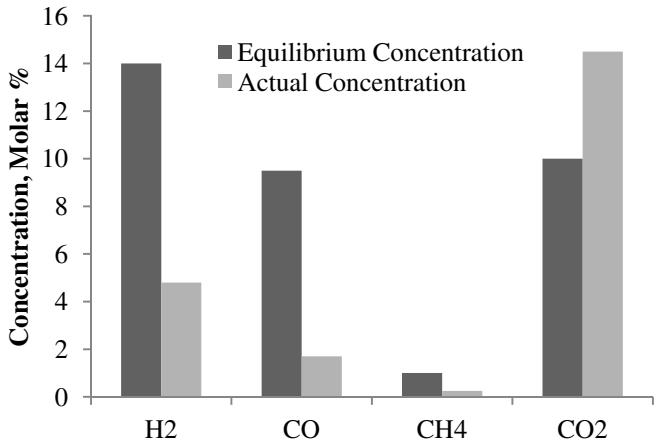

Figure 2.6 - Comparison of predicted equilibrium and actual compositions of reformate at oxidant temperature of 650°C and excess oxidant factor of 2.5 [16]

More recent experimental research conducted on a catalyst developed specifically for exhaust gas fuel reforming [79] has achieved hydrogen yields of 14% at 580°C, agreeing with results from a thermodynamic equilibrium model based on the minimisation of the Gibbs free energy (Figure 2.7). The catalyst was found to inhibit methanation reactions, resulting in higher than expected hydrogen yield for a given fuel conversion rate as predicted thermodynamically. Figure 2.7 shows the correlation in hydrogen production and significantly lower methane formation. Conversion rates of iso-octane were between 58-70% and the gas phase composition was close to that for thermodynamic equilibrium.

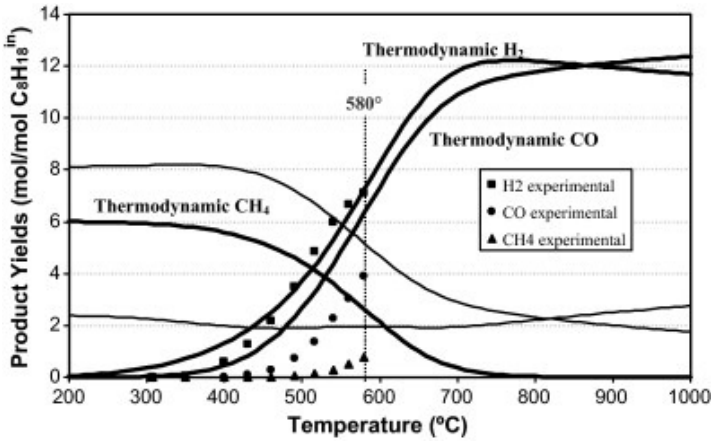

Figure 2.7 - Thermodynamic and experimental product distribution as a function of temperature for REGR conditions [79]

The extent to which temperature influences reformate composition is obvious from Figure 2.7. Of particular note is the large variation in hydrogen and CO concentration across the temperature range typical of the gasoline engine exhaust, between 400-800°C. This means that it is important to ensure efficient heat transfer from the exhaust stream to increase the temperature of the reactor bed, and that an effective catalyst is available to bring the reformate composition close to thermodynamic equilibrium.

The thermodynamic model also predicts a trend that results in lower hydrogen yield for increasing pressure, a 10% drop when raising pressure from 1.0 to 1.3bar. This result suggests that positioning of the reformer late in the exhaust system would be preferable, assuming that a significant pressure drop occurs due to the restriction imposed by the exhaust components and catalysts. However, the decreasing gas temperature along the exhaust is likely to be of greater detriment to reformer performance.

2.4.5 Automotive applications for fuel reforming

Autothermal reforming

Fuel reforming of HC fuels has uses in many industrial applications, and has been widely researched as a method for producing hydrogen onboard a vehicle in order to supply a fuel cell as part of an electrified powertrain. In a process known as autothermal reforming, the steam reforming and partial oxidation reforming reactions are combined, which requires strict control of the oxygen/ carbon ratio and steam/ carbon ratio to ensure the correct reaction pathways and hydrogen selectivity [80]. In this case, occurrence of the WGS reaction is useful for limiting the CO production, but a separate clean up catalyst is required to remove the remaining CO from the reformate and achieve a sufficiently pure hydrogen supply (< 20ppm CO) as required by the fuel cell [81]. While having not achieved commercial success for the

fuel cell application, much of the catalytic technology developed for these fuel reformers is applicable to exhaust gas fuel reforming.

Partial oxidation reformer

Based on the reaction in Equation 2.16, the partial oxidation reformer converts a rich fuel-air mixture into a hydrogen-rich gaseous fuel. There are various types of partial oxidation reformer including catalytic [82], electrically heated [83] and plasma-boosted reformers [84]. Each type is capable of rapidly increasing the reactor temperature that enables fast start up, allowing the engine to be started operating solely on reformate. None of these systems aim to achieve exhaust heat recovery.

Because the exothermic partial oxidation reaction involves the conversion of chemical energy from fuel into heat energy the efficiency of the reforming process is always less than one, in terms of gaseous fuel energy out compared to liquid fuel energy in. But due to the resulting high temperature, hydrogen yields will be higher. Partial oxidation reformers therefore rely upon the increase in engine thermal efficiency that may come as a result of reformate combustion to compensate for the energy lost in reforming. In depth analysis of system efficiency is required in order to justify the technology.

Exhaust gas fuel reformer

Uniquely to the exhaust gas fuel reformer, the engine exhaust stream is used as a heat source to drive the endothermic reforming reactions, in contrast to the autothermal and partial oxidation reformers. The aim of exhaust gas fuel reforming is to ensure that the reforming process efficiency becomes greater than one; this means increasing the enthalpy of the gaseous product fuel above that of the input gasoline by capturing waste thermal energy from the engine exhaust stream. Further efficiency gains from in-cylinder combustion of reformate

produces a compound effect, increasing the overall engine-reformer system efficiency. The potential of the system is clearly limited by the available exhaust temperature, or rather by the transfer of sufficient heat from the exhaust stream to the reformer catalyst.

At low exhaust temperature, i.e. at low engine load, some air could be introduced to induce the exothermic oxidation reactions and raise the temperature of the reformer [85], but the overall process efficiency would be reduced depending on the oxygen/fuel ratio. Thermodynamic equations that represent the exhaust gas fuel reforming reactions suggest that the fuel enthalpy can be raised by the overall endothermic process from 41.8 MJ/kg for gasoline to 55.2 MJ/kg for the reformate [16].

2.5 Combustion of hydrogen and reformate in gasoline engines

A significant amount of research has been conducted worldwide into the combustion of hydrogen in internal combustion engines, ranging from pure hydrogen combustion to the addition of a small fraction of hydrogen to the primary fuel. To a lesser extent, similar research exists for hydrogen-rich gases such as reformate. This section discusses a selection of the most relevant research.

2.5.1 Fractional hydrogen addition to gasoline engines

Combustion performance and engine efficiency

For a GDI engine operating with an undiluted, homogeneous charge it has been shown that hydrogen addition retards the ignition timing for maximum torque [38]. This can be attributed to the faster burn rate of hydrogen, which increases the rate of flame propagation and shortens the overall combustion process. If the ignition timing remains unchanged, hydrogen causes a more rapid pressure rise during the compression stroke, thus increasing the pumping work, which in turn reduces efficiency. The effect was found to be less significant for rich mixtures

as they are inherently faster burning. Hydrogen addition also improves combustion stability, again being more significant for stoichiometric than rich combustion.

Alger et al. [86] report the effect of small amounts (up to 1% vol) of hydrogen on the EGR tolerance of an SI engine. It was shown that while operating with EGR at the combustion stability limit, defined by a coefficient of variation of indicated mean effective pressure (COV of IMEP) > 5%, only a very small fraction of hydrogen was required to stabilise the engine, just 0.2% in most cases. In another set of tests, 1% hydrogen addition extended the EGR tolerance at all engine conditions tested, providing benefits to engine efficiency and emissions.

Tests by Al-Baghdadi and Al-Janabi [87] demonstrated the effect of hydrogen addition on engine performance potential, showing that peak power is increased for up to 2% hydrogen addition (fuel mass ratio) due to the high burn rate of hydrogen shortening the combustion process. Above 2% hydrogen addition engine power output is reduced due to decreased VE and mixture density.

Recent research [88-95] has focused on the effects of hydrogen addition to lean and low load conditions, finding that hydrogen increases thermal efficiency, reduces the variation of peak in-cylinder pressure, and increases and advances the peak in-cylinder temperature and pressure. In one study, the lean dilution limit was extended with only 3% hydrogen addition [89], however research elsewhere stated “the lean operating limit is extended only when the hydrogen percentage in the fuel is higher than 40 per cent by volume” [96]. The extension of the dilution limit is obviously heavily case dependent, influenced by engine design, combustion system components such as the ignition system, and also what is defined as the dilution limit. D’Andrea et al. [97] added hydrogen to a range of lean conditions, reporting

increased IMEP and combustion rates for equivalence ratios less than 0.85; for equivalence ratios above 0.85, approaching stoichiometric conditions, there was little difference in engine performance reported. Hydrogen also reduces cyclic variations for lean combustion [93, 97, 98].

There has also been research into the use of hydrogen with stratified-charge GDI engines. The presence of hydrogen in a stratified gasoline-air mixture widens the flammability window, mainly on the rich side, and therefore offers a wider range of usable ignition timings [37]. There has been little effect on thermal efficiency found when comparing homogeneous and stratified charging methods for lean iso-octane combustion with hydrogen addition [95]. Experiments by Conte and Boulouchos [37] show that hydrogen in a stratified charge consistently increases the combustion rate, and hence the heat release rate, particularly for the first stage of combustion.

Engine emissions

Hydrogen addition to lean gasoline combustion in the GDI engine reduces engine-out HCs and increases CO for a given AFR [88]. However, when compared to stoichiometric combustion of gasoline both HC and CO emissions are reduced by hydrogen enriched lean combustion [96, 98]. For a given AFR, as hydrogen is added to the charge, faster and more complete combustion occurs, hence unburned HCs are reduced. HC emissions are also reduced for increasingly lean mixtures (up to a point, until combustion becomes unstable and HCs increase) because the higher oxygen concentration enhances the oxidation of HCs during and post-combustion. The fact that hydrogen can extend the lean limit enhances this effect.

CO emissions are reduced by ensuring a more complete combustion process; therefore hydrogen can reduce CO emissions directly by ensuring a more rapid and complete burn, and

indirectly by allowing increasingly lean AFRs (again increasing the combustion efficiency). The effect of hydrogen (and hydrogen in combination with diluted combustion) on combustion temperature also influences CO emissions. A reduction in temperature reduces the level of CO_2 dissociation, reducing CO emissions [22].

NO_x emissions are frequently reported to increase with hydrogen addition [88, 98], but Tahtouh [96] states that NO_x is mostly affected by equivalence ratio and dilution. Because hydrogen addition increases the combustion rate, which raises the in-cylinder temperature and pressure, NO_x formation increases; however, charge dilution cools combustion. These competing effects may explain the disparity in the literature of the effect of hydrogen on CO and NO_x emissions. At low engine load, hydrogen addition enables the use of significantly higher EGR rates [37, 86], for instance the EGR limit can be increased to 50% from 25% for undiluted gasoline combustion [86]. Whilst hydrogen addition alone causes an increase in NO_x emissions, when coupled with EGR a large NO_x reduction can in fact be achieved.

The use of a stratified-charge also influences NO_x emissions, which tend to be lower for combustion of a hydrogen-enriched charge with stratified gasoline injection compared to combustion of a homogeneous gasoline-hydrogen charge [95]. Further to this, Conte and Boulouchos [37] report that it is possible to use retarded ignition timing, due to the faster combustion rate of hydrogen, which leads to a slight NO_x reduction despite the higher adiabatic flame temperature of hydrogen. The significant stability improvement for late ignition timings also results in lower HCs. Figure 2.8 shows the general trend for increased efficiency and reduced NO_x with increasing hydrogen concentration and EGR percentage. The data, captured from a stratified charge GDI engine at 3bar IMEP, show that NO_x emissions are reduced while indicated efficiency increases by combining hydrogen addition with high EGR rates [37].

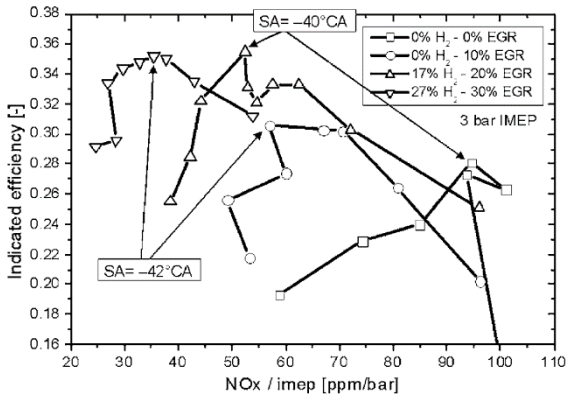

Figure 2.8 - Trade-off between indicated efficiency and NO_x in a stratified-charge GDI engine for some combinations of hydrogen addition and EGR [37]

Hydrogen enhancement has been shown to reduce PM formation in GDI engines [38, 99]; 6% hydrogen addition (energy fraction) to a stoichiometric gasoline-air mixture can reduce PM number and mass by up to 90% [38]. Similarly, EGR can reduce PM emissions from gasoline engines [30, 64-66]. Therefore it may be possible that the use of REGR (containing hydrogen) will result in greater PM reductions than can be achieved by conventional EGR alone.

The most notable effects of partial hydrogen addition to the gasoline engine on combustion performance and emissions are summarised in Table 2.5. Within the sources cited there have been an extensive range of tests performed at a variety of engine conditions. The general trends drawn from these results are identified by arrows signifying an increase or decrease in the stated parameter. Where there are two conflicting arrows shown, this identifies a case where other engine conditions may affect the same parameter so that hydrogen addition is not the primary influence; for example, NO_x emissions are generally increased when hydrogen is added to the normal gasoline-air combustion mixture due to increased in cylinder temperature and pressure, however if charge dilution is introduced through EGR or excess air then NO_x emissions will be reduced relative to stoichiometric gasoline combustion at comparable engine load.

Table 2.5 - Effects of partial hydrogen addition on engine performance compared to stoichiometric gasoline operation

Performance Parameter	Change	Performance Parameter	Change
Combustion rate	↑	Thermal efficiency	↑
Combustion stability	↑	System efficiency	↑↓
Combustion duration	↓	EGR tolerance	↑
Ignition timing advance	↓	HC and CO emissions	↓
In-cylinder pressure	↑	NO_x emissions	↑↓
Knock tendency	↓	PM emissions	↓

These studies demonstrate the potential that hydrogen offers for enhancing gasoline combustion. The problem is, as ever, in ensuring adequate supply of hydrogen for a multi-cylinder engine operating within a vehicle, outside the confines of the laboratory. This is where fuel reforming shows potential for onboard generation of hydrogen. The next section will explore the research that has used simulated reformate (hydrogen, CO and nitrogen) rather than hydrogen in isolation.

2.5.2 Reformate combustion in gasoline engines

This section discusses data in the literature from experiments that have attempted to replicate engine operation with a fuel reformer. This is usually achieved by inducting gaseous hydrogen and CO in various compositions, in so called ‘simulated reformate combustion’ studies. In this context ‘simulated’ implies that reformate is supplied from a compressed gas cylinder, where the composition has been chosen to represent that expected from a particular reforming process.

For clarity and quick comparison, the various reformate compositions used in the work cited in the following section are summarised in Table 2.6. Note that the hydrogen and CO concentrations are high, always above 20%. This is representative of either a very high

temperature reforming process, or predictions based on idealised, thermodynamic equilibrium composition at the expected process temperature.

Table 2.6 - Summary of simulated reformate compositions

Representative reforming process	Reformate component			Citation
	Hydrogen	CO	Nitrogen	
Partial oxidation	21%	24%	55%	[68, 69, 100] [1]
Partial oxidation	25%	26%	49%	[101]
Partial oxidation (Plasmatron)	23%	25%	52%	[71]
Partial oxidation (Plasmatron)	25%	26%	49%	[102]

[1] The authors of these works cite early research into gasoline partial oxidation reforming by Houseman [103] as the basis for their reformate composition selection

Influence of reformate on engine efficiency

Much of the research cited relates to partial oxidation reformers [68, 69, 100, 101]. Delphi Automotive [68] investigated combustion near the dilute limit using gasoline supplemented with 0%, 15%, 30%, 50% and 100% reformate (percentage of total fuel energy as reformate). They found that reformate extends the dilution limit and allows for significantly higher charge dilution rates to be used; the lean limit equivalence ratio was lowered by 44% as the reformate energy fraction increased from 0% to 100%, while the EGR tolerance increased by 115%.

Lean combustion of reformate tends to be more efficient than stoichiometric combustion of reformate with EGR when compared at the dilution limit [68, 69, 101]. As an example of the typical engine efficiency benefits published, stoichiometric combustion with maximum EGR and 20% reformate (energy fraction) yields a 6% efficiency improvement, while 39% reformate improves efficiency by 13%. In comparison, combustion at the lean limit produces 15% and 20% efficiency gains respectively [69].

The improvements in engine efficiency when using reformate combined with charge dilution can generally be attributed to: the reduction of pumping losses with high levels of dilution; improved combustion phasing initiated by the presence of hydrogen and CO; and the higher overall ratio of specific heats of the combustion mixture due to the high nitrogen concentration of the reformate. The presence of steam and CO_2 in EGR does in fact lower the value of the ratio of specific heats of the combustion mixture. It has been suggested by some [68] that this effect counters the efficiency gain due to reduced pumping losses, meaning that in some cases engine efficiency for reformate combustion with EGR is close to that of stoichiometric gasoline combustion. The extent to which this is true is likely to be dependent on load and the fraction of work lost to pumping.

Increasing the reformate fraction for a given dilution rate can result in lower engine efficiency, which may be attributed to a higher rate of heat loss to the cylinder walls due to increased combustion temperatures; this has been shown to occur for hydrogen enrichment [104] and leads to reduced efficiency. This increase in heat loss will not be as large when there is a lower reformate quality, i.e. lower hydrogen concentration and greater inert fraction.

Allgeier at al. [100] investigated engine operation with 100% reformate compared to pure gasoline and found that engine efficiency increased by up to 50% at low speed and load. This was attributed to: improved engine stability at high EGR rates; reduced pumping work by raising the intake manifold pressure with high volumetric flow rates (air + reformate + EGR); and high levels of EGR resulting in low combustion temperatures and therefore lower heat losses. The efficiency improvements became less significant with increasing speed and load. The maximum engine load achievable when using 100% reformate was reduced by around 40%, because a reformate-air charge has lower energy density that a gasoline-air charge. This is a result of using a gaseous fuel, that also includes inert gases in this case, which occupies a

portion of the cylinder volume and limits the oxygen available for combustion. Even so, the engine efficiency improved due to improved combustion efficiency and lower heat losses. Elsewhere, the use of 100% reformate required supercharging to restore the full load engine performance [68].

Influence of reformate on combustion

As has already been discussed, hydrogen addition speeds up gasoline combustion. In one study, when the combustion process was analysed in three phases (ignition to 5% mass fraction burned (MFB), 5-50% MFB and 50-90% MFB) it was found that all phases were shortened by reformate addition [69], with the first phase reduced most significantly; Figure 2.9 shows the trend for increasing combustion speed with reformate energy fraction. The presence of fast burning hydrogen obviously has the effect of reducing the main combustion phase durations, but it seems that it is most effective for enhancing the early flame development. This is because there is a reduced ignition energy as well as a higher laminar flame speed; early flame growth is mostly laminar, and the later stages of combustion are dominated by turbulent combustion.

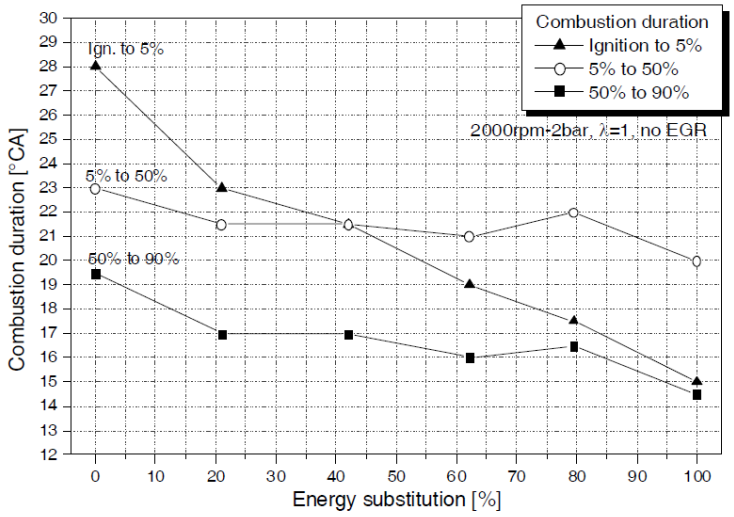

Figure 2.9 - Effect of reformate energy fraction on combustion duration (λ=1, no EGR) [69]

Unacceptable combustion stability is usually the limiting factor for increasing EGR percentage; however, as Figure 2.10 shows, the tolerance to EGR can be increased significantly by adding reformate to gasoline combustion while maintaining an acceptable COV of IMEP. It should be noted that the 3% [68] and 10% COV of IMEP [69] curves are derived from research on different engines, but using the same reformate composition.

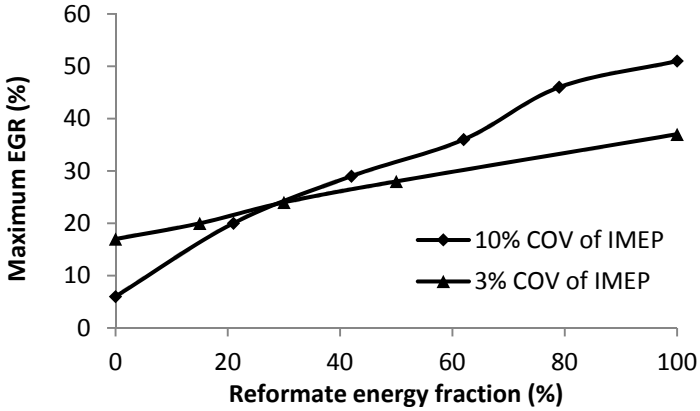

Figure 2.10 - Effect of reformate energy fraction on EGR tolerance [68, 69]

Experimental results [71] have shown that the research octane number of a fuel mixture to be increased by 10 when 15% of the liquid fuel is replaced by hydrogen and CO which, according to other research [105, 106], would allow for a CR increase of 2. Raising the CR from 10 to 14 can reduce specific fuel consumption by 10% [19]. Reformate addition, as well as hydrogen and CO addition independently, all show similar trends in reducing the tendency to knock [71].

Engine emissions

NO_x emissions can be reduced by over an order of magnitude as reformate is increased from 0% to 100% for lean and EGR dilution [68]. Significant NO_x reduction can also be achieved with relatively low reformate addition when operating with EGR, as shown in Figure 2.11. The NO_x emissions data are normalised to those for gasoline combustion with maximum EGR.

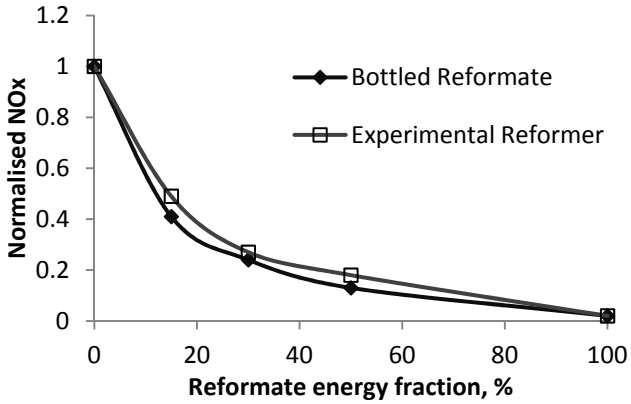

Figure 2.11 - NO_x emissions for EGR diluted gasoline combustion with reformate addition (normalised to gasoline combustion with maximum EGR) [68]

Interestingly, Figure 2.12 shows that NO_x emissions are all but eliminated (15ppm) for 37% reformate addition when operating at the lean limit [69]. This may suggest that under certain conditions an engine utilising a TWC could operate with a lean AFR because the highly oxidising nature of the lean exhaust stream wouldn't necessarily render the TWC inoperable, assuming engine-out NO_x was sufficiently low. CO and HC emissions would be easily oxidised in the 'TWC'. However, it would be a significant challenge to ensure this approach worked effectively under all possible conditions, especially during transient engine operation.

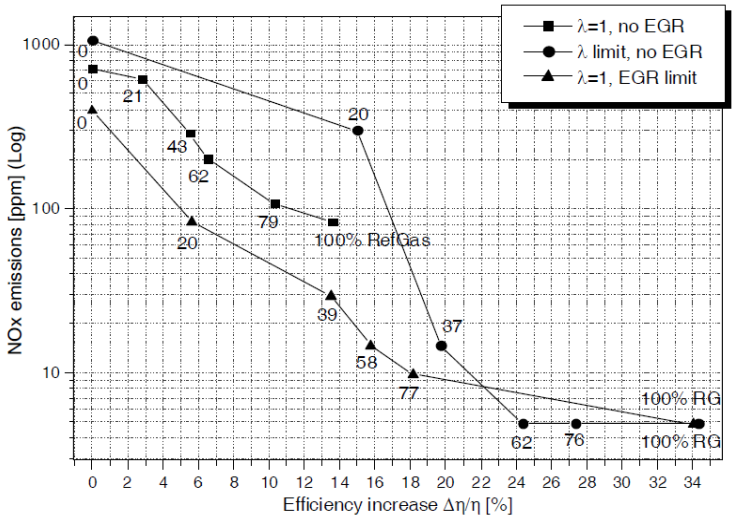

Figure 2.12 - Efficiency gain plotted against NO_x emissions for three combustion mixture strategies with reformate addition [69]
Data marker labels indicate reformate energy fraction

Both EGR and air dilution strategies have proven to be capable of reducing NO_x by 98%, enabled by the extended dilution limit with reformate enhancement. However, these results also revealed an almost linear system efficiency-NO_x trade off [101].

Some research has presented simultaneously reduced CO, NO_x and HC emissions [14] when using reformate. Others have presented slightly increased CO and relatively unchanged HC emissions [68]. In this work, HC emissions were relatively unchanged compared to undiluted gasoline combustion when using fractional reformate addition at the dilution limit, although were slightly lower with EGR than air dilution. HC emissions were effectively zero for 100% reformate use. These emissions parameters are strongly influenced by AFR, the fraction of HC fuel used, the level of charge dilution and the combustion stability; therefore, CO and HC emissions results when using reformate are very case dependant.

In 100% reformate combustion tests [100] the significantly higher EGR limit (increased to 46% from 12% for pure gasoline) effectively eliminated NO_x emissions. HC emissions were also reduced to near zero as there was no HC fuel supplied for combustion, although this may not be applicable to real reformer operation where HCs can be expected to break though the reformer to some degree.

Use of lower reformate fractions also leads to large reductions of engine-out aromatic hydrocarbons (benzene, toluene, etc), of the order of 60% to 70% [107]. This is partly because the quantity of HC fuel contained in the raw combustion charge is reduced when replaced by reformate, so there is proportionally less HC left unburned. It is also due to reformate enabling a more complete combustion process similarly to hydrogen addition. The higher flame temperature should assist with oxidation of the more stable aromatic HCs.

There was no information found in the literature as to the influence of reformate combustion on PM emissions.

System efficiency

The results for improved engine efficiency, combustion performance and emissions with reformate addition show similar trends as those summarised for hydrogen addition. In some of the reformate addition works cited, the total system performance was considered; this takes into account the reforming process, which is especially important if there is a net energy loss when reforming HC fuel to reformate.

The reported system efficiencies for simulated partial oxidation reforming vary. In one case, when reformate was added to the combustion mixture the estimated system efficiency was consistently lower compared to the baseline indolene fuelling, caused by the associated losses in the partial oxidation reforming process [101]. However, for other tests using similar reformate composition the authors state that, when operating with 100% reformate and high EGR, the increased engine efficiency was enough to compensate for losses associated with producing reformate with a partial oxidation reformer [100].

2.5.3 Engine integrated prototype reformers

This section discusses results in the literature where a prototype fuel reformer has been operated in parallel with a gasoline SI engine and reformate has been supplied to the engine for partial or complete fuelling. These prototypes are summarised in Table 2.7.

Partial reformate fuelling

Jamal et al. [16] report single-cylinder experiments using reformate derived from a prototype exhaust gas fuel reformer operating at moderate temperatures (600 – 650°C). The results showed slightly improved overall efficiency, extended lean burn operation for most ignition

timings, lower NO_x and HC emissions and lower cycle-to-cycle in-cylinder pressure variation. These effects were observed despite relatively low hydrogen concentration (2-5%) in the reformed gas, with reformate energy fractions in the region of 1% tested.

The paper by Quader et al. [68] includes tests using an engine fuelled with gasoline and a fraction of reformate from a partial oxidation reformer, with the tests replicating those performed with bottled reformate for diluted combustion (EGR and lean limit). NO_x emissions were practically identical for both sources of reformate, shown earlier in Figure 2.11. HC emissions were higher, assigned to the reformer breakthrough of HC compounds. The total system (engine + reformer) efficiency was lower due to energy lost in the exothermic partial oxidation reforming process.

An alternative plasma boosted or "Plasmatron" reformer [84, 102] has been developed based on the partial oxidation reaction. The system is electrically powered and uses resistive heating to the raise the temperature and produce reformate without the requirement for a catalyst. The reformer was integrated with a four-cylinder gasoline engine and was able to improve combustion stability at lean operation, improve engine efficiency and reduce NO_x emissions due to extended dilution. System efficiency was reduced due to the electrical power used in the reforming process.

A combined TWC and fuel reformer [15] used a traditional TWC surrounded by an annular reforming catalyst, designed to test the hypothesis that waste heat from the TWC would raise the temperature of the reformer to improve performance. The reformate produced contained a maximum of 10-11% hydrogen across the various operating points tested, both with and without the TWC core fitted, suggesting little effect on maximum yield; the maximum yields occurred when the fuel flow rate to the reformer was highest.

100% reformate fuelling

Delphi Automotive Systems developed a fast start up gasoline reformer to reduce NO_x and HCs during engine start up [82]. By rapidly and directly heating the reformer catalyst using combustion of gasoline the engine could be started from cold, being fuelled with 100% reformate. The reformer heating period was tested at 2, 5 and 10 seconds prior to firing the engine. The early combustion stability was analysed and compared to that for gasoline. Starting the engine after 10s reformer pre-heat clearly showed immediate firing and superior combustion stability, although a 5s pre-heat gave comparable performance to gasoline. The 2s pre-heat results showed misfires and unstable combustion. The resulting HC emissions were reduced by up to 75% over those for pure gasoline during early engine running for the 5s and 10s pre-heat times. Cumulative HC emissions increased for the 2s pre-heat time due to misfires and incomplete combustion. HC emissions during the pre-heating period (gasoline combustion over the catalyst) showed high test-to-test variability.

An electrically heated partial oxidation reformer was also designed to fuel a SI engine with 100% reformate during cold-start to improve combustion performance and emissions [83]. Rapid electrical-heating allowed the reformer to fuel the engine during cold starts at ambient temperatures as low as -20°C, reducing HC and CO emissions by 80% and 40% respectively.

Exhaust gas ethanol reformers designed to achieve heat recovery from ethanol-fuelled [13] and gasoline-fuelled [12] SI engines have been developed more recently. Ethanol can be reformed more easily than the longer chain and more complex (e.g. aromatic) HC components of gasoline and so it is possible at lower temperature, typically between 300-350 °C [13] with a copper-nickel catalyst. This makes ethanol reforming feasible over most of the operating range of a SI engine. While this makes ethanol reforming a potentially attractive technology

for reducing fuel consumption and emissions, its application would be limited to countries where ethanol or E85 is widely available.

Table 2.7 - Summary of prototype reformers in the literature

Operating principle	Fuel	Prototype stage	Catalyst	Reference
Partial oxidation	Gasoline	Engine integrated (single-cylinder)	Proprietary catalyst	[68, 82]
Electrically heated partial oxidation	Gasoline	Engine integrated (multi-cylinder)	Non-catalytic (Ceramic 'hot-surface igniter')	[83]
Plasma-boosted (resistive heating) partial oxidation	Gasoline	Engine integrated (multi-cylinder)	No catalyst required	[84]
Exhaust heated (TWC integration)	Gasoline	Engine integrated (multi-cylinder)	Proprietary precious metal catalyst	[15]
Exhaust heated, exhaust gas reforming	Ethanol	Engine integrated (multi-cylinder)	Cu/Pd/C and Cu/Ni	[11, 13]
Exhaust heated, exhaust gas reforming	Ethanol	Engine integrated (multi-cylinder)	Copper	[12]
Exhaust heated, exhaust gas reforming	Gasoline	Engine integrated (single-cylinder), externally heated,	Not specified	[16]
Exhaust heated, steam reforming	n-heptane	Standalone, externally heated	Not specified	[108]
Exhaust heated, exhaust gas reforming	Iso-octane	Standalone, externally heated	1% Rh on Zirconia	[79]

2.6 Predicted mechanisms for improved engine efficiency with REGR

There are multiple, additive factors that should work to improve engine efficiency with REGR across the engine range. The most influential factors are summarised pictorially in Figure

2.13, highlighting where in the engine range they are most significant. There is less clarity as to where in the engine range heat recovery will be achievable; therefore the area highlighted in Figure 2.13 is more suggestive than definitive. A more detailed summary of each of the mechanisms follows.

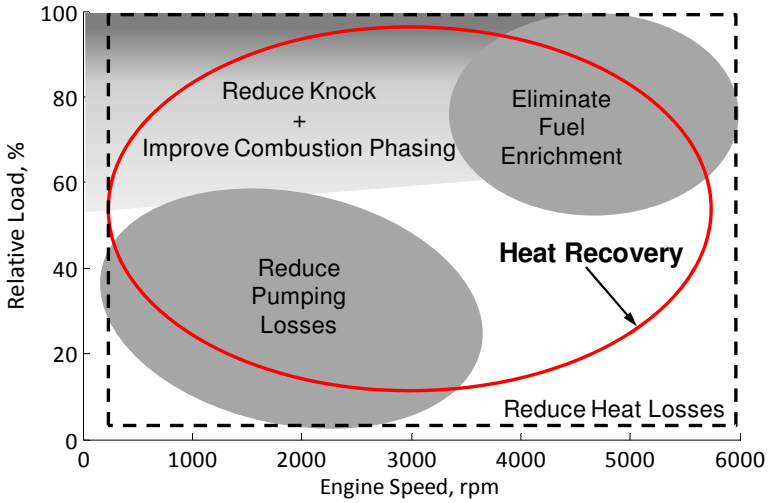

Figure 2.13 - Mechanisms for improving fuel efficiency with REGR across the engine range

Engine efficiency may be improved by REGR for the following reasons:

1. Reduced pumping losses at low-mid engine loads due to higher intake manifold pressure (there is potential for reducing the pumping work whenever the intake manifold pressure under partial vacuum without REGR)
2. Increased ideal thermodynamic efficiency due to the higher value of the ratio of specific heats, γ, of the charge due to lower temperature during combustion
3. Lower heat losses: lower rate of heat transfer to the combustion chamber walls and less energy contained in the exhaust stream due to lower combustion temperatures
4. Improved combustion phasing due to the elimination or delayed onset of knock
5. Reduced or eliminated requirement for fuel enrichment at high engine speed and load due to lower exhaust temperatures

6. Potential for increasing the compression ratio, which leads to improved efficiency across the speed/load range
7. Reduced NO_x emissions meaning there is no requirement for ignition retardation, which is sometimes used to reduce NO_x but also reduces efficiency
8. Hydrogen from reforming increases combustion stability
9. Hydrogen from reforming increases combustion efficiency
10. Heat energy is recovered from the exhaust gas stream and used to drive endothermic reforming reactions, converting gasoline into, primarily, hydrogen and CO. This process increases the chemical energy of the fuel injected into the reformer, which is later inducted into the cylinder for combustion

Points 1-7 can also be said for conventional EGR; however, REGR is expected to enhance the contribution from each factor. For many operating conditions, the maximum EGR rate is limited by the deterioration of combustion stability. The literature review has highlighted results that show hydrogen can enable higher dilution rates to be used in gasoline engines and so REGR should offer the potential to equal or excel the engine efficiency benefits of EGR, in addition to achieving heat recovery from the exhaust stream.

Much of the work cited has involved engine operation fuelled by gasoline supplemented with high quality reformate and using excess air dilution. Some sources have investigated reformate or hydrogen with EGR-diluted combustion, and a minority have used a stratified charge. There has been little work dedicated to the use of reformate with homogeneous, stoichiometric GDI engines, or with reformate having composition that is representative of a real exhaust gas fuel reforming process at gasoline engine exhaust temperatures, i.e. lower quality reformate than is predicted by thermodynamic equilibrium calculations for high process temperatures.

2.7 Conclusion

The aim when implementing an exhaust gas fuel reformer or REGR system with a GDI engine should be to maximise the REGR rate at all conditions in order to:

1. Maximise exhaust heat recovery and generate the highest possible increase in fuel energy
2. Achieve the maximum reduction in pumping loss for all low load conditions, when the intake manifold is normally under significant vacuum
3. Minimise the regions of operation when optimum combustion phasing is not achievable due to knocking combustion
4. Eliminate fuel enrichment from high speed/load regions of the engine map

Factors that may work to limit the achievable REGR rate are:

1. The reduction in combustion stability, which is heavily influenced by the hydrogen concentration in the REGR stream
2. Increased HC emissions
3. Increased boost requirement at high loads
4. Reduced reformer efficiency due to high GHSV at the maximum REGR rate
5. Cooling capacity of the re-circulated gas heat exchangers
6. Low EGT due to heavily diluted combustion leading to reduced reformer efficiency or ineffective reformer operation

If the EGT is sufficiently low to render fuel reforming impractical at low engine loads, EGR could still be used to provide the normal benefits to engine performance. Additionally, passing raw exhaust gas over the reforming catalyst acts as a regeneration process; in contrast to some other aftertreatment catalysts, the regeneration process will not result in drastically

reduced engine efficiency, in fact being regenerated while operating in a regime more efficient than the baseline.

CHAPTER 3

EXPERIMENTAL FACILITIES

Section 3.1 provides a brief overview of the single-cylinder GDI engine test cell that was used for the research presented in Chapter 4. This was an existing test cell that had been used and developed by former postgraduate researchers, and has been described in detail in previous theses [109, 110]. The remaining chapters contain the main body of research that was conducted using a multi-cylinder GDI engine. This test cell was commissioned during the first 18 months of the research period, with the test cell design, component specification, purchasing, project management and much of the installation completed by the author. Assistance was provided by Dale Turner and Jake Wallis during the design of some sub-systems, and by the laboratory technicians (acknowledged earlier) with the heavier installation and fabrication work. Section 3.2 provides a detailed overview of the multi-cylinder engine test cell installation, the various modifications that were made to the base engine, the instrumentation and the data acquisition system.

3.1 Single-cylinder engine test cell

3.1.1 Test bed and instrumentation

The single-cylinder GDI research engine was coupled to a DC dynamometer. The engine design was based on a modified production cylinder head with four valves per cylinder, dual VCT and centrally located spark plug and fuel injector. The displacement volume was 553cm^3 (89mm bore/88.9mm stroke) with a geometric compression ratio of 11.5. Engine control and data acquisition were achieved by software programmed in LabVIEW. The variable engine control parameters included: ignition advance; coil dwell time; start of injection; injector

pulse width; IVO angle; and EVC angle. The fuel system supplied gasoline at 150bar from an accumulator pressurised with compressed nitrogen. The air flow rate to the engine was measured by a positive displacement flow meter coupled to a rotary encoder. The flow of diluent gas (compressed bottled nitrogen or reformate) was measured using a variable area flow meter and fed to the intake manifold downstream of the throttle, as indicated in Figure 3.1. A water-cooled Kistler pressure transducer and charge amplifier measured in-cylinder pressure. An ETAS lambda meter measured the excess air ratio in the exhaust stream and was used to indicate AFR. For all tests the engine was operated with the dynamometer in constant speed mode, controlled to 1500rpm, and the engine water and oil temperatures were controlled to 95°C and 85°C respectively.

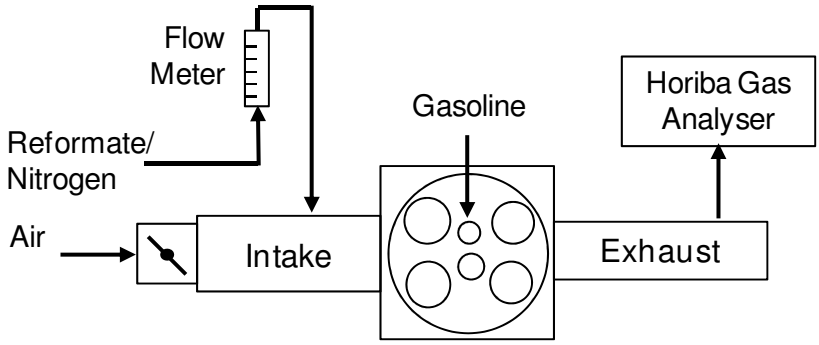

Figure 3.1 - GDI engine schematic including diluent induction

3.2 Multi-cylinder engine test cell

3.2.1 Engine

The engine used for the majority of the research was a 2L, four-cylinder turbocharged GDI engine with side-mounted solenoid fuel injectors and centrally located spark plugs. It is considered to be a first-generation air-guided DI combustion system design. The exhaust manifold is divided to the turbine entry in order to minimise detrimental pressure wave interactions between successively firing cylinders. Exhaust gas aftertreatment consists of a

conventional close-coupled TWC; therefore the engine uses a homogeneous, stoichiometric combustion strategy.

The low pressure fuel system uses a 12V electric fuel pump to supply fuel regulated at 4bar to the camshaft-driven high pressure fuel pump. Fuel rail pressure is varied depending on engine operating condition by an ECU controlled solenoid valve integrated with the fuel pump assembly. An air to water heat exchanger cooled the intake air to control charge temperature measured at the inlet port. Oil cooling was not separately controlled, but used the standard fitment heat exchanger fed by engine coolant. For the purposes of maintaining the auxiliary drive-belt arrangement, an oil to water heat exchanger cooled the fluid circulated by the power steering pump. Further details of the engine specification are listed in Table 3.1.

Table 3.1 - Engine specification

Feature	**Specification**
No. of cylinders	4
Firing order	1-2-4-3
Displacement	1999cc
Compression ratio	10:1
Bore x stroke	87.5 x 83.1mm
Turbocharger	Borg Warner k03 with variable wastegate
Rated power	149kW at 6000rpm
Rated torque	300Nm at 1750-4500rpm
Valvetrain	Four valves per cylinder, dual overhead camshafts with dual continuously variable electro-hydraulic phasing
Engine management	Bosch ME17
Emissions control	TWC, meets Euro 5 regulations
Fuel system	Camshaft driven, high pressure pump with solenoid actuated pressure control, injection pressure variable up to 200bar
Fuel injectors	Multi-hole, side mounted, solenoid actuated
Piston design	‘Flat’ top (shallow air-guiding features)

3.2.2 Dynamometer

The engine was coupled with a 75kW AC dynamometer and inverter drive capable of motoring and absorption/regeneration. The peak engine load is higher than the dynamometer is capable of for sustained operation (S1 curve in Figure 3.2), but for periodic operation the peak engine load can be absorbed up to approximately 3500rpm. This means the engine could potentially overload the dynamometer at high speed; however, this was avoided by programming appropriate warning alarms and shut-down limits into the dynamometer control system. Figure 3.3 shows the engine and dynamometer installed in the test cell installation.

3.2.3 Exhaust gas recirculation system

In production specification the engine does not use external EGR, instead utilising dual VCT to induce internal EGR when required. An external EGR system was designed to provide flexibility in comparing alternative EGR system configurations, and would allow EGR or reformer operation across the entire engine range. The system is configured as in Figure 3.4 and allows for use of two distinct types of EGR loop, defined as High Pressure (HP) and Mixed Pressure (MP). Exhaust gas is drawn from before the turbine and fed into the intake air stream either at the manifold (HP) or pre-compressor (MP). A second EGR cooler on the HP system was implemented to increase the cooling capacity and allow for high EGR rates to be used without increasing the charge temperature (at the inlet port) to unacceptable levels. With the MP system additional cooling capacity is provided by the main charge air cooler.

The EGR valves installed in each system could not be operated simultaneously, and were controlled using a standalone control unit supplied by Pierburg (the valve manufacturer). The control unit required a pulse-width modulated (PWM) input signal to specify the desired

valve position, which was provided by a custom LabVIEW application. The unit also provided an analogue output to enable EGR position feedback and logging.

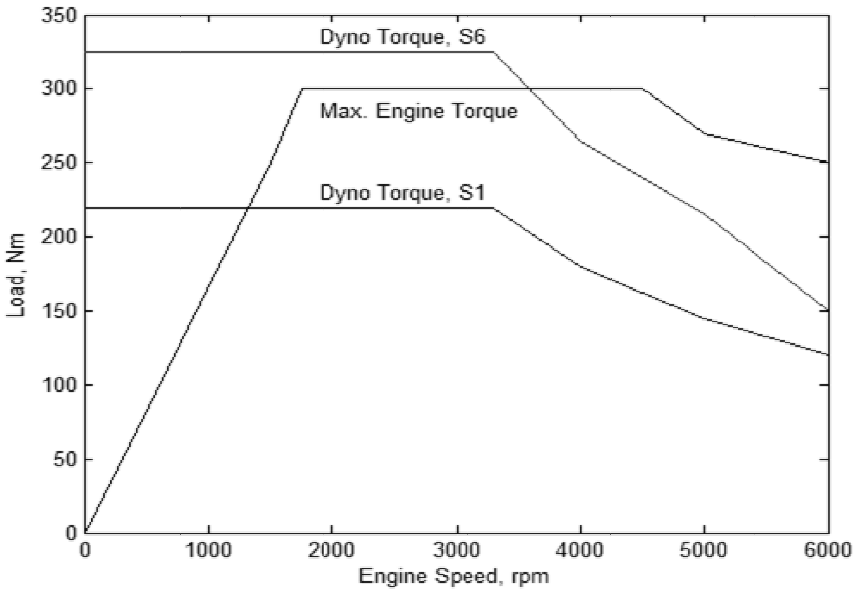

Figure 3.2 - Engine and dynamometer torque curves for sustained (S1) and periodic (S6) operation

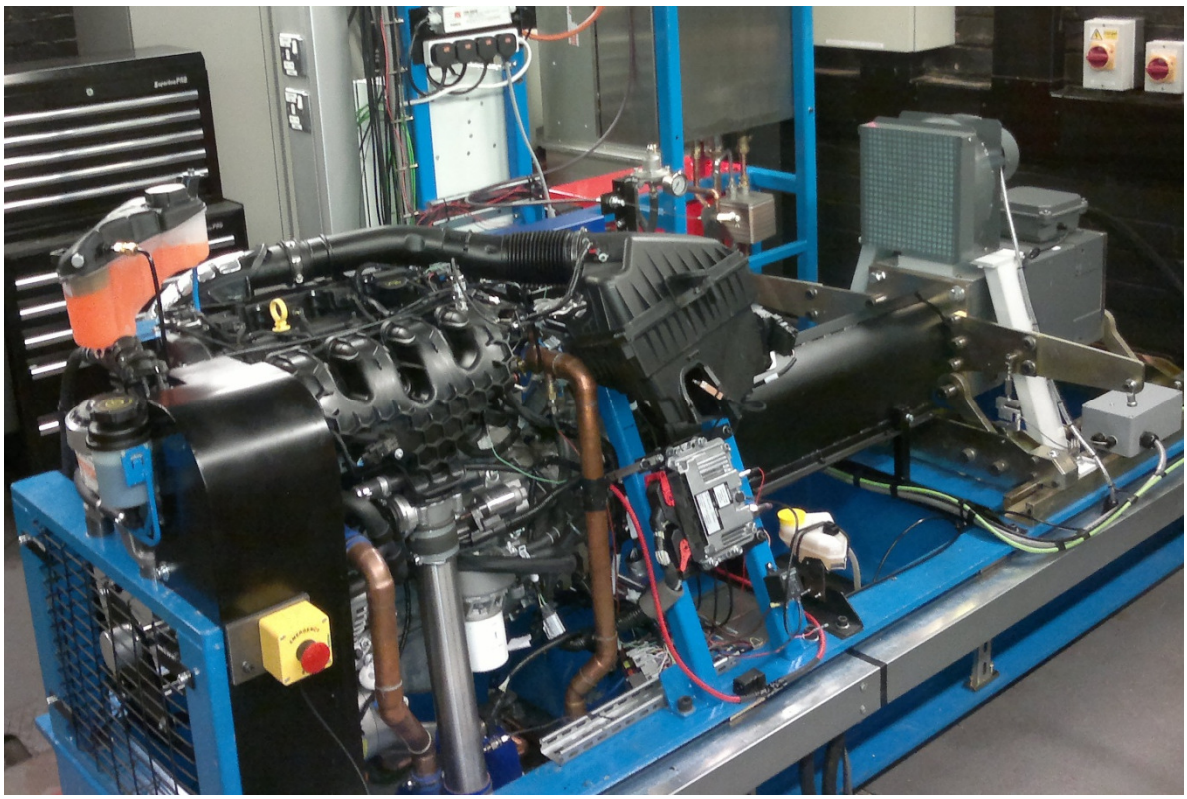

Figure 3.3 - Test cell installation

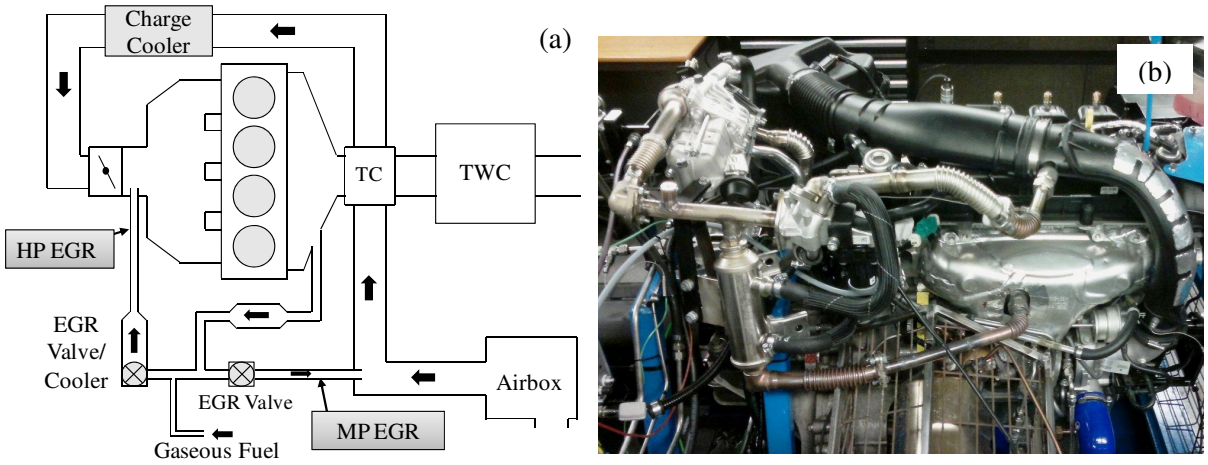

Figure 3.4 - EGR system schematic (a) showing the high pressure (HP) and mixed pressure (MP) system configurations with gaseous fuel induction, and the test cell installation (b)

3.2.4 Instrumentation and data acquisition

The CADET dynamometer control system, supplied by CP Engineering, provided data acquisition (DAQ) for engine speed and load, critical fluid temperatures and a variety of analogue and thermocouple (TC) inputs.

Fuel flow measurement was achieved with a Rheonik RM015 Coriolis fuel flow meter that provides continuous flow measurement in the range 0 to 20 kg/h, with an accuracy of ±0.12% over most of this range, increasing to 0.2% at 0.24 kg/h. The fuel supply temperature control was provided by a fuel conditioning unit sourced from CP Engineering, and set to 28°C for all tests.

The engine's cylinder head was machined to allow the cylinder pressure to be measured by a sensor mounted flush with the combustion chamber roof of cylinder number four. Pressure indication was provided by an AVL piezo-electric pressure transducer and charge amplifier, referenced to the engine cycle using a Baumer 720 pulse per revolution magnetic rotary encoder. An absolute pressure transducer located in the intake runner close to the port entry

was used to reference the cylinder pressure trace to the intake manifold pressure at bottom dead centre (BDC) after the intake stroke.

A development specification ECU provided by the engine manufacturer enabled access to the engine calibration, sensor readings and other calculated parameters. A small selection of the available data was acquired using a controller area network (CAN) hub and interface application from Accurate Technologies Inc.

Acquisition of additional data involved the utilisation of two National Instruments PCI-6251 cards, which each provide 16 analogue inputs (AI), two analogue outputs (AO), 16 digital input/outputs (DI/O) and two onboard counter/timers. A BNC-2090 breakout box is required for each card. The maximum sample rate of these cards was 2MS/s. This was deemed to be adequate for low frequency sampling of up to 16 AI channels, or high frequency sampling of fewer channels, for instance when used for combustion analysis. A LabVIEW application controlled the acquisition of in-cylinder pressure data. Samples were triggered by the shaft encoder at 0.5° crank angle (CA) intervals. Online calculation of IMEP, COV of IMEP, peak pressure and position of peak pressure was available when required, but more in-depth analysis of pressure data and calculation of combustion parameters were handled during post processing (detailed in section 3.6). Exhaust emission data was collected using another LabVIEW application with a lower sample rate of 5Hz.

Additional instrumentation required for the prototype reformer included two standalone thermocouple amplifiers used to collect 16 channels of reformer temperature data, and reformate composition data collected using the Fourier transform infra-red (FTIR) analyser. The EGR valve position and reformer injector settings were logged by the EGR valve control LabVIEW application. The arrangement of the major test cell hardware and data acquisition

components is detailed schematically in Figure 3.5. A comprehensive list of the channels of data acquired from the multi-cylinder engine test cell is included in Appendix 1. Details of measurement accuracy associated with the instrumentation are provided in Appendix 2.

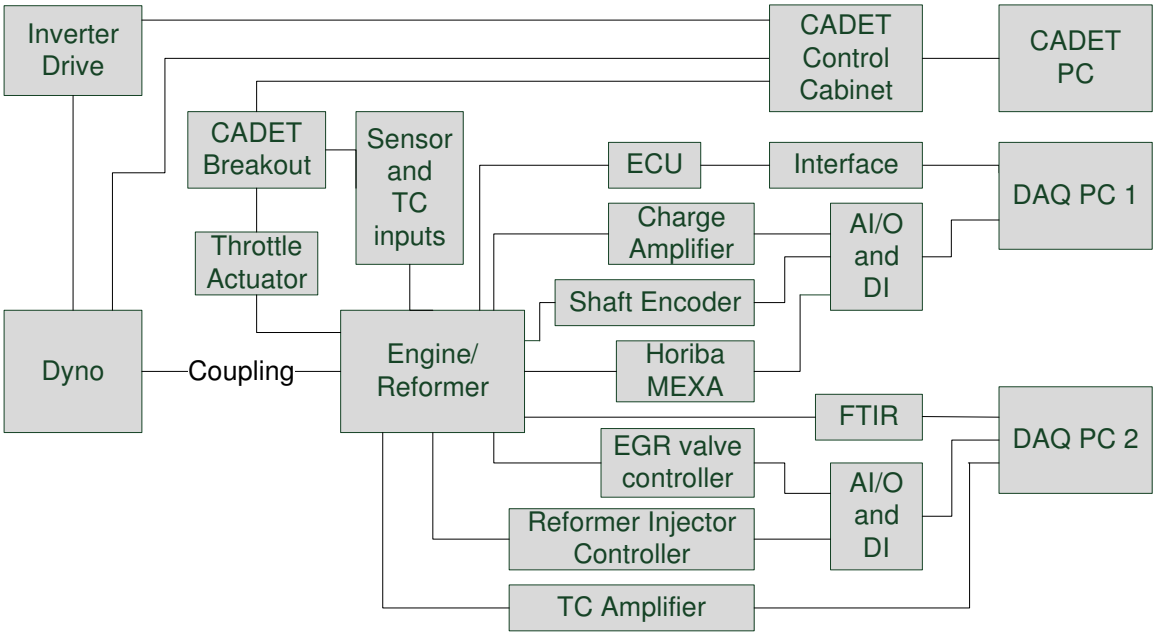

Figure 3.5 - Data acquisition (DAQ) and control system hardware schematic

3.3 Fuels

3.3.1 Gasoline specification

The pump-grade gasoline used throughout the course of the research was supplied by Shell Fuels, and the specification is provided in Table 3.2.

3.3.2 Gaseous fuel induction

A system was designed to enable dual-fuel engine operation by inducting gaseous fuel (e.g. hydrogen or simulated reformate) from a compressed gas cylinder into the intake system. This would be useful for combustion studies using model reformate.

There were various measures taken to ensure safe operation of the system. A flame arrestor was installed in the line and a digital signal from the dynamometer control system was used to enable remote and automated control of the system via a pneumatically actuated gate valve. This meant the gaseous fuel system could only be switched on when the engine was running, and the system would automatically shut down should the engine stop unexpectedly. The system was leak tested using a portable gas analyser following installation, and the test cell is equipped with an air composition/flammability monitoring system as standard.

The desired gaseous fuel flow rate was set manually using a variable area flow meter, and the line pressure set with a variable pressure regulator. The gaseous fuel line was introduced to the intake system via the EGR system, positioned after the EGR valve but well upstream of the intake manifold.

Table 3.2 - Shell gasoline specification

Parameter	**Specification**	**Measured**
Chemical formula	-	$C_{5.88}H_{11.06}O_{0.1}$
Research octane number (RON)	95 (min)	96.8
Motor octane number (MON)	85 (min)	85.2
Density at 15^{o}C, g cm-3	0.72 (min)	0.7332
Sulphur content, mg/kg	50 (max)	7
AFR (stoichiometric)	-	14.23
Enthalpy of combustion, MJ/Kg (liq.)	-	-42.258
Paraffins, % vol	-	12.6
Isoparaffins, % vol	-	33.4
Olefins (including dienes) , % vol	-	14.6
Naphthenes, % vol	-	5.1
Aromatics, % vol	-	28.9
Oxygenates, % vol	-	4.9

3.4 Prototype exhaust gas fuel reformer

3.4.1 Reformer design

The reformer was designed by Johnson Matthey and consists of a stack of five metallic catalyst plates coated with 3.6g/in^3 of CZA loaded with 3.3% Pt - 1.7% Rh. Each catalyst is mounted between two finned stainless steel plates used to seal it from the exhaust stream. The reformer plate assembly, shown alone in Figure 3.6 and installed in Figure 3.7, was designed to ensure high heat transfer from the hot exhaust gas to the catalyst, using fins on the stainless steel surround for increased surface area and a narrow catalyst construction only four cells thick. The exhaust stream flows perpendicularly over the reformer plate stack, which is positioned after the TWC.

The reformer feed gas is extracted from the exhaust stream before the TWC, mixed with gasoline, and routed around the outer skin of the TWC to assist with fuel vapourisation and feed gas pre-heating. The required flow rate of gasoline was injected into the reformer feed gas by varying the pulse-width of a solenoid injector, typically used in PFI engines. The injector was mounted to the reformer with a manifold cooled by engine water to protect the injector from high exhaust system temperatures.

Eleven thermocouples were distributed over the central reformer plate according to Figure 3.8, with additional thermocouples for the feed gas (inlet), reformate (outlet) and the exhaust stream before and after passing over the reformer assembly.

3.4.2 Reformer installation

The reformer was installed as a sub-section of the EGR system to create the REGR system. Generally this was used in the HP configuration (inducting reformate directly into the intake

manifold) at low to medium engine load, but flexibility was designed into the system to allow MP or low pressure (LP) configurations that would allow the reformer to be operated across the full engine range. The LP system involves extracting the raw exhaust gas from after the turbine. A schematic of the engine-reformer configuration with REGR system flexibility is detailed in Figure 3.9.

Thermal insulating material was used to lag the entire exhaust and reformer system in order to minimise the heat loss to atmosphere and maximise the exhaust temperature at the reformer plate interface; this would be critical to ensuring the best system performance. Figure 3.10 shows the reformer installed on the engine test bed complete with thermal insulation.

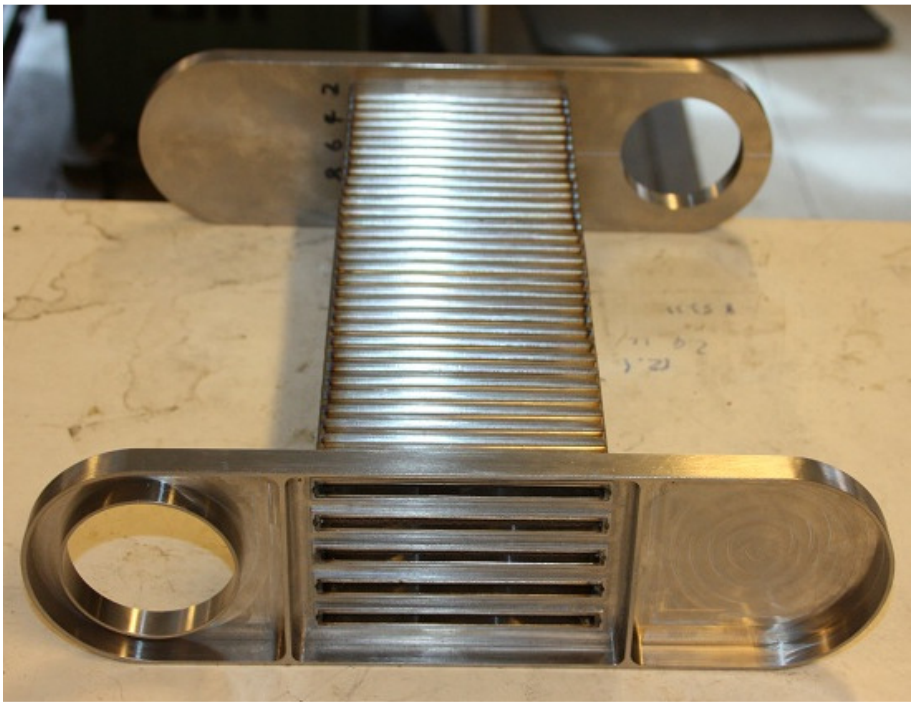

Figure 3.6 - End view of the reformer plate assembly, showing the feed gas entry to the five catalyst plates

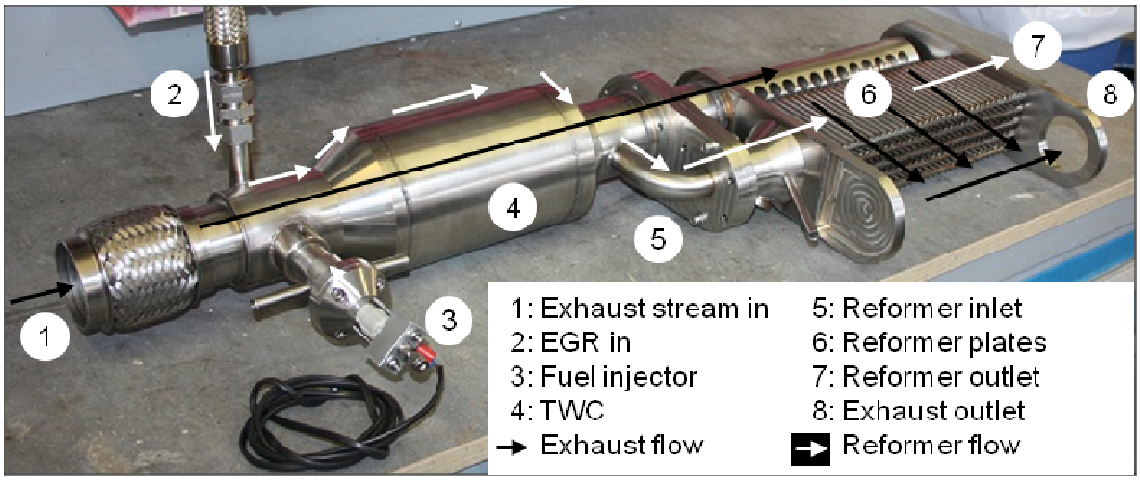

Figure 3.7 - TWC and reformer system assembly (with reformer canning removed to reveal the five reformer plates) including the feed gas inlet pipe and fuel injector installed in front of the TWC

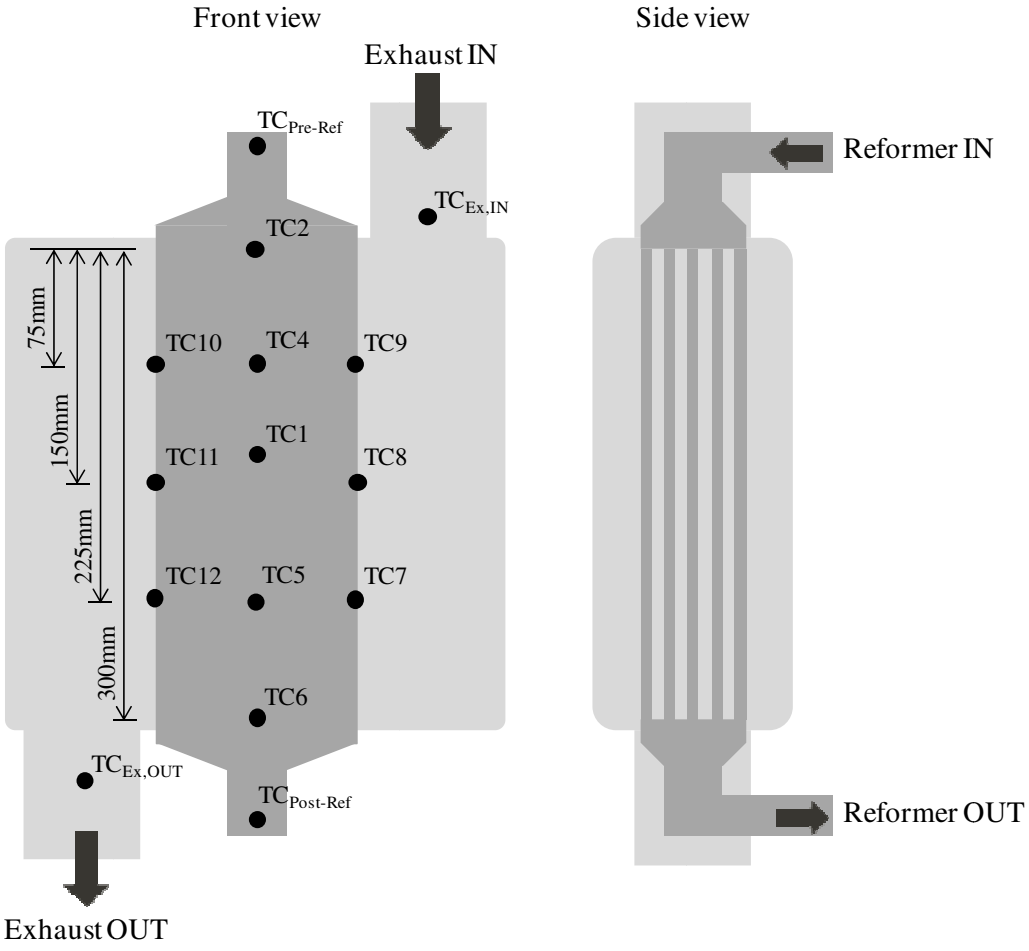

Figure 3.8 - Reformer schematic indicating thermocouple (TC) locations on the central reformer plate and in the exhaust stream

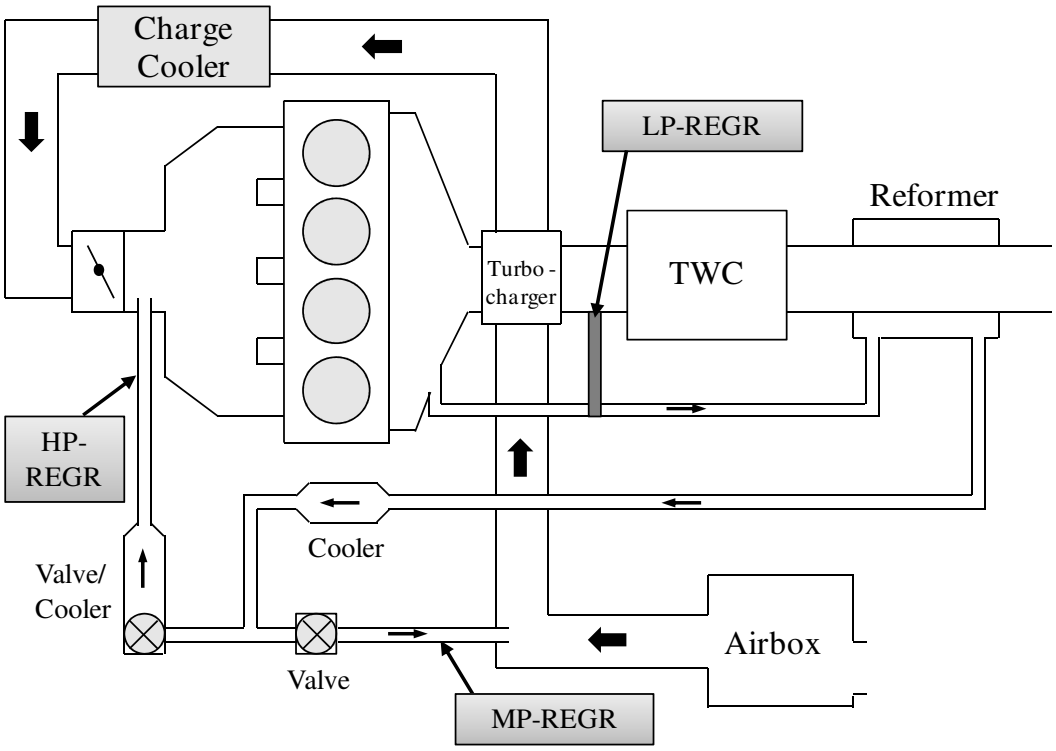

Figure 3.9 - REGR configuration with HP, MP and LP system flexibility

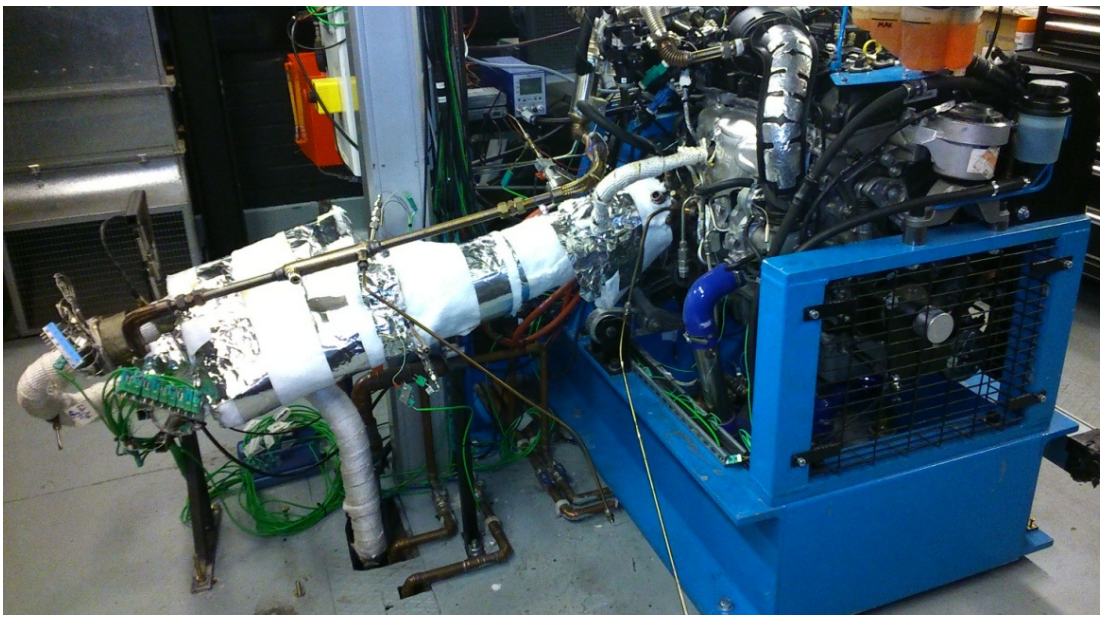

Figure 3.10 - Reformer installed on the engine test bed

3.4.3 Reformer operation

Direct control of the reformer was achieved via the EGR valve and reformer fuel injector, which together determine the feed gas composition and flow rate. The engine control

parameters (speed, load, etc) provided indirect control of other reformer operating parameters such as the exhaust stream temperature at the reformer inlet.

The variables to be investigated, i.e. those that will influence engine and reformer system performance, have been categorised as Primary and Secondary variables. Primary variables are those that can be directly controlled by the engine operating parameters or actuator settings. Secondary variables are those that are dependent on the primary variables, and have significance for the reformer operation but cannot be controlled directly. Figure 3.11 describes schematically how these variables are related, and also how the output parameters to be analysed (combustion and emissions) have an influence on the secondary variables.

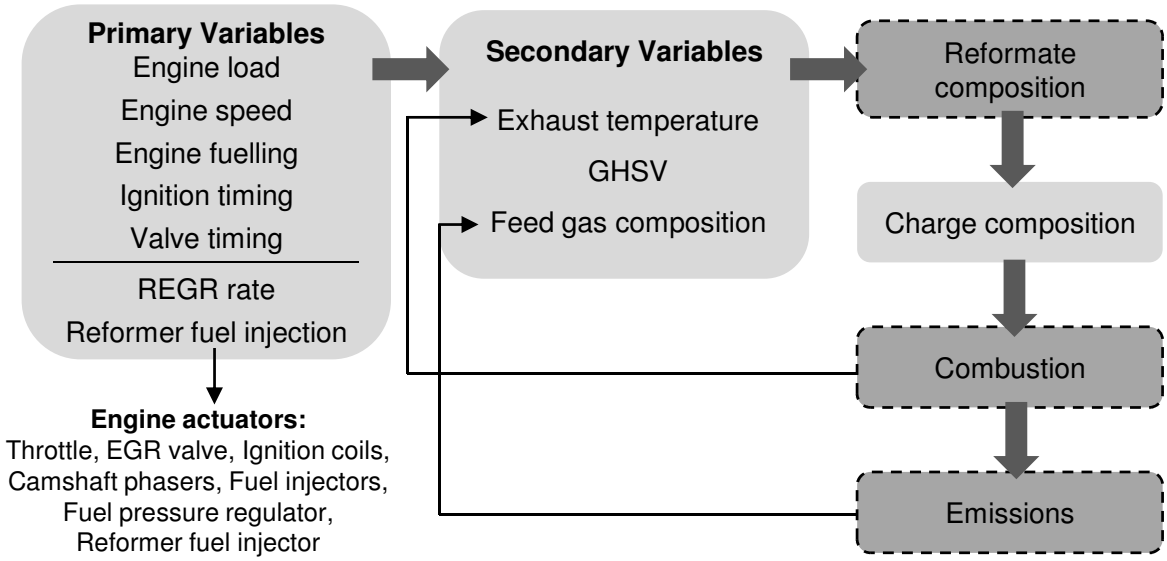

Figure 3.11 - Schematic to describe the dependence of reformer operating parameters (secondary variables) on the engine operating conditions (primary variables) and the system performance parameters (dependant variables – indicated by dashed borders)

3.4.4 Reformer fuel metering

As already stated, a solenoid fuel injector delivered gasoline to the reformer feed gas stream. All fuel supplied to the engine and reformer passed through the Coriolis fuel flow meter, described earlier in section 3.2.4, to allow accurate calculation of fuel efficiency for the total

system. The reformer fuel injector was calibrated to establish the flow rate variation with signal pulse width (Figure 3.12). Knowledge of the fuel flow rate to the reformer enabled the desired feed gas fuel concentration to be targeted, and parameters such as the reformed fuel fraction to be calculated. The injector control signal was generated using a custom made injector drive controller based on a Texas Instruments LM1949 integrated circuit. The LabVIEW application that controlled the EGR valve position also supplied the injector controller with a PWM signal, specified by the pulse-width duration (ms) and frequency (Hz), in order to vary the fuel flow rate. The calibration curve for injector fuel flow rate in Figure 3.12 was determined with the signal frequency fixed at 30Hz. This value was chosen to be as high as possible in order to minimise the effect of discontinuous fuel delivery on non-uniform feed gas composition, while still being able to supply the range of fuel flow rates required with variation of the pulse-width alone.

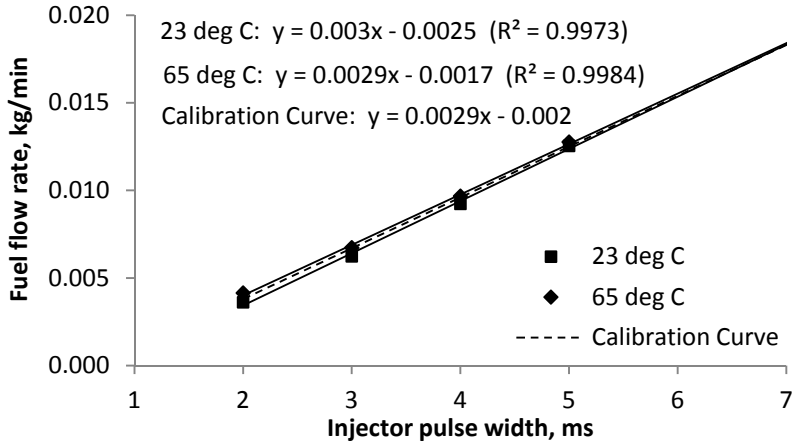

Figure 3.12 - Reformer fuel injector calibration curve

It was important to avoid accidental delivery of fuel to the reformer when not required, or when it would not be safe to do so, e.g. when the engine was not turning or firing, or the EGR valve was not open. In order to provide protection against user error or system malfunction, hardware-based logic was built into the controller circuit with input signals to clarify ignition

status (i.e. ignition is ON) and dynamometer status (i.e. dynamometer is fully operational, and the user has actively selected a digital output to request reformer operation). This approach is shown schematically in Figure 3.13, with the logic table of Table 3.3 highlighting the conditional generation of the injector signal. In addition, software-based logic was included in the LabVIEW application to prevent the PWM signal being generated until the EGR valve was opened (>10%).

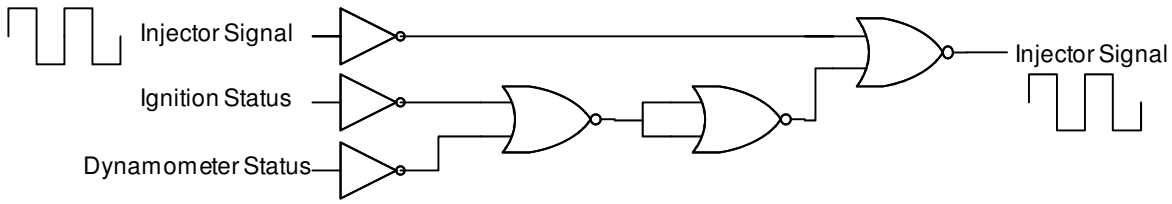

Figure 3.13 - Logic circuit to prevent unsafe reformer injector operation

Table 3.3 - Logic table for reformer injector operation

Injector Pulse In	Ignition Status	Dynamometer Status	Injector Pulse Out
0	0	0	0
0	0	1	0
0	1	0	0
0	1	1	0
1	0	0	0
1	0	1	0
1	1	0	0
1	1	1	1

3.5 Gas composition analysis

3.5.1 Exhaust gas composition analysis

Engine-out gaseous emissions were measured using a Horiba MEXA-7100DEGR, which provides multi-species analysis for all regulated gaseous (vehicle) emissions. This equipment uses the non-dispersive infra-red (NDIR) technique to detect CO_2 and CO, the

chemiluminescence phenomenon to detect NO and NO_x, magneto-pneumatic detection to measure the oxygen concentration and a flame ionisation detector (FID) to indicate the total hydrocarbon (THC) concentration. The sample line to the analyser was heated to 191°C to prevent condensation of HC species and water. The intake manifold CO_2 concentration was also measured in order to calculate the EGR rate according to Equation 3.1. The measurement accuracy of each channel is detailed in Appendix 2.

$$EGR\ Rate, \% = \frac{(CO_2)_{manifold}}{(CO_2)_{exhaust}} x100 \quad \text{Equation 3.1}$$

At times it was necessary to evaluate the re-circulated gas in terms of mass flow rate, particularly when operating with the reformer. The EGR mass flow, $\dot{m}_{EGR}$, was estimated using Equation 3.2 and Equation 3.3, where $\dot{n}_{Air}$ and $\dot{n}_{EGR}$ are the molar flow rates of intake air and EGR respectively, and $M_{r,EGR}$ is the calculated molar mass of EGR based on the exhaust gas composition.

$$\dot{m}_{EGR} = \dot{n}_{EGR} \cdot M_{r,EGR} \quad \text{Equation 3.2}$$

$$\dot{n}_{EGR} = \frac{\dot{n}_{Air}}{\left(\frac{100}{EGR, \%} - 1\right)} \quad \text{Equation 3.3}$$

Generally, the concentration of steam and hydrogen in the engine-out exhaust gas were not measured directly but were estimated using Equation 3.4 and Equation 3.5. These equations exploit knowledge of the WGS reaction equilibrium and are an accepted method for estimating these species' concentration [111, 112].

$$H_2O\ (\%) = 0.5 * \left[\frac{H}{C}\right] * \left[\frac{(CO(\%) * CO_2(\%))}{\left(\frac{CO(\%)}{3.5 * CO_2(\%)}\right) + 1}\right] \quad \text{Equation 3.4}$$

$$H_2\ (ppm) = 10000 * \left[\frac{(CO(\%) * H_2O(\%))}{3.5 * CO_2(\%)}\right]$$ Equation 3.5

3.5.2 Reformate composition analysis

An MKS Instruments Multigas 2030 FTIR spectrometer was used to analyse the reformate stream for multiple species, including CO_2, CO, water, ammonia and a selection of hydrocarbons compounds including methane. A 'method' is a collection of spectra to be analysed by the FTIR, and that has been proven to give good quantification of individual gas species. A method formulated specifically for gasoline combustion (supplied by the instrument manufacturer) was used as the basis for the analysis; however ethanol was eliminated from the analysis to avoid unfavourable interference with other compounds, on the advice of experienced individuals at Johnson Matthey.

A HP 5890 Series 2 gas chromatograph (GC) coupled with a thermal conductivity detector (GC-TCD) and HP 3395 integrator were used to measure the hydrogen concentration in the reformate stream. Argon at 40psi acted as the carrier gas to the sample gas supplied at 10psi, resulting in the hydrogen peak occurring at 2.4s retention time. The detector was calibrated with 30% hydrogen in nitrogen. The GC-TCD was also used at times to measure hydrogen in the main engine-out exhaust stream, using the same calibration settings.

Another HP 5890 Series 2 GC coupled instead with a flame ionisation detector (GC-FID) gave in-depth speciation of the HC components of the reformate. The GC was calibrated with 15 common HCs ranging from C1 to C7.

The sample lines used for reformate measurement were also heated to 191°C to avoid condensation, and were stainless steel to reduce the impact of measurement losses due to the high permeation rate of hydrogen through most materials.

Table 3.4 - Hydrocarbon species included in the GC-FID calibration

HC species	Formula	HC species	Formula	HC species	Formula
Methane	CH_4	1 - butane	C_4H_{10}	n-pentane	C_5H_{12}
Ethylene	C_2H_4	1,3-Butadiene	C_4H_6	n-hexane	C_6H_{14}
Propylene	C_3H_6	n-butane	C_4H_{10}	Benzene	C_6H_6
Propane	C_3H_8	3-Methyl-1-butene	C_5H_8	n-heptane	C_7H_{16}
Iso-butane	C_4H_{10}	Iso-pentane	C_5H_{12}	Toluene	C_7H_8

3.5.3 Particulate matter measurement

PM was sampled using a TSI scanning mobility particle sizer (SMPS) consisting of a series 3080 electrostatic classifier, a 3081 Differential Mobility Analyser and a 3775 Condensation Particle Counter. The sample and sheath flow rates were set such that the measurement (particle diameter) range was nominally 10-407nm. A TSI rotating disk thermodiluter provided heated dilution at 150°C for a wide range of dilution ratios; generally a 30:1 ratio was used. The SMPS sampled the exhaust stream after the TWC, due to its influence on removing HC species that act as precursors to volatile particle formation [113], and can become a significant source of variation in measurements.

Due to the well known low repeatability of nucleation mode particles [114-117], for some test conditions a Topas TDD 590 thermo-denuder was employed in order to guarantee the removal of the volatile component of PM, leaving a measurement of only carbonaceous soot. A thermo-denuder consists of a tube of activated carbon that, when heated, is effective for the removal of HCs by adsorption. Soot passes through, although there are some additional particle losses associated with the process. The temperature of the heater in the thermo-

denuder was set to 400°C as a compromise to ensure evaporation and adsorption of the volatile nucleation mode particles while minimising soot oxidation.

3.6 Data post-processing

A custom post-processing script was written in MATLAB. The first objective of the script was to import and time-align the channels of data obtained by the multiple data acquisition sources, as detailed in Appendix 1. After this, the relevant data for each test point could be extracted, calculations performed, and a summary file generated that contained information on the test conditions, set points, measured data and calculated parameters. It should be acknowledged that the combustion analysis calculations originate from a MATLAB script written by the ICE group in Oxford, and were previously used for analysis of the single-cylinder engine test data.

3.6.1 Combustion process analysis

Heat release rate and mass fraction burned

The measured cylinder pressure data were used for analysis of the combustion process. Equation 3.6 was used to estimate the net heat release rate. The ratio of specific heats, γ for the cylinder contents was estimated from the gradient of the logarithmic pressure-volume curve during the compression and expansion phases, and smoothed at the transition.

$$\frac{dQ}{d\theta} = \frac{\gamma}{\gamma - 1} p \frac{dV}{d\theta} + \frac{1}{\gamma - 1} V \frac{dp}{d\theta} \qquad \text{Equation 3.6}$$

The mass fraction of fuel burned was inferred from the integral of heat release rate using Equation 3.7, where the MFB at a given crankshaft rotation, θ° after combustion initiation is the ratio of the cumulative heat release, QR_{Cum} to the total heat release, QR_T. This generates a normalised MFB curve where 0 is combustion initiation and 1 is the end of combustion. The

crankshaft position that has a MFB value of 0.5 identifies when half of the fuel has been burned, is referred to as MFB50% and has been used to specify the combustion phasing. In the work that follows, the main combustion duration has been defined as MFB10-90% and the combustion initiation duration as MFB0-10%.

$$MFB_{(\theta)} = \frac{QR_{cum\,(\theta)}}{QR_T} \qquad \text{Equation 3.7}$$

Combustion efficiency

An indication of the combustion process efficiency was derived using Equation 3.8 by calculating the combustion inefficiency from the engine-out exhaust composition. This estimates the energy associated with the combustible species that remain in the exhaust gas using the lower heating value, LHV_x and the calculated mass flow, $\dot{m}_{x,ex}$ of species x in the exhaust stream. The LHV of the measured HCs is assumed to be that for gasoline.

$$\eta_{comb} = 1 - \left[\frac{\left(LHV_g.\dot{m}_{HC,ex} + LHV_{H2}.\dot{m}_{H2,ex} + LHV_{CO}.\dot{m}_{CO,ex}\right)}{(Total\ fuel\ supplied, kJ/s)}\right] \qquad \text{Equation 3.8}$$

3.6.2 Engine performance and efficiency

Mean effective pressure (MEP) provides a normalised value for engine load, useful for comparison of data from engines with alternative design or configuration. MEP was calculated for each of the four cycle strokes using Equation 3.9, where $\bar{p}$ is the mean cylinder pressure during an interval of crank rotation resulting in piston displacement volume, dV, and V_s is the total swept volume over the stroke.

$$MEP_x = \frac{\sum \bar{p} dV}{V_s} \qquad \text{Equation 3.9}$$

The total cycle IMEP can then be calculated by summation of the individual stroke MEPs (Equation 3.10). Pumping MEP (PMEP) represents the negative work associated with the exhaust and induction strokes (Equation 3.11).

$$IMEP = MEP_1 + MEP_2 + MEP_3 + MEP_4 \quad \text{Equation 3.10}$$

$$PMEP = MEP_1 + MEP_4 \quad \text{Equation 3.11}$$

A measure of the engine's operational stability, or combustion stability, was provided by analysing the COV of IMEP for 300 consecutive engine cycles using Equation 3.12.

$$COV\ of\ IMEP\ (\%) = \left[\frac{Standard\ Deviation\ (IMEP)}{Mean\ (IMEP)}\right] \cdot 100 \quad \text{Equation 3.12}$$

Indicated engine thermal efficiency, η_{Ind} was evaluated for the indicated cylinder with Equation 3.13. This quantifies the efficiency with which the engine converts fuel energy into mechanical work, and requires calculation of the indicated cylinder power, P_{Ind} (Equation 3.14) from the IMEP and the fuel flow to the cylinder in question.

$$\eta_{Ind} = \frac{P_{Ind}}{\dot{m}_{fuel} \cdot LHV_{fuel}} \quad \text{Equation 3.13}$$

$$P_{Ind} = \frac{1}{2} \cdot \frac{IMEP \cdot V_s \cdot N}{6000} \quad \text{Equation 3.14}$$

Brake specific fuel consumption (BSFC) was calculated with Equation 3.15 and was used to quantify the engine fuel efficiency, where brake power, P_{Br}, was calculated using Equation 3.16 based on engine torque, *T*, as measured by the dynamometer.

$$BSFC = 1000 \cdot \frac{\dot{m}_{fuel}}{P_{Br}} \quad \text{Equation 3.15}$$

$$P_{Br} = \frac{T \cdot 2\pi \cdot N}{60000} \quad \text{Equation 3.16}$$

CHAPTER 4

ESTABLISHING REFORMING CATALYST PERFORMANCE AND THE EFFECTS OF REFORMATE COMBUSTION ON GDI ENGINE EFFICIENCY AND EMISSIONS [1]

As discussed in Chapter 2, reformate produced by exhaust gas fuel reforming at moderate reaction temperatures tends to contain a lower concentration of hydrogen and CO in comparison with other reforming technologies that rely on exothermic reactions to raise the process temperature. For example, exhaust gas reforming experiments at 650 °C produced reformate with 5% hydrogen and 2% CO [16], whereas typical concentrations for exothermic partial oxidation reforming are likely to be in the region of 15% hydrogen and 20% CO [83] or higher. Many previous reformate combustion studies have used reformate with high quality compositions such as this, which are not necessarily achievable in practice with an exhaust gas fuel reformer.

Section 4.1 aims to establish the performance of current Pt-Rh reformer catalysts at typical gasoline engine exhaust stream temperature, and therefore offer a more realistic prediction for achievable reformate composition.

Section 4.2 uses information gained in section 4.1 in order to determine the effects of partial reformate fuelling (REGR) on GDI engine combustion and emissions performance, with tests performed on a single-cylinder GDI engine. The tests were designed to compare REGR to conventional EGR and the GDI engine baseline.

[1] This chapter forms the basis of a published technical paper [17]

4.1 Reforming studies

4.1.1 Johnson Matthey thermodynamic and experimental reforming studies

Initially, a thermodynamic study was performed by Johnson Matthey to predict the gas composition of reformate produced by reforming under gasoline exhaust conditions. Calculations were based on the minimisation of Gibbs free energy of an adiabatic reactor. Methane was considered as inert. In these fuel reforming studies and those in the literature [79], at low temperature the measured methane production was well below equilibrium and usually negligible. The thermodynamic quantities of hydrogen, CO and CO_2 expected after reforming were calculated based on the chosen reactor feed gas compositions, summarised in Table 4.1, which approximated stoichiometric GDI engine exhaust gas with the addition of iso-octane.

Table 4.1 - Reactor feed gas composition

Species	Concentration (% vol)
CO_2	10
H_2O	10
CO	2
Oxygen	1
Iso-octane	0.3, 0.5, 0.8, 1.0
Nitrogen	Balance

In the experimental study a Pt(2%)-Rh(1%)/CZA catalyst on a 1”x3” ceramic monolith with 600 cells per square inch, was used to reform iso-octane, which was vaporised and mixed with model exhaust gas (with composition as specified in Table 4.1) upstream of a furnace heated reactor vessel. Iso-octane was selected as the model fuel to avoid difficulties in vaporising and analysing a multi-component mixture such as gasoline. A range of fuel concentrations were tested to determine catalyst performance at furnace temperatures between 300 and 600°C and

a GHSV of 22,000h^{-1}. The full dataset is not included here, but a selection is compared to data from the following tests later, in Figure 4.4.

4.1.2 Furnace heated catalytic reforming of gasoline

Reforming tests were also performed by the author using real exhaust gas from the single-cylinder GDI engine for the reforming of gasoline, rather than iso-octane. The engine was operated with a stoichiometric AFR and therefore the exhaust oxygen concentration was low at 0.7%. A catalyst of identical size and formulation (Pt(2%)-Rh(1%)/CZA) was held in a reactor vessel and heated by a furnace. Figure 4.1 shows the experimental setup.

The flow rate of the reactor feed gas was 10L/min (15759hr^{-1} GHSV). Gasoline was introduced to the reactor from a syringe pump via a heated ultrasonic atomiser so that the volumetric concentration of gasoline in the feed gas was approximately 0.6% and 1.2%. The reformer performance was analysed at furnace temperatures of 400, 500, 600 and 700°C. The monolith temperature profile was recorded using a thermocouple housed in a tube mounted co-axially through the monolith.

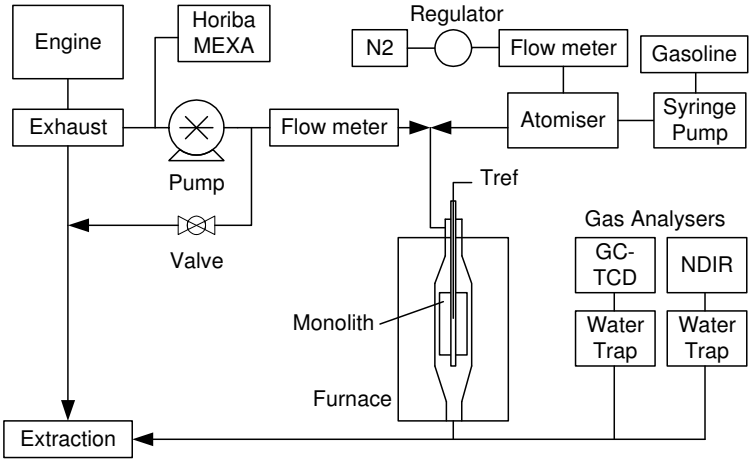

Figure 4.1 - Experimental setup for furnace heated reforming study

Figure 4.2 shows the monolith temperature profile for a range of reforming conditions. Endothermic reforming was evident when the furnace was at 600°C and above (approx 550°C at the monolith inlet), but not for lower temperature. The maximum reduction in temperature due to the endothermic reforming reactions was approximately 90°C. Hydrogen, CO and CO_2 concentrations for reforming with 0.6% and 1.2% gasoline fractions are shown in Figure 4.3. A maximum of 7% hydrogen was produced at 700°C furnace temp for 1.2% gasoline fraction.

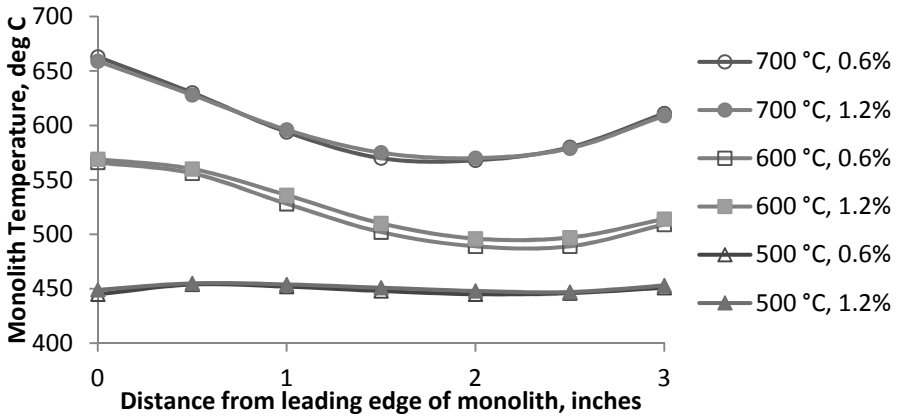

Figure 4.2 - Monolith temperature profiles at a range of furnace temperatures for 0.6% and 1.2% gasoline fraction

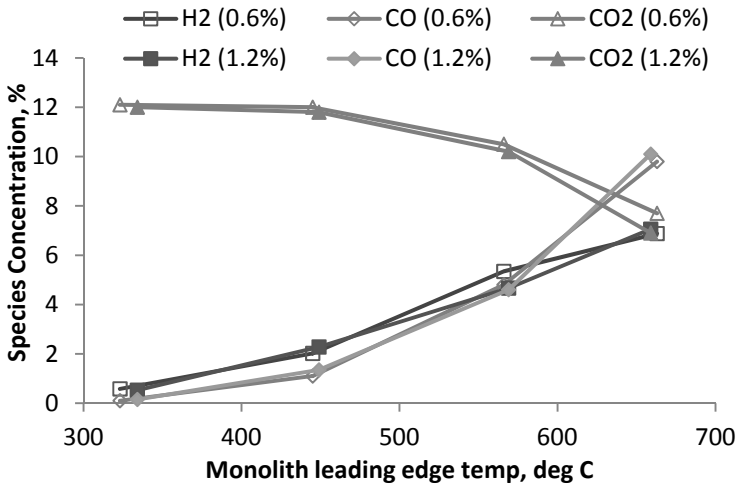

Figure 4.3 - Reformate species concentration for 0.6% and 1.2% feed gas fuel fraction

These experiments show that by using the Pt-Rh catalyst it is possible to produce hydrogen with endothermic reforming reactions when the catalyst inlet temperature is above approximately 550°C.

4.1.3 Model reformate composition

Figure 4.4 compares the experimental and thermodynamic reformate compositions obtained above. The experimental results obtained by Johnson Matthey at catalyst inlet temperatures above 450°C show that the hydrogen yield was approximately half of that predicted by the thermodynamic model, as was the CO. Hydrogen production was low in comparison to the thermodynamic equilibrium concentrations at low temperatures (≤350°C) where the reforming reactions are kinetically limited. The CO_2 measured experimentally was consistent across the temperature range, suggesting there is little influence of dry reforming under these conditions.

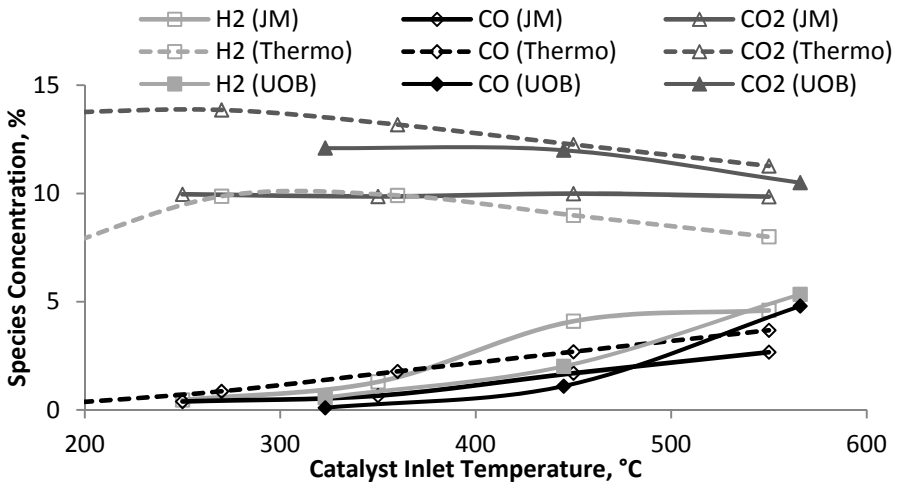

Figure 4.4 - Comparison of experimental and thermodynamic reformate compositions (Tests performed at Johnson Matthey (JM) with 0.5% (vol) iso-octane (GHSV 22,000 h^{-1}) and at the University of Birmingham (UOB) with 0.6 % (vol) gasoline (GHSV 16,000 h^{-1}))

Hydrogen production was lower at 450°C in the gasoline reforming experiments (UoB data in Figure 4.4), which may be attributed to the differences between iso-octane and gasoline with

the latter proving to be more difficult to reform due to the presence of aromatic hydrocarbons. At higher temperature the production of hydrogen and CO increased, with a corresponding drop in CO_2 concentration that, in contrast to the previous data, may indicate some dry reforming activity.

It was seen as important to select an achievable reformate composition to use in the later combustion tests, rather than an 'ideal' composition based on thermodynamic equilibrium models. This ultimately means lower hydrogen and CO concentrations. Guided by the experimental data, the model reformate used in the series of engine tests that follow in section 4.2 approximates gasoline reforming at 550°C, and its composition is summarised in Table 4.2. It was decided that steam would be eliminated from the simulated reformate mixture in order to simplify the test procedure. Reformate from exhaust gas fuel reforming contains steam in lower concentrations than EGR due to being consumed in steam reforming reactions. Additionally, the approximation of EGR used in this study contained no steam.

Table 4.2 - Properties of the simulated reformate

Component	Molar conc., %	Molar Mass	Mass, %	LHV, MJ/kg	AFR (λ=1)
H_2	5	2	0.4	120	34.1
CO	4	28	4.0	10.1	2.45
CO_2	10	44	15.5	-	-
N_2	81	28	80.1	-	-
Reformate	**-**	**28.30**	**-**	**0.824**	**0.217**

The reforming process efficiency was calculated from the experimental data using the measured composition that most closely matched the simulated reformate composition. This involved estimating the energy content of the reformate relative to the gasoline fuel energy supplied to the reformer. When the gasoline concentration in the feed gas was 0.6%, with a

catalyst inlet temperature of approximately 550°C, the product reformate contained 5.3% hydrogen, 4.8% CO and 10.5% CO_2. Reforming at this temperature resulted in 30% of the HC fuel passing through the reformer. The calculated reforming process efficiency was 1.34. That is, the total fuel enthalpy was increased by 34% by endothermic reforming, with energy supplied in this case by a furnace, simulating the hot exhaust stream of the real REGR application.

4.2 Experimental study of simulated reformate combustion

The tests in this section were designed to compare GDI engine operation with REGR to that of conventional EGR, and enabled analysis of combustion and emissions performance for the two methods of charge dilution. In order to simplify the experimental procedure and aid repeatability, reformate was supplied to the engine from a compressed gas cylinder, rather than a real fuel reformer. The reformate composition was summarised in Table 4.2. Due to the absence of an EGR loop on the single-cylinder engine, conventional EGR was approximated by inducting nitrogen.

4.2.1 Test conditions

Initially, the engine performance was established for operation with gasoline and no external charge dilution; this is referred to throughout as the baseline condition. The target AFR throughout all tests was stoichiometric. Other controlled parameters for all tests included valve timings, fixed at -16° and 36° after top dead centre (aTDC) for intake and exhaust respectively, as well as fuel pressure, start of injection (SOI) timing, ignition coil dwell time and engine speed. Table 4.3 summarises these parameters. Ignition timing sweeps established the ignition timing for maximum torque (MBT) at each engine condition; data recorded at MBT would later be used when comparing engine and emissions performance between

operating conditions. Combustion data were captured and averaged over 300 cycles at each steady state test point. Once the baseline engine performance had been established, each test point was repeated with charge dilution, first by nitrogen to simulate EGR, then by reformate to simulate REGR. In order to maintain engine load and AFR for each test point the throttle opening and GDI fuelling were adjusted. It should be noted that the lambda sensor reader was programmed with the C:H:O ratio of the gasoline (detailed in Section 3.3.1) and was not modified with the addition of reformate.

Table 4.3 - Fixed engine parameters

Engine speed	1500rpm	Fuel pressure	150bar
Coolant temp.	95°C	Start of Injection	280°bTDC
Oil temp.	85°C	IVO	-16°aTDC
AFR	λ = 1	EVC	36°aTDC

The matrix of test conditions (engine load and dilution rate) is detailed in Table 4.4. The column labelled 'Max' relates to the level of charge dilution that causes a reduction in combustion stability such that the COV of IMEP becomes greater than 5%; this was then the maximum achievable charge dilution. The definition of charge dilution in this context differs from that defined in Chapter 3, and was instead defined as the percentage of diluent flow (nitrogen or reformate) in the total flow into the cylinder and was calculated with Equation 4.1; the total flow comprises of the combustion air and the diluent. It should be noted that reformate was treated as a diluent, despite the presence of combustible gases, to enable comparison between EGR and REGR. Results are also presented in later sections that compare total inert fraction in the combustion charge.

$$Dilution, \% = \frac{\dot{V}_{diluent}}{\dot{V}_{air} + \dot{V}_{diluent}} \times 100 \qquad \text{Equation 4.1}$$

Table 4.4 - Matrix of test conditions

Load, bar IMEP	Charge Dilution, %					
	0	**5**	**10**	**15**	**20**	**Max**
3.5						
6.5						
7.5						

4.2.2 Combustion stability

It is accepted that charge dilution by EGR causes a reduction in combustion stability, which becomes a limiting factor in determining the maximum possible recirculation rate. This is especially significant at low engine load when combustion is generally less stable. At higher engine load, other factors may determine the maximum recirculation rate, such as ensuring that sufficient air is available for combustion (dependent on VE) or providing adequate heat rejection from the re-circulated gas to maintain an acceptable charge temperature. Limiting the deterioration of combustion stability is also important to minimise the adverse effects on NVH, which is an important issue in the modern automotive industry. In the following analysis, the maximum allowable deterioration of combustion stability is defined by a COV of IMEP of 5%.

Figure 4.5 shows the reduction of combustion stability (rising COV of IMEP) for increasing charge dilution, with the maximum allowable dilution being 21% and 27% for EGR and REGR respectively. This seems to imply that the presence of hydrogen and CO in REGR, even in low concentration, enables higher dilution rates than EGR. This is significant because reforming potential, i.e. heat recovery, shouldn't be limited as severely by the deterioration of combustion stability. The combustion stability at the higher load of 6.5bar IMEP didn't deteriorate for either REGR or EGR, being maintained below 1.5% COV of IMEP for all dilution rates tested.

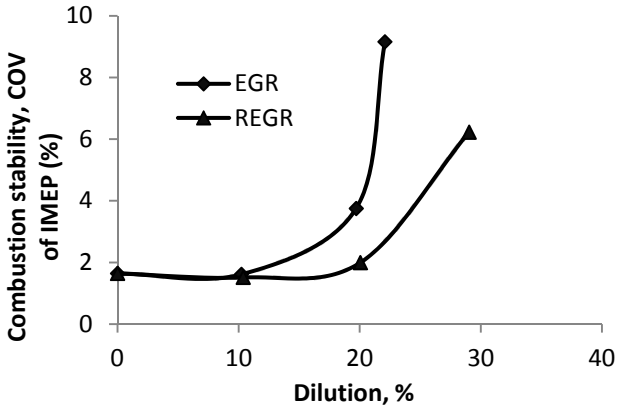

Figure 4.5 - Effect of EGR and REGR dilution on combustion stability at 3.5bar IMEP

An alternative way to view the same combustion stability data is to plot against inert fraction of the combustion charge instead of dilution percentage. This eliminates the dubious inclusion of combustible gases in the diluent flow. Figure 4.6 presents this alternative plot, and shows that REGR combustion stability deteriorates more quickly with increasing inert fraction than conventional EGR. This may indicate then that the lower inert content of reformate is part of the reason for improved combustion stability seen here, rather than it being a beneficial effect from the presence of hydrogen and CO alone.

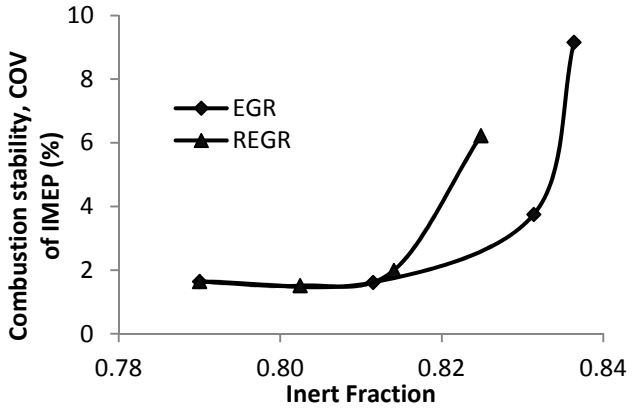

Figure 4.6 - Effect of inert fraction on combustion stability at 3.5bar IMEP

At this point it may be useful to reiterate the benefits of using increased recirculation rates. Lower pumping work occurs as a result of de-throttling and higher intake manifold pressure. The higher fraction of inert gas in the combustion charge results in lower combustion

temperature and pressure; this leads to reduced heat loss to the cylinder walls and lower NO_x emissions. A negative effect is that slower combustion rates, indicated by an advanced MBT shift and longer combustion durations, will inevitably result in reduced thermodynamic efficiency.

The advancement of MBT with increasing REGR rate at 3.5bar IMEP is apparent in Figure 4.7; the ignition timing sweep performed for each charge dilution was primarily to find MBT but also indicates that the combustion rate slows. The effect of the increasing concentration of inert gases in the combustion mixture seems to outweigh any beneficial effect from the hydrogen, which has previously been shown to enhance burn rate at concentrations below 1% [86]. Figure 4.7 also shows that with REGR there was a wider range of usable ignition timings that produce maximum, or close to maximum torque; this is identified by a flatter curve near the MBT point and indicates that a lower efficiency penalty will arise if using retarded ignition timings for NO_x suppression, or if the ignition timing is not calibrated optimally.

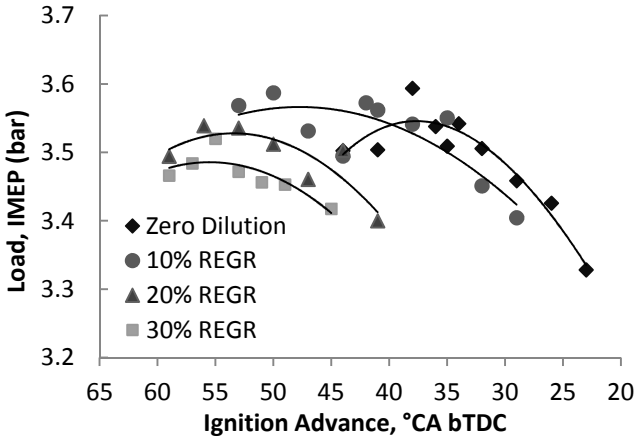

Figure 4.7 - Ignition timing sweeps at 3.5bar IMEP for a range of REGR rates

Regarding the MBT shift of EGR and REGR, Figure 4.8 shows that there was very little difference at 6.5bar IMEP, just one degree less for REGR. This supports the previous

statement that the presence of hydrogen is showing little effect on the combustion rate. In this case, because the load is sufficiently high, MBT was limited by knock so these positions have been marked in the figure.

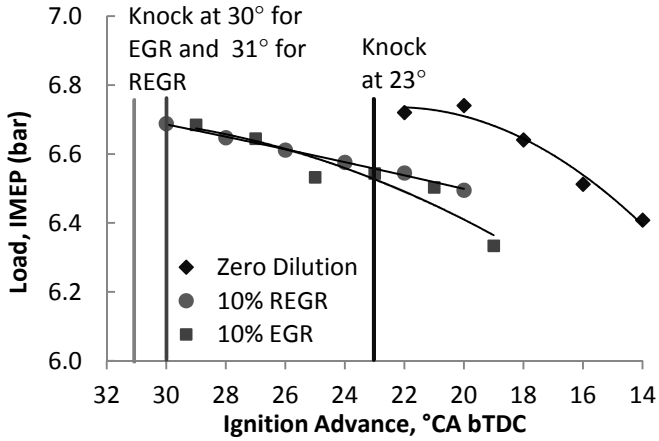

Figure 4.8 - Ignition timing sweeps at 6.5bar IMEP with 10% dilution

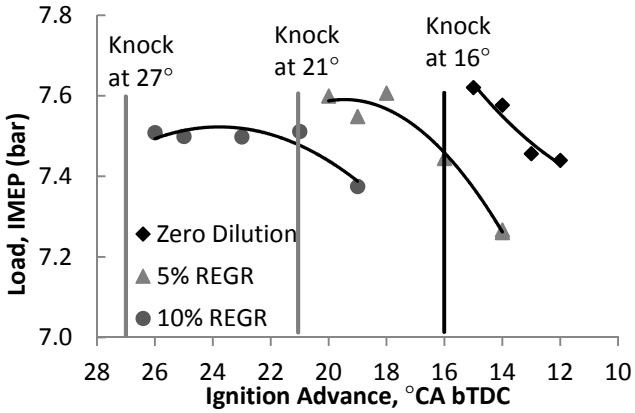

Figure 4.9 - Ignition timing sweeps at 7.5bar IMEP with 0, 5% and 10% REGR

The 7.5bar IMEP engine load test points were included in order to further investigate knock for the engine operating with REGR. The onset of knock in these tests was defined as the minimum ignition timing advance that induces audible knock. Figure 4.9 shows ignition timing sweeps for 5% and 10% REGR with the expected advancing MBT shift, similarly to lower engine loads. It can also be seen that when REGR is introduced, MBT is no longer knock-limited. This is likely to be due to the increased inert fraction of the combustion charge

resulting in lower combustion temperatures. Hydrogen and CO have previously been identified as octane enhancers [71] and so could also be assisting in the delay of knock onset.

The ignition timing for knock onset was further advanced by REGR, making true MBT achievable, which for a fixed engine condition that is normally knock-limited would imply increased engine thermal efficiency. In this case, because the throttle opening and gasoline fuelling both change in order to maintain engine load when REGR is introduced, this doesn't necessarily translate directly into an efficiency increase and will require further analysis. The advancement of knock onset with increasing REGR is clearer to see when engine load is plotted against ignition timing relative to MBT, as in Figure 4.10. When the engine operates on gasoline with zero charge dilution, knock occurs 1°CA in advance of MBT, although MBT is knock-limited in this case. As REGR is introduced, the onset of knock is advanced 3° and 4°CA before MBT for 5% and 10% REGR respectively. This suggests that an engine operating with REGR could operate closer to true MBT ignition timing with less risk of small fluctuations in operating conditions resulting in knock.

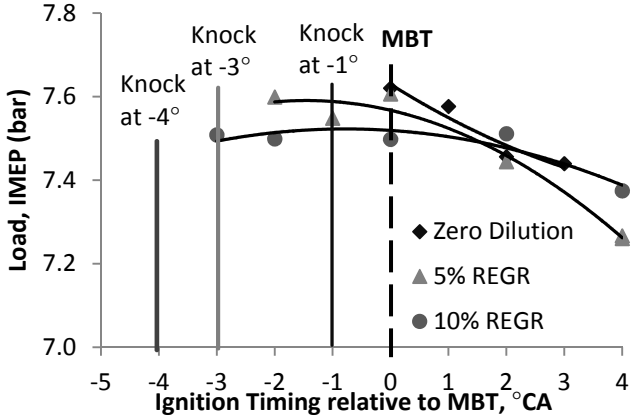

Figure 4.10 - Ignition timing sweeps at 7.5bar IMEP (relative to MBT) with 0, 5% and 10% REGR

When comparing the dilution strategies across the ranges of engine load and dilution rates tested, REGR tended to advance knock between 2 - 3° more than EGR for the higher dilution rates. The difference between EGR and REGR was negligible for the lower dilution rates.

4.2.3 Combustion

Figure 4.11 plots the two major phases of combustion. The flame initiation phase is represented by the 0-10% MFB duration and the main combustion period by the 10-90% MFB duration. Data for 3.5 and 6.5bar IMEP are plotted for EGR and REGR at MBT ignition timings. As might be expected, the effect of increasing charge dilution was to slow down the rate of early flame propagation, resulting in a longer 0-10% MFB duration compared to the baseline. Hydrogen has a higher laminar flame speed (1.9 to 2.7ms^{-1}) compared to gasoline (0.4ms^{-1}) [68]. This suggests that during the early stages of combustion, when flame growth is fundamentally laminar, an air/fuel mixture with a higher concentration of hydrogen would exhibit a faster rate of flame growth.

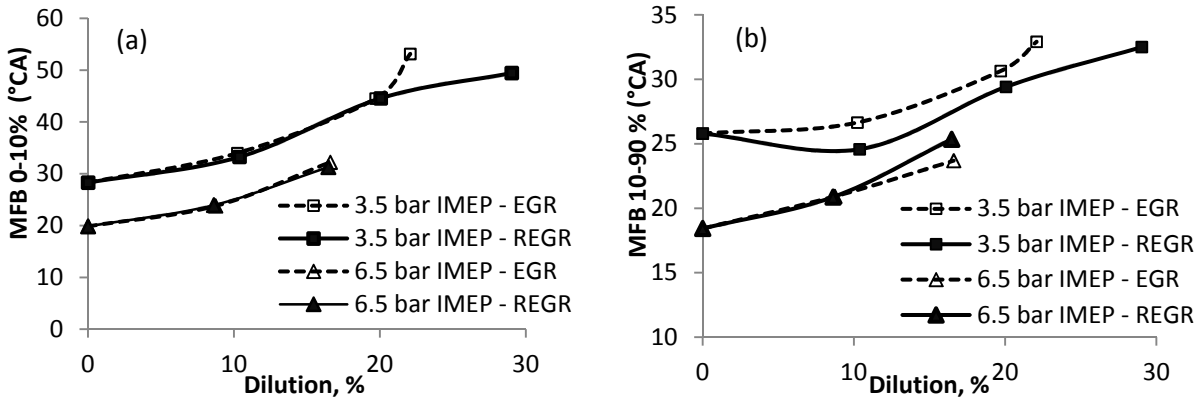

Figure 4.11 - Effect of dilution on flame initiation phase (a) and main combustion phase (b) duration

Figure 4.11a, however, shows that there is no discernible difference in 0-10% MFB duration between EGR and REGR, indicating that the small amount of hydrogen present is not aiding

early flame growth. A small difference is seen at 3.5bar IMEP as the maximum dilution rates are approached – when combustion stability has deteriorated – and REGR flame initiation remains slightly faster.

Burn rate during the main combustion phase is represented in Figure 4.11b by the 10 to 90% MFB combustion duration. There is a similar upward trend for both EGR and REGR, confirming that combustion rate is reduced by dilution; however, it is apparent that in general REGR was able to maintain a slightly faster burn rate for the same level of charge dilution. This is due to both the presence of hydrogen and a lower inert fraction in the cylinder charge working to slow down the deterioration of combustion rate with increasing dilution. Despite the relatively low concentration of hydrogen in the cylinder charge, 0.5% and 1% at 10% and 20% REGR respectively, the hydrogen has a beneficial effect on combustion speed. This apparent effect may be attributed to the stabilising effect of hydrogen rather than a physical increase in burn rate, as the data presented are averaged over 300 engine cycles.

The absence of CO_2 in the approximation of EGR used here may be causing an under-estimation of burn rates compared with actual EGR, as CO_2 has a greater deteriorating effect on flame growth than nitrogen. The simulated reformate contained 10% CO_2 and this, to some degree, will have masked the effect that hydrogen and CO had on increasing the combustion rate of REGR when compared to EGR.

The composition of the reformate used in this study approximates that produced by exhaust gas fuel reforming at 550°C. Figure 4.12 shows the reduction in EGT with increasing dilution. At the higher load of 6.5bar IMEP there was a 40°C drop in EGT from the baseline to approximately 560°C at maximum EGR and REGR. At lower load, EGTs were slightly below 550°C for all conditions, which would result in slightly lower quality reformate than that used

in these tests. Referring to Figure 4.4, however, it can be seen that hydrogen production drops off rapidly below 450°C. It is therefore significant and encouraging that EGT was maintained above 500 °C in these tests, even at low load, and means that a real exhaust gas fuel reformer mounted in the exhaust stream should not be 'switched off' as a result of recirculation of its own product reformate.

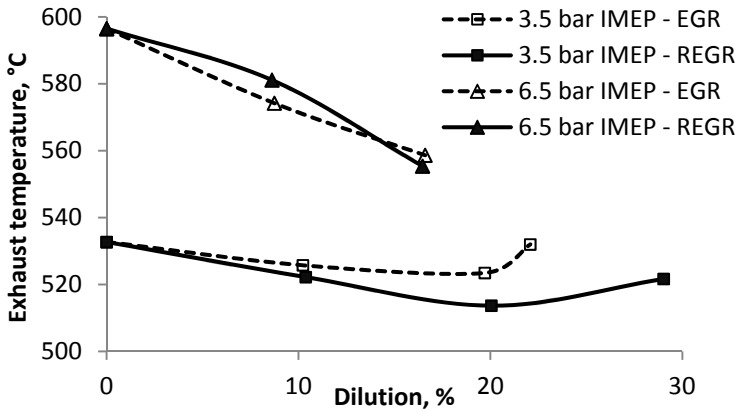

Figure 4.12 - Effect of dilution on exhaust gas temperature

4.2.4 Engine thermal efficiency

The primary objective of the exhaust gas fuel reforming process is to capture waste heat from the exhaust stream and convert it to usable energy in the form of gaseous fuel; therefore analysis of the overall system including the reforming process is required, as well as the standalone performance of the engine. Indicated efficiency is used to assess engine performance in terms of the work generated by the combustion process from the total fuel energy supplied to the cylinder in the form of gasoline and reformate. System efficiency instead uses the total energy of the gasoline supplied to the cylinder and to the reformer.

In this case, because there is no actual reforming process, only the indicated engine efficiency can be measured directly. System efficiency can be estimated by using the calculated

reforming process efficiency from the earlier reforming tests to approximate the amount of gasoline required to produce a given flow rate of reformate.

Figure 4.13 plots the change in indicated efficiency with dilution for 3.5 and 6.5bar IMEP. Taking first the lower engine load data, it is apparent that with EGR, efficiency was almost constant with only a slight increase up to 20% dilution before dropping off rapidly due to poor combustion stability. In contrast, for REGR the indicated efficiency drops off almost linearly as the fraction of gasoline replaced by reformate becomes larger with increasing REGR dilution.

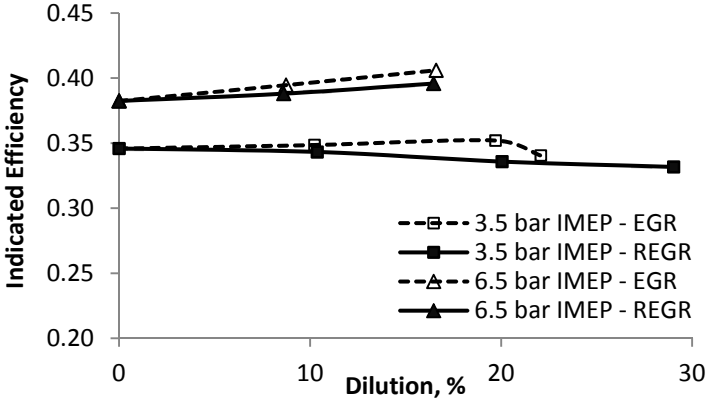

Figure 4.13 - Effect of dilution on Indicated Efficiency

At higher load the trend for both EGR and REGR was for increased indicated efficiency with dilution. This can be attributed to the increased intake manifold pressure as a result of de-throttling, which in turn leads to reduced pumping work. In addition, true MBT becomes achievable with dilution at higher load. It is clear, however, that the improvement in indicated efficiency is smaller for REGR. Presumably this deficit could be reduced to some extent with a higher maximum recirculation rate associated with REGR, as for 3.5bar IMEP.

In Figure 4.14 the estimated system efficiency has been plotted against inert fraction. The equivalent gasoline flow rate for each reformate flow rate was calculated, on an energy basis,

for a reforming process efficiency of 1.34. This representation indicates similar performance for both REGR and EGR. At higher load, both EGR and REGR show increased efficiency relative to the baseline gasoline condition. At lower load, the system efficiency for REGR was closer to that for EGR when accounting for the reforming process efficiency, but does not show an overall increase. These results indicate that to yield a more significant increase in system efficiency, the proportion of fuel processed by the reformer should be increased in order to recover more exhaust heat.

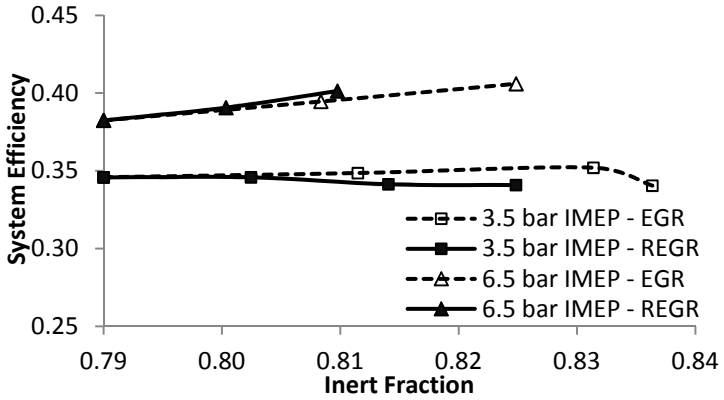

Figure 4.14 - Effect of inert fraction on system efficiency

4.2.5 Emissions

The concentration of NO_x in the exhaust stream was measured, and converted into an engine power specific value to eliminate the influence of the increased exhaust flow rate due to the additional nitrogen or reformate when operating with charge dilution. This allowed for a meaningful comparison to the baseline engine NO_x emissions. Figure 4.15a plots the reduction in specific NO_x emissions with charge dilution for both 3.5 and 6.5bar IMEP. At 3.5bar IMEP the NO_x emissions for both EGR and REGR were essentially the same for increasing dilution, however both showed a dramatic reduction compared to the baseline performance (0% dilution). A further reduction was made possible with REGR due to the higher achievable charge dilution, resulting in a 90% drop in engine-out specific NO_x.

Baseline engine condition NO_x emissions were almost doubled at 6.5bar IMEP due to the increase in engine load, but were reduced by half for approximately 15% charge dilution with both EGR and REGR. These significant NO_x reductions can be attributed to lower in-cylinder temperatures, resulting from the greater mass, therefore heat capacity, of the cylinder charge.

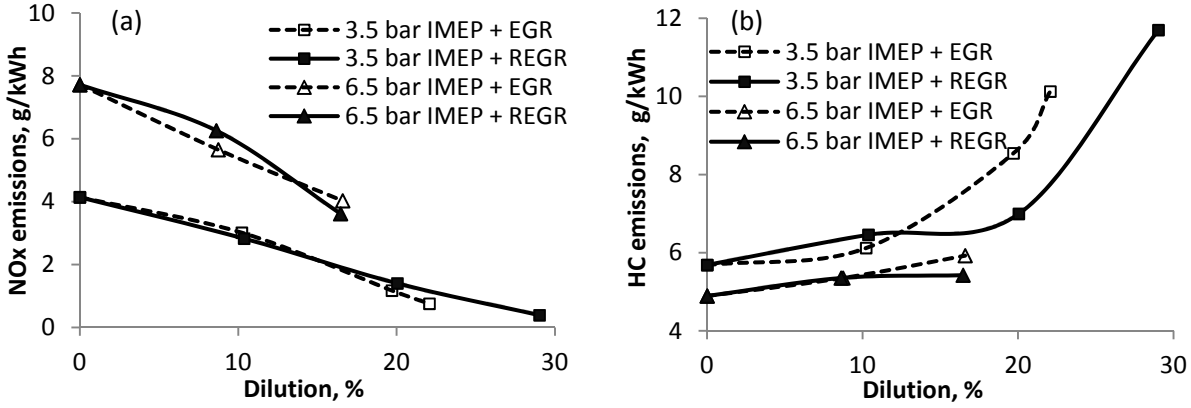

Figure 4.15 - Effect of dilution on specific NOx (a) and HC (b) emissions

Engine-out unburned HCs were also measured. Referring to Figure 4.15b, at 3.5bar IMEP the specific HC emissions were approximately doubled for maximum EGR and REGR compared to the baseline. It has already been shown that there was deterioration in combustion stability with increasing dilution at 3.5bar IMEP. The rapid increase in HCs after 10% dilution at 3.5bar IMEP signifies that higher cycle-to-cycle variations in combustion performance led to more occurrences of incomplete combustion, or misfires, and therefore unburned HCs. It is clear that REGR delays the increase in HC emissions, following a similar trend to that for combustion stability in Figure 4.5; specifically this means that at 20% dilution REGR, HC emission performance is improved by 18% relative to EGR.

A slight upward trend in specific HC emissions with increasing EGR, and to a lesser degree for REGR, is seen at 6.5bar IMEP. Lower in-cylinder temperatures associated with dilution result in a reduced rate of reaction in the late stages of combustion, i.e. towards the end of the

expansion stroke, and during the exhaust stroke. In a similar way, lower EGTs seen with dilution will have slowed down the rate of oxidation of unburned HCs in the exhaust manifold. Peak cylinder pressures were relatively consistent for all levels of dilution at each engine load, so differences in the amount of unburned mixture forced into crevice volumes is likely to have been small.

The increase in specific HCs is less significant for REGR, and can possibly be attributed to the replacement of HC fuel (gasoline) with gaseous fuel in the form of hydrogen and CO in the reformate. A more complete burn may also occur due to the homogeneous dispersal of hydrogen in the combustion chamber. The quench distance of hydrogen is also smaller than gasoline, 0.6mm compared to 2.8mm [69], meaning that the flame front may be able to penetrate further into crevice volumes, burning otherwise unburned HCs. Combustion stability was consistently good for all test points at this, higher engine load and so doesn't have any impact on HC emissions as for 3.5bar IMEP. Overall, REGR tends to reduce HC emissions relative to EGR, although performance is very similar for low levels of charge dilution, and a reduction in combustion stability due to either charge dilution method has a negative effect on HC emissions.

4.3 Summary

The results presented so far have shown how the combustion of reformate in a GDI engine can be beneficial to engine performance and emissions. Bottled reformate approximating an achievable composition from an exhaust gas fuel reformer was used to compare REGR to conventional EGR, and nitrogen was used to approximate EGR. Experimental work using a fuel reforming catalyst informed the selection of an achievable reformate composition.

The engine test results showed an improvement in combustion stability when operating with REGR relative to EGR, allowing for increased charge dilution. This implies that higher recirculation rates would enable a greater fraction of fuel to be reformed, thus increasing the potential for waste energy capture by an exhaust gas fuel reformer.

REGR results in a large NO_x reduction relative to the baseline gasoline condition, and a reduction in HCs relative to EGR. Additionally, REGR enables a wider range of usable ignition timings, which would lead to a lower efficiency penalty if additional NO_x suppression is required by ignition retard. REGR also reduces the tendency to knock.

Indicated efficiency is slightly reduced at low engine load by both EGR and REGR, while at higher engine load both yield increased indicated efficiency, although less so with REGR. Because of this, any increase in system efficiency with reformate of this quality would occur as a result of exhaust energy capture – i.e. from the associated increase in fuel enthalpy – and is not likely to be as a result of increased engine efficiency. Estimated system efficiency results that account for the possible fuel enthalpy increase due to a reforming process were also presented, showing that performance is comparable for EGR and REGR under the conditions tested.

The benefits of the combustion of reformate presented in this chapter are not as significant as those cited in the literature, where reformate with higher energy content has been used. It may be expected that REGR will perform better relative to real EGR, rather than the nitrogen approximation of EGR used here, because real EGR containing steam and CO_2 will have a greater influence on engine deterioration than nitrogen dilution. This will be investigated in the following chapter.

CHAPTER 5

IMPROVING THERMAL EFFICIENCY, EMISSIONS AND PM WITH REGR: A MULTI-CYLINDER GDI ENGINE STUDY USING SIMULATED REFORMATE

This chapter is concerned with simulating a REGR system on a multi-cylinder GDI engine, developing the research detailed in Chapter 4. When planning the experiments, further attention was placed on being able to generate a charge composition to more closely represent an engine operating with an exhaust gas fuel reformer. Firstly, a custom EGR system allowed real exhaust gas diluents to be included in the analysis, unlike in chapter 4 where nitrogen was used as the diluent. Secondly, the simulated reformate was not of pre-mixed composition; instead, a hydrogen/ CO mixture was added to the EGR flow to create a REGR-like charge composition, allowing more flexibility for varying the reformate quality, i.e. the hydrogen and CO concentration. Emphasis was placed throughout on comparing performance with REGR to the baseline gasoline engine, and also to engine performance with conventional EGR. Following further catalyst testing at Johnson Matthey, the reformate composition that may be expected from an exhaust gas fuel reformer was re-considered.

5.1 Preliminary results [2]

The preliminary results in this section were used to inform the selection of test conditions for the investigations presented later in this chapter.

[2] Parts of this section appear in a research article published by the Int. J. Hydrogen Energy [18]

5.1.1 Establishing valve timings for low exhaust residuals

Because of the influence that EGR and REGR has on reducing combustion stability, it was important to establish suitable valve timings that result in low trapped exhaust residuals (internal EGR) in order to maximise the achievable REGR rate; ultimately, this equates to increasing the reformed fuel fraction and the potential for exhaust heat recovery with a real fuel reformer.

Suitable valve timings were determined by analysing the effects of modifying the VCT settings on burn rate, combustion stability, emissions (mainly NO_x) and manifold pressure; taken as a whole, this information quickly gives an indication of the relative concentration of trapped exhaust residuals.

The engine was operated without external EGR at the conditions specified in Table 5.1, and ignition timing sweeps were performed for a selection of intake and exhaust valve timing combinations. The scripting application of the ECU interface software was used to automate the ignition timing and valve timing sweeps. Figure 5.1 displays some data traces recorded during one script run. This facility was re-used for EGR and REGR conditions in later tests. Data was recorded for each valve timing setpoint at the MBT ignition timing, and the results are summarised in Figure 5.2.

Table 5.1 - Engine conditions during valve timing selection

Engine speed	2100rpm	Air (post-intercooler) temp	30°C
Engine load	35Nm	Fuel temp	28°C
External EGR	0%	Fuel pressure	5.1 MPa
AFR	λ= 1	Start of injection timing	305 °bTDC
Engine Coolant exit temp	95°C		

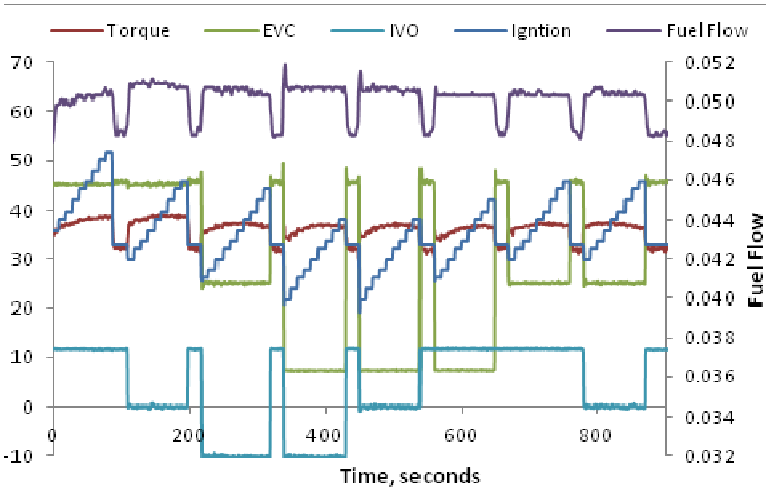

Figure 5.1 - Ignition timing and valve timing sweep

The ECU limits for IVO retard and EVC advance were 11° and 8°aTDC respectively. The standard homologated ECU calibration valve timing at the test point in question was 11° IVO and 45° EVC. The results for the baseline calibration valve timing are indicated by a dashed border in Figure 5.2. In general the results suggest lower exhaust residuals towards the upper left of the valve timing matrix, where the combined valve timings result in a relatively short overlap period centred close to TDC. This is immediately obvious from the retardation of MBT ignition timings relative to the baseline, where later ignition timing implies a faster burn rate. This is confirmed by the combustion duration data; both the early combustion (MFB0-10%) and main combustion (MFB10-90%) durations are shortened towards the top left of the matrix.

Combustion stability was good for all valve timings at MBT, with COV of IMEP values consistently below 2%, and so wasn't useful as an indicator of trapped residuals. It should be noted that the standard calibration does not use MBT ignition timing at this engine condition, instead using ignition retard of approximately 8°, presumably for NO_x suppression and to reduce the pumping work by raising the intake manifold pressure. With retarded ignition

timing, combustion stability performance worsens to 4% COV of IMEP, close to the 5% limit, and MFB10-90% combustion duration is increased to 32°CA.

MBT ignition timings

	EVC				
IVO	**8**	**15**	**25**	**30**	**45**
-10	29		32		
0	28		30		34
11	32	32	34	35	40

Combustion stability, COV of IMEP

	EVC				
IVO	**8**	**15**	**25**	**30**	**45**
-10	1.7				
0	1.5		1.8		
11	1.9	1.8		1.9	1.9

Combustion duration, MFB 10-90% (°CA)

	EVC				
IVO	**8**	**15**	**25**	**30**	**45**
-10	23.5				
0	26.1		28.2		
11	26.0	25.1		28.1	29.1

Combustion duration, MFB 0-10% (°CA)

	EVC				
IVO	**8**	**15**	**25**	**30**	**45**
-10	26.2				
0	25.5		27.9		
11	28.4	28.3		31.2	37.1

Indicated efficiency

	EVC				
IVO	**8**	**15**	**25**	**30**	**45**
-10	0.272				
0	0.276		0.282		
11	0.274	0.278		0.272	0.281

Engine-out NO_X (ppm)

	EVC				
IVO	**8**	**15**	**25**	**30**	**45**
-10	2042				
0	2002		1697		
11	2038	-		-	952

Manifold pressure (mbar)

	EVC				
IVO	**8**	**15**	**25**	**30**	**45**
-10	400				
0	406		420		
11	433	444		433	487

Pumping work, PMEP (bar)

	EVC				
IVO	**8**	**15**	**25**	**30**	**45**
-10	0.65				
0	0.63		0.63		
11	0.60	0.60		0.62	0.59

Valve overlap period (°CA)

	EVC				
IVO	**8**	**15**	**25**	**30**	**45**
-10	18	25	35	40	55
0	8	15	25	30	45
11	-3	4	14	19	34

Overlap midpoint timing (°aTDC)

	EVC				
IVO	**8**	**15**	**25**	**30**	**45**
-10	-2	3	8	10	18
0	4	8	13	15	23
11	9	13	18	21	28

Figure 5.2 - A selection of results across the valve timing test matrix used to establish valve timings for low exhaust residuals

Of the valve timings tested, -10° IVO and 8° EVC showed combustion performance indicating the lowest trapped exhaust residuals. This was supported by the highest NO_x emissions occurring at this valve timing. Indicated efficiency was 1% lower than the baseline valve timing (at MBT) due to the lower intake manifold pressure and associated increased pumping loss. These valve timings were selected as the low exhaust residuals condition to be used in the low engine load REGR combustion study in section 5.2.1.

5.1.2 Selection of appropriate reformate composition

The reformate composition that may be expected from an exhaust gas fuel reformer was re-considered following further reformer catalyst performance tests at Johnson Matthey. In particular, it was important to determine the hydrogen/CO ratio as these fuels would be supplied from a single compressed gas cylinder. Figure 5.3a shows the variation of hydrogen/CO ratio with temperature for a selection of Pt-Rh catalyst formulations and loadings. The experimental results are also plotted against those predicted by a thermodynamic model that is closely matched at all temperatures by the 2%Pt-1%Rh catalyst loaded at 2.5g/in^3.

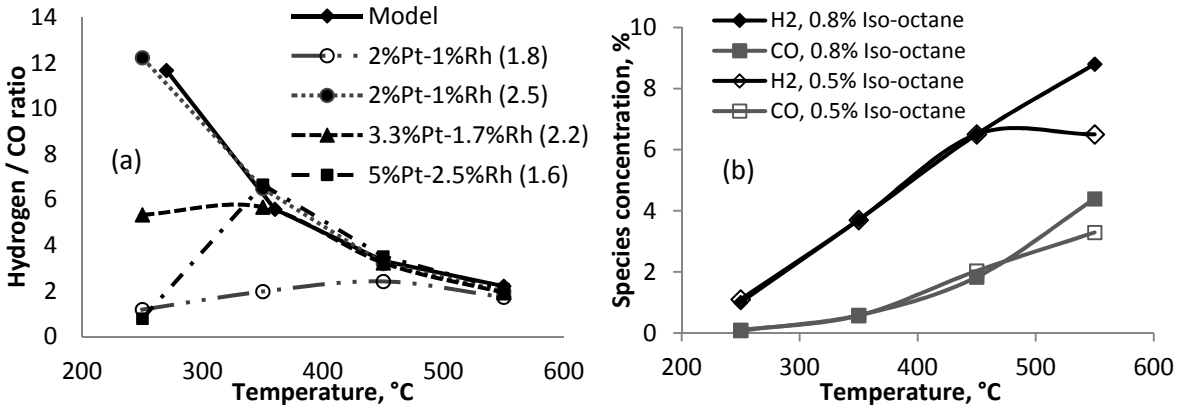

Figure 5.3 - a) H_2/CO ratio in reformate produced by Pt-Rh reforming catalysts with various formulation and loading (g/in^3), b) Hydrogen and CO yields with the 2%Pt-1%Rh (2.5g/in^3) reformer catalyst, with 0.5% and 0.8% iso-octane in the feed gas [Data courtesy of Johnson Matthey]

A fixed 3:1 H_2/CO ratio was selected to be used throughout the study, based on the Pt-Rh catalyst performance in the region of 500°C. This was anticipated to be the least favourable but still functional temperature for fuel reforming, corresponding to a GDI engine operating at low load.

5.2 Engine thermal efficiency, gaseous emissions and PM emissions with REGR [3]

Using the information gained in the preliminary tests, a series of studies were designed to establish the effect of a REGR system on combustion performance, engine efficiency, gaseous emissions and PM emissions. The two engine conditions selected for investigation were:

- Low load: 35Nm (3bar IMEP) at 2100rpm, which represents a key steady state condition in the urban section of the new European drive cycle (NEDC) for a typical mid-size/large family vehicle with this 2L engine
- Middle load: 105Nm (7.2bar IMEP) at 2100rpm which is typical of the highest load transient in the extra-urban drive cycle

The baseline GDI engine condition was compared to each EGR and REGR condition with the ignition timing optimised for MBT. The HP-EGR system configuration was used throughout. Injection timing, fuel pressure and other engine parameters were held at the standard calibration values, with the exception of cam phasing that was varied for the low engine load condition. Engine performance was assessed at increasing EGR and REGR rates until the combustion stability limit was reached, again defined by the COV of IMEP exceeding 5%.

In section 5.2.1 the low engine load condition will be considered, followed by results from the mid-load condition in section 5.2.2. A full system analysis attempts to predict the total

[3] Sections 5.2.1 to 5.2.4 have been published in a research article by the Int. J. Hydrogen Energy [18]

engine-reformer system efficiency in section 5.2.3. An investigation into the influence of EGR and REGR on PM emissions is presented in section 5.2.4. Section 5.2.5 takes a brief look at the influence of increased charge air temperature with EGR dilution on engine efficiency, with consideration for cooling requirements.

5.2.1 Low-load engine performance and gaseous emissions with REGR

In order to test the effect of reformate quality on engine performance, the flow rate of the hydrogen/CO gas mixture was adjusted at a range of REGR dilution rates so that the total volumetric combustible gas fraction in the REGR was 0.05 or 0.1. Therefore, the hydrogen concentration in the REGR stream at each condition would be 3.75% or 7.5% respectively, with 1.25% or 2.5% CO. The hydrogen concentration in the intake charge at each test point is shown in Table 5.2, which also specifies the energy fraction of the total fuel supplied as reformate (hydrogen and CO) for each test.

Initially the engine retained the standard calibration valve timings, which employ a late, high overlap configuration that results in a high residual gas fraction for reduced pumping work and low NO_x formation at low engine load.

Table 5.2 - Hydrogen concentration in REGR stream and intake charge

	REGR combustible gas fraction	**Percentage REGR**			
		7%	**14%**	**21%**	**28%**
REGR stream hydrogen, %	0.05	3.8%			
	0.1	7.5%			
Intake hydrogen concentration, %	0.05	0.2%	0.5%	0.7%	1.0%
	0.1	0.5%	1.0%	1.5%	2.0%
Reformate energy fraction, %	0.05	1.6%	3.7%	6.1%	8.8%
	0.1	3.2%	7.3%	12.5%	17.7%

For the standard calibration valve timing, indicated efficiency (Figure 5.4a) was initially increased with EGR due to reduced pumping work and lower heat losses. As the EGR rate was increased further the efficiency dropped off due to a reduction in combustion stability to the point of misfire (Figure 5.4b). Combustion durations increased monotonically with dilution rate, more significantly for the initiation phase than the main combustion phase; these are represented by the MFB0-10% and MFB10-90% durations in Figure 5.4c and d. This deterioration in combustion speed was associated with the increasing inert gas fraction.

Significantly increased unburned HCs at the higher EGR rates was caused by the deterioration of combustion stability and the resulting misfire (Figure 5.4e). Lower in-cylinder temperature with EGR also reduced the rate of post-combustion HC oxidation. As expected, NO_x emissions dropped with increasing EGR (Figure 5.4f). This is again due to reduced combustion temperature, which decreases the rate of NO_x formation; the thermal dilution effect of the inert gases in the charge with EGR (i.e. greater total heat capacity) coupled with the reduction of the heat release rate reduce the in-cylinder temperature. This counters any incremental increase in temperature due to higher cylinder pressure (associated with greater charge mass) or advanced ignition timing. EGR dilution also leads to a slightly lower oxygen concentration in the charge and the exhaust stream; if the oxygen concentration is also lower while the temperature is sufficiently high for NO_x formation, then it follows that the rate of NO_x formation would be reduced.

The indicated efficiency for REGR was slightly lower relative to EGR for the same dilution rate, until the combustion stability with EGR deteriorated. For REGR the COV of IMEP remained below 5%, indicating that the hydrogen/CO in the REGR had a stabilising effect on combustion. These figures also show that an incremental increase in combustion rate was achieved with REGR relative to EGR, for a given dilution rate. This was attributed to the

beneficial combustion properties of hydrogen, in particular the higher laminar flame speed [68], which explains the large reduction in the flame initiation period (MFB 0-10%) when combustion is primarily laminar.

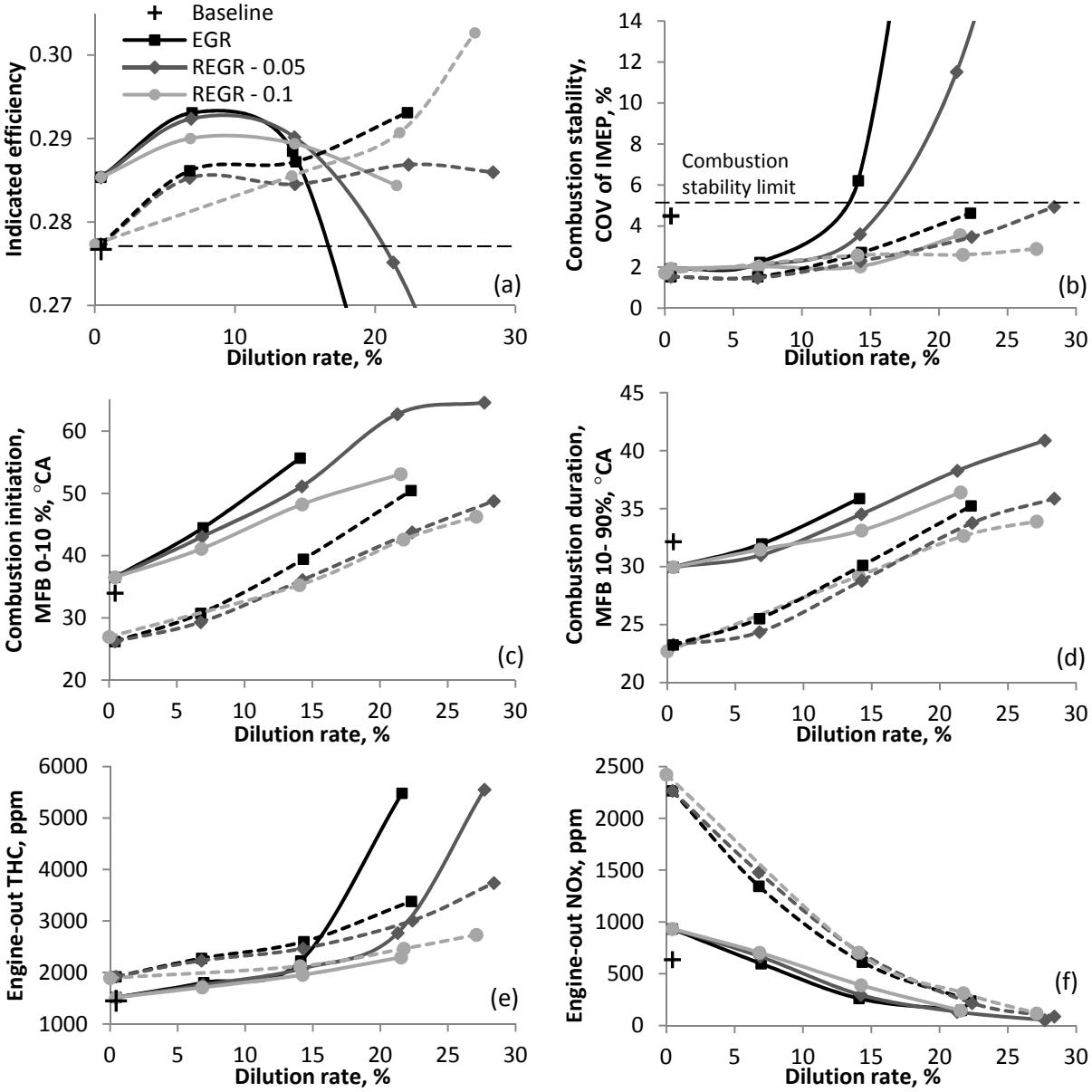

Figure 5.4 - Effect of EGR and REGR dilution rate on various engine performance parameters a) indicated efficiency, b) combustion stability, c) combustion initiation duration, d) main combustion duration, e) engine-out THC and f) engine-out NO_x

Standard valve timings (solid lines); valve timings for low exhaust residuals (dashed lines)

The mechanisms for reducing NO_x formation with EGR are also applicable to REGR due to the very similar charge composition, and the net result is again significantly reduced NO_x emissions with respect to the baseline condition. However, the higher adiabatic flame temperature of hydrogen and CO compared to gasoline and slightly faster combustion result in higher in-cylinder temperature, leading to slightly increased NO_x formation rate for REGR relative to EGR. For the same reason HC oxidation is increased and HC emissions are lower.

As anticipated, the results obtained with the standard valve timings confirm that the level of exhaust residuals should be reduced in order to increase the achievable REGR rate, and increase the concentration of hydrogen and CO in the charge. Therefore, the valve timings for low exhaust residuals determined in section 5.1.1 (IVO at -10°aTDC and EVC at 8°aTDC) were adopted and the REGR and EGR test points repeated.

When there was no external charge dilution, altering the valve timings to the low exhaust residuals setting reduced the indicated efficiency (Figure 5.4a), primarily due to lower intake manifold pressure that increased the pumping work. The introduction of external dilution improved indicated efficiency monotonically up to the dilution limit, which was extended to 21% for EGR and 28% with REGR. The peak efficiency achieved with the EGR dilution method was very similar for both valve timings, albeit while using very different external EGR rates. This implies that the total dilution rate (internal + external EGR) was similar in both cases, supported by comparable emissions and combustion results (Figure 5.4b-f).

It is apparent that the presence of hydrogen and CO in REGR, in low concentration, does not lead directly to improved indicated efficiency relative to EGR; however, the possibility to operate the engine with higher overall dilution rate does. This is also combined with significantly reduced NO_x emissions and only moderately increased HCs.

5.2.2 Mid-load engine performance and gaseous emissions with REGR

The following section presents results for the engine operating at a higher, mid-load condition of 105Nm/7.2bar IMEP at 2100rpm. The target dilution rate was 21%, the maximum achievable with the HP-EGR system under these manifold conditions. The ignition timing was set for either optimum combustion phasing (defined by MFB50% = 8° ± 2°aTDC) or knock-limited timing minus 2°CA. For this condition, higher combustible gas fractions in REGR of 0.1 and 0.15 were used. This was based on the knowledge that higher engine load will raise the exhaust and reformer temperature, and should lead to generally higher hydrogen and CO yields [79]. Table 5.3 defines the conditions for the 7.2bar IMEP tests and the results are summarised in Table 5.4. Combustion was stable for all test conditions at this engine load.

Table 5.3 - Test conditions at 7.2bar IMEP, 2100rpm

Test point	Dilution rate, %	H_2,% REGR	CO,% REGR	H_2,% intake	CO,% intake	REGR energy, %	Ignition, °bTDC	Manifold pressure (bar)
Baseline	0	0	0	0	0	0	21	0.85
EGR	21	0	0	0	0	0	44	1.00
REGR (0.1)	20	8.1	2.7	1.8	0.6	9	33	1.01
REGR (0.15)	20	11.9	4.0	2.8	0.9	15	31	1.02

Table 5.4 - Summary of results for 7.2bar IMEP at optimum ignition timing

Test point	η_{ind} [1]	$\Delta\eta_{ind}$ (%) [2]	Specific emissions, g/kWh			η_{comb} [3]	EGT [4]	EGT [5]	PMEP (bar)
			HC	NO_x	CO				
Baseline	0.340	0	2.4	16.0	28.6	0.960	743°C	727°C	-0.47
EGR	0.356	+4.7	3.9	2.6	20.6	0.962	655°C	645°C	-0.34
REGR 0.1	0.357	+4.8	3.3	2.7	17.5	0.967	661°C	642°C	-0.33
REGR 0.15	0.354	+4.0	3.0	3.0	16.4	0.970	658°C	635°C	-0.31

[1] Indicated engine efficiency; [2]Percentage increase in efficiency;
[3]Combustion efficiency; [4] Pre-turbine EGT; [5]Post-TWC EGT

The effect of EGR on combustion was, as expected, to reduce the burn rate. As was the case at lower engine load this was most significant in the ignition phase of combustion, indicated in Figure 5.5 by longer MFB0-10% duration. Figure 5.5 also shows that the trend was similar but less pronounced for the main combustion phase duration.

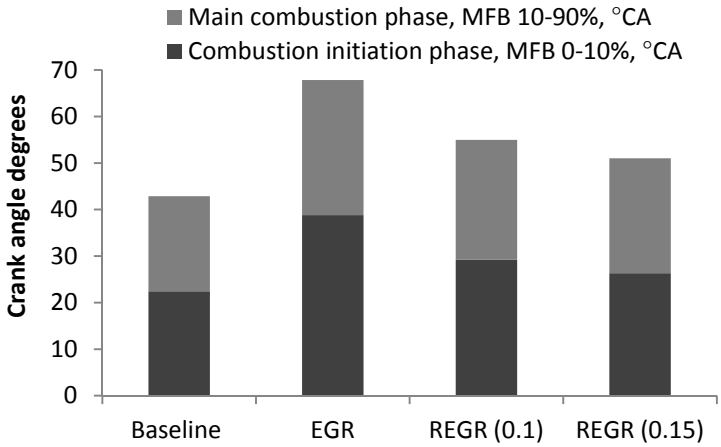

Figure 5.5 - Combustion phase durations at 7.2bar IMEP

HC emissions were almost doubled by EGR due to lower cylinder temperatures and reduced oxidation rate, but despite these effects the combustion efficiency was maintained (Table 5.4). This can be attributed to the simultaneous reduction in CO emissions, which also reduces the estimated value for hydrogen concentration in the exhaust stream (Equation 3.5). Together these offset the reduction of combustion efficiency caused by increased unburned HCs.

Similarly to the low engine load results, the presence of hydrogen and CO in the charge for REGR influenced combustion by increasing the burn rate towards that of the baseline case, and resulted in further improvements to combustion efficiency. Slightly higher combustion temperatures relative to EGR led to an incremental increase in NO_x formation and HC oxidation rates. Despite this, REGR offers greater than 80% reduction in NO_X compared to the baseline.

The simultaneous reduction of CO and slightly increased NO_x with REGR may have implications for TWC operation, with regards to the suitable ratio of reducing and oxidising species in the feed gas. The CO/NO_x ratio with REGR remains favourable to remove NO_x by the CO reduction mechanism; in fact, this ratio is increased when compared to the baseline. It may be the case that complete conversion of CO is not possible if NO_x becomes too low, in which case more oxygen should be made available in the exhaust stream. This may be achieved with engine control by shifting the stoichiometry fluctuations in the lean direction. This would also restore the overall reducing/oxidising balance by incrementally increasing NO_x formation and reducing CO and HCs.

The improvement to indicated efficiency with EGR (Table 5.4) was attributed to optimised combustion phasing and slightly lower pumping work due to the increased intake manifold pressure. In addition, lower combustion temperatures reduce the rate of heat loss from the combustion chamber. Indicated efficiency for REGR with both compositions was similar to that of EGR. It seems that the addition of hydrogen and CO provides no further efficiency benefit for the same recirculation rate, even though the hydrogen concentration in REGR was higher at 7.5% and 11.25%. The incremental improvement in combustion efficiency with REGR was not sufficient to improve indicated efficiency compared to EGR.

Dilution with either EGR or REGR allowed for the combustion phasing to be advanced closer to the optimum, apparent by the advancement of the MFB50% timing from 12°aTDC (knock-limited) for the baseline to 7°aTDC for each of the other conditions, visible in the MFB curves of Figure 5.6. This supports previous research that has shown EGR dilution [26, 28, 29] and hydrogen enhancement [71, 118] to be effective for attenuating knock.

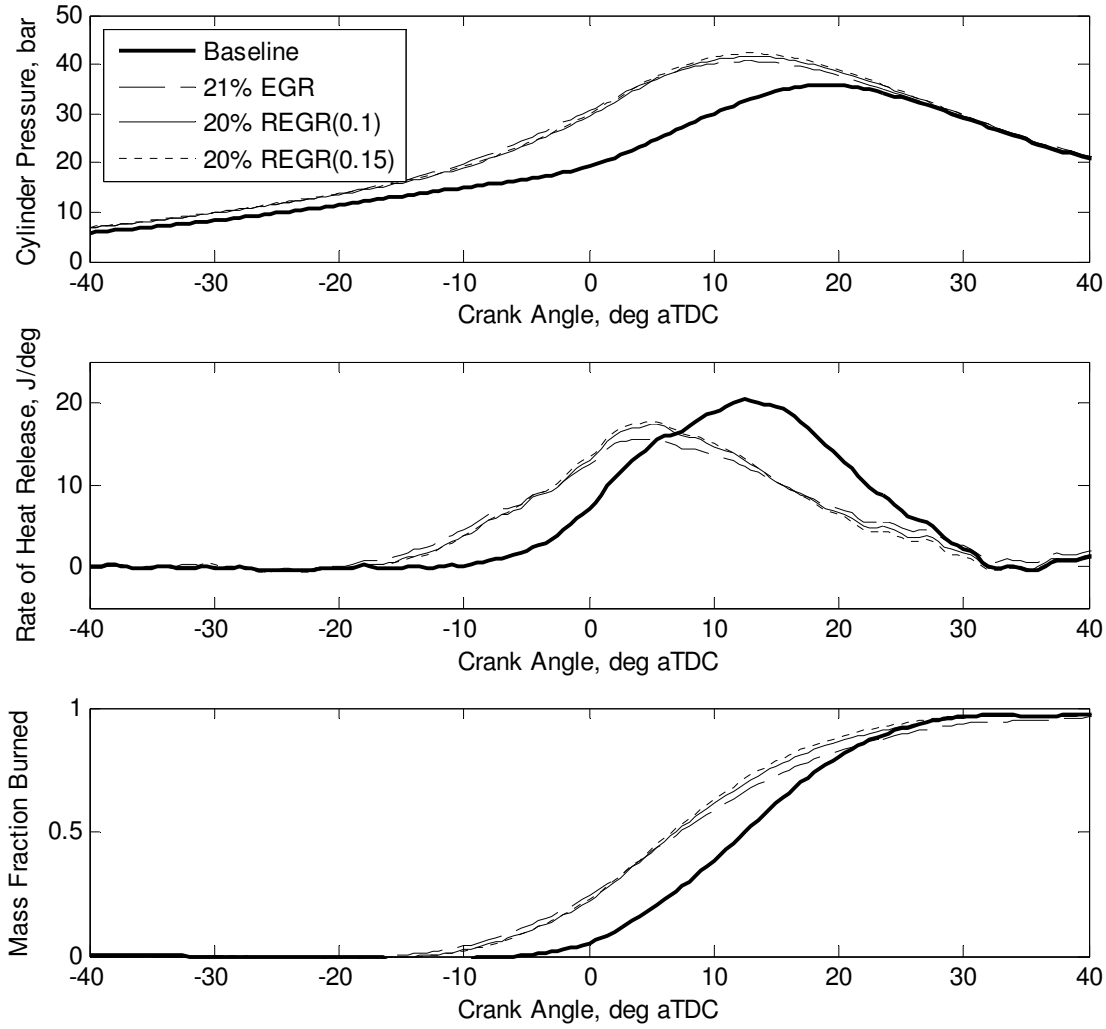

Figure 5.6 - In-cylinder pressure, rate of heat release and MFB curves for the baseline gasoline combustion, and diluted combustion with EGR and REGR

Figure 5.6 also shows that higher peak cylinder pressures are generated with dilution, which is due to the increased charge mass relative to the baseline. Studying the rate of heat release curves it is seen that the baseline gasoline combustion process is appreciably retarded from the optimum (due to knock) meaning that the combustion process is releasing energy at the highest rate once the piston is too far into the expansion stroke. This ultimately reduces efficiency as it is a poor approximation of the idealised constant volume combustion process that is characteristic of the Otto cycle. Although the maximum rate of heat release is lower with diluted combustion, the position of the maximum is advanced much closer to TDC. It is

also obvious that the hydrogen and CO in REGR results in a higher maximum rate of heat release than for EGR, meaning that marginally less energy is released during the compression stroke and also later in the expansion stroke, and so represents a closer approximation to constant volume combustion.

5.2.3 System efficiency for a GDI engine operating with a fuel reformer

The following section provides an estimate of the total engine-reformer system efficiency, accounting for the exhaust heat recovery that might be achieved by an exhaust gas fuel reformer. First, the reforming process efficiency was calculated. This considers the change in enthalpy of the portion of gasoline converted to gaseous fuel by a reformer, which in this case excludes any gasoline that breaks through unreacted. This approach was most suitable here because the simulated reformate contains no HC component. Therefore, HCs that would enter the combustion chamber as part of the reformate following a real reforming process were, in these tests, supplied as normal via the fuel injector.

Experimental data from the reformer catalyst tests in section 5.1.2 were applied to Equation 5.1 in order to estimate the reforming process efficiency, where LHV_X is the lower heating value of species x, $\dot{m}_{g,ref,in}$ represents the mass flow of gasoline into the experimental reformer, and the mass flows of hydrogen, CO and methane are products in the reformate. The reformer process efficiency can be considered a fuel enthalpy multiplier that represents the change in total fuel enthalpy during the reforming process, and as such may be less than or greater than one. The reformer process efficiency was calculated to be η_{ref} = 1.1 at 550°C with 0.5% feed gas fuel.

$$\eta_{ref} = \frac{LHV_{H2}.\dot{m}_{H2} + LHV_{CO}.\dot{m}_{CO} + LHV_{CH4}.\dot{m}_{CH4}}{LHV_g.(\dot{m}_{g,ref,in} - \dot{m}_{g,ref,out})} \qquad \text{Equation 5.1}$$

A prediction of total engine-reformer system efficiency was then calculated using Equation 5.2 for the best performing REGR condition at each load tested, detailed in Table 5.5. Indicated engine efficiency ($\eta_{eng,ind}$) relates to the engine as used in this study, operating with gasoline, EGR, hydrogen and CO to simulate reforming. Indicated system efficiency ($\eta_{sys,ind}$) assumes the engine operates with an integrated reformer that has a reformer process efficiency (η_{ref}) of 1.1 or 1.3. The larger value represents a more optimistic prediction of reformer performance, which may be achieved with operation at higher temperature or following further catalyst development. The delta engine and system efficiencies ($\Delta\eta$) in Table 5.5 are relative to the baseline GDI engine performance at each engine load, and predict the potential benefit of using a fuel reformer integrated with a GDI engine to improve thermal efficiency.

$$\eta_{sys,ind} = \frac{\dot{W}_{ind}}{LHV_g . \dot{m}_{g,eng} + \left(\frac{LHV_{H2} . \dot{m}_{H2} + LHV_{CO} . \dot{m}_{CO}}{\eta_{ref}}\right)} \qquad \text{Equation 5.2}$$

Table 5.5 - Predicted total engine-reformer system performance ($\eta_{sys,ind}$) based on two possible reformer process efficiencies (η_{ref})

			$\eta_{ref} = 1.1$		$\eta_{ref} = 1.3$	
Engine condition	$\eta_{eng,ind}$	$\Delta\eta_{eng,ind}$	$\eta_{sys,ind}$	$\Delta\eta_{sys,ind}$	$\eta_{sys,ind}$	$\Delta\eta_{sys,ind}$
3bar IMEP, 2100rpm 28% REGR (0.1) IVO = -10°/EVC = 8°	0.299	+7.9%	0.303	+9.1%	0.308	+11.1%
7.2bar IMEP, 2100rpm 20% REGR (0.1)	0.357	+4.8%	0.360	+5.7%	0.365	+7.1%

Finally, it is accepted that diluted combustion leads to lower EGT, which clearly has implications for the operation of an exhaust gas heated fuel reformer. For example at the 3bar IMEP engine load the EGTs (pre-turbine and post-TWC) were reduced from around 650°C

for the baseline condition to 550°C for REGR. Using REGR resulted in a slight increase in pre-turbine EGT relative to EGR (Table 5.4) due to higher combustion temperature. One result that was not anticipated was the influence of REGR on lowering the post-TWC EGT. The oxidation of unburned combustion products normally induces a rise in temperature across the TWC, but because the REGR combustion process is more complete and the exhaust contains lower HCs and CO this effect is reduced and the resulting EGT is lower. This fact could be important for future reformer design and integration.

5.2.4 Influence of EGR and REGR on PM emissions

At elevated engine load, PM formation in GDI engines becomes more significant than at lower load. The mid-load, 7.2bar IMEP engine condition studied in section 5.2.2 was used to examine the effects of EGR and REGR on reducing PM emissions. The same general test conditions were used, with the addition of 14% EGR and REGR test points in order to identify the influence of dilution rate on PM emissions. Of particular interest was whether the presence of hydrogen and CO in REGR would enable a further PM reduction over that achieved by conventional EGR.

The formation of PM by nucleation of volatile species in the exhaust stream, and the adsorption of volatile species onto existing solid particles are processes that occur primarily during cooling and dilution of the exhaust gas [24]; for instance at the tailpipe exit, or in the PM sampling system. In these experiments, the PM sampling system was positioned after the TWC to minimise the influence of these two mechanisms on measurement variability, on the basis that the TWC removes the majority of the volatile fraction from the exhaust stream. Heated dilution also aimed to limit nucleation mode particle formation.

Figure 5.7 illustrates the benefit that both EGR and REGR have on reducing total PM number and mass relative to the baseline gasoline condition. Further to that, REGR results in lower PM emissions compared to EGR. This reduction in PM with EGR dilution is opposite to when cooled EGR is used in diesel engines. Because the average exhaust stream oxygen concentration is low and essentially fixed (0.5 - 0.8% for effective TWC operation) and the combustion temperatures with EGR are lower, it follows that the rate of PM oxidation in the end-gas is reduced so it may be logical to expect an incremental increase in PM emissions. This is clearly not the dominant effect though, so there must be other mechanisms leading to reduced PM emissions. Hedge et al. conclude in their work that "EGR significantly inhibits the nucleation of the particles, to the extent that it overcomes the decrease in post-flame oxidation and the increased potential for agglomeration" [30]. There has been only a limited amount of research that demonstrates this effect of EGR on PM emissions in GDI engines, and as yet no fundamental research has established the exact mechanisms at work. That said the reduced in-cylinder temperature with EGR will inhibit both soot formation and oxidation.

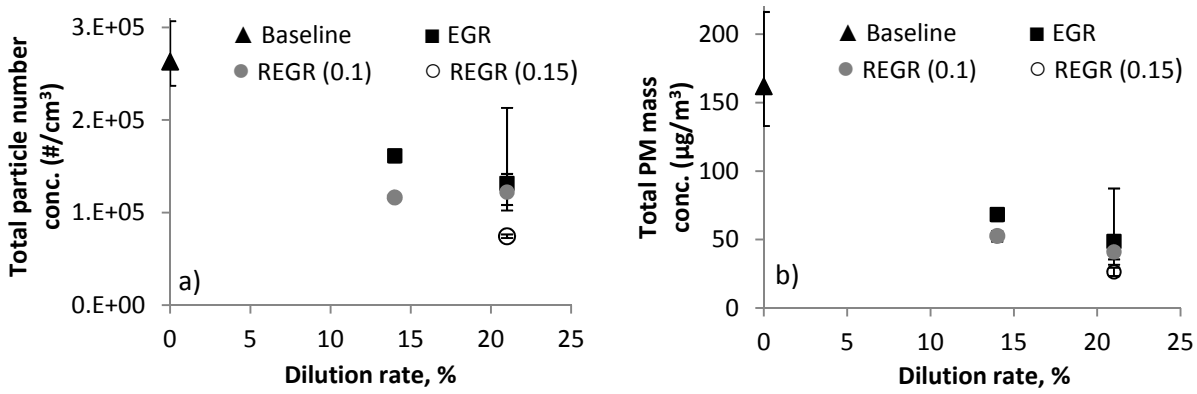

Figure 5.7 - Total PM number (a) and mass (b) concentration for a range of conditions at 7.2bar IMEP/2100rpm

Another reason for lower PM formation can be attributed to the fact that EGR improves engine efficiency. Therefore, for a given engine load, a smaller quantity of fuel is injected into

the cylinder compared to the baseline condition and will lead to proportionally less PM being formed.

As well as this, in order to maintain engine load with the induction of EGR, the charge mass must be increased by raising the intake manifold pressure. The rate of mass transfer (and therefore kinetic energy) through the intake valve must be higher than for the baseline case. The influence of greater charge motion could be improved mixing, fuel vapourisation and charge homogeneity. Although this effect is difficult to quantify without thorough experimental or simulation effort, it could feasibly be leading to an incremental reduction of locally fuel rich regions where particles are formed.

A clear reduction in PM formation occurs with REGR due to the presence of hydrogen and CO. This reduction is seemingly monotonic as the reformate quality improves, i.e. the hydrogen and CO concentration increases. This is partly due to the decreasing proportion of the total fuel injected as gasoline, meaning that there is less liquid fuel to be vaporised and mixed; as a result there should be fewer fuel droplets and rich regions that remain once combustion begins. There is also a shorter injection duration associated with the reduced volume of gasoline injected, which means that the end of injection is earlier (because the SOI is fixed at 294° bTDC); therefore the fuel spray is less likely to impinge the piston top and there is more time available for vaporisation. The incrementally higher combustion temperature due to higher hydrogen and CO flame temperatures will also assist in HC and PM pre-cursor oxidation.

Because of the fixed H_2/CO ratio in these tests it is not possible to determine the individual contribution from either species on influencing PM formation. Previous research into hydrogen enhanced gasoline combustion [39] has indicated that hydrogen initiates a

significant reduction in nucleation mode particle number, by around 96% with 6% hydrogen (energy fraction). The reduction was less pronounced for accumulation mode particles, but still of the order of 90%. Guided by work elsewhere on soot formation in ethylene-hydrogen flames [119], it was concluded that hydrogen addition inhibits soot nucleation by slowing or reversing the hydrogen abstraction reaction, the mechanism by which polycyclic aromatic hydrocarbons grow to form soot. It seems likely that this route to reduced PM formation is applicable here.

Fundamental combustion studies have proven CO addition to ethylene [120] and acetylene [121] flames to be effective for reduced PM formation. Although these works derived that the chemical effect of CO is to enhance PM formation, overall PM formation was reduced due to the dominance of the dilution and thermal effects. The application of the current study differs in that the molar charge concentration of CO is low (<1%), and the large proportion of CO_2, steam and nitrogen in the charge will render the dilution and thermal effects of the CO insignificant. It is possible then that the chemical effect of CO will lead to an incremental increase in PM formation in this case, but it is offset by the presence of hydrogen.

The advanced ignition timing shift required for diluted combustion will tend to increase PM formation to some degree by allowing less time for charge mixing, meaning that more locally fuel-rich regions remain during combustion. This effect should not be as pronounced for the 'homogeneous charge' GDI engine compared with stratified charge GDI or diesel engines as the early injection timing (294° bTDC in this case) means that the increment of time lost for charge mixing with advancing ignition will be small relative to the overall time between injection and ignition. With REGR the ignition timing is retarded from that with EGR, which may be contributing factor that reduces PM with REGR. Ignition timing variation also alters the prevailing in-cylinder conditions during combustion and post-combustion, which has a

significant influence on the formation and destruction of soot pre-cursors and soot, and therefore may influence overall PM emissions more than the charge mixing effect. This will be revisited in section 5.3.3.

Ultimately, the nucleation of PM in the combustion chamber is heavily influenced by the gas-phase and liquid-phase fuel concentrations, along with temperature [66]. For the various reasons discussed above, it is likely that both the gas-phase and liquid-phase fuel concentrations are reduced by the use of EGR, and more so by REGR, leading to lower PM nucleation. Similarly, the in-cylinder temperature is lower with EGR and REGR during the period when PM formation occurs.

Figure 5.8 plots the particle size distributions for number and mass concentration. These are included to provide information on the influence of REGR on particle size, which is important when considering the negative health and environmental effects of PM. Particles with smaller diameter are considered more detrimental to health. The distributions show no evidence of bi-modal distribution normally associated with the nucleation and accumulation modes. A similar, uni-modal particle size distribution has been seen with post-TWC exhaust sampling from a PFI gasoline engine [67].

The geometric number mean particle diameter (GNMD) for the baseline case was 58nm, and the addition of EGR reduced the GNMD substantially to 51nm. An increase in primary particles with larger diameter might reasonably be expected with EGR because the lower post-flame temperature increases the rate of particle surface growth [66] as well as decreases the rate of particle oxidation. However this effect doesn't appear to lead to a larger GNMD. The addition of hydrogen and CO in the charge with REGR does not strongly influence the

mean particle diameter with respect to EGR, but does serve to further reduce the particle count across the range.

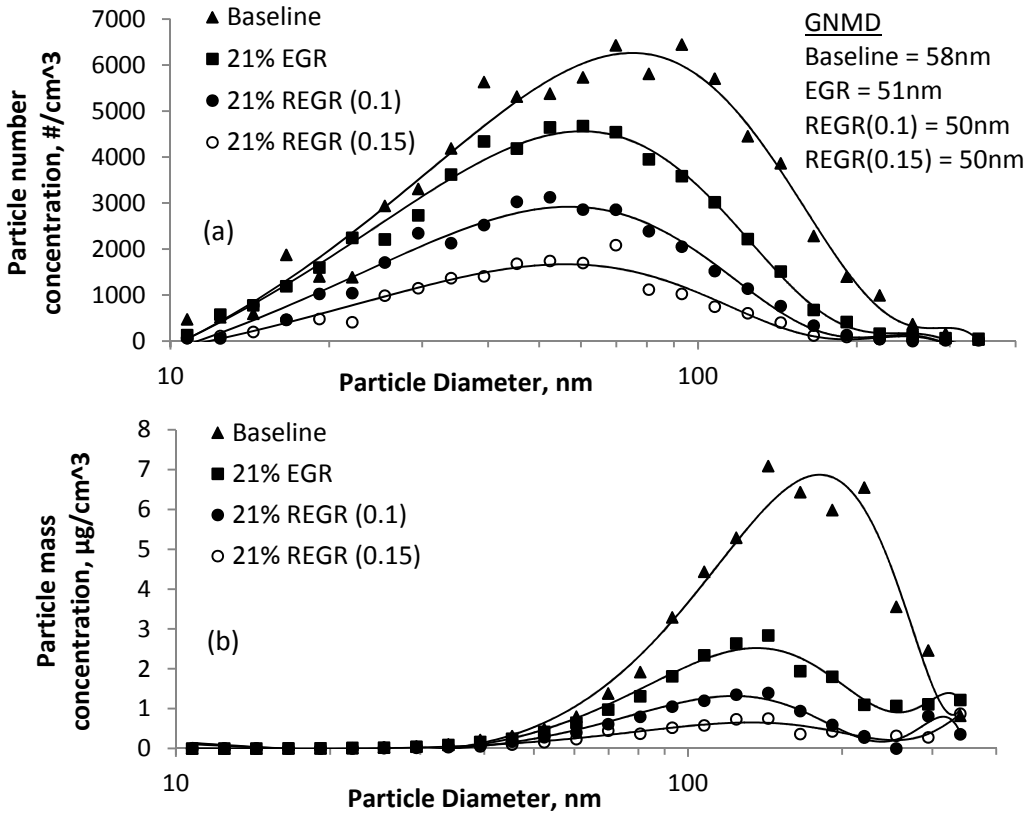

Figure 5.8 - Particle size distributions by (a) number and (b) mass concentration for the baseline, EGR and REGR conditions

The concentration of particles with diameter above 200nm was very low for both EGR and REGR, whereas for the baseline condition particles were measured in greater numbers up to 250nm. This effect, and the overall reduction of the GNMD, was due to the reduced particle formation with EGR and REGR meaning there was a lower probability of agglomeration to form the larger particles. The significance of this can be seen in the particle mass distributions of Figure 5.8b, with a greater contribution of these large particles to the total particulate mass concentration. It is clear that the reduced GNMD with EGR and REGR is not caused by an increase in particles with smaller diameter.

5.2.5 Effect of increased charge air temperature on engine efficiency with consideration of the EGR cooling requirement

The use of EGR inevitably causes an increase in charge air temperature unless a high capacity gas cooling system is used. The extent to which charge air temperature influences engine efficiency was investigated at a fixed engine condition (105Nm/7.2bar IMEP, 2100rpm, 14% EGR) and three charge temperature set points (35°C, 45°C and 55°C). For these tests the MP-EGR system was used to enable greater control of the charge air temperature. The EGR gases were cooled to around 125°C with a single EGR cooler before mixing with the pre-compressor air path. The air-to-water heat exchanger (i.e. the charge cooler) provided the final cooling to the setpoint temperature.

Referring to Figure 5.9 and Table 5.6 it can be seen that raising the charge air temperature increased fuel efficiency and a greater reduction in pumping loss was achieved due to the reduced charge density at higher temperature. Manifold depression was relatively small at this mid-range load, and so the pumping work was a small fraction of the indicated work. Increasing the charge air temperature should therefore offer a greater benefit at lower loads when the pumping work is more significant.

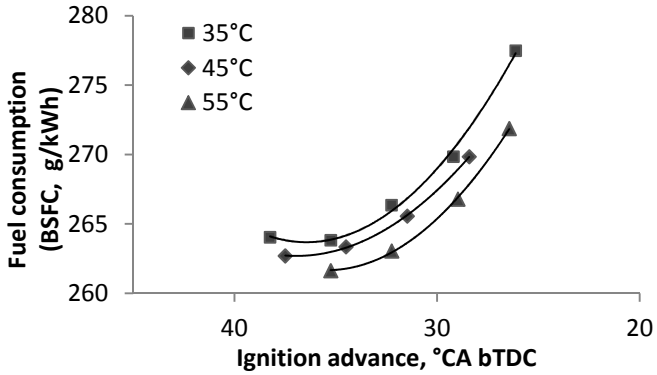

Figure 5.9 - Effect of charge air temperature on fuel efficiency at 7.2bar IMEP (14% EGR)

Table 5.6 - Results for various charge temperatures at 7.2bar IMEP, 14% EGR (MBT ignition timing)

Charge Air T	Ignition, °bTDC	η_{ind}	$\Delta\eta_{ind}$	PMEP, bar	Intake P, bar	COV of IMEP	MFB10-90, °CA	NOx, g/kWh	Intercooler ΔT
35°C	35	0.348	-	-0.45	0.925	2.3%	27	4.3	38°C
45°C	37.5	0.349	0.5%	-0.43	0.936	2.0%	26	5.3	26°C
55°C	35	0.352	1.4%	-0.42	0.952	1.7%	26	5.1	15°C

The optimum ignition timing remained essentially the same for these conditions, but the onset of knock was retarded for higher charge temperature; this could result in reduced efficiency for some engine conditions when the optimum ignition timing is no longer achievable. Another slight negative effect is increased NO_x formation due to higher compression temperature and the resulting higher prevailing combustion temperature.

Finally, there was a lower demand placed on the EGR and charge air cooling systems for the higher charge temperature set points. In practice, the use of 35°C charge air temperature with this level of EGR would be impractical using conventional heat exchangers as used in production vehicles, due to the high temperature drop required (ΔT = 38°C in Table 5.6). Ground water was used to control the engine water and charge air temperature in the test cell, which provided high cooling capacity. On the vehicle air-to-air charge coolers offer lower cooling capacity; typical ambient air temperatures experienced by the vehicle result in a low temperature gradient and poor heat exchange potential. Gas-to-water EGR coolers reject heat to the engine coolant, feasibly reducing the gas temperature to below 100°C but must not be cooled to below approx 60°C to avoid condensation. Heat removed from the EGR circuit is eventually rejected to atmosphere by the main water-to-air heat exchanger, or 'radiator'. It is important for overall vehicle efficiency to reduce the cooling system ancillary work and parasitic losses, e.g. fluid pumping work, electrical power required by the fan, and

aerodynamic losses associated with air flow over the heat exchangers. Therefore charge air cooling to 45°C or 55°C is more feasible due to the lower temperature drop required, and may also assist by further increasing efficiency if the compromise to increased NO_x and advanced knock initiation can be tolerated.

5.3 Effects of reformate species (hydrogen and CO) concentration on combustion, engine efficiency and PM emissions

The simulated REGR investigations of this chapter have so far used a fixed H_2/CO ratio of 3:1. This section aims to establish the effects of small changes to the hydrogen and CO concentration in REGR on the engine efficiency and combustion performance, as well as any possible effect on PM emissions. At the same time, this would allow for the relative effect of ignition timing advance on PM emissions to be studied.

5.3.1 Test conditions

Ignition timing sweeps were performed at 80Nm/5.7bar IMEP, 2000rpm and 21% REGR while varying the composition of the simulated REGR. Three compositions of REGR (C1-C3) were generated with differing hydrogen and CO concentration. The combustible gas compositions of the simulated REGR were:

C1: A total of 10% hydrogen and CO, in a 3:1 ratio

C2: 10% hydrogen, having equivalent energy content to composition 1 (No CO)

C3: 7.5% hydrogen, having equivalent hydrogen content to composition 1 (No CO)

For the PM measurements the thermodenuder was installed in the diluted exhaust gas sample line.

5.3.2 Combustion and engine efficiency

The indicated efficiency and combustion initiation results are plotted in Figure 5.10, with results for 21% EGR and the baseline condition included for further comparison. Comparing compositions C1 and C2, when CO was present (in composition C1) the optimum ignition timing was advanced, indicating slower combustion compared to composition C2. While the amount of gaseous fuel energy supplied was the same, indicated efficiency was slightly lower for composition C1 meaning that CO is a less efficient energy carrier than hydrogen for in-cylinder combustion. Combustion stability also dropped off more rapidly with ignition retard resulting in a large drop in efficiency, meaning that the use of optimum ignition timing is more important. This suggests that the extra hydrogen in composition C2 was useful for maintaining reliable combustion at retarded ignition timings. Combustion initiation was slightly faster (as is the main combustion phase) when the CO fraction was replaced with hydrogen, which is indicative of hydrogen's superior laminar flame speed and lower ignition energy.

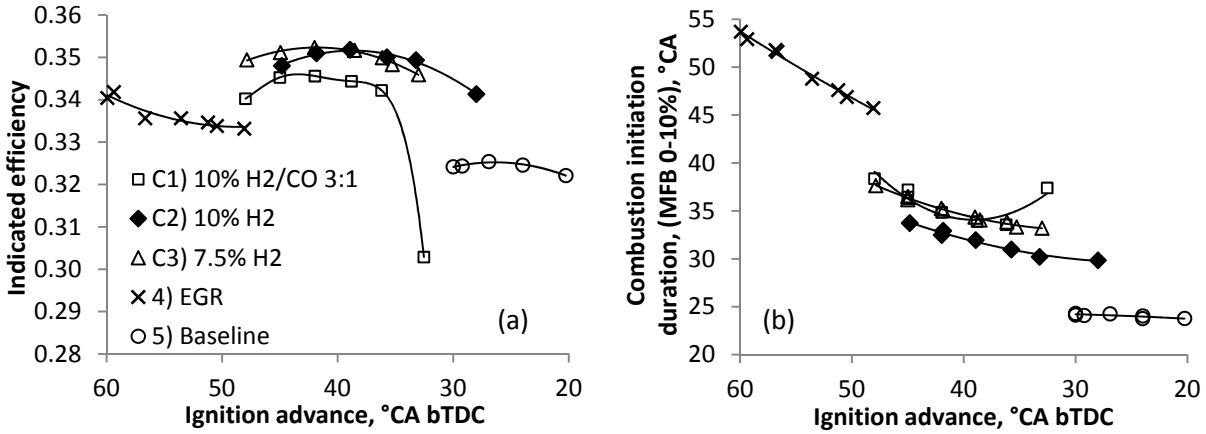

Figure 5.10 - Effect of REGR composition on indicated efficiency (a) and combustion initiation (b) at 5.7bar IMEP, 2000rpm and 21% REGR

Comparing composition C1 and C3, which have equivalent hydrogen concentration but C3 does not contain CO, it is apparent that the optimum ignition timing was essentially the same.

Indicated efficiency was generally higher without CO in the REGR, and was maintained for longer as ignition was retarded. It appears that CO is detrimental to combustion stability as both compositions have the same hydrogen concentration, but with the addition of 2.5% CO the COV of IMEP increased abruptly to 7.5% at 35°bTDC ignition timing. The combustion initiation phase duration (as well as the main combustion phase) was the same until the combustion stability deteriorates, which implies the CO had very little influence on combustion initiation.

The efficiency-ignition timing curves for compositions C2 and C3 (different hydrogen concentration, no CO) have very similar shape, but the curve is advanced by approximately 6°CA when the hydrogen concentration was decreased from 10% to 7.5%. Both curves are quite flat, indicating a wide range of useable ignition timings (efficiency changes only 1.4% across 9°CA). Reducing the hydrogen concentration also lengthened the combustion initiation period slightly.

It is also apparent that the relative changes in performance for each REGR composition were small compared to the difference in performance with 21% EGR, and the baseline condition. In every case, REGR was more efficient than both EGR and the baseline, and REGR goes some way to regaining the loss in combustion performance with EGR when compared to the baseline.

These results indicate that, for a fixed diluent fraction: hydrogen concentration determines the optimum ignition advance due to its strong influence on combustion rate; CO concentration influences the extent to which the useable ignition timing window is reduced, but does not have as significant an effect on combustion rate (for the incremental change in CO concentration tested); and hydrogen is a more effective energy carrier than CO.

These factors may be of consideration in future experimental work to optimise the reforming reaction routes, and produce the desired relative quantities of hydrogen and CO. For example, it may be beneficial to overall engine performance to increase the hydrogen/ CO ratio, for instance by promoting the WGS reaction, even if it marginally decreases the reforming process efficiency.

5.3.3 Influence of REGR composition and ignition timing on PM emissions

The results in Figure 5.11 indicate a trend for increasing PM mass with advanced ignition timing, particularly for undiluted combustion at the baseline. This is consistent with the well known effect that reducing the time for fuel-air mixing has on increasing PM formation.

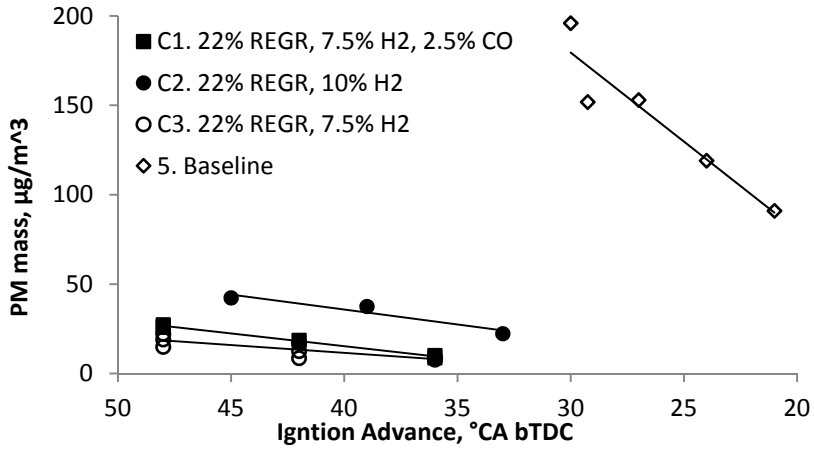

Figure 5.11 - PM mass concentration against ignition timing advance

As was the case in section 5.2.4, the use of REGR significantly reduced PM emissions compared to the baseline. Composition C3, which uses 7.5% hydrogen in REGR (equating to 7.5% of the total fuel energy), results in a 91% reduction in PM mass relative to the baseline at optimum ignition timings. By way of further comparison, PM mass reductions of the order of 90% have been demonstrated in research elsewhere with the addition of 6% hydrogen (energy fraction) to gasoline combustion [38].

Interestingly, the gradient of the PM increase with ignition timing advance is significantly lower for combustion with REGR, such that the magnitude of the PM variation due to 12° ignition timing shift with REGR is smaller than the PM reduction seen with REGR compared to the baseline. Put another way, the sensitivity of PM emissions to ignition advance is reduced from 10 to 1.6 $\mu g/m^3$ per degree. This is likely to be partly due to the replacement of some gasoline with gaseous fuel, meaning less liquid fuel is injected into the cylinder and therefore reducing the time for charge mixing is not as critical. When comparing the various REGR compositions, there is only a small difference between C1 and C3, which contain the same hydrogen concentration. Composition C2 contains 2.5% additional hydrogen, and the results show slightly greater PM formation.

5.4 REGR performance across a wider range of engine operating conditions

The objective of this section is to provide an estimate of engine performance characteristics with REGR across a wider range of engine speed/load conditions. Previous sections have presented results at a small number of engine conditions of interest. These tests broaden the scope to a larger portion of the engine map, using hydrogen enhanced EGR to approximate REGR. Again, the results are discussed in direct comparison to equivalent data for the baseline and EGR conditions. In addition, the performance maps produced offer some insight into the interaction of the reformer/REGR system with the engine.

5.4.1 Test conditions

For these tests, the HP gas recirculation configuration was used, supplying a fixed 7.5% hydrogen concentration in order to replicate REGR. It was decided that the CO fraction in REGR would be excluded. Given the increased flow rates required and the extended test matrix, it was seen as more economical to use industrial grade hydrogen rather than pre-mixed

hydrogen/CO gas; this decision could be justified based on the results from section 5.3.2, where compositions C1 and C3 showed comparable performance.

At each test point the maximum EGR or REGR rate was used, defined either by a combustion stability limit of 5±1% COV of IMEP, or by the physical flow limit of the EGR system. The speed/load map of interest was 30 to 110Nm and 1500 to 3000rpm at increments of 20Nm and 500rpm. For the baseline condition the valve timing remained at the standard calibration settings, while for EGR and REGR valve timing was fixed at a setting resulting in low trapped residuals (0° IVO/ 10° EVC). Ignition timing was modified such that combustion was phased for MFB50% = 8° ± 2°aTDC.

The charge air temperature at the inlet port was controlled to 35°C for the baseline condition. With the use of high recirculation rates it was not possible to maintain this temperature, so higher set points of 45°C and 50°C were used for the EGR and REGR conditions.

5.4.2 Analysis of the EGR and REGR test conditions

The recirculation rates used across the speed/load range for the EGR and REGR cases are shown in Figure 5.12. The limiting factor that determined the maximum recirculation rate varied across the speed/load range. At lower engine speeds and loads this was combustion stability, particularly for the EGR case. As engine speed and/or load increased, the flow capacity of the EGR system became important and was found to be limiting the recirculation rate. Flow capacity is determined by the flow resistance of the recirculation system and the manifold pressure ratio that varies with operating point. The maximum (combustion stability limited) recirculation rate was 34% for REGR at low load, when the manifold pressure ratio was high.

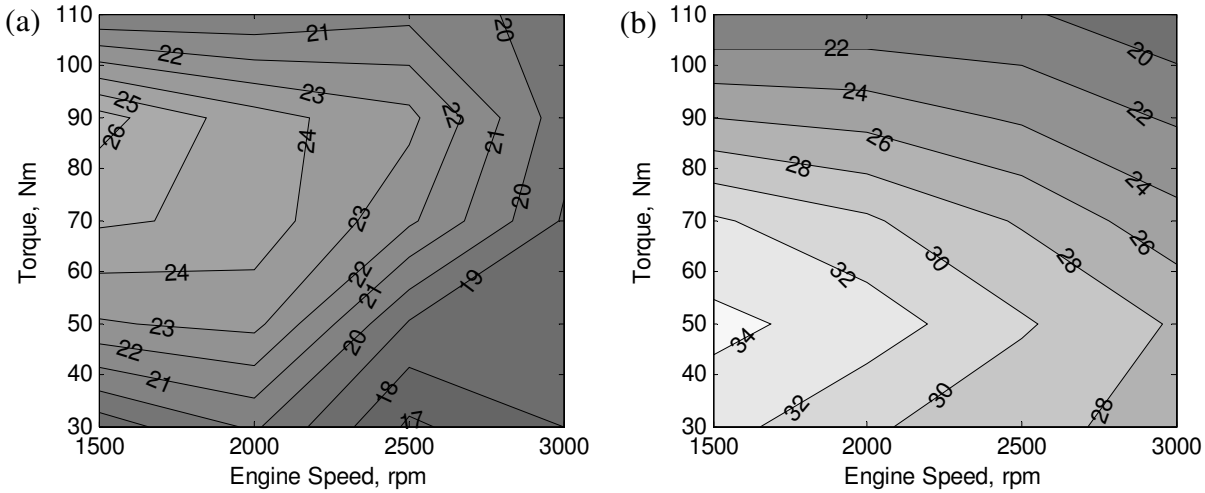

Figure 5.12 - Recirculation rate maps for (a) EGR and (b) REGR, %

Figure 5.13 plots the combustion stability, represented by the COV of IMEP, across the tested range for the REGR case; where numbers are greater than 4%, the test point can be considered as having the REGR rate limited by combustion stability. Numbers below 4% indicate the regions in which the recirculation rate was determined by the EGR system and the manifold pressure ratio, and there was not sufficient diluent present to cause a significant deterioration in combustion stability. When viewed alongside Figure 5.14, which shows the increase in recirculation rate for REGR relative to EGR, the extent to which the recirculation system installation is limiting the potential for increasing the REGR rate when hydrogen is present to enhance combustion can be seen. At the lowest speed and load the recirculation rate was increased from 18% to 33%, while at loads above 80Nm the increase was limited to 2% or less.

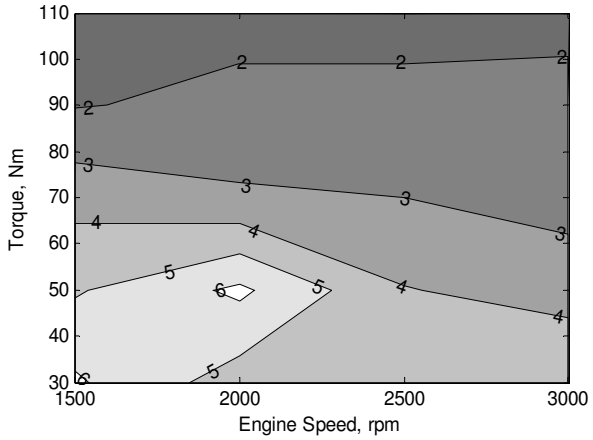

Figure 5.13 - Combustion stability with REGR (COV of IMEP, %)

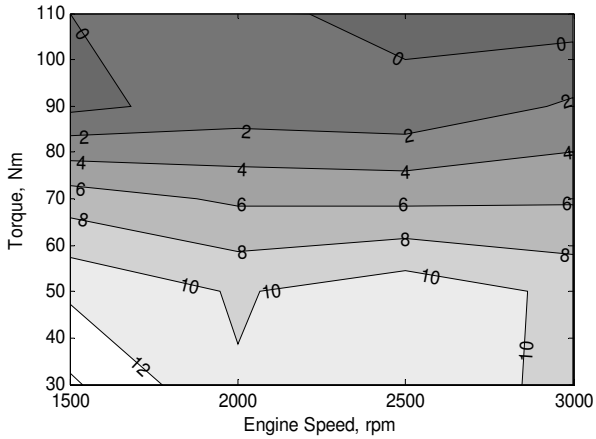

Figure 5.14 - Increase in recirculation rate with REGR relative to EGR, %

Because of the large variance in REGR rate and fixed hydrogen concentration, the fraction of total fuel energy supplied by REGR (in this case, as hydrogen) also varied, between 6% and 11% as shown in Figure 5.15.

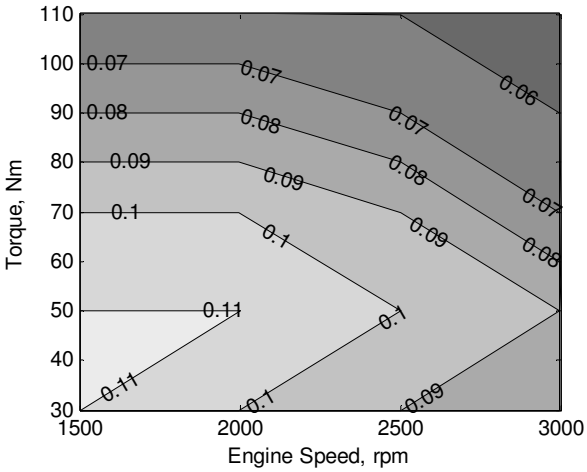

Figure 5.15 - Fraction of total fuel energy supplied as hydrogen in REGR

5.4.3 Engine performance and emissions maps

Indicated efficiency maps for the baseline, EGR and REGR cases are compared in Figure 5.16. There was a general trend for increasing efficiency across the map with EGR, and further so with REGR. This is clearer to see in Figure 5.17, which plots the relative indicated efficiency improvement (compared to the baseline), with peak efficiency increases of 7% and

9% for EGR and REGR respectively. It is apparent in the lower left quadrant of Figure 5.17a, i.e. at low engine speed/load, that conventional EGR is unable to offer significant efficiency gains. However EGR does provide a reasonably uniform benefit of 4-7% in the upper half of the map. REGR substantially improves the low speed/load performance (Figure 5.17b) relative to both the baseline and EGR because of largely increased recirculation rates while maintaining combustion performance. Elsewhere, REGR provides a consistent efficiency improvement of between 2-3% beyond EGR, reaching 7-9% improvement compared to the baseline across a large proportion of the map.

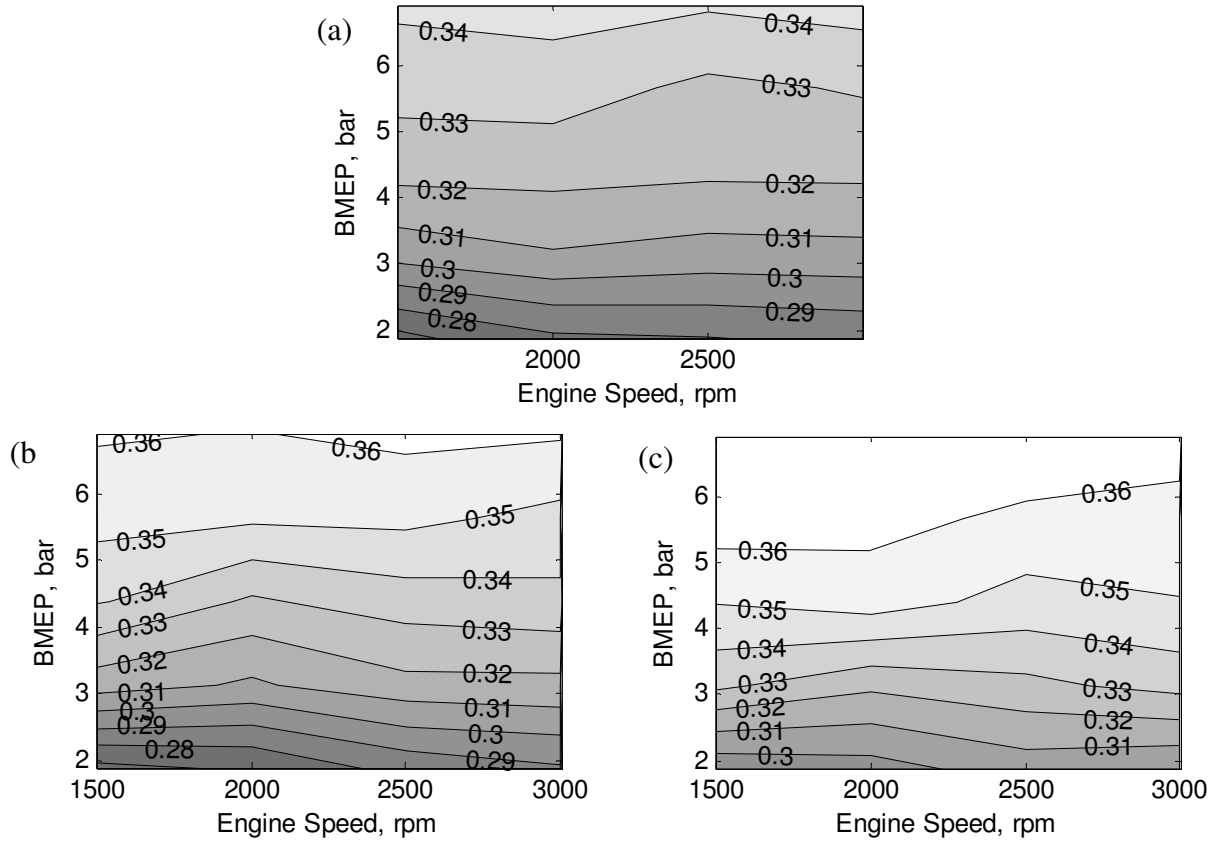

Figure 5.16 - Indicated efficiency performance maps for the (a) Baseline, (b) EGR and (c) REGR cases

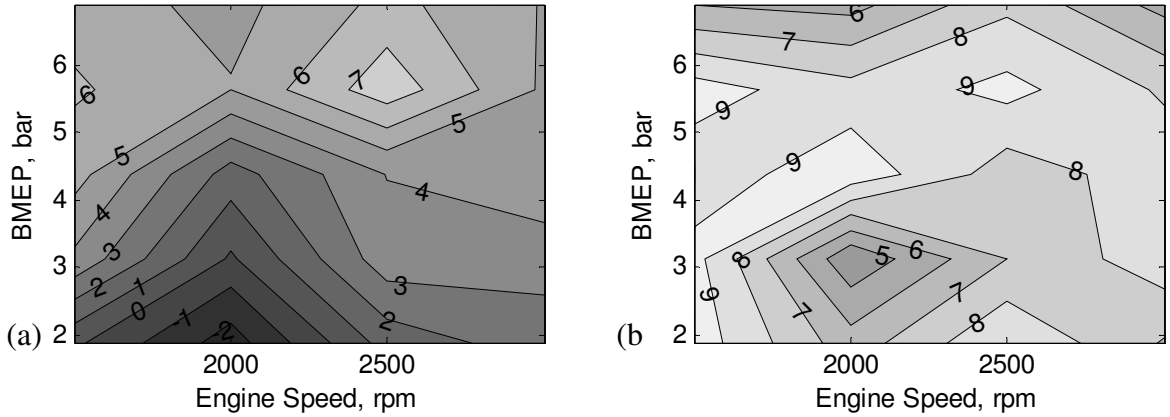

Figure 5.17 - Indicated efficiency improvement of (a) EGR and (b) REGR relative to the baseline

Figure 5.18 plots the NO_x emissions with EGR and REGR; the values are normalised against the baseline GDI engine NO_x emissions. The plots clearly indicate lower NO_x across the range, with between 40-90% reduction achieved by EGR (Figure 5.18a). NO_x was reduced markedly by REGR, particularly in the lower half of the map due to extended dilution rates, and more consistently than EGR; engine-out NO_x was between 82-96% lower across the map with REGR.

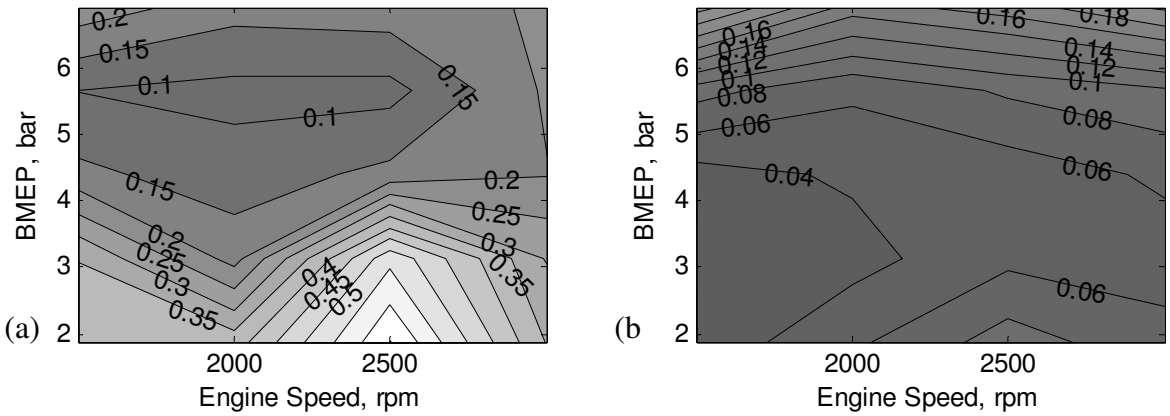

Figure 5.18 - Normalised NO_x emissions for (a) EGR and (b) REGR relative to the baseline

5.4.4 Exhaust gas temperature

Finally, it is important to note the shift to lower exhaust temperatures across the range when REGR is implemented. Figure 5.19 plots the engine-out and post-TWC exhaust temperature for the baseline and REGR conditions. There is a relatively substantial and uniform reduction of engine-out EGT across the range when comparing the baseline (Figure 5.19ai) and REGR plots (Figure 5.19bi).

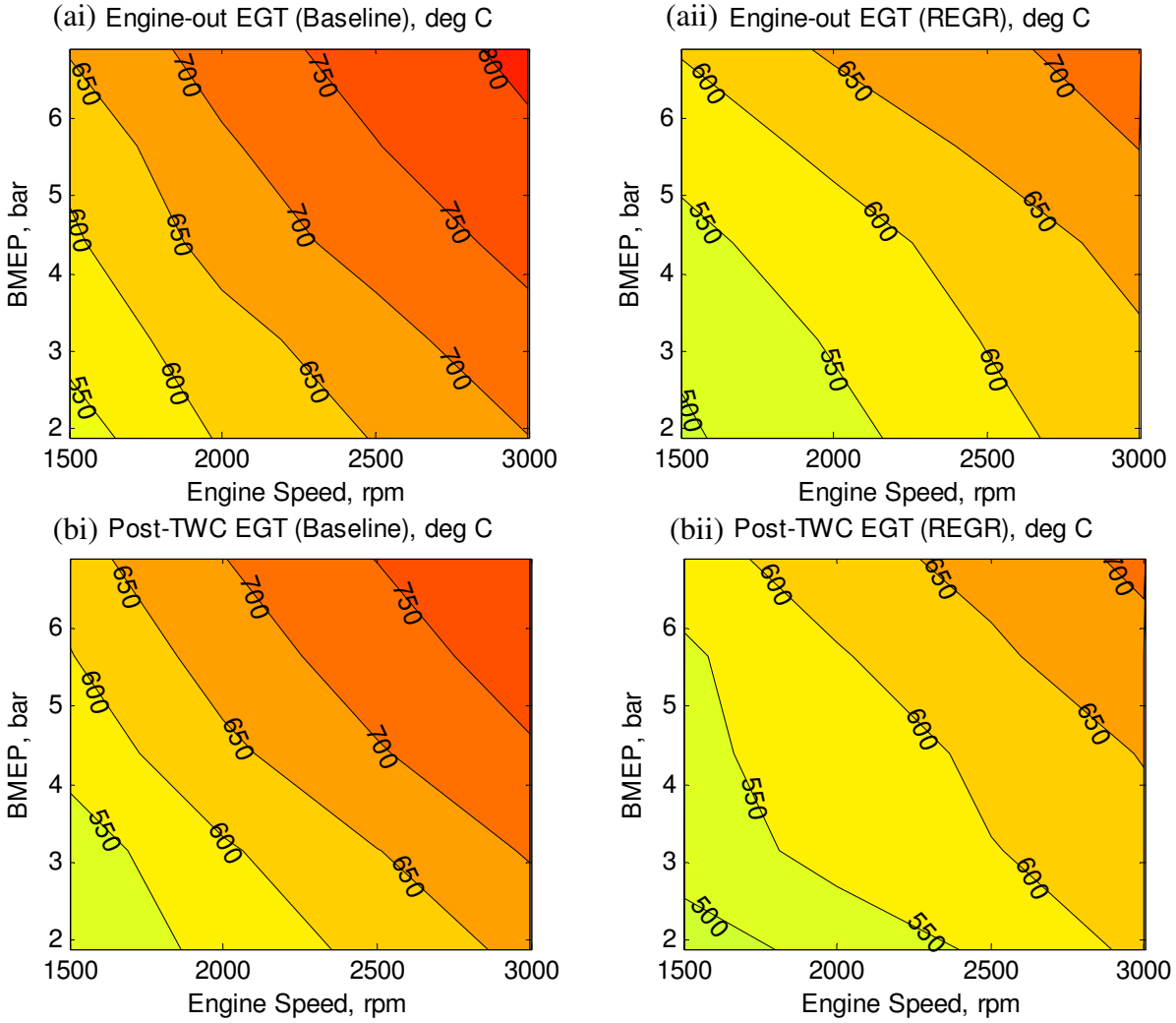

Figure 5.19 - Maps of engine-out (a) and post-TWC (b) exhaust temperature for the baseline (i) and REGR (ii) conditions

Positioning a fuel reformer as close as possible to the exhaust ports in order to utilise the highest exhaust stream temperature would be optimal for promoting endothermic reforming

reactions and maximising reformer performance. However, packaging a fuel reformer in a downstream location is likely to be more practical, certainly at the prototype stage. While a fuel reformer could potentially be designed to be mounted close to the exhaust ports, which would be before the turbine in the case of this multi-cylinder GDI engine, there would be many additional considerations for the reformer design and engine integration. These include: the effect of increasing exhaust backpressure on engine performance; modification of exhaust pressure-wave reflection characteristics that strongly influence cylinder scavenging; and high thermal loading of relatively intricate (thin walled) reformer components, such as the catalyst housing that would be required to seal the exhaust and reformate streams while providing good heat transfer. Not least, packaging in this location would also be detrimental to turbocharger performance to some degree. The act of fuel reforming would reduce the exhaust enthalpy and the physical restriction would result in a pressure drop, reducing the turbine inlet pressure as well as dampening exhaust pressure pulses into the turbine housing. Therefore, lower peak turbine work would result. Additionally, a larger pre-turbine volume would deteriorate transient performance.

With all this is mind, the post-TWC exhaust temperature is included in Figure 5.19 as an indication of the conditions to be expected for a fuel reformer located after the TWC. What Figure 5.19aii shows is that the baseline post-TWC temperature is substantially lower than the engine-out temperature due to the expansion across the turbine and heat lost from the exhaust system to the surroundings. However the post-TWC temperature with REGR (Figure 5.19bii) is quite comparable to the baseline, with only a small further drop in temperature. As identified earlier in section 5.2, slightly increased engine-out HCs with high REGR dilution compared to the baseline result in a higher exotherm over the TWC, therefore the temperature

drop isn't as substantial. Even so, the post-TWC EGT was below 600°C for over half of the observed range.

5.5 Summary

The potential benefits that an exhaust gas fuel reformer may offer the GDI engine have been demonstrated with the series of studies in this chapter. The tests have used either bottled hydrogen, or hydrogen and CO, added to EGR in order to simulate REGR and generate reformate with realistic, achievable compositions.

In all cases REGR has improved indicated engine efficiency relative to the baseline GDI engine. At low engine load REGR outperforms conventional EGR due to extension of the dilution limit and improved combustion. VCT was found to offer an advantage to engine operation by extending the maximum achievable REGR rate when utilising valve timings for low exhaust residuals. In the case of a real exhaust gas fuel reformer this would increase the reformed fuel fraction, maximising the potential for exhaust energy recovery.

Both EGR and REGR were found to reduce PM number and mass emissions across the range of studied particle diameters. The presence of hydrogen and CO in REGR leads to lower PM relative to EGR. The results indicate that there is an additive benefit achieved by combining the mechanisms for reducing PM emissions with EGR and hydrogen.

Engine performance maps showed that REGR increased indicated engine efficiency between 6-9% across most of the engine range compared to the baseline GDI engine. NO_x was consistently very low with REGR, being reduced by 82-96%. Engine-out EGTs were found to be significantly cooler with REGR, but the reduction of post-TWC temperature relative to the baseline was not as large due to exothermic reactions across the TWC. Even so, due to its strong influence on the reforming process, EGT could become the limiting factor when

determining the maximum REGR rate for some engine conditions, and not the deterioration of combustion stability.

CHAPTER 6

STUDIES OF A PROTOTYPE EXHAUST GAS FUEL REFORMER INTEGRATED WITH A GDI ENGINE

This chapter is focused on the experimental study of a prototype exhaust gas fuel reformer that has been integrated with a multi-cylinder GDI engine. The test cell configuration and reformer specification were described in sections 3.2 and 3.4. Various methods are implemented in order to analyse the effectiveness of the reforming process under GDI engine exhaust conditions. These include examination of the reformer temperature distribution, reformate speciation, calculation of the reforming process efficiency, estimation of exhaust heat recovery and analysis of the exhaust exergy.

The effect of the fuel reformer on engine performance is presented in Chapter 7.

6.1 Test conditions

Three engine speed/load conditions were selected in order to generate a suitable range of reformer temperature and flow conditions while still being relevant to normal, sustained load driving conditions. These were 35Nm/3bar IMEP at 2100rpm, 50Nm/4bar IMEP at 3000rpm, and 105Nm/7.2bar IMEP at 2100rpm. The first two are key steady state conditions used on the NEDC for a mid-size/large family vehicle with a 2L engine, and the third is typical of a higher load transient condition on the NEDC. The engine was operated with the maximum achievable charge dilution rate, and also a lower dilution rate to investigate the effect of reformer mass flow rate, or GHSV. Gasoline was injected into the reformer feed gas such that the molar concentration was 0.5% or 1% (fuel composition assumed to be octane) to test the influence of fuel concentration on reformer performance.

The cam timings were fixed at a short overlap setting (0° IVO and 10° EVC) to ensure low exhaust residuals when using external EGR or REGR. Engine fuelling was controlled for an overall stoichiometric AFR but the ratio of DI gasoline to reformate fuel energy varied depending on the reformer conditions. The charge air temperature measured at the inlet port was controlled to 45°C. Ignition timing was varied in order to phase combustion with MFB50% occurring at 8°±2°aTDC, or at the knock-limited ignition timing. Otherwise, the standard ECU calibration settings were used.

The engine-out exhaust gas composition (Table 6.1), which determines the reformer feed gas composition (prior to gasoline injection), varied little across the range of conditions tested because the engine uses a homogeneous, stoichiometric combustion strategy. The slight variations were caused by the differing overall charge dilution rate, which influences combustion and pollutant formation. The oxygen content of the exhaust stream varies only between 0.5 to 0.7%, which is of particular relevance to the reformer process efficiency as the oxygen concentration is directly proportional to the amount of fuel that is consumed by oxidation reactions in the reformer and the resulting increase in temperature.

Table 6.1 - Exhaust gas temperature and composition at each engine condition

Engine condition	**EGT [1]**	**CO_2 (%)**	**O_2 (%)**	**CO (%)**	**H_2O [2] (%)**	**NO_x (ppm)**	**THC, (ppm)**
35Nm/ 2100rpm	595 - 605°C	14.8 - 15.0	0.60 - 0.70	0.50 - 0.60	14.3- 14.4	100 - 1200	1900 - 3000
50Nm/ 3000rpm	655 - 680°C	14.8 - 14.9	0.50 - 0.65	0.50 - 0.55	14.3- 14.4	200 - 600	1500 - 1900
105Nm/ 2100rpm	685 - 720°C	14.8 - 15.0	0.60 - 0.65	0.55 - 0.70	14.4- 14.5	900 - 2300	1300 - 1600

[1] Reformer inlet EGT; [2] Calculated

6.2 Reformer temperature

The reformer operating temperature is directly influenced by many parameters. These include: the REGR flow rate; the fuel concentration; the reactant composition that determines the prevailing reforming reactions, which may be exothermic or endothermic; and the temperature of the exhaust stream that passes over and heats the reformer plates.

The reduction in EGT that occurs with the use of EGR or REGR has been discussed in previous chapters. To provide context for the following discussions, Figure 6.1 plots the variation of the exhaust stream temperature at the reformer inlet (post-TWC) for all the reforming conditions used in the investigation, as well as for the baseline condition (0kg/h REGR).

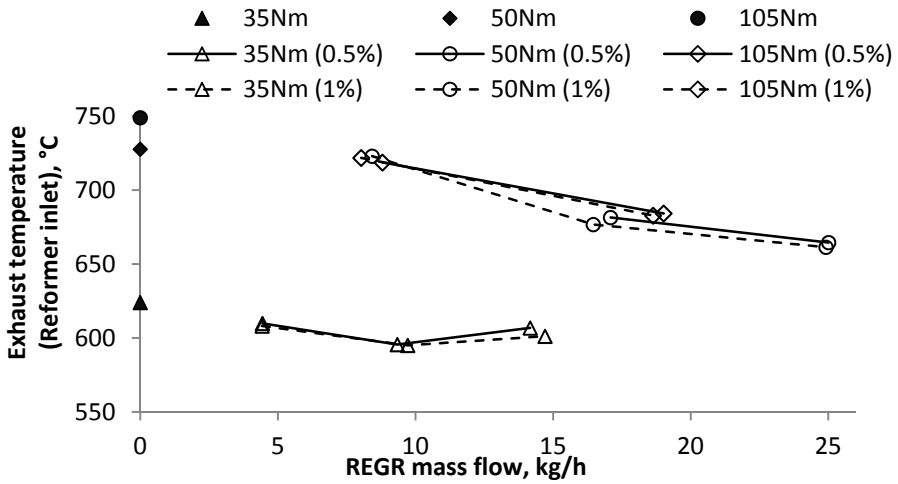

Figure 6.1 - Variation of exhaust temperature (at the reformer inlet) with REGR flow rate and reformer feed gas fuel concentration (0.5% and 1%)

[The baseline condition is identified by filled markers]

6.2.1 Reformer temperature distribution

Figure 6.2 shows how the temperature distribution across the middle reformer plate varies with engine condition, REGR flow rate, fuel concentration and the resulting reforming activity. In these plots the reformer feed gas flows from top to bottom and the engine exhaust

stream flows over the plate from right to left. The temperatures were generally higher along the right edge due to the exhaust stream heating. The baseline plots clearly show that the reformer plates were more effectively heated as the exhaust stream temperature increased with engine load.

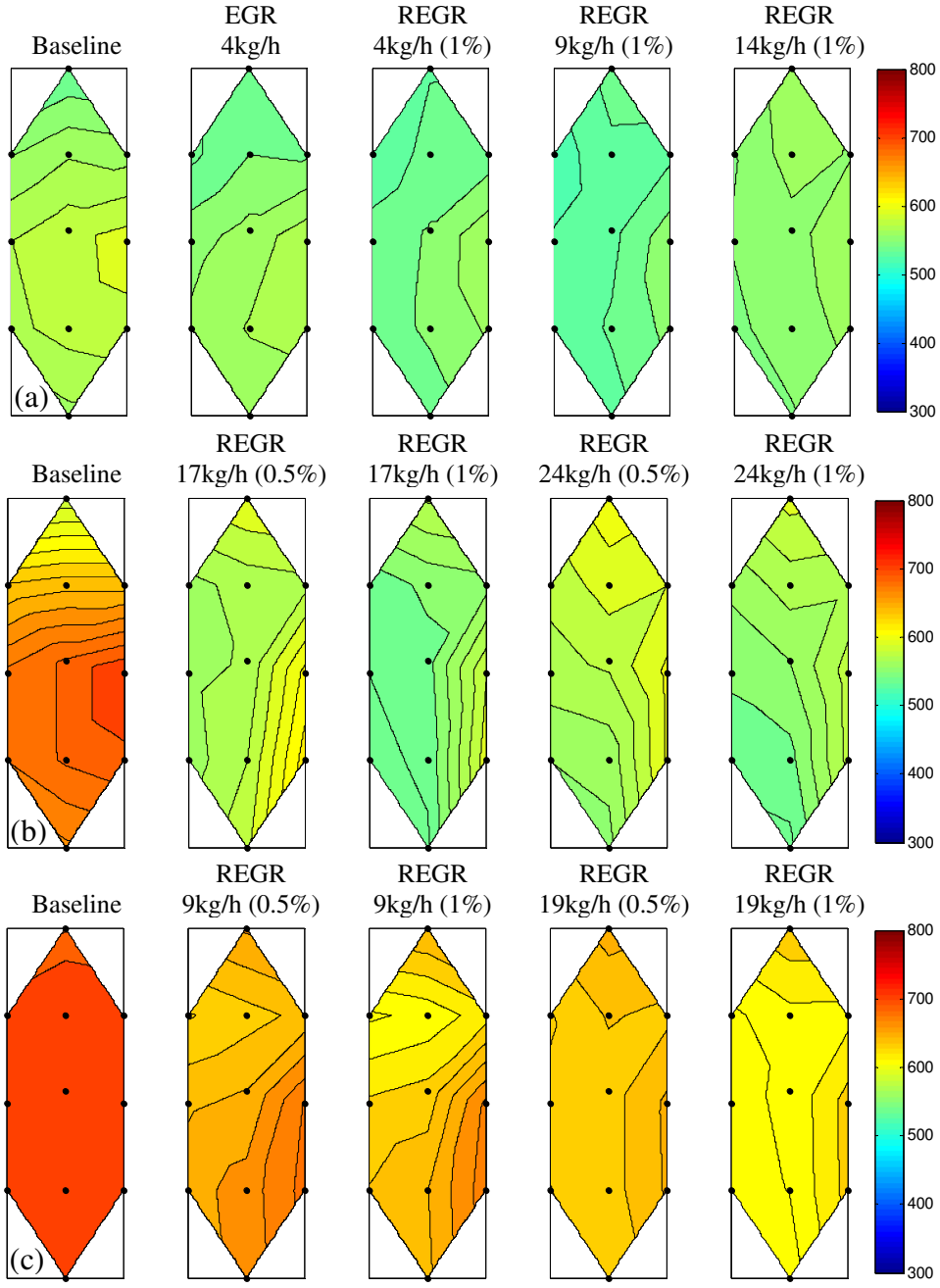

Figure 6.2 - Temperature (°C) distribution across the middle reformer plate at a) 35Nm, b) 50Nm and c) 105Nm engine conditions

At the lowest temperature condition (35Nm/2100rpm) the plate temperatures dropped as the REGR flow was increased up to 20% due to reforming activity. There was also a slight cooling effect just by flowing gas through the reformer (i.e. with EGR), analogous to a forced-convection cooling process. At the highest REGR flow rate there was a slight increase in reformer temperature with a more even distribution. This is the result of multiple effects associated with increasing the flow rate: more oxygen is available for fuel oxidation, which increases the temperature in the front section of the reformer; the high flow rate moves the high temperature gas along the reformer more quickly resulting in the more even temperature distribution; and reforming activity tends to be lower as the flow rate increases.

At the two higher engine load conditions the reformer was heated to significantly higher temperature when there was no REGR flow (baseline condition). Increasing either the REGR flow or the fuel concentation lowered the reformer temperature. Both of these changes increased the availability of fuel while, importantly, at sufficiently high temperature for the endothermic reforming reactions to be feasible. Again, increasing the REGR flow rate led to a more even temperature distribution.

6.2.2 Linear reformer temperature profiles

Figure 6.3 compares the linear reformer temperature profiles for two REGR mass flows, 4.5 and 14.5kg/h - this equates to 10% and 25% REGR in terms of the dilution rate at the 35Nm/2100rpm engine condition. Temperature profiles are included for 0.5% and 1% fuel in the reformer feed gas. At low reactant mass flow rate in the reformer, there was only a small amount of heating due to exothermic reactions in the front of the catalyst. There was no indication of endothermic reforming cooling the reformer. It appears that a small amount of endothermic reforming did occur in the first 75mm of the reformer as the temperature

remained reasonably constant. This indicates that the energy consumed by reforming reactions was approximately balanced by heat flow from the exhaust. After this the temperature increased due to heating by the main engine exhaust stream, which was around 600°C (Figure 6.1). At the higher reactant flow rate there was a greater quantity of fuel and oxygen passing through the reformer which led to a larger temperature increase at the front face. The combination of higher temperature and more fuel being available for reforming meant that there was a clear drop in temperature along the length of the reformer due to endothermic reforming reactions.

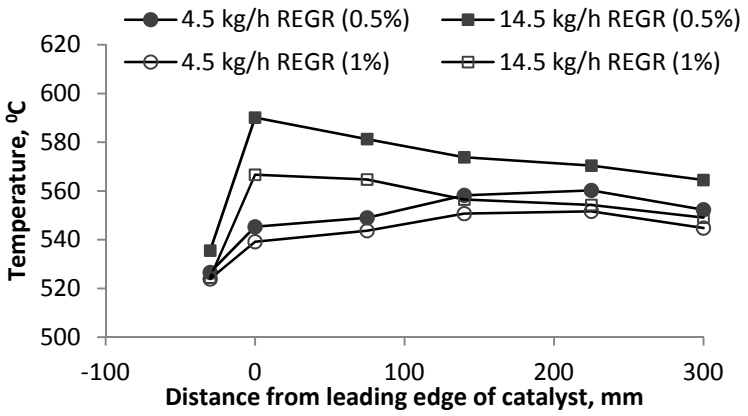

Figure 6.3 - Effect of reformer flow rate and feed gas fuel concentration on linear reformer temperature profile at the low temperature (35Nm/2100rpm) condition

Increasing the fuel concentration in the feed gas (for a given reactant flow rate) results in a reasonably uniform reduction of the temperature along the reformer. The feed gas temperature (-30mm from leading edge) was slightly lower for the higher fuel flow conditions due to greater cooling by fuel vapourisation, and the gradient of the rise in temperature between the feed gas (-30mm) and the leading edge (0mm) was similar when comparing each fuel concentration condition. The amount of oxygen available for oxidation is mainly dependent on the reactant flow rate and determines the amount of heating at the leading edge. The slight

reduction of heating with increasing fuel concentration is likely due to the higher rate of endothermic reforming (decrease in the oxygen/carbon ratio).

The effect of reactant mass flow rate in the reformer on the linear temperature profile is shown in Figure 6.4 for two engine loads with 1% feed gas fuel concentration in each case. This shows the location of endothermic reforming moving further along the reformer with increasing flow rate. The initial drop in temperature is greater for the lower flow condition at each load.

When the reformer flow is low and the reformer plate temperature is relatively high at the inlet, 650°C at the 105Nm condition, most of the reforming occurs in the first section of the reformer and is followed by re-heating. This implies that the reformer is able to process more fuel than is being supplied at the low flow condition.

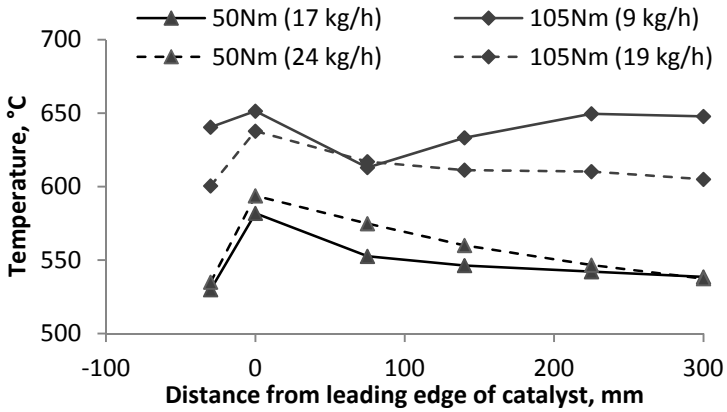

Figure 6.4 - Comparing linear reformer plate temperature profiles with high and low REGR flow at two engine conditions (1% feed gas fuel concentration)

Comparing the two curves for the high temperature condition (105Nm) there is a large temperature difference in the final 100mm of the reformer. The conditions in this section can be used to give an insight into the equilibrium position of the WGS reaction. The reformer temperature is reduced for the higher REGR rate, which reduces the WGS reaction equilibrium constant (Figure 2.5) and results in an equilibrium shift towards higher product

concentration (H_2 + CO_2). For this reason, increasing the REGR rate generally results in a greater H_2/CO ratio (providing that the conditions are reasonable for reforming). This can be seen by comparing the hydrogen and CO data in Figure 6.5, particularly for the 1% feed gas fuel concentration conditions. However, increasing the REGR flow rate (the GHSV) means that the reaction equilibrium is less likely to be achieved.

It should be emphasised that the linear profiles offer a 1-dimensional view of the reformer operating temperature. This information disregards the temperature distribution across each reformer plate and any difference between the five individual plates. Different operational temperature between plates may be expected to some degree as a result of non-uniform flow distribution of the exhaust stream or the feed gas/reformate.

6.3 Reformate speciation

The production of hydrogen at each engine condition varied with REGR mass flow rate and the fuel concentration in the reformer feed gas (Figure 6.5). The maximum hydrogen production was observed when the consumption of steam was greatest, which indicates successful promotion of the steam reforming reaction. This occurred at the 50Nm/3000rpm engine condition when there was 11% hydrogen produced and 6% un-reacted steam measured in the reformate, and there was a combination of high temperature and intermediate reactant flow rate. For the high exhaust temperature condition (105Nm/2100rpm), when the reactant flow rate was low, reformer temperatures were higher than all other conditions; this may go some way to explain the slightly lower hydrogen production than for the lower temperature (50Nm/3000rpm) condition because there was less promotion of the WGS reaction at higher temperature. That said there was also less CO produced. When comparing the two similar REGR flow conditions (17kg/h at 50Nm and 19kg/h at 105Nm), when the exhaust

temperature at the reformer inlet was very similar (678°C and 675°C in Figure 6.1), it can be seen that the hydrogen and CO production were both lower at the 105Nm condition, implying less reforming activity. This was confirmed by lower HC conversion compared with the 50Nm condition; however, the cause was not completely clear. There will have been some influence of GHSV that was slightly higher at the 105Nm condition (19kg/h), which will have reduced the fuel conversion and H_2/CO yields to some degree, but not to the extent seen. This may suggest that the reformer experienced some temporary catalyst deactivation, perhaps due to the deposition of carbon onto the catalyst surface (coking), which may be expected to occur during sustained operation. However, there was no evidence collected to confirm this, and the normal test procedure involved periodically operating with EGR to expose the catalyst to steam and oxygen in order to reverse any coking.

Some CO_2 can be expected to be produced by the oxidation and WGS reactions that occur as part of the overall reforming process, as well as being consumed in the dry reforming reaction. The CO_2 concentration in the reformate was relatively consistent at most test points, but was reduced slightly for low REGR mass flow rates while at high temperature (Figure 6.5). This implies that there was some dry reforming activity when the reformer inlet exhaust stream temperature was high (i.e. >700°C in Figure 6.1). It should be noted that, for a given engine load, at lower REGR mass flows the reformer plate temperatures are higher. This means that the reversible WGS reaction has a greater equilibrium constant, is therefore less favourable towards the reaction products, and so less hydrogen and CO_2 are produced by this reaction.

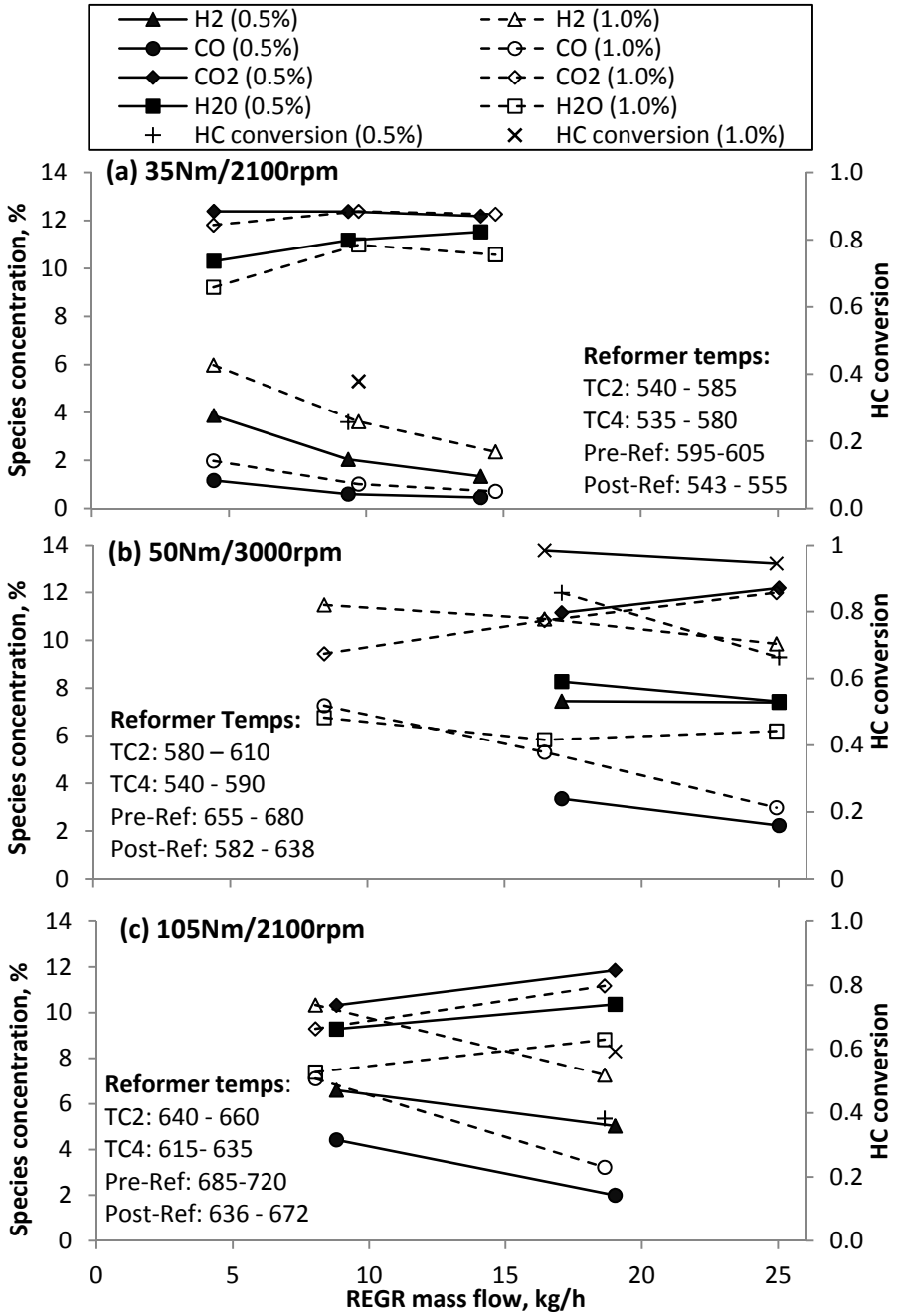

Figure 6.5 - Reformate species concentrations at various engine conditions (a) 35Nm, (b) 50Nm and (c) 105Nm

6.3.1 Hydrocarbon speciation

The GC-FIC was used to identify the relative proportion of a selection of individual HC species in the reformate. The results are plotted in Figure 6.6 for two REGR flow rates with 1% fuel concentration at the 50Nm engine condition. It should be noted that not all HCs are

accounted for using this method; only the calibrated species detailed in Table 3.4 can be identified and quantified. The calibration gas used contains many of the major components of gasoline and there were no significant peaks in the chromatogram spectrum unaccounted for.

The proportion of HCs that break through the reformer increases with REGR flow rate; therefore at 17kg/h REGR (Figure 6.6a) there is a lower THC concentration. Methane made up a greater proportion of the HCs in the reformate at lower REGR flow, partly because the total breakthrough HC quantity was lower, but also due to higher methane (CH_4) production by the 'methanation' reforming side reactions (Equation 2.18 and Equation 2.19); these consume hydrogen in reactions with CO, CO_2 or HCs to produce methane, but tend to be relatively unfavoured under REGR conditions [79]. The higher concentration of hydrogen and CO (the methanation reactants) produced by the primary reforming reactions at lower REGR flow will have led to the methanation reactions being increasingly favoured.

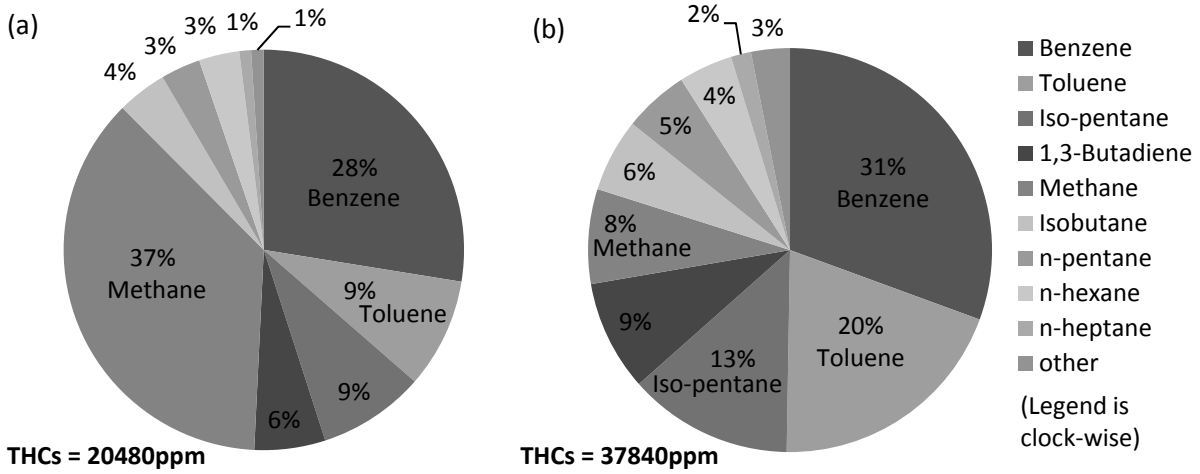

Figure 6.6 - Proportion of HC species of the total HCs in reformate as measured by GC-FID at 50Nm/3000rpm with REGR (1% fuel): 17kg/h (a) and 24kg/h (b)

The molar composition of the gasoline (detailed in Table 3.2) was 12.6% paraffins, 33.4% isoparaffins, 14.6% olefins, 5.1% naphthenes, 28.9% aromatics and 4.9% oxygenates. The measured aromatic fraction (benzene + toluene) in the reformate was higher in each case at

37% and 51%. This supports the idea that the aromatic fraction of the gasoline is not reformed as readily as the less complex HCs such as the paraffins, which constitute nearly half of the gasoline mixture and appear in significantly lower quantity in the reformate. There was also a smaller toluene/benzene ratio at low REGR reactant flow, which implies toluene is reformed more readily than benzene. It may be that some toluene is partially reformed to the more stable/less reactive benzene.

6.4 Reformer process efficiency

The effectiveness of the reformer can be analysed by calculating the reformer process efficiency using Equation 6.1. This provides a measure of the reformer's ability to increase fuel energy when converting from liquid to gaseous fuel, and calculates the ratio of the fuel energy contained in the reformate to the fuel energy in the reformer feed gas. The feed gas consists of EGR and gasoline; the energy associated with the small fraction of CO and HCs in the EGR is included in the analysis. The non-methane HCs measured in the reformate were assumed to have the properties of gasoline when calculating the total reformate fuel energy. 'Dry' measurements were converted to 'wet' molar fractions (using knowledge of the steam concentration in the feed gas/reformate) before calculating the mass flow rate of individual species.

$$\eta_{ref} = \frac{LHV_{H2}.\dot{m}_{H2} + LHV_{CO}.\dot{m}_{CO} + LHV_{CH4}.\dot{m}_{CH4} + LHV_{g}.\dot{m}_{HC,out}}{LHV_{g}.\dot{m}_{g,in} + LHV_{CO}.\dot{m}_{CO,exh} + LHV_{g}.\dot{m}_{HC,exh}}$$

Equation 6.1

At the two highest engine load conditions, when the exhaust temperature was above 650°C, the reformer process efficiency was calculated to be greater than one (Figure 6.7a and b). This means that the total fuel enthalpy was increased by reforming (Figure 6.7c and d). The reformer process efficiency was similar for each feed gas fuel concentration; however,

increasing the fuel concentration to 1% increased the magnitude of the total fuel enthalpy increase achieved by reforming (Figure 6.7c & d), which is obviously beneficial.

At the low temperature condition the reformer process efficiency is less than one, meaning some energy was lost in reforming the gasoline to reformate. As presented in Figure 6.5 though, some hydrogen was produced that may still enable enhanced engine and total system efficiency.

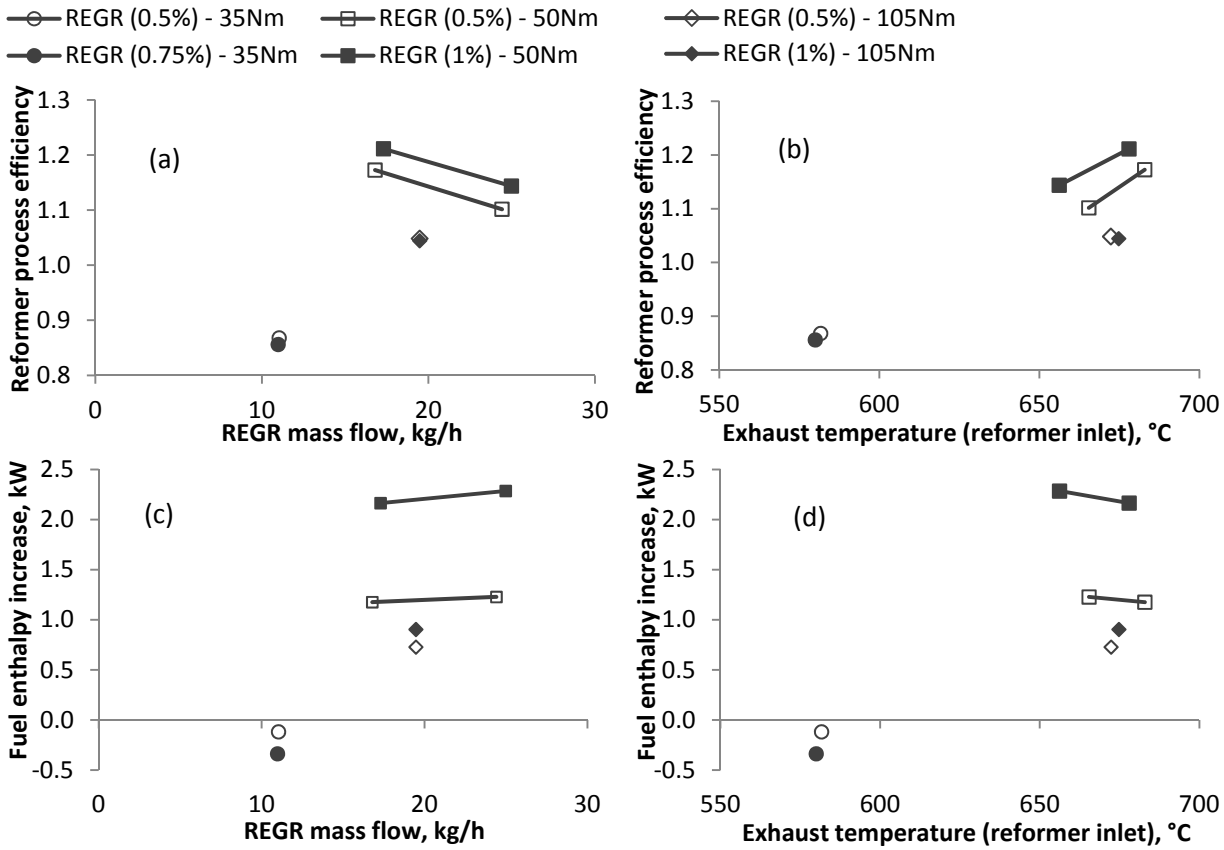

Figure 6.7 - Reformer process efficiency (a & b) and fuel enthalpy increase (c & d) plotted against REGR mass flow (a & c) and exhaust temperature at the reformer inlet (b & d)

In the above analysis of the reformer process efficiency the HCs and CO contained in the exhaust gas (reformer feed gas) were included. These species were included because they have chemical energy (i.e. they are combustible) but they are supplied to the reformer as products of incomplete in-cylinder combustion. Usually they would be considered wasted

energy, being oxidised in the TWC or lost to atmosphere. In effect then, some of the HCs and CO in the exhaust gas are being reclaimed. Figure 6.8 compares the reformer process efficiency with and without these species included in the calculation. It can be seen that this modification increases the reformer efficiency.

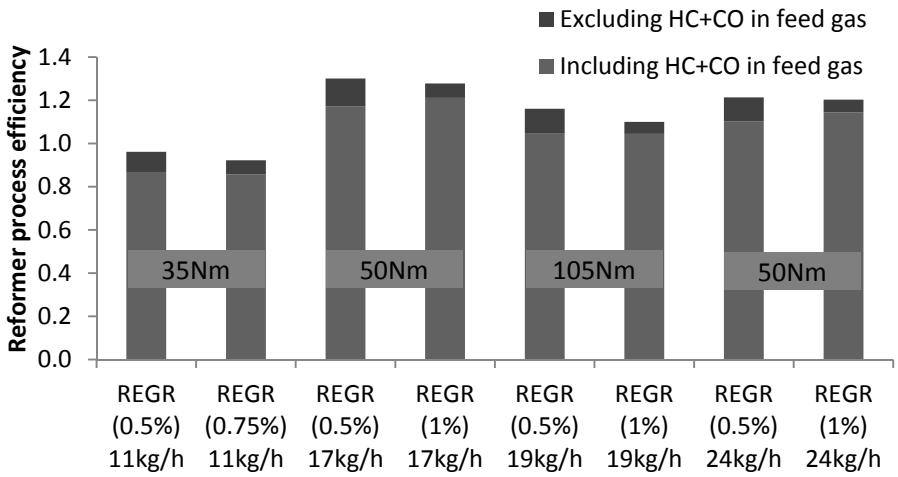

Figure 6.8 - Effect of including fuel energy from HCs and CO contained in the feed gas on reformer process efficiency

6.5 Exhaust energy recovery

6.5.1 First law analysis: exhaust stream energy

Under normal engine operating conditions, i.e. when there is no reforming, the exhaust stream temperature drops by some amount ΔT as it passes across the reformer due to heat loss to the atmosphere. This is perhaps an obvious statement; however, it is necessary to consider this heat loss when estimating the amount of exhaust energy recovery achieved by the reformer. When operating with EGR or REGR at a given engine load and recirculation rate, the exhaust stream mass flow, composition, and temperature at the reformer inlet are very similar; therefore, it may be assumed that the heat loss to atmosphere is the same under each condition.

When the reformer is switched on there will be a greater exhaust stream temperature differential (ΔT_{REGR}) if energy is extracted by the overall endothermic reforming process. This means that the exhaust stream temperature drop due to reforming, ΔT_{Ref} can be estimated for each condition using $\Delta T_{Ref} = \Delta T_{REGR} - \Delta T_{EGR}$. The rate of exhaust heat recovery is then approximately equal to the change in enthalpy of the exhaust gases as they drop in temperature by ΔT_{Ref}, and is calculated using Equation 6.2. The specific heat capacity of the exhaust stream, c_{exh}, was calculated for the mixture of nitrogen, CO_2 and steam (post-TWC composition) at the average of the pre- and post-reformer exhaust stream temperature.

Exhaust heat recovery, $\dot{Q} = \dot{H} = \dot{m}_{exh} \cdot \bar{c}_{p,exh} \cdot \Delta T_{Ref}$ (kW) Equation 6.2

The rate of exhaust stream heat recovery achieved by fuel reforming at each engine condition is plotted in Figure 6.9. The highest rate of heat recovery was achieved at the 105Nm engine condition when the reformer temperature was highest. This engine condition used intermediate REGR mass flow rates and so the reformer's ability to recover exhaust energy was not compromised by high GHSV. At the 50Nm engine condition, increasing the REGR flow to the highest rate reduced heat recovery due to the combined effects of increased GHSV and lower exhaust stream temperature (increased charge dilution causes lower combustion and exhaust temperatures). Therefore, there was a smaller temperature differential between the exhaust stream and the reformer resulting in less heat transfer. In general, increasing the reformer fuel flow increases the amount of exhaust heat recovery.

Figure 6.10 presents the exhaust heat recovery as a fraction of the total fuel energy, effective engine work and pre-reformer exhaust stream energy. When working close to optimally at the 50Nm and 105Nm conditions, the reformer is able to extract energy from the exhaust stream to recover around 1% of the total fuel energy supplied to the engine and reformer, which equates to between 3-4% of the effective engine work.

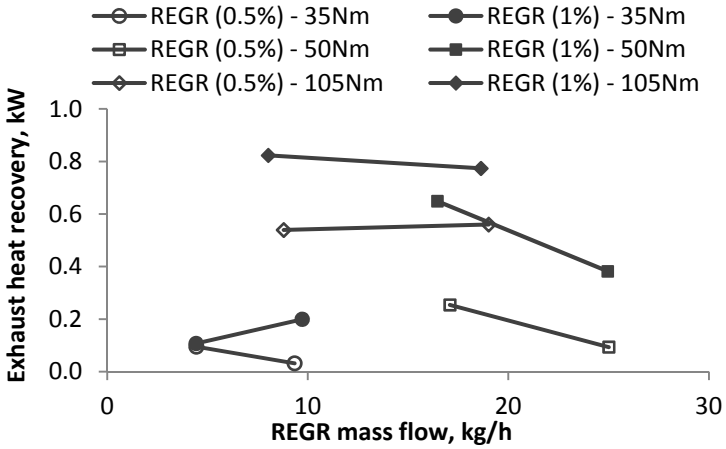

Figure 6.9 - Rate of exhaust stream heat recovery with fuel reforming

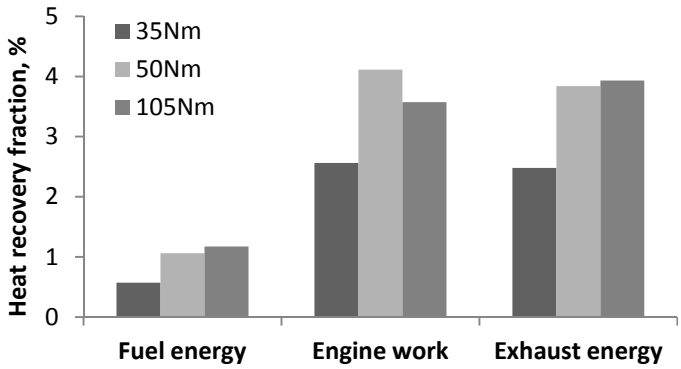

Figure 6.10 - Exhaust stream heat recovery as a fraction of total fuel energy, engine effective work and pre-reformer exhaust energy

6.5.2 Second law analysis: exhaust stream exergy

According to the second law of thermodynamics, exergy represents the maximum amount of work that may be extracted by bringing a system at temperature T to the ambient temperature T_0. The exergy of a fluid stream can be evaluated using Equation 6.3 [63]. This considers the exergy of the enthalpy, kinetic energy and potential energy of the fluid stream. This analysis was applied to the exhaust stream, which contains multiple gas species, using Equation 6.4 to calculate the 'energy availability' of the pre- and post-reformer exhaust gas, where $\dot{N}_{exh}$ is the molar flow of the exhaust stream (kmol/s) and n_i is the molar fraction of gas species i. In this case, T_0 was taken as 298K.

$$\psi = (h - h_0) - T_0(s - s_0) + \frac{V^2}{2} + gz \quad \text{(kJ/kmol)} \qquad \text{Equation 6.3}$$

$$\psi_{exh} = \sum \dot{N}_{exh} \cdot n_i \cdot \left[\left(h_i - h_{i,0}\right) - T_0\left(s_i - s_{i,0}\right)\right] \quad \text{(kW)} \qquad \text{Equation 6.4}$$

There were various assumptions made during the analysis. These included: the exhaust stream is a mixture of ideal gases; specific heat values are taken at the average process temperature, and were calculated using 3rd order polynomial relationships [63]; the TWC converts the exhaust stream to a mixture of inert gases (nitrogen, carbon dioxide and steam) with 100% efficiency and therefore the exhaust contains no species with chemical potential energy; the exergy of the kinetic and gravitational potential energy components of the exhaust stream are negligible.

As the reformer was designed to recover energy from the exhaust stream, there should be a reduction in exergy, or available energy, across the reformer. A more efficient overall engine-reformer system should also result in a reduction of the exhaust stream exergy (for a given load) at the reformer inlet. This accounts for the influence of REGR on the engine and combustion efficiency, which directly influences the exhaust exergy.

Figure 6.11 plots the pre- and post-reformer exhaust stream exergy as a percentage of the engine brake power for each test condition at each engine load. These plots show the general trend for reducing exhaust stream exergy with increasing dilution rate and reformed fuel fraction. In each case the baseline condition exhaust exergy was highest; both EGR and REGR reduced the exhaust exergy. The 50Nm engine condition represents the highest 'relative' exergy with 60% of the brake power available for recovery; the highest absolute exergy was at the 105Nm condition.

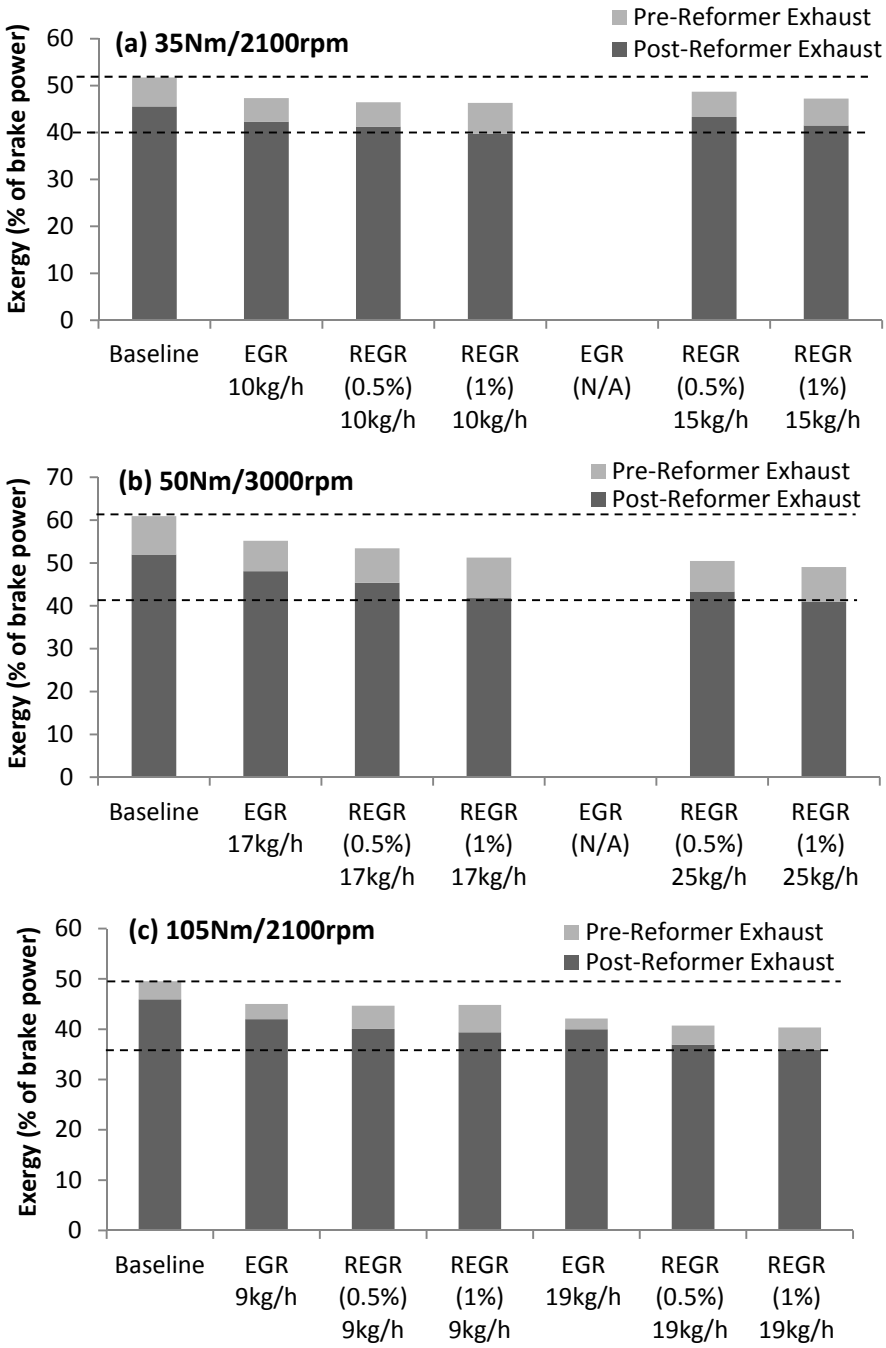

Figure 6.11 - Comparing pre- and post-reformer exhaust stream exergy for a variety of engine conditions (a) 35Nm, (b) 50Nm and (c) 105Nm

6.6 Summary

This chapter has demonstrated a full-scale prototype exhaust gas fuel reformer coupled with a multi-cylinder GDI engine. The results confirm that endothermic reforming of gasoline is feasible at typical GDI engine exhaust temperature.

At higher exhaust temperatures (above 650°C) the reformer is capable of converting gasoline to hydrogen-rich gas in an overall endothermic process while recovering some exhaust energy. Performance is borderline effective at lower exhaust temperature (around 600°C). This means that some reforming is possible, which produces hydrogen that may be beneficial to engine operation, but a small amount of fuel energy is lost in the reforming process.

Speciation of the reformate at a range of engine conditions indicates a large variation in its quality, with a strong dependence on process temperature. Reformate quality also drops off with increasing feed gas flow rate, however the rate of hydrogen production is increased while also raising the engine's dilution rate.

While the quantities of exhaust heat recovery are relatively low compared to the total energy content of the exhaust stream, the potential of a fuel reformer to efficiently produce hydrogen onboard a vehicle has been demonstrated. It was shown in Chapter 5 that quantities of hydrogen of the magnitude produced by the fuel reformer increases the engine's dilution tolerance and, as well as providing other benefits to combustion and emissions, improves engine thermal efficiency. The effect of the integrated exhaust gas fuel reformer on engine efficiency and emissions will now be discussed in Chapter 7.

CHAPTER 7

ASSESSING GDI ENGINE PERFORMANCE WITH EXHAUST GAS FUEL REFORMING

This chapter investigates whether the prototype exhaust gas fuel reformer is able to improve engine fuel efficiency as predicted by the simulated system in Chapter 5 and how the real REGR system affects engine emissions. Sections 7.1 and 7.2 discuss engine efficiency and emissions results for the engine and reformer operating conditions used in Chapter 6. Engine data are presented to identify the factors that influence engine efficiency when REGR is implemented. The effect that engine down-speeding has on GDI engine operation with exhaust gas fuel reforming is investigated in section 7.3. The chapter concludes with a study of the effects of fuel reforming at full engine load, including the use of two alternative gas recirculation system configurations.

7.1 Engine fuel efficiency

Figure 7.1 shows that the use of exhaust gas fuel reforming can provide a significant fuel saving at each of the engine conditions tested, particularly at the higher loads when conditions are more favourable for effective fuel reforming, i.e. the exhaust temperature is higher. The fuel efficiency results at the 105Nm engine condition were generally consistent with the trends presented in Table 5.5 in that REGR outperforms both EGR and the baseline condition. At the 35Nm condition the peak fuel efficiency improvement with REGR was lower than the other engine conditions, and lower than predicted in Table 5.5. There are various reasons for this. Firstly, the hydrogen concentration produced by the fuel reformer was lower at around 3%, compared to 7.5% used in the simulated reformate (0.1 combustible gas fraction), which,

as shown in Figure 5.4, results in marginally lower combustion speed and stability for a given dilution rate. For the real system the reformer process efficiency was lower, calculated to be 0.87 in section 6.4, meaning that some fuel energy was lost to the reforming process; therefore, the thermal efficiency of the total system will have been incrementally reduced. In contrast the 'reformer efficiency' of the simulated system was assumed to be 1, 1.1 or 1.3. Finally, there was a slightly lower maximum charge dilution rate of 26% compared to 28% for the simulated system. This was caused by the combustion stability limit being reached at lower dilution rate, again due to the lower hydrogen concentration.

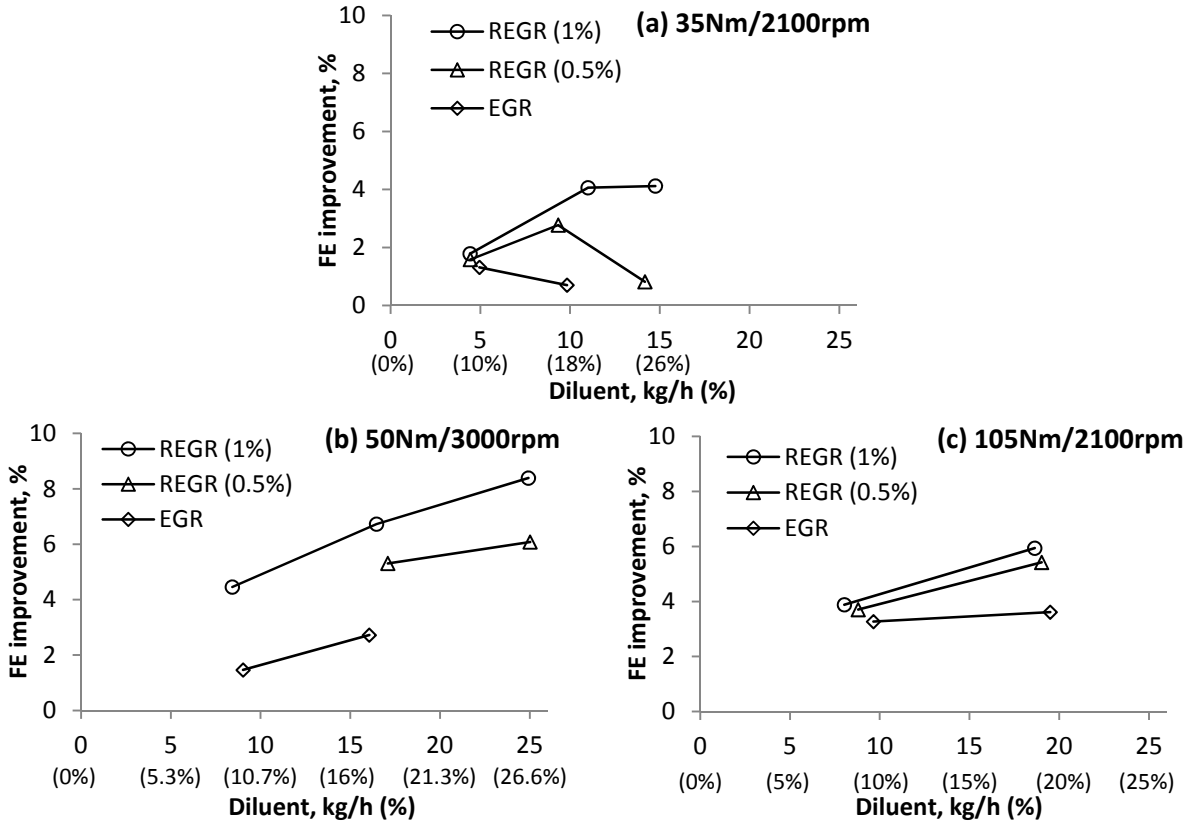

Figure 7.1 - Fuel efficiency (FE) improvement with EGR and REGR at three engine conditions

Referring again to Figure 7.1, it is seen that raising the gasoline flow rate to the reformer (from 0.5% to 1% feed gas concentration) improved the engine fuel efficiency in every instance. At the higher temperature conditions, this was partly because some of the additional

gasoline was successfully consumed in endothermic fuel reforming reactions that increased the enthalpy of the reformate, although this was not the case at the lower temperature (35Nm) condition; this was identified earlier in Figure 6.7c. In every case though, even at the lower temperature, increasing the fuel concentration did supply additional hydrogen to the engine (Figure 6.5), which was able to accelerate and stabilise the combustion process with some benefit to its thermal efficiency. This is particularly apparent in Figure 7.1a for the 14kg/h REGR conditions. In this case increasing the fuel concentration from 0.5% to 1% increased the hydrogen yield from 1.5% to 2.8%, which was enough to stabilise combustion (reducing the COV of IMEP from 11% to 6%) and raise the engine efficiency.

At the 35Nm engine condition the maximum REGR rate was limited by combustion stability, and at the other two conditions by the flow capacity of the gas recirculation system, so could not be increased further. However, it is evident that, in general, increasing the REGR rate improves engine fuel efficiency. The greatest engine fuel efficiency improvement observed was 8% at 50Nm/3000rpm. Because combustion was still stable at this condition, a further increase in the engine efficiency may be feasible if a higher REGR rate could be achieved. Being able to use a higher REGR rate would raise the reformed fuel fraction (of the total fuel supplied to the engine), which, providing the reforming conditions were adequate, would result in a greater enthalpy increase of the reformed fuel (ΔH_{ref}). Additionally, increasing the charge dilution rate should continue to enhance thermal efficiency providing that the combustion performance is maintained. Aside from those benefits, the reformate quality would be reduced to some degree due to higher GHSV, which would make it harder to achieve stable combustion with the increasingly high charge dilution.

These results show that the engine fuel efficiency improvement with REGR is always greater than can be achieved by conventional EGR, and generally offers at least double the fuel

saving. This is due to a combination of extended dilution rate (at the lower engine loads), which further reduces pumping and heat losses, as well as improved combustion (for similar dilution rates) and the successful conversion of waste exhaust energy to reformate fuel energy. The contribution from each of these factors will be discussed below with reference to Table 7.1, which summarises some important parameters that provide a measure of the engine and reformer performance and indicates the various sources of improved engine fuel efficiency. It also provides a quick comparison between the most efficient EGR and REGR conditions to the baseline condition at each engine load. Data are shaded where a result contributed to improved engine fuel efficiency.

For any thermodynamic cycle applied to an IC engine the ideal thermodynamic efficiency is determined by the engine's CR and the ratio of specific heats, γ, of the working fluid, as shown by Equation 2.12. It is preferable for thermodynamic efficiency (ideal and actual) to increase the values of CR and γ. In particular, γ is influenced by the working fluid composition and is reduced for increasing temperature, which is particularly relevant because the working fluid (the charge) temperature increases significantly during combustion. In this engine, because the AFR is fixed at stoichiometric, the charge composition varies mainly with overall dilution rate, which is ultimately defined by the residual gas fraction (influenced by valve timing) and the external EGR/REGR rate. The reforming process and specific reformate composition will also affect the charge composition. There are opposing affects on γ when EGR or REGR is introduced to the charge; γ is reduced when the concentration of steam or CO_2 in the charge increases (this was demonstrated in Table 2.2), but generally the temperature is lower during combustion and the expansion stroke so γ may be lower than for undiluted combustion.

Table 7.1 - Summary of engine and reformer results to highlight the sources of improved engine efficiency with REGR

ENGINE											Exhaust exergy (% of engine power)	
Test conditions [1]		BSFC, g/kWh	η_{ideal} [2]	COV of IMEP	η_{comb} [3]	MFB 10-90% (°CA)	$\dot{Q}_{max}$ [4] (J/deg)	PMEP bar	PMEP (% of IMEP)	EGT [5]	Engine-out	Post-reformer
35Nm/ 2100rpm	**Baseline**	390	0.452	2.8%	96.8%	32°	7.8	0.61	21%	648°C	55%	46%
	10% EGR	384	0.472	2.4%	96.5%	29°	8.0	0.62	22%	621°C	50%	42%
	26% REGR (1%)	374	0.411	6.0%	96.1%	36°	7.9	0.53	18%	595°C	48%	41%
50Nm/ 3000rpm	**Baseline**	352	0.460	1.6%	96.6%	24°	12.8	0.72	18%	749°C	64%	52%
	17% EGR	343	0.441	6.1%	95.7%	32°	9.8	0.59	15%	693°C	55%	48%
	26% REGR (1%)	325	0.466	2.4%	96.6%	30°	10.0	0.53	13%	669°C	50%	41%
105Nm/ 2100rpm	**Baseline**	269	0.462	1.6%	96.1%	20°	22.1	0.50	7%	745°C	48%	46%
	19% EGR	260	0.455	2.5%	95.8%	28°	17.6	0.29	4%	675°C	40%	40%
	19% REGR (1%)	254	0.465	1.5%	96.4%	25°	18.6	0.28	4%	676°C	40%	36%

REFORMER					Reformate		Reforming process		Exhaust heat recovery [11]	
Test conditions [1]		Reformed fuel [6]	EGT [7]	Reformer temp. [8]	H_2	CO	η_{ref} [9]	ΔH_{ref} [10], kW	kW	% of eng. power
35Nm/ 2100rpm	**26% REGR (1%)**	21.2%	592°C	558°C	2.5%	0.8%	0.86	-0.34	0.1	1.3%
50Nm/ 3000rpm	**26% REGR (1%)**	19.8%	661°C	568°C	9.8%	3.0%	1.14	2.29	0.4	2.4%
105Nm/ 2100rpm	**19% REGR (1%)**	13.9%	683°C	615°C	7.3%	3.2%	1.04	0.90	0.8	3.4%

Shaded regions identify parameters that contribute to increasing the engine thermal efficiency with REGR

[1] Data for EGR and REGR correspond to the highest fuel efficiency conditions in Figure 7.1; [2] Ideal thermodynamic efficiency calculated using Equation 2.12 and γ estimated from the log(p-V) gradient during the expansion stroke; [3] Combustion efficiency; [4] Maximum rate of heat of release from combustion; [5] Engine-out EGT; [6] Fraction of total fuel processed by the reformer; [7] Pre-reformer EGT; [8] Reformer temperature (M4 thermocouple in Figure 3.8); [9] Reforming process efficiency; [10] Enthalpy increase of reformed fuel; [11] Estimate of exhaust heat recovery based on the EGT drop due to reforming (section 6.5.1)

There are also experimental influences on the calculated value of γ. For instance the deterioration of combustion stability implies that combustion occurs later for an increasing number of cycles, resulting in higher gas temperature during the expansion stroke and a lower γ value.

The ideal thermodynamic efficiency was calculated using Equation 2.12. γ was estimated from the measured cylinder pressure data, the value taken as the gradient of a linear curve fit applied to the expansion stroke of the average log(p-V) curve over 300 engine cycles.

In general, the use of external EGR resulted in a lower value of γ and reduced the calculated value of ideal thermodynamic efficiency (Table 7.1). The opposite was true when the EGR rate was lower (10% at the 35Nm condition) and the alternative cam timing had also reduced the residual fraction, so the overall dilution rate was low. For the REGR conditions at the two higher engine loads, γ and the ideal thermodynamic efficiency slightly exceeded that of the baseline. This was due to a combination of lower combustion temperature (than the baseline) and reduced steam (and to a lesser extent CO_2) concentration in the raw charge (compared to EGR) after being consumed in reforming reactions. A sharp reduction of γ at the 35Nm REGR condition is expected to be partly a result of engine operation at the combustion stability limit resulting in more cycles with late combustion leading to high temperature, as well as the high dilution rate.

Information that describes the combustion performance is provided in Table 7.1, specifically the combustion efficiency, main combustion phase duration, and the maximum rate of heat release. Together these indicate that combustion performance with REGR does not directly contribute to increasing engine efficiency. The combustion efficiency is not increased by REGR, and is relatively unchanged in any case, although is slightly lower for EGR. Therefore

the fraction of the total chemical energy released during combustion is not increased by REGR compared to the baseline, but it is not reduced as it is by EGR. The maximum heat release rate with REGR is never greater than at the baseline, which means combustion is generally slower and the combustion durations are longer. From these results it is concluded that combustion performance is not improved by REGR relative to the baseline, but it is enhanced compared to EGR for the same dilution rate or maintained while achieving higher charge dilution.

It is well established that charge dilution reduces pumping losses and Chapter 5 confirmed this to be the case with REGR too. In these tests the pumping work at the baseline condition was of similar magnitude for each engine load, between 0.5-0.7bar PMEP in Table 7.1. However, the pumping work was a far greater proportion of the IMEP at lower engine load and is therefore a more significant cause of engine inefficiency. REGR reduced the pumping work at all engine conditions by a similar fraction of the IMEP, between 3 and 5 percentage points, therefore providing a contribution to the overall increased engine efficiency with REGR in each case.

Cam timing also has a strong influence on the pumping work. The standard cam timings, which result in a long valve overlap during the intake stroke, aim to reduce NO_x emissions by generating high exhaust residuals. This approach also reduces the pumping work by de-throttling the engine and increases engine efficiency. The short valve overlap cam timings used here for low exhaust residuals have the opposite effect, and it requires the use of moderate to high EGR or REGR rates to reduce the pumping work significantly below that for the baseline case.

The rate of heat transfer from the cylinder contents to the combustion chamber walls is controlled to large degree by the temperature gradient that arises as a result of combustion; the total heat loss therefore increases with combustion temperature. Charge dilution reduces the combustion temperature and the total heat loss, thereby improving engine efficiency to some degree. Additionally the hot exhaust gases leaving the cylinder contain a significant proportion of the energy released from combustion. Although not quantified, it can be inferred that REGR reduced heat losses. The large reductions in EGT (Table 7.1) and lower NO_x formation with REGR (Figure 7.2 below) imply that lower in-cylinder temperatures prevailed during the combustion process, inevitably reducing the rate of heat transfer and the total heat loss.

Details of the reforming process efficiency, amount of exhaust heat recovery and the exhaust exergy for each condition are also included in Table 7.1. These results were presented in Chapter 6 and are included here to highlight that the reforming process directly contributes to increasing the engine efficiency by increasing the reformed fuel enthalpy.

7.2 Engine emissions

Figure 7.2 confirms that NO_x, CO and PM emissions were all reduced by REGR, similarly to the results obtained in the simulated REGR experiments of Chapter 5. Again there was a moderate increase in HC emissions due to the highly diluted combustion and reduced in-cylinder temperature, but the increase was less than for equivalent EGR dilution. The mechanisms for reduced emissions with EGR and REGR have been adequately discussed and justified and will not be repeated here. However, it is important to demonstrate that exhaust gas fuel reforming provides a complete solution for reducing fuel consumption, gaseous emissions and PM.

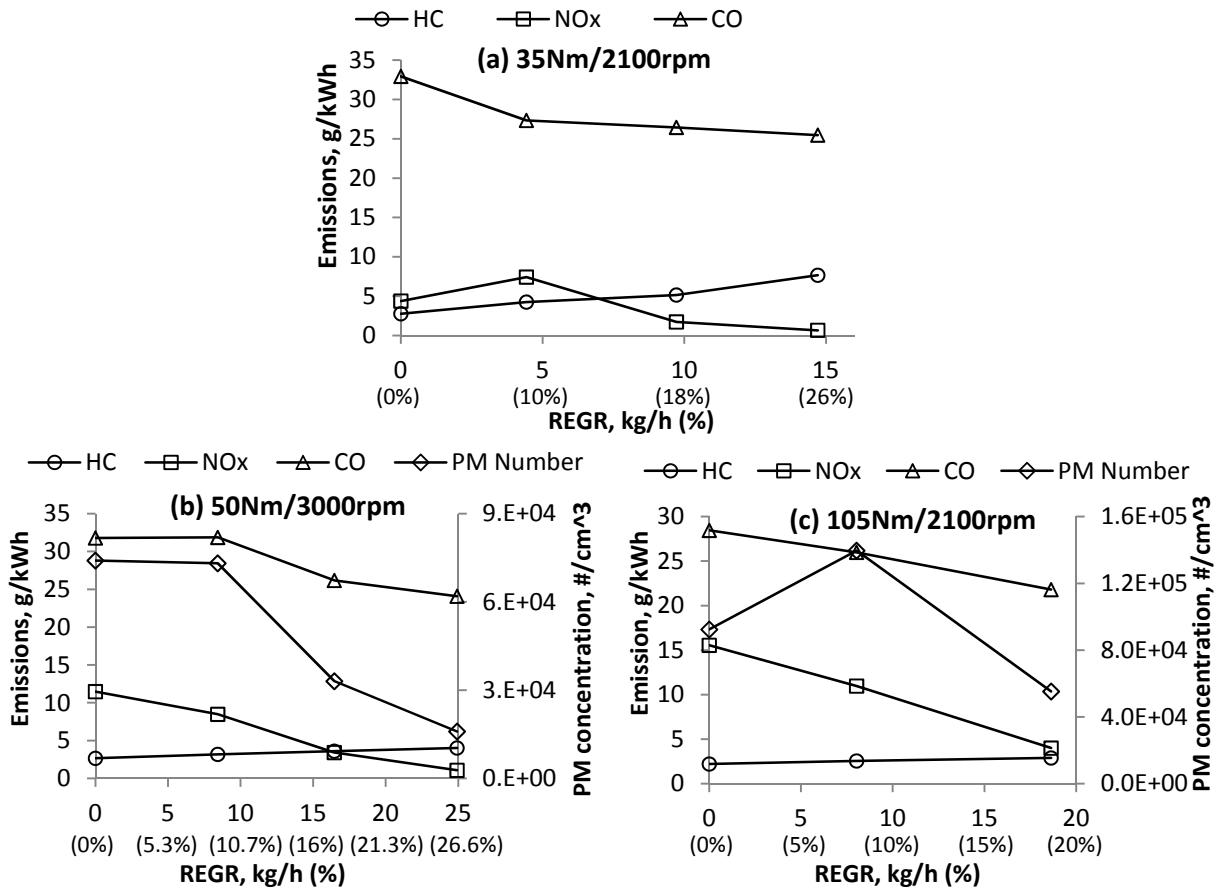

Figure 7.2 - Effect of REGR on engine-out specific NO_x, HC, CO emissions and PM number concentration at 35Nm (a), 50Nm (b) and 105Nm (c) [PM sampled using thermodenuder]

Table 7.2 details the percentage variation in engine emissions with REGR compared to the baseline emissions performance. The 50Nm engine condition showed perhaps the best overall change in emissions when using REGR; NO_x was reduced by 91% and CO by 24%, PM number and mass were reduced by 78% and 84% respectively, while HC suffered a moderate increase of 51%.

Table 7.2 - Percentage change in engine emissions with REGR from baseline performance

	CO	HC	NOx	PM #	PM Mass
35Nm	-23%	+177%	-85%	-	-
50Nm	-24%	+51%	-91%	-78%	-84%
105Nm	-31%	+19%	-78%	-71%	-86%

Maximum REGR rate (with 1% fuel) used at each load

7.2.1 PM emissions

A more detailed analysis of the effect of EGR and REGR on PM emissions is provided by Figure 7.3, which compares the total PM number and mass concentration with EGR and REGR with 0.5% and 1% reformer feed gas fuel concentration at 105Nm/2100rpm. The error bars show some variability in the particulate measurements, but the general trend is that both EGR and REGR reduce PM number and mass. This replicates Figure 5.7 from the simulated REGR testing that revealed REGR reduces PM more than a comparable EGR dilution. This effect was repeated with the use of the prototype fuel reformer at the high dilution rate (19kg/hr) condition. With moderate dilution (~8kg/hr) both EGR and REGR gave very similar particulate measurements, although both were lower than the baseline. Section 5.2.4 described in detail the reasons for PM emissions reduction with EGR and REGR containing hydrogen and CO.

The influence of cam timing on PM at the baseline condition (with no external dilution) should also be noted. The standard cam timing uses a long overlap period well into the induction stroke, resulting in higher exhaust residuals than with the modified cam timings used elsewhere. Changing to the cam timings for low exhaust residuals increases the PM number and mass. This is indicative of the effect that internal EGR has on reducing PM emissions [30]. Another reason PM is lower with the standard cam timings is that the exhaust valve opens later which extends the high temperature period for soot oxidation. Introducing low levels of EGR or REGR with the modified cam timing reduces the PM emissions to some degree, but it requires the use of high REGR to bring the PM emissions below that for the engine in baseline configuration. EGR was not able to match this PM reduction.

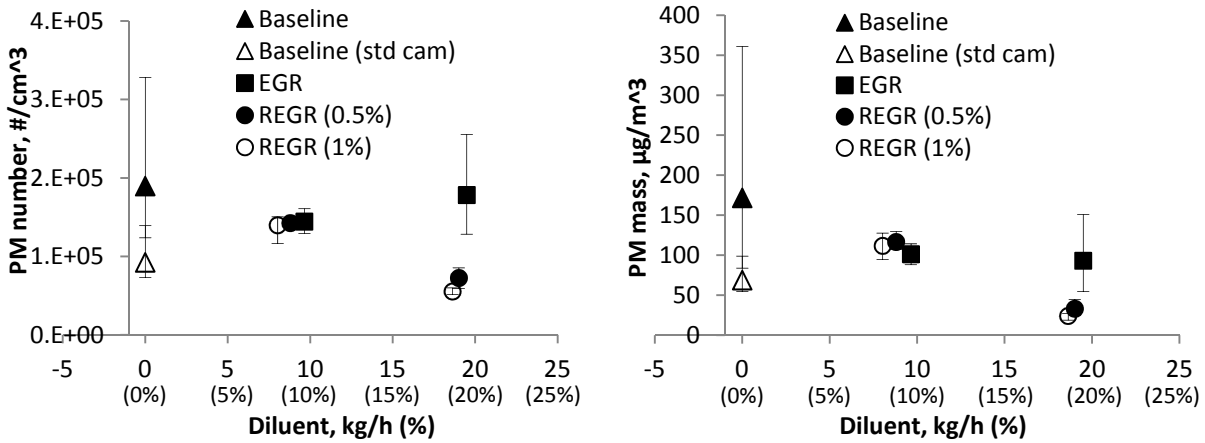

Figure 7.3 - Total particle number and mass concentration with alternative dilution strategies at 105Nm/2100rpm [PM sampled using thermodenuder]

7.3 Effect of exhaust gas fuel reforming on engine performance when combined with down-speeding

So far the fuel reformer and engine performance has been presented for three engine conditions. Of these, engine efficiency was improved most significantly at the 50Nm/3000rpm condition, which equates to 15.7kW effective engine power. This section investigates how reducing the engine speed from 3000rpm to 2500rpm and 2000rpm, while the engine power is maintained at 15.7kW by increasing the load, influences the fuel reformer's ability to improve fuel efficiency. This is of relevance because engine down-speeding is a technique increasingly used in vehicle development in order to operate the engine more frequently in higher efficiency regions of the performance map.

The EGT and the maximum recirculation rate both vary with engine speed and load, which are parameters of particular importance to reformer operation. For example, Figure 7.4, which was obtained in section 5.4.4, shows the variation of post-TWC exhaust temperature across the engine range; the three constant power engine conditions selected for this investigation are identified by Δ markers. This demonstrates that the temperature drops by approximately 50°C as the engine speed is reduced from 3000rpm to 2000rpm. This may be expected to be of

some detriment to reformer performance, but it was not known if this would reduce or eliminate the engine fuel efficiency benefit experienced when implementing REGR at the 50Nm/3000rpm condition. At each of the three engine conditions the EGR valve was fully opened to achieve the maximum REGR rate, and the reformer feed gas fuel concentration was fixed at 1%.

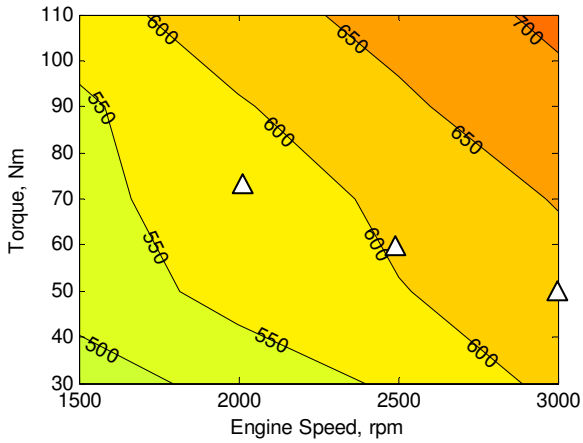

Figure 7.4 - Map of post-TWC exhaust temperature with simulated REGR
Δ markers identify the three selected constant power (15.7kW) engine conditions

7.3.1 Reformer performance

Table 7.3 summarises the reforming conditions and the reformate composition for the three constant power engine conditions used. The reformate hydrogen and HC concentrations were not measured for these tests. The reformer inlet EGTs were higher than predicted by Figure 7.4 due to the thermal insulation applied to the exhaust system, but there was still a 45°C drop in temperature as a result of reducing the engine speed from 3000rpm to 2000rpm. The reformer plate temperatures were higher at the lower engine speeds because the lower REGR flow rate meant there was less fuel injected into the reformer. In each case the resulting reformed fuel fraction of the total gasoline supplied to the system was similar at around 20%. This was a consequence of the parallel reduction of REGR flow and fuel flow to the engine, which were caused by the increased intake manifold pressure and more efficient engine

operation, respectively. Lower CO and higher CO_2 and steam concentrations in the reformate clarify the slight reduction in reformer activity at lower engine speed when the EGT was lower.

Table 7.3 - Summary of reforming conditions and reformate composition

	REGR (kg/h)	Reformed fuel [1] (%)	EGT (Pre-reformer)	Reformer temp. [2]	Reformate composition		
					CO,%	CO_2, %	Steam, %
50Nm/ 3000rpm	25	20	662°C	545°C	3.3	11.9	5.1
60Nm/ 2500rpm	23	19	654°C	577°C	3.1	11.7	6.1
75Nm/ 2000rpm	21	20	617°C	568°C	2.0	12.2	7.6

[1] Fraction of total fuel processed by the reformer; [2] Reformer temperature (M4 thermocouple in Figure 3.8)

7.3.2 Engine efficiency

Table 7.4 summarises the engine efficiency and emissions performance when down-speeding with REGR. The shaded data identify the best performance in each case. Down-speeding requires the engine to be de-throttled in order to increase load and maintain power, which increases the intake manifold pressure thereby reducing the pumping work (Table 7.4). Engine friction and other parasitic losses are also reduced for lower engine speeds. These factors combine to raise the thermal efficiency and reduce the BSFC.

Figure 7.5 demonstrates the steady reduction of fuel consumption achieved by engine down-speeding for the baseline GDI engine condition. The trend is also closely matched when operating with REGR, but is offset to lower BSFC. This confirms there is a consistent fuel efficiency benefit of around 7%, meaning that exhaust gas fuel reforming is equally effective at the lower engine speeds and is therefore compatible with the engine down-speeding approach to increasing fuel efficiency.

Table 7.4 - Engine efficiency and emissions when down-speeding with REGR

		MAP [1] (bar)	PMEP (bar)	EGT (Pre-reformer)	BSFC (g/kWh)	Emissions (g/kWh)		
						CO	HC	NO_x
50Nm/ 3000rpm	**Baseline**	0.58	0.75	704°C	348	31	2.3	9.2
	REGR	0.63	0.57	662°C	325	27	3.8	1.0
60Nm/ 2500rpm	**Baseline**	0.67	0.67	719°C	316	35	2.0	8.9
	REGR	0.70	0.45	654°C	294	23	3.4	0.9
75Nm/ 2000rpm	**Baseline**	0.72	0.58	686°C	291	31	2.1	9.2
	REGR	0.78	0.33	617°C	272	20	3.6	1.2

[1] Intake manifold air pressure. Shaded data identifies the best performance

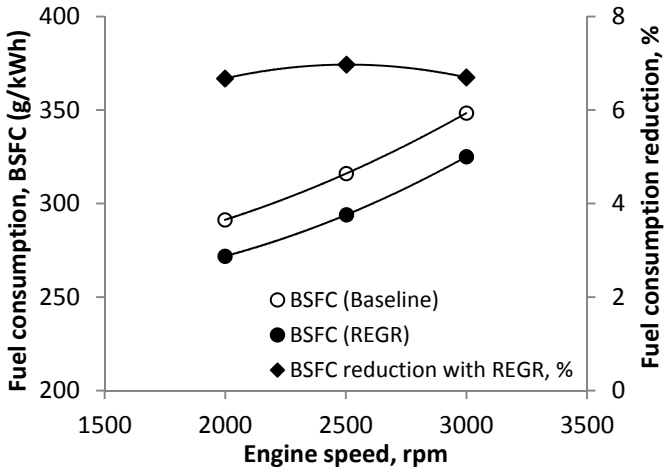

Figure 7.5 - BSFC and percentage BSFC reduction with REGR for different engine operating points (fixed power - 15.7kW)

7.3.3 Combustion

Figure 7.6 depicts the combustion process with pressure-volume diagrams, rate of heat release and MFB curves plotted for each engine speed/load condition with REGR. It can be seen clearly in Figure 7.6b that the pumping loop generated by the exhaust and induction strokes is reduced significantly by moving to lower engine speed, and this is a primary factor that increases engine efficiency when down-speeding a throttled SI engine.

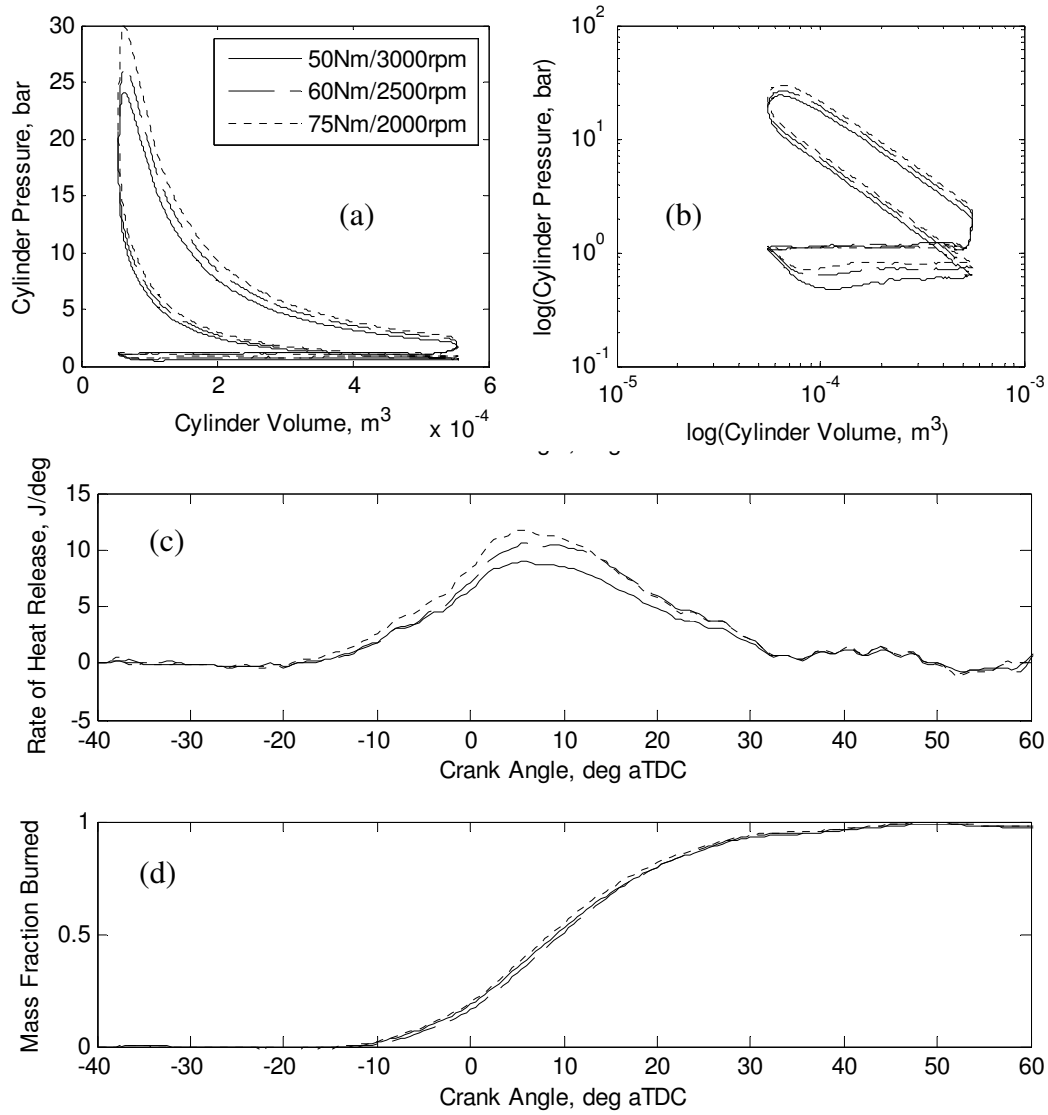

Figure 7.6 - Combustion plots for the three constant power (15.7kW) engine conditions with REGR: (a) pressure-volume diagram, (b) log(pressure-volume) diagram, (c) rate of heat release, (d) MFB curve

Reducing the engine speed also results in higher peak cylinder pressure (Figure 7.6a) near to TDC, increasing the work generated. This is partly because the heat released from combustion per degree of crank rotation becomes higher as the engine speed is reduced (Figure 7.6c) leading to a higher rate of cylinder pressurisation. Also, the cylinder pressure at BDC is increased at lower engine speed, matching the intake manifold pressure, which leads to higher pressure for the duration of the compression stroke (Figure 7.6b) although this does increase the compression work slightly. Aside from this the combustion performance at each condition

is quite similar, certainly in terms of the combustion phasing (visualised by the MFB curve in Figure 7.6d).

Of the engine conditions investigated, 75Nm/2000rpm with maximum REGR offers the best overall performance in terms of fuel efficiency and emissions (Table 7.4). Partly this is due to the effect that engine down-speeding has on increasing thermal efficiency. Importantly, exhaust gas fuel reforming continues to offer a fuel efficiency improvement as the engine speed is reduced and reforming conditions become less favourable.

7.4 Full load engine performance with exhaust gas fuel reforming

This section investigates and compares the use of EGR and REGR at full engine load. Abnormal combustion is often encountered at high load, particularly knock which occurs readily at lower engine speeds. EGR has proven to be able to attenuate knocking combustion [28, 32, 122] and low speed pre-ignition [31] at high engine load. Similarly, the knock susceptibility of gasoline combustion is reduced by the addition of hydrogen and CO which act as octane enhancers [71]. The REGR system combines hydrogen and CO addition with EGR-like dilution, therefore may also be expected to successfully attenuate knock.

For this investigation the fuel reformer was operated with the engine at wide-open throttle at 1500rpm. This low speed condition was selected as it would be suitable to establish the influence of REGR on the engine's combustion performance and knock characteristics. The standard cam timings (-28° IVO and 28° EVC) were used which provide a long valve overlap period centred around TDC to ensure good cylinder scavenging and high VE under boosted intake manifold conditions. For each test point the knock-limited ignition timing was used and the charge air temperature controlled to 45°C. In each case the reformer feed gas fuel concentration was 1.5%.

For turbocharged engines operating at full load the intake manifold pressure is similar to or higher than the exhaust pressure, which means it is generally not feasible to use a HP gas recirculation system. Therefore the MP and LP gas recirculation system configurations illustrated in Figure 3.9 were implemented for this investigation. These systems extract exhaust gas from either before (MP) or after (LP) the turbine; therefore, they influence the turbocharger and engine operating characteristics, such as turbine mass flow and backpressure, which strongly influence peak load and engine efficiency. In both cases the re-circulated gas is inducted into the intake system upstream of the compressor. The maximum recirculation rate was found to be 13% using the MP system and, due to the lower manifold pressure ratio, 6% for the LP system.

Before the full load engine performance with REGR is examined, details of the exhaust and reformer temperatures and the reformate composition will be presented.

7.4.1 Reformer operation at full engine load

Ignition retardation implemented to avoid knock at the full load baseline condition results in the EGT approaching 800°C, higher than if a more advanced combustion process were possible. Figure 7.7a indicates that there is a more significant drop in EGT when introducing EGR or REGR than seen at lower engine loads because there is a greater influence from advanced combustion phasing, which reduces the EGT. Referring back to Figure 6.1, the use of 17kg/h REGR caused a 40°C drop in EGT at 50Nm/3000rpm, and by 70°C for 19kg/h at 19kg/h at 105Nm/2100rpm. Figure 7.7a shows that at this full load condition the EGT was reduced by 100 degrees to around 700°C with just 13kg/h REGR. The resulting reformer plate temperatures, which were generally between 610-660°C (Figure 7.7b), were quite similar to the 105Nm/2100rpm condition used in Chapter 6.

It should be considered that these tests were performed under steady state conditions meaning that the exhaust and reformer temperatures had the opportunity to equilibrate. During normal transient engine use, which may experience relatively short durations at full load and large variations in engine speed, thermal inertia associated with the exhaust and reformer system could lead to substantially different reformer temperature distributions.

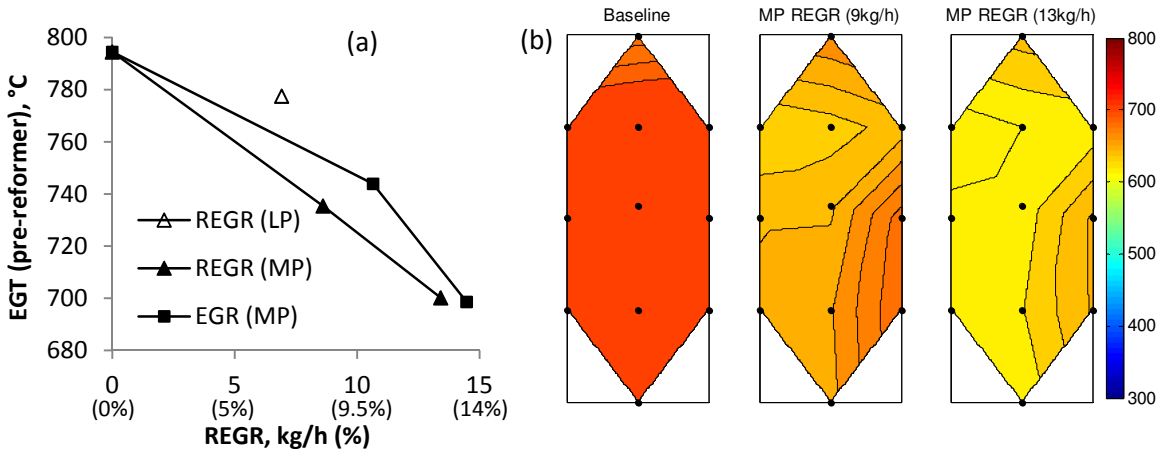

Figure 7.7 - (a) Variation of pre-reformer EGT with EGR and REGR flow rate and (b) temperature distribution across the middle reformer plate at full engine load, 1500rpm

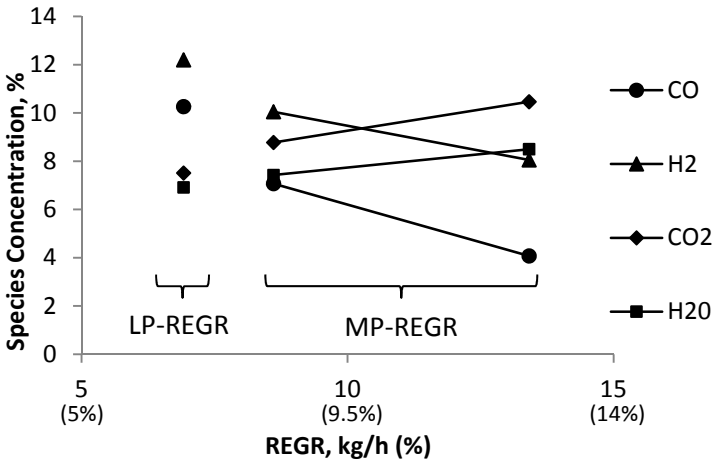

Figure 7.8 - Reformate composition variation with reformer flow rate at full engine load, 1500rpm using the LP and MP systems

The relatively low REGR flow rates combined with high EGTs improved the reforming activity compared to the earlier tests, which meant that a higher feed gas fuel concentration of

1.5% could be used without excessive HC breakthrough. For these reasons the maximum hydrogen and CO yields (Figure 7.8) were higher than the results presented in Chapter 6.

7.4.2 Full load engine performance and fuel efficiency

Figure 7.9a plots the peak torque achieved at full engine load and the corresponding fuel efficiency for MP and LP REGR, and shows that the peak torque produced by the engine was reduced as the REGR flow rate increased. This was a result of fresh charge being displaced by REGR, reducing the volume of oxygen available for combustion. Therefore less fuel (gasoline and reformate) was supplied to the cylinder in order to maintain a stoichiometric AFR, meaning that the total energy released from combustion was reduced, which results in lower peak torque.

In addition, when REGR is introduced using the MP system the engine's VE is reduced considerably, more than for the LP system. This is because exhaust gases are extracted from before the turbine, which reduces the pre-turbine pressure, the exhaust mass flow and the resulting rate of turbine work; in turn, there is lower compressor work and the intake manifold pressure is reduced. This causes the drop in VE, which also reduces the fresh charge mass for combustion. It is also apparent that higher engine torque was achievable with the LP system that the MP system. This is because the exhaust gas is extracted after the turbocharger; therefore, the mass flow through the turbine is higher with the LP system, which increases the turbine work.

Although REGR was detrimental to peak torque the engine fuel efficiency was improved significantly in all cases, by up to 8% at the highest REGR flow condition (Figure 7.9). There was a slightly smaller fuel efficiency benefit with the LP system, partly because the REGR flow rate was lower compared to the MP system, and also because there was a higher exhaust

backpressure due to increased turbine mass flow. The various reasons for improved engine efficiency with REGR were discussed in section 7.1, most of which are also applicable at high engine load, and will be expanded upon in section 7.4.3.

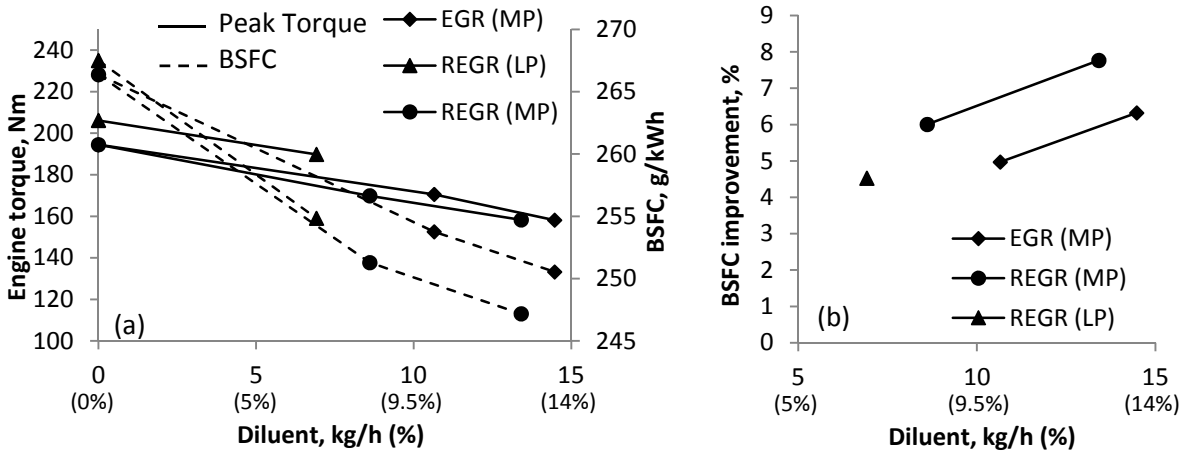

Figure 7.9 - (a) Peak torque and fuel efficiency and (b) percentage fuel efficiency improvement at 1500rpm using EGR and REGR with the MP and LP systems

It should be emphasised that the engine speed was selected to be 1500rpm because it is a low speed condition, and will therefore be susceptible to knock at high load. This happens to be below the speed at which the engine is able to produce maximum torque, which is achieved between approximately 1750 and 4500rpm. This means that 1500rpm is outside of the turbocharger's optimum operating range. Therefore it may be expected that with some redesign of the turbine and compressor characteristics, the full load performance at low speed may be restored to some degree while implementing REGR by providing higher intake manifold pressurisation.

7.4.3 Combustion with REGR at full engine load

Increasing the EGR or REGR mass flow rate advanced the initiation of knock and so the ignition timing could also be advanced. This is demonstrated in Figure 7.10, which shows that the combustion phasing (position of MFB50%, °aTDC) was steadily advanced as EGR or REGR was introduced. At the baseline GDI engine condition MFB50% occurred at around

21°aTDC, which is considerably retarded and of detriment to thermodynamic efficiency. The ability to advance the combustion phasing when using EGR or REGR works to increase the engine thermal efficiency. The optimum combustion phasing will vary to some degree depending on the exact engine conditions and combustion performance, but MFB50% values in the range 6-10°aTDC may be considered close to optimum. In these tests the use of greater than 13kg/h EGR or REGR allowed the optimum combustion phasing to be achieved.

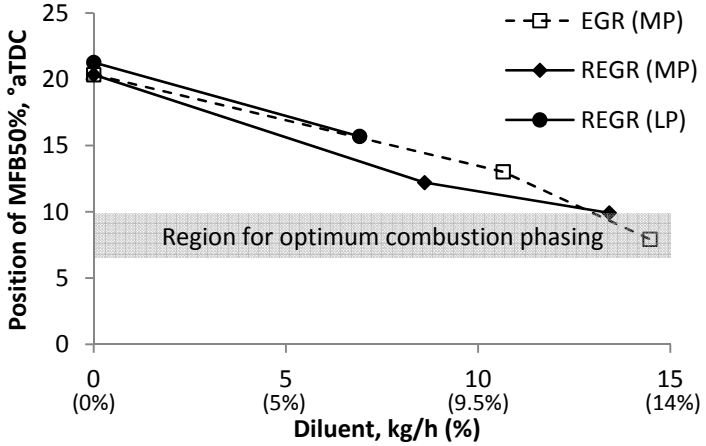

Figure 7.10 - Combustion phasing at the knock-limited ignition timing using EGR and REGR at full engine load, 1500rpm with the MP and LP systems

Arguably, maximising thermal efficiency is less critical at full load due to the typically low duty cycle, and achieving what is considered to be acceptable peak load performance is the most important criteria. From the above it is obvious that the LP system has the superior maximum load performance at this engine condition. With this in mind, the combustion performance with LP-REGR will now be studied in more detail.

Table 7.5 summarises the variation of some important engine parameters at the knock-limited ignition timing for LP-EGR, LP-REGR and the baseline. This demonstrates that lower exhaust pressure and EGT (which is proportional to exhaust enthalpy) with EGR and REGR lead to reduced intake manifold pressure and air mass flow, which reduce the maximum

engine torque. The relative changes to engine emissions are small compared to earlier results because the EGR and REGR rates were low at around 8%.

Table 7.5 - Summary of engine conditions, efficiency and emissions at full load, 1500rpm at the baseline, with LP-EGR and LP-REGR

	Max torque (Nm)	Exhaust Pressure [1] (bar)	EGT [2] (°C)	MAP [3] (bar)	MAF [4] (kg/h)	BSFC (g/kWh)	Emissions (g/kWh)		
							CO	HC	NOx
Baseline	213	1.43	839	1.34	129	267	42	2.5	18
EGR	195	1.39	764	1.29	115	261	37	3.5	12
REGR	194	1.37	750	1.27	111	254	37	3.1	14

[1] Pre-turbine exhaust pressure; [2] Pre-turbine EGT; [3] Intake manifold air pressure; [4] Air mass flow

The cylinder pressure trace, rate of heat release and MFB curves are plotted in Figure 7.11 for each condition. For combustion with REGR the cylinder pressure begins to rise above the compression pressure curve earlier in the cycle (Figure 7.11a) due to a combination of advanced ignition timing relative to the baseline, and faster and more advanced combustion compared to EGR (Figure 7.11b). Together these result in the peak cylinder pressure occurring closer to TDC and the combustion phasing being advanced toward the optimum position (Figure 7.11c).

Referring to the pressure-volume diagrams of Figure 7.12 it can be seen that REGR shifts the work loop towards TDC, which increases thermodynamic efficiency as it is closer to the ideal Otto cycle shape. Even so, there is a large departure from the typical Otto cycle around TDC, particularly for the baseline due to late ignition timing and combustion initiation. It should be noted that the air and fuel flow rate was different in each case due to the variation in manifold conditions caused by the shift in turbocharger performance. Because there was a higher air mass flow to the cylinder at the baseline condition (Table 7.5), there was more potential fuel energy to be released during combustion and this, combined with higher and later rate of heat

release (Figure 7.11b), resulted in higher cylinder pressure for the duration of the expansion stroke. This meant that the work generated was higher than when EGR or REGR were used, but at the expense of efficiency. It is also apparent from Figure 7.11b that the pumping work was insignificant at full engine load while under boosted intake manifold conditions, with the pressure-volume diagram pumping loop virtually eliminated.

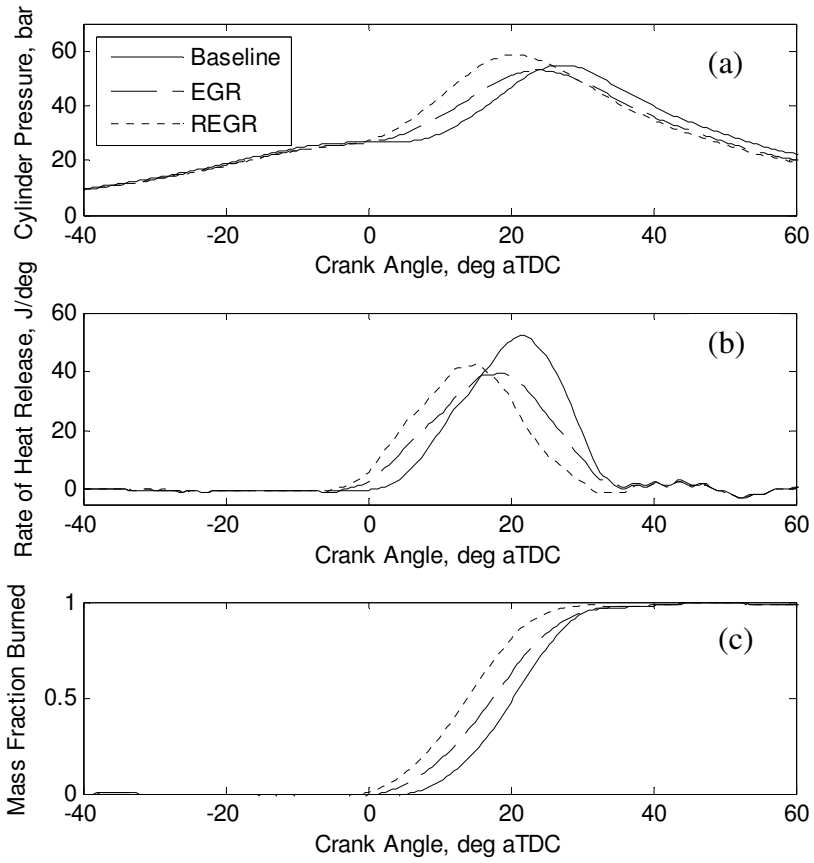

Figure 7.11 - (a) Cylinder pressure, (b) rate of heat release and (c) MFB curve for combustion at full load, 1500rpm at the baseline, with LP-EGR and LP-REGR

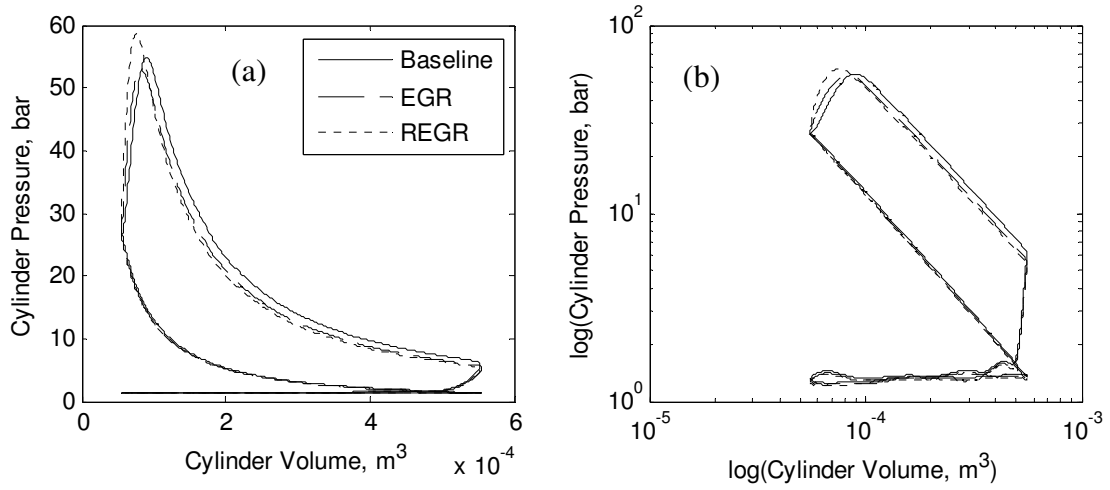

Figure 7.12 - (a) Pressure-volume and (b) log(pressure-volume) diagrams for combustion at full load, 1500rpm at the baseline, with LP-EGR and LP-REGR

7.5 Summary

This chapter has confirmed that exhaust gas fuel reforming is a technology capable of improving GDI engine efficiency and emissions with the demonstration of a full-scale prototype coupled with a multi-cylinder GDI engine. Analysis of the reformer process in chapter 6 showed that GDI engine exhaust conditions are favourable for fuel reforming and can promote endothermic reforming reactions to achieve exhaust heat recovery and increase the fuel enthalpy, although this was not true for the lower engine load condition tested. This chapter has shown that, in any case, operating with the reformer improves engine efficiency, by up to 8% for the higher temperature conditions and 4% for the lower temperature condition. Gaseous and PM emissions are largely reduced with the implementation of REGR with the exception of HCs, which are slightly increased.

Further tests identified that engine down-speeding does not reduce the effectiveness of exhaust gas fuel reforming in terms of the percentage reduction of fuel consumption, providing a consistent benefit of around 7% between 2000 and 3000rpm under steady state conditions.

The use of REGR at full engine load was found to be effective for advancing the onset of knock, allowing for advanced combustion phasing as well as increasing engine efficiency. However, the peak engine torque was reduced substantially with increasing REGR mass flow. A LP gas recirculation system offers higher peak load performance than a MP system due to higher exhaust mass flow through the turbine. The MP system does allow higher REGR rates to be used that result in a larger efficiency increase, although at the expense of peak engine torque.

CHAPTER 8

CONCLUSIONS

8.1 Summary of findings

The thesis has explored how exhaust gas fuel reforming can be beneficial to GDI engine efficiency and emissions, and has investigated the characteristics of the exhaust gas fuel reforming process applied to a GDI engine under stoichiometric exhaust conditions. Experimental results were collected from simulated reformate combustion studies using a single-cylinder GDI engine and a 2L turbocharged GDI engine, as well as from tests using a full-scale prototype exhaust gas fuel reformer. A summary of the major findings from this collection of research follows.

8.1.1 Reformate combustion studies

Single-cylinder engine

Experimental data from reforming catalyst testing informed the selection of an achievable reformate composition to be used for the study of reformate combustion in the single-cylinder engine. Bottled reformate was used to replicate a REGR system and, due to the absence of an EGR system on the single-cylinder engine, nitrogen was used to approximate conventional EGR. The reformate composition was 5% hydrogen, 4% CO, 10% CO_2 and 81% nitrogen.

The results showed that REGR improves combustion stability, results in a large NO_x reduction relative to the baseline engine condition, and a reduction in HCs relative to EGR. REGR enables a wider range of usable ignition timings at low engine load and reduces the tendency to knock at higher load. Because nitrogen was used to approximate EGR there were

some limitations when interpreting the results, specifically because the steam and CO_2 contained in real EGR influence the charge properties and the resulting combustion process.

Multi-cylinder engine

These limitations were addressed in tests on the multi-cylinder GDI engine by adding hydrogen and CO to the intake via a conventional EGR system in order to replicate REGR. This approach enabled the generation of reformate with realistic, achievable compositions that included CO_2 and steam. Again REGR and EGR performance were directly compared to the baseline GDI engine. The simulated REGR system consistently improved engine efficiency and emissions relative to the baseline GDI engine and engine operation with EGR.

At low engine load (3bar IMEP) REGR outperforms EGR by improving the ignitability of the charge and increasing the combustion rate, which together improve combustion stability thereby extending the dilution limit. Additionally, the use of valve timings for low exhaust residuals was found to extend the maximum achievable REGR rate, which may otherwise be limited by poor combustion stability. This enabled an 8% improvement to indicated efficiency with REGR at low load. At higher load (7.2bar IMEP) EGR and REGR performance were more comparable because the dilution rate was limited by the maximum flow rate of the gas recirculation system, in each case increasing indicated efficiency by around 5%. Data from reforming studies were used to estimate the reforming process efficiency, which was estimated to be 1.1, and enabled a prediction of the total engine-reformer system efficiency. This increased the predicted indicated system efficiency benefit of REGR to 9% and 6% at 3bar and 7.2bar IMEP.

Engine performance maps were generated to identify the relative performance of REGR at a wider range of engine conditions. The performance maps showed that REGR increases

indicated engine efficiency quite consistently, between 6% and 9% compared to the baseline GDI engine across the engine range explored (between 1000 and 3000rpm and up to 110Nm/7.5bar IMEP).

It is well accepted that charge dilution with EGR slows the combustion process, and this was also found to be the case for REGR when compared to the standard GDI engine. Generally it was found that the combustion rate was increased when hydrogen and CO were present in the charge with REGR compared with an equivalent EGR dilution, resulting in shorter combustion initiation and main phase durations. The improved ignitability and faster combustion enhanced the combustion stability and contributed to increasing the combustion efficiency. The overall combustion performance with REGR could not be restored to that for the baseline GDI engine, but it was possible to operate with higher dilution rates relative to EGR at low load engine conditions.

The engine-out EGT was reduced significantly by increasing the REGR rate, but exothermic reactions across the TWC meant that the reduction of the reformer inlet EGT was not as large. These results suggested that, due to its strong influence on the reforming process, the drop in EGT with increasing REGR may limit the maximum REGR rate for lower load engine conditions.

Overall, REGR has a positive effect on engine emissions. The primary factor that leads to reduced NO_x and CO emissions is the lower combustion temperatures experienced with REGR. This same factor combined with slower combustion and advanced exhaust cam phasing increases HC emissions, but less than with EGR. NO_x emissions were reduced by 82-96% across the range with REGR compared to the baseline. This was greater than was

achieved by EGR, which reduced NO_x by 40-90%. This improvement is due to the higher charge dilution rates possible with REGR.

PM emissions measurements found that REGR reduces PM number and mass in a similar manner to EGR, as well as reducing the mean particle diameter. The results also identified that the hydrogen and CO contained in REGR reduces PM emissions further than EGR alone, suggesting that there are complimentary mechanisms that reduce PM formation. Importantly, the energy content of reformate replaces a fraction of the liquid gasoline injected into the cylinder, which improves the charge homogeneity and reduces the possibility for PM to be formed when fuel rich regions of charge are burned. Generally speaking, advancing the ignition timing increases PM emissions, and the results revealed that using REGR reduces the sensitivity of PM emissions to ignition timing from 10 to 1.6 $\mu g/m^3$ per degree.

8.1.2 Exhaust gas fuel reformer performance

Experimental work using a full-scale prototype exhaust gas fuel reformer integrated with a multi-cylinder GDI engine has demonstrated that producing hydrogen by endothermic reforming of gasoline is possible. In doing so, some waste exhaust energy is recovered.

When the exhaust temperature was greater than 650°C, which is typical for moderate engine loads, exhaust gas fuel reforming was capable of converting gasoline to hydrogen-rich gas in an overall endothermic process. The reforming process efficiency was calculated to be greater than one, up to a maximum of 1.21, indicating that the fuel enthalpy was increased by reforming. The reformer was less effective when the exhaust temperature was lower (≈600°C) at lower engine load, and reforming process efficiencies were lower at around 0.87 meaning that some fuel energy was lost in the reforming process.

Analysis of the reformate composition for a range of reforming conditions confirmed a large variation in reformate quality with a strong dependence on process temperature, as predicted by thermodynamics. Increasing the reformer reactant flow rate reduced the reformate quality, which, while not unexpected, is a significant result because the preceding research suggested that it is generally preferable to maximise the engine's REGR rate.

At the higher temperatures the measured hydrogen concentration varied between 7 and 11% depending on the specific reforming conditions, decreasing as the REGR flow rate increased. Reforming activity was reduced at lower temperature but the system was still able to produce reformate with between 2.5 and 6% hydrogen. Measurements with a GC-FID provided in-depth speciation of the HC components of reformate, indicating that the aromatic fraction of gasoline is most difficult to reform.

The maximum rate of exhaust heat recovery achieved by the reforming process (based on the drop in EGT resulting directly from reforming) was estimated to be 0.8kW, which equated to approximately 4% of the effective engine power. The energy content and exergy of the exhaust stream were more substantially reduced when operating with REGR compared to the baseline GDI engine. For example, at the 50Nm/3000rpm engine condition, REGR reduced the exhaust exergy at the reformer inlet from 61% to 49% of the effective engine power, implying that the engine operates more efficiently and the exhaust stream exhibits lower 'energy availability'.

8.1.3 GDI engine performance with exhaust gas fuel reforming

The research has confirmed that exhaust gas fuel reforming is capable of improving GDI engine efficiency and emissions with the demonstration of a full-scale prototype coupled with a multi-cylinder GDI engine.

Exhaust gas fuel reforming consistently increases the engine fuel efficiency due to a number of factors including reduced pumping work, lower engine heat losses, enhanced combustion (relative to EGR diluted combustion), and reduced exhaust enthalpy. These are on top of the benefits provided by the reforming process, which achieves exhaust heat recovery and increases the fuel enthalpy. At the higher temperature reforming conditions (>650°C) engine fuel efficiency was increased by up to 8%, with a smaller benefit of 4% when the reformer temperature was lower (≈600°C).

The fraction of gasoline processed by the reformer (of that supplied to the total system, i.e. the engine and reformer) varied between engine conditions up to a maximum of 21%.

Analysis of the combustion process has shown that combustion with REGR is faster and more stable compared to EGR when the dilution rate is similar, but is degraded relative to the baseline GDI engine. The improved combustion stability with REGR allows higher dilution rates to be used. The results demonstrate that hydrogen can be produced by the fuel reformer in sufficient quantity to positively affect combustion. Experiments with the real exhaust gas fuel reformer confirmed the emissions trends predicted in the simulated REGR tests.

The effect of engine down-speeding on engine and reformer performance was investigated by using REGR at three constant power engine conditions between 2000 and 3000rpm. The results indicated that in addition to the fuel efficiency benefit provided by engine down-speeding, REGR was able to provide a consistent benefit of around 7% despite the lower EGTs and slightly reduced reformate quality at lower engine speed.

REGR potential has also been demonstrated at full engine load with multiple benefits including knock attenuation, lower exhaust gas temperatures and superior combustion phasing leading to increased engine efficiency and reduced emissions. However, the peak engine

torque was reduced as the REGR flow rate increased due to the displacement of fresh charge for combustion.

Two gas recirculation systems were compared and the results showed that a LP system offers higher peak load performance than a MP system due to higher exhaust mass flow through the turbine. However, the MP system does allow higher REGR rates to be used that result in a larger efficiency increase, attributed to increasingly advanced combustion phasing and higher reformed fuel fraction, although at the expense of reduced peak engine torque. This could be addressed in future development with alterations to the pressure charging system in order to raise the intake manifold pressure while using REGR, increase the fresh charge mass and restore the peak engine torque to some degree.

The application of various gas recirculation system configurations throughout the experimental research has highlighted that factors such as back pressure, turbine work potential, cooling requirements and maximum flow rate must be considered in future system design.

8.2 Concluding remarks

Experimental analysis of a prototype exhaust gas fuel reformer has shown that GDI engine exhaust conditions are favourable for fuel reforming, and can promote endothermic reforming reactions to increase the reformed fuel enthalpy and achieve some exhaust heat recovery. Ultimately this enables hydrogen to be efficiently produced by an integrated system onboard a vehicle, which in turn allows the engine to be operated in a more efficient manner.

Exhaust gas fuel reforming therefore shows good potential as a future technology to improve the thermal efficiency and emissions performance of GDI engines. In particular it is effective for reducing fuel consumption during sustained mid-load operation (e.g. motorway driving),

and may also be expected to perform well for 'real-world' operation in the cases where torque demand may be higher than is required by regulated drive cycles.

The outlook for exhaust gas fuel reforming may be improved should the trend for engine downsizing continue. By placing a higher demand on the engine by downsizing, there is a shift to higher engine IMEPs for a given road load. The mean exhaust temperature will be increased as a result.

The ability to achieve or exceed the benefits presented in this thesis with a vehicle integrated system will be greatly influenced by how the engine management is optimised. Away from the engine test bench and under transient conditions the instantaneous reformate composition will vary significantly, with implications for providing suitable engine control.

It would be advantageous to provide the engine management system with a means for assessing the instantaneous reformate or charge composition, allowing for more accurate prediction of in-cylinder fuelling requirements. This would enable relevant engine control parameters, such as fuel injector settings and ignition timing, to be modified as necessary, helping to ensure appropriate AFRs and combustion phasing, which ultimately determine the engine efficiency and emissions performance. The requirement for a robust calibration that will ensure safe engine operation under all conditions may reduce the fuel efficiency benefit to some degree.

There is much work still required to develop an exhaust gas fuel reformer system with production feasibility. If future development of the exhaust gas fuel reformer is to be successful it will be necessary to:

- Improve low temperature catalyst performance to ensure effective reformer operation across more of the 'normal' engine operating range

- Ensure that the engine is able to correctly modulate fuelling while there is a continuous and potentially significant variation in the energy content of the raw charge with REGR
- Generate a robust calibration for transient engine and reformer operation, which may require the development of predictive models or sensors to feedback on instantaneous reformer performance
- Develop diagnostics capability
- Ensure acceptable warm-up and 'switch-on' time for adequate drive-cycle performance
- Justify the requirement for additional precious metals with regards to increased cost and supply chain security
- Ensure stability of catalytic performance with sufficient durability for the lifetime of the vehicle, avoiding the various mechanisms that may cause catalyst poisoning or deactivation
- Navigate the reliability, safety and emissions implications of injecting fuel directly into the exhaust system
- Design intricate exhaust system and reformer components to withstand the thermally stressed and highly corrosive environment with acceptable mass and heat transfer characteristics
- Overcome the inclusion of non-compatible technologies in existing or future engine architectures (e.g. water-cooled IEM)
- Develop an effective system with a viable production cost

8.3 Future work

8.3.1 Effect of oxygen concentration in the reformer feed gas

In this work the reformer feed gas oxygen concentration was fixed at between 0.5 - 0.6%, which was determined by the engine-out exhaust gas composition associated with stoichiometric combustion. Increasing the oxygen concentration in the reformer feed gas would result in higher local catalyst temperature due to fuel being consumed in exothermic oxidation reactions. This should increase the hydrogen yield, although at the expense of the reforming process efficiency. This approach may be especially useful when the exhaust temperature is insufficient to promote endothermic reforming, e.g. at low engine load, but supplying hydrogen for combustion would be beneficial to engine operation.

In practise, more oxygen could be supplied to the reformer by operating the engine with a slightly lean AFR. Additionally this may improve the engine's combustion efficiency. Higher NO_X emissions normally associated with slightly lean AFRs would be avoided due to the REGR dilution effect. Another option would be injecting air directly into the reformer feed gas.

Conversely, reducing the oxygen concentration would result in less fuel oxidation, potentially increasing the reforming process efficiency providing the process temperature was sufficiently high. The elimination of oxygen from the reformer feed gas may be achieved by extracting exhaust gas from after the TWC.

The investigation should aim to determine whether a small amount of oxygen stimulates reforming or unnecessarily consumes fuel, and whether this is dependent on the engine condition and exhaust temperature.

8.3.2 Increasing the REGR rate

During the research certain engine conditions were identified that could feasibly accept higher REGR rates, with potential further benefits to engine efficiency and emissions; however, this could not always be achieved due to flow limitations of the gas recirculation system. This was generally experienced at moderate engine load conditions when combustion is inherently more stable and there is a smaller manifold pressure differential than at lower load. Therefore the use of higher REGR rates warrants further investigation. This could be achieved by a variety of methods, which may include:

- Re-designing the gas recirculation system to reduce the pressure drop and increase the maximum flow rate
- Using an EGR/REGR pump, which have been proposed for diesel EGR systems [123]
- Simultaneous delivery of REGR to the intake system before and after the compressor by using a combined HP/MP or HP/LP configuration

Higher overall charge dilution could also be achieved with the use of REGR in combination with conventional, external EGR. This approach would enable the charge dilution rate to be increased without increasing the reformer flow rate, and might also employ a split HP/MP/LP system. Alternatively, a similar result could be achieved by combining REGR with higher internal EGR via tuning of the VCT settings.

8.3.3 Ignition system

In these tests the engine used the standard ignition system and spark plug. High energy and continuous discharge ignition systems are able to increase EGR dilution tolerance [57, 124]. This technology could be expected to translate to increasing REGR tolerance, particularly at low engine load when the deterioration of combustion stability limits the REGR rate. The

application of advanced ignition systems to the REGR case could improve combustion performance and yield further engine efficiency improvements. More simply, the effect of spark plug specification and electrode gap on ignition quality, combustion stability and dilution tolerance could be investigated.

8.3.4 Split fuel injection strategy

Fuel delivery in the base engine is achieved with single-pulse DI to generate a homogeneous charge mixture. This approach was maintained throughout the experimental work, with the exception of using some gaseous fuel (hydrogen/CO/reformate) to replace a fraction of the DI gasoline. Utilising split injection to generate a partially stratified charge has been shown to benefit combustion stability and fuel economy with an EGR diluted charge [29], and may be expected to enhance REGR tolerance at low engine load. The multi-cylinder GDI engine used side mounted solenoid injectors for the air-guided combustion system. A spray-guided combustion system with centrally mounted piezo-electric injector may be better suited to exploiting the benefits of split injection due to the requirement for short injection duration and fuel placement close to the spark plug.

8.3.5 Exhaust gas fuel reformer design

In any future development of the fuel reformer it would be constructive to consider:

- The optimum reformer location and packaging to maximise the exhaust temperature at the reformer inlet
- Analysing the reformer catalyst/exhaust stream interface, perhaps with computational methods, in order to maximise heat transfer from the exhaust stream
- Reducing the thermal mass to minimise the warm-up time

- The effect of exhaust flow path on reformer temperature distribution and heat exchange, perhaps comparing a multi-pass configuration to the single-pass arrangement of the current design
- Increasing the reformer feed gas heating after fuel injection to maximise the gas temperature before entering the reformer in order to raise the catalytic process temperature

APPENDIX 1: DATA ACQUISITION CHANNELS

[1] Dynamometer and engine control (10Hz)	
Engine speed	rpm
Engine load	Nm
Engine coolant temperature	°C
Charge air temp	°C
Oil temperature	°C
Temp - Intake Manifold	°C
Exhaust temperature (Pre-turbo)	°C
Exhaust temperature (Pre-TWC)	°C
Exhaust temperature (Post-TWC)	°C
Intake air temperature	°C
EGR temperature	°C
Fuel temperature	°C
Fuel Mass Flow	kg/h
Ambient Pressure	bar

LabVIEW data acquisition

[2] High speed - 0.5° CA	
Cylinder pressure	bar
Intake port pressure	°C
Exhaust pressure (Pre-turbo)	°C
Exhaust pressure (Pre-TWC)	°C
Exhaust pressure (Post-TWC)	°C

[3] Low speed (5Hz)	
Exhaust CO (High)	%
Exhaust CO (Low)	ppm
Exhaust CO_2	%
Exhaust O_2	%
Exhaust THC	ppm
Exhaust NO_x	ppm
Exhaust NO	ppm
Intake CO_2	%
Relative Humidity (Ambient)	%

[3] EGR and Reformer settings (1Hz)	
EGR valve position	%
Reformer injector duration	ms
Reformer injector frequency	Hz

[2] ECU parameters (10Hz)	
Engine speed	rpm
Throttle plate position	%
Throttle pedal position	%
IVO timing	°aTDC
EVC timing	°aTDC
Waste-gate duty cycle	%
Start of injection timing	°bTDC
Injection duration	ms
Ignition advance	°bTDC
Ignition dwell	ms
Engine temperature	°C
Oil temperature	°C
Charge air temperature	°C
Fuel temperature	°C
Charge Air pressure	mbar
Oil Pressure	MPa
Fuel Pressure	MPa
Mass air flow	kg/h
Oxygen sensor (HEGO)	V

[3] Thermocouple amplifier (1Hz)	
Reformer temperature (x13)	°C
Exhaust stream (x2)	°C
EGR cooling water temperature	°C

[3] FTIR gas analyser (1Hz)	
Reformate CH_4	ppm
Reformate CO	%
Reformate CO_2	%
Reformate H_2O	%
Reformate Ammonia	ppm
Reformate Toluene	ppm

Data channels acquired by [1] CADET PC, [2] DAQ PC1 and [3] DAQ PC2

APPENDIX 2: INSTRUMENTATION MEASUREMENT ACCURACY

Instrument	Range	Accuracy
Rheonik RM015 fuel flow meter	0 to 20 kg/h	±0.12%
Dynamometer load cell	0 to 1000N	±0.05% FS
AVL GM12D pressure transducer	0 to 200bar	±0.3% FS
Variohm EPT3100 pressure transducer	0 to 4bar (absolute)	±0.5%
TSI Model 3775 CPC (SMPS)	0 to 10^7 particles/cm^3	±10% < $5x10^4$ particles/cm^3 ±20% < 10^7 particles/cm^3
Horiba MEXA 7100 D-EGR		
CO	0 to 12% vol	±1% FS
CO_2	0 to 20% vol	±1% FS
THC	0 to 50000ppm C1	±1% FS
O_2	0 to 25% vol	±1.5% FS
NO/NO_X	0 to 10000ppm	±1% FS

APPENDIX 3: AUTHOR PUBLICATIONS AND AWARDS

Publications

1. Fennell, D.; Herreros, J.M.; Tsolakis, A.; Xu, H.; Cockle, K.; Millington, P. GDI Engine Performance and Emissions with Reformed Exhaust Gas Recirculation (REGR). SAE Technical Paper: 2013-01-0537. DOI: 10.4271/2013-01-0537. Presented at SAE World Congress 2013.

2. Fennell, D.; Herreros, J.M.; Tsolakis, A. Improving Gasoline Direct Injection (GDI) engine efficiency and emissions with hydrogen from exhaust gas fuel reforming. International Journal of Hydrogen Energy. 2014 *(In press)*. DOI: http://dx.doi.org/10.1016/j.ijhydene.2014.01.065

3. Fennell, D.; Herreros, J.M.; Tsolakis, A.; Cockle, K.; Millington, P.; Pignon, J. Achieving exhaust energy recovery with exhaust gas fuel reforming - Part 1: Analysis of reformer performance. Applied Energy. *(In review)*

4. Fennell, D.; Herreros, J.M.; Tsolakis, A.; Cockle, K.; Millington, P.; Pignon, J. Achieving exhaust energy recovery with exhaust gas fuel reforming - Part 2: Effect on GDI engine performance, efficiency and emissions. Applied Energy. *(Future publication)*

Awards

FK Bannister Prize 2011

Hufton Postgraduate Scholarship 2013

LIST OF REFERENCES

[1] Tsolakis A, Megaritis A, Wyszynski ML. Application of Exhaust Gas Fuel Reforming in Compression Ignition Engines Fueled by Diesel and Biodiesel Fuel Mixtures. Energy & Fuels. 2003;17:1464-73. DOI:10.1021/ef0300693

[2] Tsolakis A, Megaritis A. Catalytic exhaust gas fuel reforming for diesel engines—effects of water addition on hydrogen production and fuel conversion efficiency. International Journal of Hydrogen Energy. 2004;29:1409-19. DOI:http://dx.doi.org/10.1016/j.ijhydene.2004.01.001

[3] Tsolakis A, Megaritis A. Partially premixed charge compression ignition engine with on-board production by exhaust gas fuel reforming of diesel and biodiesel. International Journal of Hydrogen Energy. 2005;30:731-45. DOI:http://dx.doi.org/10.1016/j.ijhydene.2004.06.013

[4] Abu-Jrai A, Tsolakis A, Theinnoi K, Megaritis A, Golunski SE. Diesel exhaust-gas reforming for H2 addition to an aftertreatment unit. Chemical Engineering Journal. 2008;141:290-7. DOI:http://dx.doi.org/10.1016/j.cej.2007.12.028

[5] Rodriguez-Fernandez J, Tsolakis A, Cracknell RF, Clark RH. Combining GTL fuel, reformed EGR and HC-SCR aftertreatment system to reduce diesel NOx emissions. A statistical approach. International Journal of Hydrogen Energy. 2009;34:2789-99. DOI:10.1016/j.ijhydene.2009.01.026

[6] Tsolakis A, Torbati R, Megaritis A, Abu-Jrai A. Low-Load Dual-Fuel Compression Ignition (CI) Engine Operation with an On-Board Reformer and a Diesel Oxidation Catalyst: Effects on Engine Performance and Emissions. Energy & Fuels. 2010;24:302-8. DOI:10.1021/ef900796p

[7] Lau CS, Allen D, Tsolakis A, Golunski SE, Wyszynski ML. Biogas upgrade to syngas through thermochemical recovery using exhaust gas reforming. Biomass and Bioenergy. 2012;40:86-95. DOI:http://dx.doi.org/10.1016/j.biombioe.2012.02.004

[8] Tsolakis A, Megaritis A, Yap D. Application of exhaust gas fuel reforming in diesel and homogeneous charge compression ignition (HCCI) engines fuelled with biofuels. Energy. 2008;33:462-70. DOI:10.1016/j.energy.2007.09.01

[9] Leung P, Tsolakis A, Rodriguez-Fernandez J, Golunski S. Raising the fuel heating value and recovering exhaust heat by on-board oxidative reforming of bioethanol. Energy Environ Sci. 2010;3:780-8. DOI:10.1039/b927199f

[10] Park C, Choi Y, Kim C, Oh S, Lim G, Moriyoshi Y. Performance and exhaust emission characteristics of a spark ignition engine using ethanol and ethanol-reformed gas. Fuel. 2010;89:2118-25. DOI:http://dx.doi.org/10.1016/j.fuel.2010.03.018

[11] Wheeler JC, Stein RA, Morgenstern DA, Sall ED, Taylor JW. Low-Temperature Ethanol Reforming: A Multi-Cylinder Engine Demonstration. 2011. 2011-01-0142]. DOI:10.4271/2011-01-0142

[12] Ji C, Dai X, Ju B, Wang S, Zhang B, Liang C, et al. Improving the performance of a spark-ignited gasoline engine with the addition of syngas produced by onboard ethanol steaming reforming. International Journal of Hydrogen Energy. 2012;37:7860-8. DOI:http://dx.doi.org/10.1016/j.ijhydene.2012.01.153

[13] Sall ED, Morgenstern DA, Fornango JP, Taylor JW, Chomic N, Wheeler J. Reforming of Ethanol with Exhaust Heat at Automotive Scale. Energy & Fuels. 2013;27:5579-88. DOI:10.1021/ef4011274

[14] West H. The on-line characterisation of hydrocarbon species in engine exhaust gases using a mass spectrometer, with applications to the reduction of harmful hydrocarbon species by fuel reforming. [PhD Thesis]. Birmingham: University of Birmingham; 1993.

[15] Ashur M, Misztal J, Wsyzynski ML, Tsolakis A, Xu HM, Qiao J, et al. On board Exhaust Gas Reforming of Gasoline using Integrated Reformer & TWC. 2007. [SAE Technical paper No. 2007-24-0078]

[16] Jamal Y, Wagner T, Wyszynski ML. Exhaust Gas Reforming of Gasoline at Moderate Temperatures. Int J Hydrogen Energy. 1996;21:pp.507 - 19. DOI:10.1016/0360-3199(95)00103-4

[17] Fennell D, Herreros JM, Tsolakis A, Xu H, Cockle K, Millington P. GDI Engine Performance and Emissions with Reformed Exhaust Gas Recirculation (REGR). 2013. 2013-01-0537]. DOI:10.4271/2013-01-0537
[18] Fennell D, Herreros JM, Tsolakis A. Improving Gasoline Direct Injection (GDI) Engine Efficiency and Emissions with Hydrogen from Exhaust Gas Fuel Reforming. International Journal of Hydrogen Energy. 2014;39:5153–62. DOI:http://dx.doi.org/10.1016/j.ijhydene.2014.01.065
[19] Zhao H. Advanced direct injection combustion engine technologies and development. Volume 1: Gasoline and gas engines: Woodhead Publishing; 2010.
[20] Preussner C, Döring C, Fehler S, Kampmann S. GDI: Interaction Between Mixture Preparation, Combustion System and Injector Performance. 1998. 980498]. DOI:10.4271/980498
[21] Steimle F, Kulzer A, Richter H, Schwarzenthal D, Romberg C. Systematic Analysis and Particle Emission Reduction of Homogeneous Direct Injection SI Engines. 2013. 2013-01-0248]. DOI:10.4271/2013-01-0248
[22] Stone R. Introduction to Internal Combustion Engines. Third edition ed: MacMillan Press; 1999.
[23] Heywood JB. Internal combustion engine fundamentals: McGraw-Hill; 1988.
[24] Eastwood PG. Critical Topics in Exhaust Gas Aftertreatment: Research Studies Press Limited; 2000.
[25] Sgro LA, Sementa P, Vaglieco BM, Rusciano G, D'Anna A, Minutolo P. Investigating the origin of nuclei particles in GDI engine exhausts. Combustion and Flame. 2012;159:1687-92. DOI:http://dx.doi.org/10.1016/j.combustflame.2011.12.013
[26] Duchaussoy Y, Lefebvre A, Bonetto R. Dilution Interest on Turbocharged SI Engine Combustion. 2003. 2003-01-0629]. DOI:10.4271/2003-01-0629
[27] Cairns A, Blaxill H, Irlam G. Exhaust Gas Recirculation for Improved Part and Full Load Fuel Economy in a Turbocharged Gasoline Engine. 2006. 2006-01-0047]. DOI:10.4271/2006-01-0047
[28] Potteau S, Lutz P, Leroux S, Moroz S, Tomas E. Cooled EGR for a Turbo SI Engine to Reduce Knocking and Fuel Consumption. 2007. 2007-01-3978]. DOI:10.4271/2007-01-3978
[29] Alger T, Chauvet T, Dimitrova Z. Synergies between High EGR Operation and GDI Systems. SAE Int J Engines. 2008;1:101-14. DOI:10.4271/2008-01-0134
[30] Hedge M, Weber P, Gingrich J, Alger T, Khalek I. Effect of EGR on Particle Emissions from a GDI Engine. V120-3EJ. 2011;4:650-66. DOI:10.4271/2011-01-0636
[31] Amann M, Alger T, Mehta D. The Effect of EGR on Low-Speed Pre-Ignition in Boosted SI Engines. SAE Int J Engines. 2011;4:235-45. DOI:10.4271/2011-01-0339
[32] Kaiser M, Krueger U, Harris R, Cruff L. "Doing More with Less" - The Fuel Economy Benefits of Cooled EGR on a Direct Injected Spark Ignited Boosted Engine. 2010. 2010-01-0589]. DOI:10.4271/2010-01-0589
[33] Cairns A, Fraser N, Blaxill H. Pre Versus Post Compressor Supply of Cooled EGR for Full Load Fuel Economy in Turbocharged Gasoline Engines. 2008. 2008-01-0425]. DOI:10.4271/2008-01-0425
[34] Bourhis G, Chauvin J, Gautrot X, de Francqueville L. LP EGR and IGR Compromise on a GDI Engine at Middle Load. SAE Int J Engines. 2013;6:67-77. DOI:10.4271/2013-01-0256
[35] Galloni E, Fontana G, Palmaccio R. Effects of exhaust gas recycle in a downsized gasoline engine. Applied Energy. 2013;105:99-107. DOI:http://dx.doi.org/10.1016/j.apenergy.2012.12.046
[36] Li T, Wu D, Xu M. Thermodynamic analysis of EGR effects on the first and second law efficiencies of a boosted spark-ignited direct-injection gasoline engine. Energy Conversion and Management. 2013;70:130-8. DOI:http://dx.doi.org/10.1016/j.enconman.2013.03.001
[37] Conte E, Boulouchos K. Hydrogen-enhanced gasoline stratified combustion in SI-DI engines. J Eng Gas Turb Power. 2008;130. DOI:02280110.1115/1.2795764
[38] Stone R, Zhao HY, Zhou L. Analysis of Combustion and Particulate Emissions when Hydrogen is Aspirated into a Gasoline Direct Injection Engine. 2010. [SAE Technical paper No. 2010-01-0580]. DOI:10.4271/2010-01-0580

[39] Zhao H, Stone R, Zhou L. Analysis of the particulate emissions and combustion performance of a direct injection spark ignition engine using hydrogen and gasoline mixtures. Int J Hydrogen Energy. 2010;35:11-. DOI:10.1016/j.ijhydene.2010.02.087
[40] He X, Ratcliff MA, Zigler BT. Effects of Gasoline Direct Injection Engine Operating Parameters on Particle Number Emissions. Energy & Fuels. 2012;26:2014-27. DOI:10.1021/ef201917p
[41] Fraidl G, Hollerer P, Kapus P, Ogris M, Vidmar K, Particulate Number for EU6+: Challenges and Solutions, presentation at the IQPC Advanced Emission Control Concepts for Gasoline Engines, May 2012, Stuttgart
[42] Johnson T. Vehicular Emissions in Review. SAE Int J Engines. 2013;6. DOI:10.4271/2013-01-0538
[43] Richter JM, Klingmann R, Spiess S, Wong K-F. Application of Catalyzed Gasoline Particulate Filters to GDI Vehicles. SAE Int J Engines. 2012;5:1361-70. DOI:10.4271/2012-01-1244
[44] Spiess S, Wong KF, Richter JM, Klingmann R, Investigations of Exhaust Aftertreatment Systems for Removal of Particulate Emissions from Gasoline Injection Engines, presentation at the 9th Catalysts for Automotive Pollution Control (CAPoC) Conference, September 2012, Brussels
[45] Kirwan JE, Shost M, Roth G, Zizelman J. 3-Cylinder Turbocharged Gasoline Direct Injection: A High Value Solution for Low CO2 and NOx Emissions. SAE Int J Engines. 2010;3:355-71. DOI:10.4271/2010-01-0590
[46] Coltman D, Turner JWG, Curtis R, Blake D, Holland B, Pearson RJ, et al. Project Sabre: A Close-Spaced Direct Injection 3-Cylinder Engine with Synergistic Technologies to Achieve Low CO2 Output. SAE Int J Engines. 2008;1:129-46. DOI:10.4271/2008-01-0138
[47] Miller J, Taylor J, Freeland P, Warth M, Dingelstadt R, Mueller R. Future Gasoline Engine Technology and the Effect on Thermal Management and Real World Fuel Consumption. 2013. 2013-01-0271]. DOI:10.4271/2013-01-0271
[48] Wheeler J, Polovina D, Frasinel V, Miersch-Wiemers O, Mond A, Sterniak J, et al. Design of a 4-Cylinder GTDI Engine with Part-Load HCCI Capability. SAE Int J Engines. 2013;6:184-96. DOI:10.4271/2013-01-0287
[49] Eichhorn A, Lejsek D, Hettinger A, Kufferath A. Challenge Determining a Combustion System Concept for Downsized SI-engines - Comparison and Evaluation of Several Options for a Boosted 2-cylinder SI-engine. 2013. 2013-01-1730]. DOI:10.4271/2013-01-1730
[50] Kramer U, Phlips P. Phasing Strategy for an Engine with Twin Variable Cam Timing. 2002. 2002-01-1101]. DOI:10.4271/2002-01-1101
[51] Alkidas AC. Combustion advancements in gasoline engines. Energy Conversion and Management. 2007;48:2751-61. DOI:DOI: 10.1016/j.enconman.2007.07.027
[52] Li T, Gao Y, Wang J, Chen Z. The Miller cycle effects on improvement of fuel economy in a highly boosted, high compression ratio, direct-injection gasoline engine: EIVC vs. LIVC. Energy Conversion and Management. 2014;79:59-65. DOI:http://dx.doi.org/10.1016/j.enconman.2013.12.022
[53] Fontana G, Galloni E. Variable valve timing for fuel economy improvement in a small spark-ignition engine. Applied Energy. 2009;86:96-105. DOI:http://dx.doi.org/10.1016/j.apenergy.2008.04.009
[54] Turner JWG, Pearson RJ, Kenchington SA. Concepts for improved fuel economy from gasoline engines. Int J Engine Res. 2005;6:137-57. DOI:10.1243/146808705x7419
[55] Faulkner B, Continuously variable valve lift systems, presentation at the Institution of Mechanical Engineers Lecture, 2013, School of Mechanical Engineering, University of Birmingham, England
[56] Alger T, Gingrich J, Mangold B, Roberts C. A Continuous Discharge Ignition System for EGR Limit Extension in SI Engines. SAE Int J Engines. 2011;4:677-92. DOI:10.4271/2011-01-0661
[57] Alger T, Gingrich J, Roberts C, Mangold B, Sellnau M. A High-Energy Continuous Discharge Ignition System for Dilute Engine Applications. 2013. 2013-01-1628]. DOI:10.4271/2013-01-1628
[58] Attard WP, Blaxill H. A Gasoline Fueled Pre-Chamber Jet Ignition Combustion System at Unthrottled Conditions. SAE Int J Engines. 2012;5:315-29. DOI:10.4271/2012-01-0386

[59] Srivastava D, Agarwal AK. Laser Ignition of Single Cylinder Engine and Effects of Ignition Location. 2013. 2013-01-1631]. DOI:10.4271/2013-01-1631
[60] Alger T, Mehta D, Chadwell C, Roberts C. Laser Ignition in a Pre-Mixed Engine: The Effect of Focal Volume and Energy Density on Stability and the Lean Operating Limit. 2005. 2005-01-3752]. DOI:10.4271/2005-01-3752
[61] Saidur R, Rezaei M, Muzammil WK, Hassan MH, Paria S, Hasanuzzaman M. Technologies to recover exhaust heat from internal combustion engines. Renewable and Sustainable Energy Reviews. 2012;16:5649-59. DOI:http://dx.doi.org/10.1016/j.rser.2012.05.018
[62] Alger T, Mangold B. Dedicated EGR: A New Concept in High Efficiency Engines. SAE Int J Engines. 2009;2:620-31. DOI:10.4271/2009-01-0694
[63] Cengel YA, Boles MA. Thermodynamics: An Engineering Approach: Mcgraw-Hill; 1998.
[64] Alger T, Gingrich J, Khalek IA, Mangold B. The Role of EGR in PM Emissions from Gasoline Engines. SAE Int J Fuels Lubr. 2010;3:85-98. DOI:10.4271/2010-01-0353
[65] Gu X, Huang Z, Cai J, Gong J, Wu X, Lee C-f. Emission characteristics of a spark-ignition engine fuelled with gasoline-n-butanol blends in combination with EGR. Fuel. 2012;93:611-7. DOI:http://dx.doi.org/10.1016/j.fuel.2011.11.040
[66] Kayes D, Hochgreb S. Mechanisms of Particulate Matter Formation in Spark-Ignition Engines. 1. Effect of Engine Operating Conditions. Environmental Science & Technology. 1999;33:3957-67. DOI:10.1021/es9810991
[67] Arsie I, Di Iorio S, Vaccaro S. Experimental investigation of the effects of AFR, spark advance and EGR on nanoparticle emissions in a PFI SI engine. Journal of Aerosol Science. 2013;64:1-10. DOI:http://dx.doi.org/10.1016/j.jaerosci.2013.05.005
[68] Quader AA, Kirwan JE, Grieve MJ. Engine performance and emissions near the dilute limit with hydrogen enrichment using an on-board reforming strategy. 2003. [SAE Technical paper No. 2003-01-1356]
[69] Conte E, Boulouchos K. Influence of hydrogen-rich-gas addition on combustion, pollutant formation and efficiency of an IC-SI engine. 2004
[70] Richard AY, Guillaume R, Vigor Y, Zhe W, Piyush T. Fundamental Combustion Characteristics Of Syngas. Synthesis Gas Combustion: CRC Press; 2009. p. 99-128.
[71] Topinka JA, Gerty MD, Heywood JB, Keck JC. Knock Behavior of a Lean-Burn, H_2 and CO Enhanced, SI Gasoline Engine Concept. 2004. [SAE Technical paper No. 2004-01-0975]
[72] Gomes SR, Bion N, Blanchard G, Rousseau S, Duprez D, Epron F. Study of the main reactions involved in reforming of exhaust gas recirculation (REGR) in gasoline engines. RSC Advances. 2011;1:109-16. DOI:10.1039/C1RA00003A
[73] Tsolakis A, Megaritis A. Partially premixed charge compression ignition engine with on-board H-2 production by exhaust gas fuel reforming of diesel and biodiesel. International Journal of Hydrogen Energy. 2005;30:731-45. DOI:10.1016/j.ijhydene.2004.06.013
[74] Abu-Jrai A, Rodriguez-Fernandez J, Tsolakis A, Megaritis A, Theinnoi K, Cracknell RF, et al. Performance, combustion and emissions of a diesel engine operated with reformed EGR. Comparison of diesel and GTL fuelling. Fuel. 2009;88:1031-41. DOI:10.1016/j.fuel.2008.12.001
[75] Peucheret S, Feaviour M, Golunski S. Exhaust-gas reforming using precious metal catalysts. Applied Catalysis B: Environmental. 2006;65:201-6. DOI:http://dx.doi.org/10.1016/j.apcatb.2006.01.009
[76] Reynolds WC. STANJAN. . 1981. p. Software for Chemical Equilibrium Analysis.
[77] Praharso, Adesina AA, Trimm DL, Cant NW. Supported Rh catalysts for the indirect partial oxidation of isooctane. Korean Journal of Chemical Engineering. 2003;20:468-70.
[78] Bartholomew CH. Mechanisms of catalyst deactivation. Applied Catalysis A: General. 2001;212:17-60.

[79] Gomes SR, Bion N, Blanchard G, Rousseau S, Bellière-Baca V, Harlé V, et al. Thermodynamic and experimental studies of catalytic reforming of exhaust gas recirculation in gasoline engines. Applied Catalysis B: Environmental. 2011;102:44-53. DOI:DOI: 10.1016/j.apcatb.2010.11.023
[80] Villegas L, Guilhaume N, Provendier H, Daniel C, Masset F, Mirodatos C. A combined thermodynamic/experimental study for the optimisation of hydrogen production by catalytic reforming of isooctane. Applied Catalysis A: General. 2005;281:75-83. DOI:http://dx.doi.org/10.1016/j.apcata.2004.11.015
[81] Golunski S. What is the point of on-board fuel reforming? Energy Environ Sci. 2010;3:1918-23. DOI:10.1039/c0ee00252f
[82] Kirwan JE, Quader AA, Grieve MJ. Fast Start-Up On-Board Gasoline Reformer for Near Zero Emissions in Spark-Ignition Engines. 2002. [SAE Technical paper No. 2002-01-1011]
[83] Isherwood KD, Linna JR, Loftus PJ. Using on-board fuel reforming by partial oxidation to improve SI engine cold-start performance and emissions. 1998. [SAE Technical paper No. 980939]
[84] Green J, J.B. , Domingo N, Storey JME, Wagner RM, Armfield JS, Bromberg L, et al. Experimental evaluation of SI engine operation supplemented by hydrogen rich gas from a compact plasma boosted reformer. 2000. [SAE Technical paper No. 2000-01-2206]
[85] Tsolakis A, Megaritis A. Catalytic exhaust gas fuel reforming for diesel engines--effects of water addition on hydrogen production and fuel conversion efficiency. International Journal of Hydrogen Energy. 2004;29:1409-19.
[86] Alger T, Gingrich J, Mangold B. The Effect of Hydrogen Enrichment on EGR Tolerance in Spark Ignited Engines. 2007. 2007-01-0475]. DOI:10.4271/2007-01-0475
[87] Al-Baghdadi M, Al-Janabi H. Improvement of performance and reduction of pollutant emission of a four stroke spark ignition engine fueled with hydrogen-gasoline fuel mixture. Energy Conversion and Management. 2000;41:77-91.
[88] Ji CW, Wang SF. Effect of hydrogen addition on combustion and emissions performance of a spark ignition gasoline engine at lean conditions. International Journal of Hydrogen Energy. 2009;34:7823-34. DOI:10.1016/j.ijhydene.2009.06.082
[89] Ji CW, Wang SF. Effect of Hydrogen Addition on Idle Performance of a Spark-Ignited Gasoline Engine at Lean Conditions with a Fixed Spark Advance. Energy & Fuels. 2009;23:4385-94. DOI:10.1021/ef900517t
[90] Ji CW, Wang SF. Experimental Study on Combustion and Emissions Characteristics of a Spark Ignition Engine Fueled with Gasoline-Hydrogen Blends. Energy & Fuels. 2009;23:2930-6. DOI:10.1021/ef900209m
[91] Ji CW, Wang SF. Effect of hydrogen addition on the idle performance of a spark ignited gasoline engine at stoichiometric condition. International Journal of Hydrogen Energy. 2009;34:3546-56. DOI:10.1016/j.ijhydene.2009.02.052
[92] Ji CW, Wang SF. Combustion and emissions performance of a hybrid hydrogen-gasoline engine at idle and lean conditions. International Journal of Hydrogen Energy. 2010;35:346-55. DOI:10.1016/j.ijhydene.2009.10.074
[93] Ji CW, Wang SF, Zhang B. Combustion and emissions characteristics of a hybrid hydrogen-gasoline engine under various loads and lean conditions. International Journal of Hydrogen Energy. 2010;35:5714-22. DOI:10.1016/j.ijhydene.2010.03.033
[94] Ji CW, Wang SF, Zhang B. Effect of spark timing on the performance of a hybrid hydrogen-gasoline engine at lean conditions. International Journal of Hydrogen Energy. 2010;35:2203-12. DOI:10.1016/j.ijhydene.2010.01.003
[95] Suzuki T, Sakurai Y. Effect of Hydrogen-Rich Gas and Gasoline Mixed Combustion on Spark Ignition Engine. 2006. [SAE Technical paper No. 2006-01-3379]
[96] Tahtouh T, Halter F, Samson E, Mounaim-Rousselle C. Effects of hydrogen addition under lean and diluted conditions on combustion characteristics and emissions in a spark-ignition engine. Int J Engine Res. 2011;12:466-83. DOI:10.1177/1468087411409309

[97] D'Andrea T, Henshaw P, Ting DSK. The addition of hydrogen to a gasoline-fuelled SI engine. International Journal of Hydrogen Energy. 2004;29:1541-52. DOI:10.1016/j.ijhydene.2004.02.002
[98] Akif Ceviz M, Sen AK, Küleri AK, Volkan Öner İ. Engine performance, exhaust emissions, and cyclic variations in a lean-burn SI engine fueled by gasoline–hydrogen blends. Applied Thermal Engineering. 2012;36:314-24. DOI:10.1016/j.applthermaleng.2011.10.039
[99] Zhao HY, Stone R, Zhou L. Analysis of the particulate emissions and combustion performance of a direct injection spark ignition engine using hydrogen and gasoline mixtures. International Journal of Hydrogen Energy. 2010;35:4676-86. DOI:10.1016/j.ijhydene.2010.02.087
[100] Allgeier T, Klenk M, Landenfeld T, Conte E, Boulouchos K, Czerwinski J. Advanced emission and fuel economy concept using combined injection of gasoline and hydrogen in SI engines. 2004. [SAE Technical paper No. 2004-01-1270]
[101] Ivanič Ž, Ayala F, Goldwitz J, Heywood JB. Effects of Hydrogen Enhancement on Efficiency and NO_X Emissions of Lean and EGR-Diluted Mixtures in a SI Engine. 2005. DOI:10.4271/2005-01-0253
[102] Tully EJ, Heywood JB. Lean-Burn Characteristics of a Gasoline Engine Enriched with Hydrogen from a Plasmatron Fuel Reformer. 2003. [SAE Technical paper No. 2003-01-0630]
[103] Houseman J, Cerini DJ. On-board hydrogen generator for a partial hydrogen injection internal combustion engine. 1974. [SAE Technical paper No. 740600]
[104] Shudo T, Nabetani S. Analysis of Degree of Constant Volume and Cooling Loss in a Hydrogen Fuelled SI Engine. 2001
[105] Chevron. Chevron Technical Review, "Motor Gasolines". 1996.
[106] Russ S. A Review of the Effect of Engine Operating Conditions on Borderline Knock. 1996. [SAE Technical paper No. 960497]
[107] Lehrle RS, West H, Wyszynski ML. On-line mass spectrometric characterisation of hydrocarbons in engine exhaust gases. Proceedings of the Institution of Mechanical Engineers. 1995;209:307-24.
[108] Posada F, Bedick C, Clark NN, Kozlov A, Linck M, Boulanov D, et al. Low Temperature Combustion with Thermo-Chemical Recuperation. 2007. 2007-01-4074]. DOI:10.4271/2007-01-4074
[109] Turner DM. The combustion and emissions performance of fuel blends in modern combustion systems [Ph.D. thesis]: University of Birmingham.; 2010.
[110] Daniel RL. Combustion and emissions performance of oxygenated fuels in a modern spark ignition engine [Ph.D. thesis]: University of Birmingham; 2012.
[111] Sharma CS, Ramanathan K, Li W. Post-processing of vehicle emission test data for use in exhaust after-treatment modelling and analysis. Proceedings of the Institution of Mechanical Engineers, Part D: Journal of Automobile Engineering. 2012;226:840-54. DOI:10.1177/0954407011427812
[112] Mueller M. General Air Fuel Ratio and EGR Definitions and their Calculation from Emissions. 2010. 2010-01-1285]. DOI:10.4271/2010-01-1285
[113] Samuel S, Hassaneen A, Morrey D. Particulate Matter Emissions and the Role of Catalytic Converter During Cold Start of GDI Engine. 2010. 2010-01-2122]. DOI:10.4271/2010-01-2122
[114] Armas O, Gomez A, Herreros J. Uncertainties in the determination of particle size distributions using a mini tunnel-SMPS system during Diesel engine testing. . Measurement Science and Technology. 2007;18:2121-30. DOI:10.1088/0957-0233/18/7/044
[115] Burtscher H. Physical characterization of particulate emissions from Diesel engines: a review Journal of Aerosol Science. 2005;36:896–932. DOI:10.1016/j.jaerosci.2004.12.001
[116] Kittelson D, Watts W, Watts W. Review of Diesel particulate matter sampling methods Supplemental Report 2: Aerosol Dynamics, Laboratory and On-road Studies 1998
[117] Wei Q, Kittleson D, Watts W. Single-stage dilution tunnel performance 2001
[118] Shinagawa T, Okumura T, Furuno S, Kim K-O. Effects of Hydrogen Addition to SI Engine on Knock Behavior. 2004. 2004-01-1851]. DOI:10.4271/2004-01-1851

[119] Guo H, Liu F, Smallwood GJ, Gülder ÖL. Numerical study on the influence of hydrogen addition on soot formation in a laminar ethylene–air diffusion flame. Combustion and Flame. 2006;145:324-38. DOI:http://dx.doi.org/10.1016/j.combustflame.2005.10.016
[120] Guo H, Thomson KA, Smallwood GJ. On the effect of carbon monoxide addition on soot formation in a laminar ethylene/air coflow diffusion flame. Combustion and Flame. 2009;156:1135-42. DOI:http://dx.doi.org/10.1016/j.combustflame.2009.01.006
[121] Jiang Y, Qiu R. Numerical Analysis of the Effect of Carbon Monoxide Addition on Soot Formation in an Acetylene/Air Premixed Flame. Acta Physico-Chimica Sinica. 2010;26:2121-9.
[122] Alger T, Gingrich J, Roberts C, Mangold B. Cooled exhaust-gas recirculation for fuel economy and emissions improvement in gasoline engines. Int J Engine Res. 2011;12:252-64. DOI:10.1177/1468087411402442
[123] Teng H, Regner G, Hunter G, inventor., assignee. EXHAUST POWER TURBINE DRIVEN EGR PUMP FOR DIESEL ENGINES. US patent 20100293943. Nov 25, 2010
[124] Chen W, Madison D, Dice P, Naber J, Chen B, Miers S, et al. Impact of Ignition Energy Phasing and Spark Gap on Combustion in a Homogenous Direct Injection Gasoline SI Engine Near the EGR Limit. 2013. 2013-01-1630]. DOI:10.4271/2013-01-1630